



DEPARTAMENTO DE PARASITOLOGÍA
UNIVERSIDAD DE GRANADA

*Memoria de Tesis doctoral presentada por **D. Francisco Olmo Arévalo** para aspirar a la obtención del título de DOCTOR INTERNACIONAL por la Universidad de Granada (Programa Oficial de Doctorado en Medicina Clínica y Salud Pública, D12.56.1)*

Application of supramolecular chemistry in the search for active compounds against *Trypanosoma cruzi* infection in mouse model.

Aplicación de la química supramolecular en la búsqueda de compuestos activos frente a la infección por *Trypanosoma cruzi* en modelo murino

Fdo: Francisco Olmo Arévalo

Granada, Marzo de 2015

Directores de la Tesis Doctoral



Dr. Manuel Sánchez Moreno

Catedrático de Parasitología de
la Universidad de Granada



Dra. Clotilde Marín Sánchez

Profesora Titular de la
Universidad de Granada

Editorial: Universidad de Granada. Tesis Doctorales
Autor: Francisco Olmo Arévalo
ISBN: 978-84-9125-097-5
URI: <http://hdl.handle.net/10481/40132>

INDEX:

1. Title page.	1
2. Acknowledgments.	5
3. Summary / Resumen.	9/15
4. Introduction.	21
4.1. Chagas Disease and <i>Trypanosoma cruzi</i> .	23
4.2. History, discovery and Epidemiology.	23
4.2.1. <i>T.cruzi</i> : morphology and life cycle.	27
4.2.2. Genetic diversity of <i>T. cruzi</i> .	31
4.2.3. Metabolism.	33
4.3. Clinical forms and pathogenesis.	34
4.4. Diagnosis.	39
4.5. Current treatments & new compounds under study.	43
4.6. Vaccines against <i>T.cruzi</i> .	47
5. Objectives/Objetivos.	51
6. Methodology.	55
6.1. Published techniques.	57
6.2. Synthesis of compounds.	58
6.3. Set up of techniques (unpublished).	58
6.3.1. Establishment of an <i>in vivo</i> model for Chagas disease.	58
6.3.2. Drug-combination studies.	63

6.3.3. New technologies for the study of chronic phase: Advanced experimental murine model.	65
7. Results.	69
7.1. Publications already published.	71
7.2. Publications submitted.	139
7.3. Unpublished results.	233
7.3.1. In vitro drug-combination.	233
7.3.2. In vivo drug-combination.	235
7.4. Invention Patents.	237
8. Discussion & Conclusions / Discusión & Conclusiones.	239/247
9. References.	259



Universidad de Granada

El doctorando **D. Francisco Olmo Arévalo** y los directores de la tesis **Dr. Manuel Sánchez Moreno** y **Dra. Clotilde Marín Sánchez**, garantizamos, al firmar esta tesis doctoral, que el trabajo ha sido realizado por el doctorando bajo la dirección de los directores de la tesis y hasta donde nuestro conocimiento alcanza, en la realización del trabajo, se han respetado los derechos de otros autores a ser citados, cuando se han utilizado sus resultados o publicaciones.

En Granada a 2 de Marzo de 2015

Director/es de la Tesis

Doctorando

Fdo.: Manuel Sánchez Moreno
Clotilde Marín Sánchez

Fdo.: Francisco Olmo Arévalo



2. ACKNOWLEDGEMENTS

*" Who only seek applause of others, put its
happiness in someone else's hands"*

*("Quién sólo busca el aplauso de los demás, pone su felicidad en manos
ajenas")*

Oliver Goldsmith

[ACKNOWLEDGEMENTS]

Quiero dar las gracias en primer lugar al Dr. Manuel Sánchez Moreno por haberme permitido realizar este trabajo en su laboratorio, haberme acogido desde aquella llamada telefónica apurada en Septiembre de 2008 cuando le pedí solicitar la Beca de Colaboración hasta estos últimos días en que me anima con este último esfuerzo y se asegura personalmente de que sigo vivo cada día y vengo por el laboratorio; muchas gracias por todo lo que me has enseñado tanto en lo profesional como en lo personal y siempre guardaré recuerdo de quien ha sido mi mentor o “padre científico”. Del mismo modo, a la Dra. Clotilde Marín Sánchez por haber aceptado codirigir este trabajo, por su ayuda técnica desde los inicios y por su confianza a lo largo en todo este camino que me ha permitido no solo crecer como investigador sino encontrar una amiga cercana, son innumerables los momentos que hemos compartido, y de todos ellos guardo un gran aprecio, en los que me ha mostrado su apoyo y también en los que me ha tirado de las orejas o recolocado los pies en el suelo.

I wanna thank professors RL Krauth-Siegel (Heidelberg, Germany) and J.M Kelly (London, UK) for the opportunity of being part of their groups during the time that I spent in their laboratories. Thank you both for your help and make me feel like home there; this work has been also possible for their collaboration.

Por supuesto agradecer a todas las personas que forman parte del grupo CTS-944 de Parasitología Molecular y resto de personal del laboratorio (Encarna y Carlos), tanto a los que siguen como a los que ya continúan su camino fuera de allí, a los que creen en ti y te animan de corazón y también aquellos que intentan poner la “zancadilla”, pues de tod@s se aprende en este circo de la vida. Mi agradecimiento más especial para Kristína, Rubén y sobre todo a la Dra. María José Rosales, por haber compartido tantos desayunos donde a costa de “foquear” hemos tenido nuestro pequeño desahogo en el “mundi dulce”; gracias

[ACKNOWLEDGEMENTS]

también a todo el personal que allí trabaja (Carlos, Carmen, Eli, Rocio) no hay nada como empezar el día con una sonrisa.

Dar las gracias también a todos mis amigos, pues si el refrán es cierto y quien tiene un amigo tiene un Tesoro: Yo soy RICO; tanto a los de toda la vida con Jose y Torres a la cabeza hasta los demás miembros de la “Familia Capisci”. No son menos los que mi llegada a Granada trajo a mi vida “el Veci”, Pepino, Xano, Begoña, Tradis, Aroa, Marina y todos los que en estos años han sabido estar ahí para lo bueno y para lo malo.

No hay duda que tengo que agradecer a mi familia, principales financiadores de esta aventura, a mi padre y a mi madre, a mi hermano Jesús y a mis tías Domi y Manoli (ventajas de tener tres madres) y a mis primos Sergio y Ana, gracias a todos por confiar siempre en mí y por vuestro apoyo incondicional pese a no saber exactamente en muchos momentos que hacia exactamente, ese es uno de los misterios de la confianza que dan los lazos familiares. Hablar de apoyo no es posible en mi vida sin mencionar a mi abuela Felipa que con solo una mirada sabe hacerme cargar mis energías para seguir cualquier viaje.

Quiero dedicar esta tesis doctoral a la memoria de mi hermano Mario,

“Allá donde estés Mario, Gracias por ser el viento en empuja mis alas”





3. SUMMARY

*" Sometimes you have to decide between a thing
that you are used and one that we would like to
know "*

Paulo Coelho

According to the World Health Organization (WHO) Chagas disease or American trypanosomiasis is a parasitic, systemic, chronic disease caused by the protozoan *Trypanosoma cruzi*. It is spread naturally by triatomine insects, especially the so-called "kissing bugs" that normally colonize poor-quality housing. It is also transmitted by transfusions, congenitally, via organ transplants and through contaminated food. Chagas disease is endemic in 21 countries in the Americas, where it is estimated that about 100 million people are at risk of infection, with around 8 million infected, and a total of 56,000 new cases annually including all forms of transmission, leading to 12,000 deaths per year. Current treatments, benznidazole and nifurtimox, exhibit limited effectiveness, only being curative during the acute phase of infection and not in the chronic phase, which is when most cases are diagnosed. Furthermore, administration involves a series of high-toxicity side effects. In addition, there is no vaccine against this parasitic infection.

For several years we have been collaborating with various chemical synthesis groups around Spain, which has resulted in the production of a series of joint publications, as well as national and international collaborative projects. This cooperative work has allowed us to gain a wide experience and knowledge of a number of chemical families which display anti-protozoal activity against *Trypanosoma cruzi* and *Leishmania* sp.

In this study, we looked at five specific families with different chemical natures to observe their *in vitro* and *in vivo* activity against *T. cruzi*. These were: **N, N'**-**Squaramides** (Department of Chemistry, Faculty of Science, University of the Balearic Islands, Palma de Mallorca), **Phthalazines** (Department of Organic Chemistry, Faculty of Chemistry, Complutense University, Madrid / Institute of Medical chemistry, Organic Chemistry Center M. Lora-Tamayo, CSIC), **Abietic Acid Derivatives**

[SUMMARY]

(Department of Organic chemistry, University of Granada), **Tetradentated polyamines** (QBIS Research Group, Institute of Computational Chemistry and Catalysis (IQCC) and the Department of Chemistry, University of Girona), and **Scorpiand-like azamacrocycles** (Institute of Molecular Science, Department of Inorganic Chemistry, University of Valencia / Department of Organic Chemistry, University of Valencia).

The experimental biology was conducted entirely in the Department of Parasitology, Faculty of Sciences, University of Granada, with the exception of the "Trypanothione reductase (TR) inhibition assay" and the "*in vivo* bioluminescence imaging study", which were developed in the Biochemie-Zentrum der Universität Heidelberg (Germany) and the London School of Hygiene and Tropical Medicine (UK) respectively, during two pre-doctoral stays. The entire study was carried out through a series of experiments that can be classified into three phases: the *in vitro* stage, *in vivo* stage, and a study of the mechanism of action. During the first two stages, compounds were screened: those with elevated activity were selected and those that did not meet minimum requirements of effectiveness were discarded.

During the first stage of *in vitro* screening, the compounds were tested at different concentrations against different forms of the parasite and mammalian cells (cytotoxicity); dividing parasite IC_{50} between mammalian cells IC_{50} (the concentration at which 50% growth inhibition occurs) a specific selectivity index (SI) for each compound was obtained. This SI was indicative of the specificity toxicity of that compound had against parasites versus mammalian cells. Based on this, the compounds exhibiting the best selectivity indices according to the criteria established in the literature were selected for the next stage.

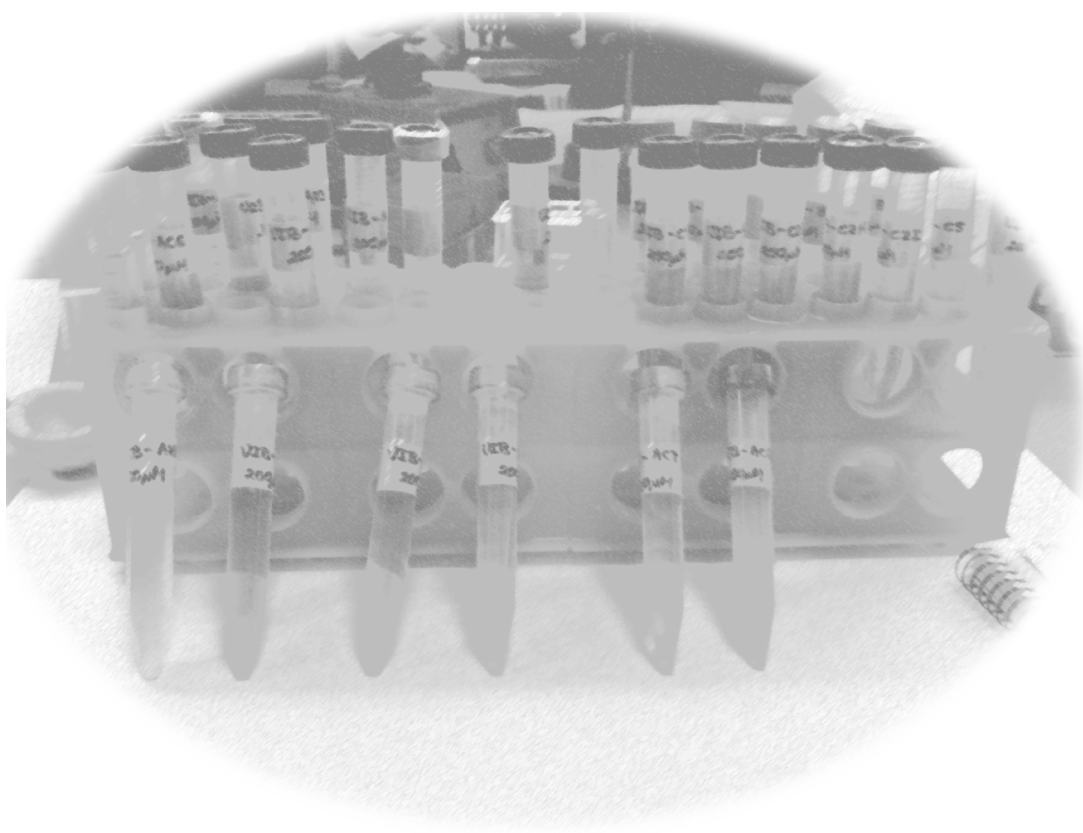
The next step was to test these compounds selected from the *in vitro* phase in an experimental animal model, the Balb/c murine model. The mice were infected and once the infection had been confirmed the treatment was started. This treatment was continued for 5 days (acute phase). Throughout the acute phase (up to 40 days post-infection), the mice were bled every three days to follow the parasitemia levels, and blood samples were obtained for serum as well as to assess the levels of antibodies, and identify common biochemical parameters in the serology that could reveal signs of toxicity associated with the compounds. The mice were kept in the same conditions for at least 120 days, i.e., the time period of the chronic phase of infection characterized by a decrease in blood parasitemia that reaches an almost undetectable level. To determine the degree of effectiveness/cure of the therapy administered, an immunosuppressive treatment was applied to the mice, to induce reactivation of parasitemia in cases where there was no cure. Similarly, the specific target organ for this strain of parasite, the heart, was analyzed *post mortem* by PCR to determine the presence or absence of the parasite.

The final stage of this study included a search for possible mechanisms of action of those compounds that had been effective in the *in vivo* treatment. For this, tests were performed at three levels: energy metabolism, by analyzing the variation in metabolite excretion to the culture medium by ¹H-NMR; ultrastructural analysis, by transmission electron microscopy; and antioxidant defense, by *in vitro* inhibition studies of the parasite-specific enzymes iron superoxide dismutase and trypanothione reductase.

Finally, the possible synergistic actions of these selected compounds were studied using *in vitro* drug-combination assays and later *in vivo* studies of combinations with very similar working protocols to those in a clinical situation.

[SUMMARY]

The results obtained are summarized in several conclusions about the potential use of these compounds as trypanocidal agents, areas for improvement in this line of research, and what future guidelines could be implemented to take an immediate step further in the preclinical phase. Also, it should be noted that many of these families of compounds are patent-protected and there is a commitment to continued improvements in their pharmaco-kinetic properties and working protocols in order to achieve better results.



3. RESUMEN

" Algunas veces hay que decidirse entre una cosa a la que se está acostumbrado y otra que nos gustaría conocer "

Paulo Coelho

Según la Organización Mundial de la Salud (OMS) la enfermedad de Chagas o tripanosomiasis americana es una enfermedad parasitaria, sistémica, crónica, causada por el protozoo *Trypanosoma cruzi*. Se transmite de manera natural por insectos triatomíneos, comúnmente llamados "vinchucas" que normalmente colonizan viviendas precarias. Otras modalidades de transmisión son transfusional, congénita, trasplantes de órganos, y a través de los alimentos contaminados. La enfermedad de Chagas es endémica en 21 países de las Américas, donde se estima que cerca de 100 millones de personas están en riesgo de infectarse, unos 8 millones infectadas, con 56.000 nuevos casos anuales por todas las formas de transmisión, motivando 12.000 muertes anuales. Los tratamientos actuales: el Benznidazol y Nifurtimox, presentan limitada efectividad, siendo solo curativos durante la fase aguda de la infección y no en la fase crónica donde la mayoría de los casos son diagnosticados. Además su administración acarrea una serie de efectos secundarios consecuencia de su alta toxicidad. Además, no existe vacuna capaz de prevenir esta infección parasitaria.

Nuestro grupo colabora desde hace varios años con diversos grupos de síntesis química de diferentes puntos de España, lo que se ha reflejado en la producción de una serie de publicaciones conjuntas y proyectos nacionales e internacionales coordinados. Esta serie de trabajos conjuntos nos han permitido tener una amplia experiencia y conocimiento de una serie de familias químicas con actividades anti-protozoarias frente a *Trypanosoma cruzi* y *Leishmania* sp.

En esta tesis doctoral se han estudiado cinco familias concretas de diferentes naturalezas químicas: **N,N'-Squaramides** (Departamento de Química, Facultad de Ciencias, Universidad de las Islas Baleares, Palma de Mallorca), **Phthalazines** (Departamento de Química Orgánica, Facultad de Química, Universidad Complutense, Madrid / Instituto de Química Médica, Centro de Química Orgánica M. Lora-Tamayo,

CSIC), **Abietic acid derivatives** (Departamento de Química Orgánica, Universidad de Granada), **Tetradentated polyamines** (QBIS Research Group, Institut de Química Computacional i Catàlisi (IQCC) y Departament de Química, Universitat de Girona) y **Scorpiand-like azamacrocycles** (Instituto de Ciencia Molecular, Departamento de Química Inorgánica, Universidad de Valencia / Departamento de Química Orgánica, Universidad de Valencia), con objeto de ver la actividad que presentan *in vitro* e *in vivo* frente a *T. cruzi*.

El desarrollo del trabajo experimental de actividad biológica ha sido íntegramente realizado en el Departamento de Parasitología, en la Facultad de Ciencias de la Universidad de Granada, con excepción de los ensayos de “inhibición de la actividad Trypanothiona reductasa (TR)” y “tratamientos *in vivo* de fase crónica por técnicas de bioluminiscencia”, llevados a cabo en el BIOCHEMIE-ZENTRUM DER UNIVERSITÄT HEIDELBERG (Alemania) y en el LONDON SCHOOL OF HYGIENE AND TROPICAL MEDICINE (Reino Unido), respectivamente mediante dos estancias pre-doctorales realizadas. El trabajo se ha realizado en una serie de fases de experimentación que pueden clasificarse en tres: fase *in vitro*, fase *in vivo* y fase de estudio del mecanismo de acción. Durante las dos primeras fases se ha realizado un cribado y selección de los compuestos con mejor actividad y eliminación de aquellos que no cumplían unos requisitos mínimos de efectividad.

Durante la primera fase de cribado *in vitro*, los compuestos fueron testados a diferentes concentraciones frente a las diferentes formas celulares del parásito, así como frente a cultivos de células de mamífero (citotoxicidad); enfrentando ambas IC₅₀ (concentración a la cual se produce un 50% de inhibición del crecimiento) se obtuvo un índice de selectividad específico para cada compuesto, indicativo de la toxicidad especificidad de ese compuesto sobre los parásitos frente a las células de mamífero. Con

esta base, fueron seleccionados para la siguiente fase los compuestos que presentan los mejores índices de selectividad de acuerdo a los criterios establecidos en la literatura.

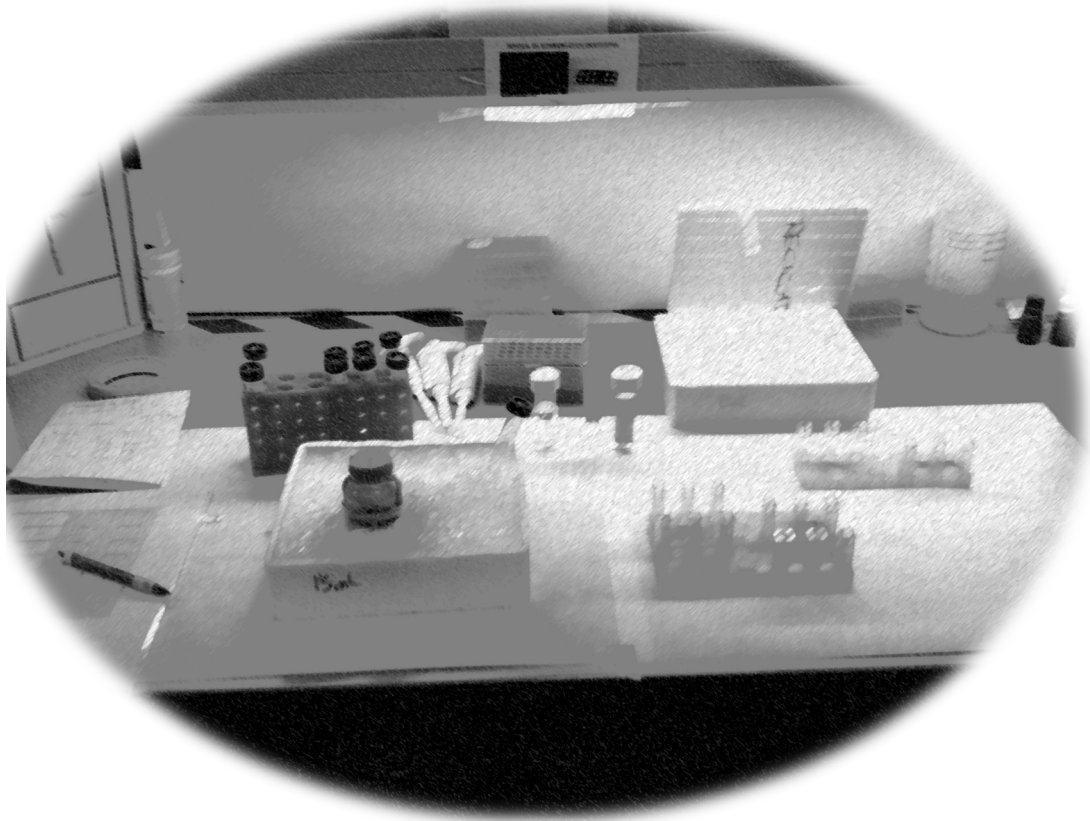
La siguiente fase consistió en testar esos compuestos seleccionados de la fase *in vitro* en un modelo de experimentación animal, el modelo murino Balb/c. Los ratones fueron infectados y una vez confirmada la infección se comenzó el tratamiento, este tratamiento se aplicó durante 5 días (fase aguda), durante toda la fase aguda (hasta 40 días post-infección) se extrajo sangre cada tres días para conteo en fresco de la parasitemia, del mismo modo se obtuvieron muestras de sangre para obtención de suero y evaluar los niveles de anticuerpos, así como la determinación de los parámetros bioquímicos comunes en una serología que pudiesen mostrar indicios de toxicidad asociada al compuesto. Los ratones fueron mantenidos en las mismas condiciones hasta superados los 120 días, es decir, en fase crónica de la infección caracterizada por una disminución de la parasitemia en sangre que llega a un nivel casi indetectable. Con objeto de determinar el grado de efectividad/curación del tratamiento sobre los ratones se aplicó un tratamiento inmunosupresor con objeto inducir la reactivación de la parasitemia en los casos donde no hubo una curación. Del mismo modo, el órgano diana específico para esta cepa del parásito, el corazón, fue analizado *post mortem* mediante la técnica de PCR para determinar la presencia o ausencia del parásito.

La última fase de este estudio comprendió la búsqueda del posible mecanismo de acción de los compuestos que habían mostrado una eficacia en el tratamiento *in vivo*. Para ello, se realizaron ensayos a tres niveles: metabolismo energético, analizando la variación en la excreción de metabolitos al medio de cultivo mediante $^1\text{H-NMR}$; análisis de la ultraestructura mediante microscopía electrónica de transmisión; defensa antioxidante, mediante estudios de inhibición *in vitro* de las enzimas específicas del parásito hierro superóxido dismutasa y trypanotona reductasa.

[RESUMEN]

Finalmente, se estudió la posible acción sinérgica de los compuestos seleccionados mediante ensayos de combinación *in vitro* y posteriormente su estudio *in vivo* sobre modelo murino con un protocolo de trabajo muy próximo a la situación clínica.

Los resultados obtenidos se resumen en varias conclusiones acerca del potencial uso como agentes tripanocidas de estos compuestos, los puntos a mejorar en esta línea de investigación, así como qué directrices futuras podríamos seguir para dar un paso más allá en los estudios de fase preclínica en un futuro inmediato. Cabe también destacar que, muchas de estas familias de compuestos han sido protegidas bajo patente y existe el compromiso de seguir trabajando para mejorar sus propiedades farmacocinéticas y los protocolos de trabajo con objeto de alcanzar mejores resultados.



4. INTRODUCTION

"Speak, So That I May See You"

("Habla para que yo te conozca")

Sócrates

4.1. Chagas Disease and *Trypanosoma cruzi*.

According to the World Health Organization Chagas disease is an important public health problem in Latin America currently affecting an estimated 8 million people in 21 countries and spreading by human migration to a number of non-endemic regions. This parasitic, chronic, and systemic disease is caused by the protozoan *Trypanosoma cruzi* and the predominant modes of transmission are vectorial, through infected dejections of triatomine bugs ('kissing bugs') and by blood transfusion. Additionally, congenital transmission, and oral infection following ingestion of food contaminated with the parasite are important (WHO, 2012).

T. cruzi is associated with a very high clinical and epidemiological pleomorphism. Clinically, Chagas disease presents a short acute phase with detectable parasites in the bloodstream, followed by a life-long chronic phase maintained with scarce parasitaemia (Rassi et al., 2010). The chronic disease presents different clinical manifestations, ranking from an absence of symptoms to severe disease. Twenty to thirty per cent of those infected will suffer irreversible cardiovascular, gastrointestinal, and/or neurological problems. The outcome of infection in a particular individual is the result of a set of complex interactions among the host genetic background, environmental and social factors, and the genetic composition of the parasite (Campbell et al., 2004).

4.2. History, discovery and epidemiology.

The 15th of April, 1909, Carlos Chagas (1878-1934), Instituto Oswaldo Cruz, announced to the scientific world the discovery in Lassance, state of Minas Gerais, of a new tropical disease caused by the protozoan *T. cruzi* (also described by him in 1908) and transmitted by a hematophagous bug popularly known as 'barbeiro' that proliferated

in the mud walls of typical houses of the poor in rural areas. The 'triple discovery' (vector, pathogen and human disease) was communicated by Oswaldo Cruz to the prestigious Academia Nacional de Medicina on April 22th (*Kropf et al., 2009*).

Chagas disease was originally confined to poor, rural areas of South and Central America, in which vector-borne transmission to man occurs. In the past 20 years, improved vector control programmes (such as the Southern Cone Initiative to Control/Eliminate Chagas Disease, Andean Pact Initiative to Control/Eliminate Chagas Disease, and Central America Initiative to Control/Eliminate Chagas Disease), and compulsory blood-bank screening have substantially reduced new cases of infection and decreased the burden of Chagas disease in Latin America (*Moncayo, 2003*).

In countrywide surveys done in the 1980s, 100 million people (ie, 25% of all inhabitants of Latin America) were estimated to be at risk of infection, and 17.4 million were infected in 18 endemic countries in 1980–85 (*WHO, 2002*) (**Table 1**). According to estimates by the Pan American Health Organization, 20% of Latin America's population were at risk (109 million individuals) and nearly 7.7 million individuals were infected in 2005 (*PAHO, 2006; Aguilar et al., 1999*). According to the report of WHO in 2012: since 1990, regional control initiatives have substantially reduced the number of new infections in Latin America (*Mott et al., 1990*). Transmission of *T. cruzi* by the main domestic vectors was certified as interrupted in Uruguay in 1997, Chile in 1999, Brazil in 2006 and much of Central America (Guatemala, Honduras, El Salvador, Nicaragua) in 2009 - 2010. The number of transfusion-related infections has also decreased substantially in all Latin American countries since blood bank screening was made compulsory (*Schmunis, 1991*). Therefore, the burden of Chagas disease in Latin America has decreased over recent years. Estimates of the number of infected people were revised to 9.8 million in 2001. The number of new cases of Chagas disease has

also decreased substantially (from 700,000 per year in 1990 to 41,200 per year in 2006), and whereas in the 1980s an estimated 5 million people in the Americas had clinical symptoms of Chagas disease, this was revised to 1.2 to 2.8 million in the 1990s (*WHO, 1991*). The estimated number of deaths from Chagas disease has decreased from about 50,000 per year to 12,500 per year (*WHO, 2002; Moncayo et al., 2009*); and the estimated burden of disease in terms of disability-adjusted life years (DALYs) declined from 2.7 million in 1990 to 586,000 in 2001 (*Mathers et al., 2003*). Estimations of aggregate treatment costs for Chagas disease in several Latin American countries in the 1990s are available. Still however, the millions of chronically infected persons who are at risk for developing cardiovascular and/or digestive pathology and the high number of cases, make Chagas disease one of the leading causes of cardiovascular morbidity and premature death in Latin America (*Schofield et al., 1991; Schenone, 1998; Salvatella et al., 1996; Jamison, 2006*).

In spite of the mechanism of control in Latin America, the recent influx of immigrants from countries endemic for disease has meant that Chagas disease is becoming an important health issue in the USA and Canada and in many parts of Europe and the western Pacific, where an increasing number of infected individuals has been identified (*Schmunis, 2007; Bern et al., 2009; Gascon et al., 2009; Guerri-Guttenberg et al., 2008*) (**Figure 1**).

Table 1. Prevalence of *Trypanosoma cruzi* infection in Latin American countries in 1980-85 and 2005, and effect of initiatives to control or eliminate Chagas disease. Taken from *Rassi et al., 2010*

	1980-85		2005	
	Infected individuals	Individuals at risk of infection	Infected individuals	Individuals at risk of infection
Southern Cone Initiative (launched in 1991)				
Argentina	2 640 000 (10.0%)	23%	1 600 000 (4.1%)	19%
Bolivia	1 300 000 (24.0%)	32%	620 000 (6.8%)	35%
Brazil	6 180 000 (4.2%)	32%	1 900 000 (1.0%)	12%
Chile	1 460 000 (16.9%)	63%	160 200 (1.0%)	5%
Paraguay	397 000 (21.4%)	31%	150 000 (2.5%)	58%
Uruguay	37 000 (3.4%)	33%	21 700 (0.7%)	19%
Andean Pact Initiative (launched in 1997)				
Colombia	900 000 (30.0%)	11%	436 000 (1.0%)	11%
Ecuador	30 000 (10.7%)*	41%	230 000 (1.7%)	47%
Peru	621 000 (9.8%)	39%	192 000 (0.7%)	12%
Venezuela	1 200 000 (3.0%)	72%	310 000 (1.2%)	18%
Central America Initiative (launched in 1997)				
Belize	2 000 (0.7%)	50%
Costa Rica	130 000 (11.7%)	45%	23 000 (0.5%)	23%
El Salvador	900 000 (20.0%)	45%	232 000 (3.4%)	39%
Guatemala	1 100 000 (16.6%)	54%	250 000 (2.0%)	17%
Honduras	300 000 (15.2%)	47%	220 000 (3.1%)	49%
Nicaragua	58 600 (1.1%)	25%
Panama	200 000 (17.7%)	47%	21 000 (0.01%)	31%
Mexico	1 100 000 (1.0%)	28%
Total	17 395 000 (4.3%)	25%	7 694 500 (1.4%)†	20%

..= data not available. *Prevalence of infected individuals was underestimated.³³ †Includes about 150 000 infected individuals living in the USA and 18 000 in the Guianas, but data for these regions are not shown in the table.

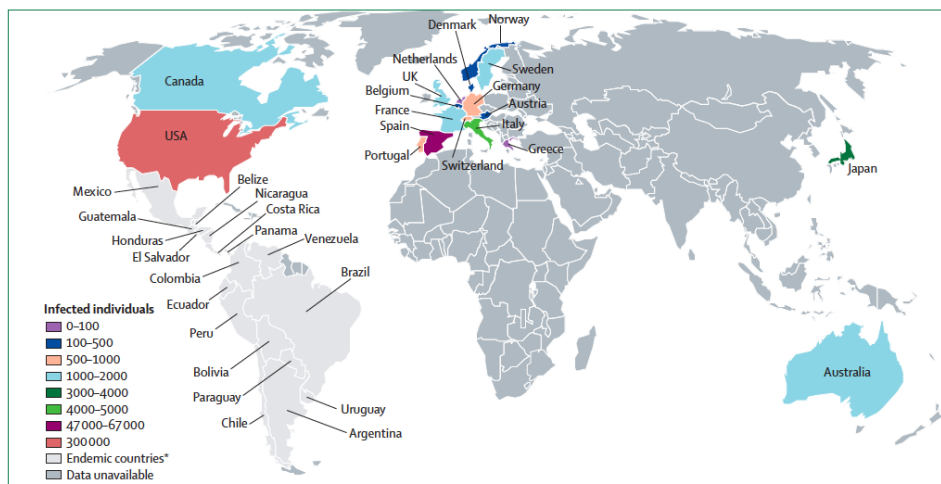


Figure 1 Estimated number of immigrants with *Trypanosoma cruzi* infection living in non-endemic countries. Taken from *Rassi et al., 2010*

The most common destination for migrants from Latin America is the USA, where an estimated 300,167 individuals (mainly from Mexico) are infected with *T cruzi*.

Spain has the second highest number of infected immigrants, an estimated 47,738 - 67,423, with most originating from Ecuador, Argentina, Bolivia, and Peru (*Bern et al., 2009*).

4.2.1. *Trypanosoma cruzi*: morphology and life cycle.

T. cruzi has the classical features of a eukaryotic cell: membrane bound nucleus, plasma membrane, Golgi apparatus and endoplasmic reticulum. However, in common with other members of the Kinetoplastida, *T. cruzi* has several peculiar features, such as a single mitochondrion, the DNA of which lies within a single unit, suborganellar structure - the kinetoplast. The kinetoplast DNA is a linked (catenated) network of hundreds of circular molecules, the minicircles which encode guide RNAs and maxicircles are similar to the mitochondrial DNA in higher eukaryotes, and they encode the rRNA and the subunits of the respiratory complexes (*Tyler et al., 2003*).

T. cruzi also compartmentalizes glycolysis in membrane bound vesicles called glycosomes, stores minerals in dense and acidic structures known as acidocalcisomes and big compartments with similar function to that mammalian lysosomes, named reservosomes (*Tyler et al., 2003*).

The cytoskeleton of *T. cruzi* is unusual, in that it is predominantly microtubular with no evidence of microfilament or intermediate filament systems. However, biochemical and molecular analyses have shown the presence of actin, myosin, and other actin-related proteins (actin-depolymerizing factor (ADF)/cofilin) located in rounded and punctuated structures throughout the cytoplasm and along the flagellum (*Melo et al., 2008; Cevallos et al., 2011*). *T. cruzi* does not possess centrioles. The replicative stages undergo a “closed” mitosis, with a microtubule spindle arising from poorly defined structures in the nuclear membrane. The trypanosome's distinctive

[INTRODUCTION]

morphologies are dictated by a “pellicular” corset of microtubules, which closely apposes the plasma membrane. *T. cruzi* possesses a single flagellum subtended by a basal body and probasal body which lie within the cell. The basal body is the trypanosome's only defined microtubule organizing centre. The flagellum varies in length during the life cycle from over 20 μm to less than 2 μm . The flagellar motor is a ciliary axonemal complex, with the typical 9 + 2 configuration of parallel microtubules. Once the axoneme exits the cell body, it is appended to an unusual semi-crystalline structure called the paraflagellar rod. It is believed that this structure provides support to the flagellar axoneme, increasing its rigidity and playing an essential role in motility. The exterior flagellum is surrounded by a specialized membrane, which is rich in sterols and sphingolipids, which contains proteins that do not diffuse into other domains of the surface membrane. Where the flagellum enters the cell there is a gap in the subpellicular corset, the junction between the pellicular plasma membrane and flagellar membrane at this point takes the form of an invagination known as the flagellar pocket. The majority of vesicular trafficking and nutrient uptake is believed to occur in this area and many receptors localize specifically to this region. A second, smaller invagination proximal to the flagellar pocket, the cytostome, has also been implicated in nutrient uptake. Also associated with the flagellar pocket, it is a contractile vacuole involved with the osmoregulation and with the phosphate metabolism (Tyler *et al.*, 2003).

T. cruzi has a complex life cycle involving both vertebrate and invertebrate hosts in three well-defined developmental stages (**Figure 2**): (A) amastigotes, which are the proliferative forms found inside the vertebrate host cells; (B) epimastigotes, which are the proliferative forms found in the intestine of the invertebrate host; and (C) trypomastigotes, which are highly infective and originate from the amastigotes at the end of the intracellular cycle following their release into the intercellular space and into

bloodstream. Trypomastigotes also arise from epimastigotes in the posterior regions of the digestive tract of the invertebrate host (*Teixeira et al., 2012*).

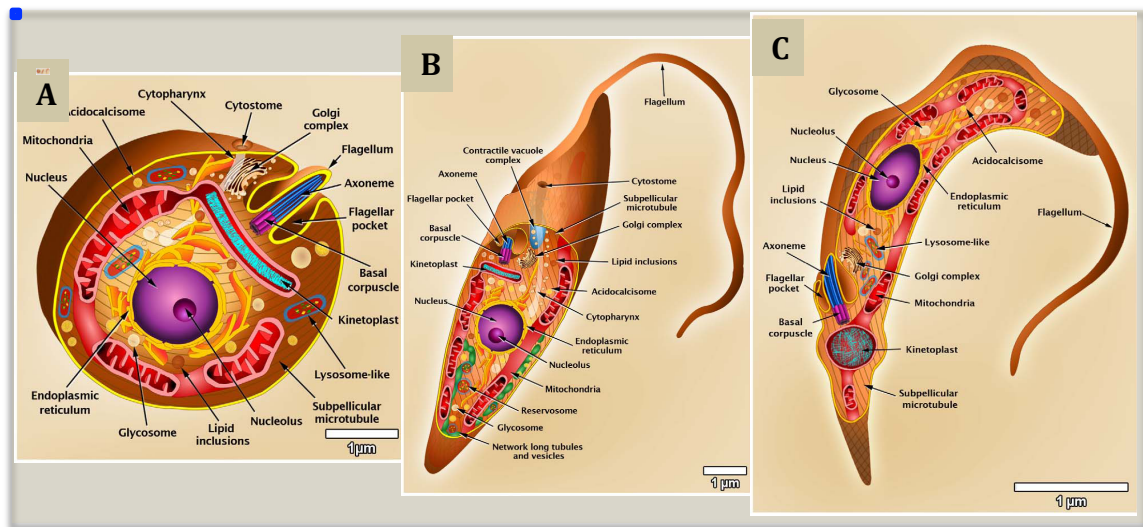


Figure 2. Schematic representations of *T. cruzi*: amastigote organelles (A), epimastigote organelles (B) and trypomastigote organelles (C). These images were made based on micrographs of light microscopy as well as scanning and transmission electron microscopy. Taken from *Teixeira et al., 2012*

In spite of the three previous form presented are the more common described for

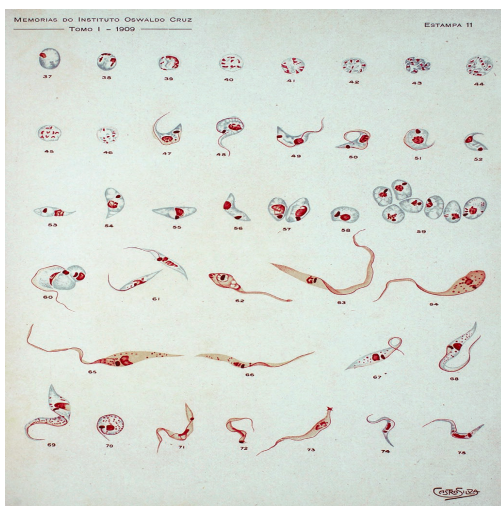


Figure 3. Reproduction of the original drawings of the first description of *Trypanosoma cruzi* by Carlos Chagas in 1909 where developmental stages found in both the invertebrate and invertebrate hosts were seen. Taken from *de Souza, 2009*

the parasite, there are a bunch of intermediate forms that can be found in the mammalian and invertebrate hosts, they also can be easily found in the axenic cultures. Since its initial description in 1909, the morphology of the various developmental stages of *T. cruzi* has been the subject of intense investigation (Chagas 1909). A colour drawing found in the original paper describing *T. cruzi* points to variations in the general shape of the protozoan and the presence of several

structures that can be stained with Giemsa (*de Souza, 2009*).

The infection of a mammalian host begins with the metacyclic trypomastigotes present in the excreta of the blood-feeding reduviid bug vector (**Figure 4**). These are introduced into the host by contamination of the insect bite wound or a variety of mucosal membranes. The non-dividing metacyclic form is able to invade a wide range of phagocytic and nonphagocytic nucleated cells, initially entering a membrane bound (parasitophorous) vacuole. Upon entry, the parasite begins to differentiate to the amastigote form and escapes the vacuole into the cell cytoplasm where the dramatic morphologic transformation, including flagellar involution, is completed. The amastigote re-enters the cell cycle and proliferates until the cell fills with these forms. At this point the amastigotes elongate, reacquiring their long flagella, differentiating to the slender trypomastigote forms via an intracellular epimastigote intermediate. Slender trypomastigotes escaping the cell can invade adjacent cells; alternatively, they can enter the blood and lymph and disseminate, in which case they may begin to differentiate extracellularly. Extracellular differentiation gives rise to the broad trypomastigotes and extracellular amastigotes. A mixture of these three forms may be present in the blood of infected individuals and can be taken up in the blood meal of a reduviid bug. In the bug midgut, remaining trypomastigotes differentiate into amastigotes. As a population, amastigotes first extend their flagella to become spheromastigotes, which then lengthen to become (midlog) epimastigotes. These epimastigotes continue to elongate as nutrients from the blood meal are exhausted. Finally, after migration to the bug's hindgut, the elongate (late-log) epimastigotes attach to the waxy gut cuticle by their flagella and differentiate into infectious metacyclic trypomastigotes, completing the life cycle (Tyler *et al.*, 2003).

The insect vector seems to be unaffected by infection with the parasite. Non-replicative bloodstream trypomastigotes and replicative intracellular amastigotes are the

typical forms of the organism that are identified in mammalian hosts, whereas replicative epimastigotes and infective metacyclic trypomastigotes infect the triatomine vector (**Figure 4**). During the acute stage, all types of nucleated cells in the human host are potential targets for infection. With development of the immune response, parasitaemia reduces to a sub-patent concentration and the number of parasites in the tissues declines substantially, signalling the end of the acute phase. However, since the parasite is not completely eliminated, infection of specific tissues, such as muscle or enteric ganglia, persists indefinitely for the life of the host (*Rassi et al., 2010*).

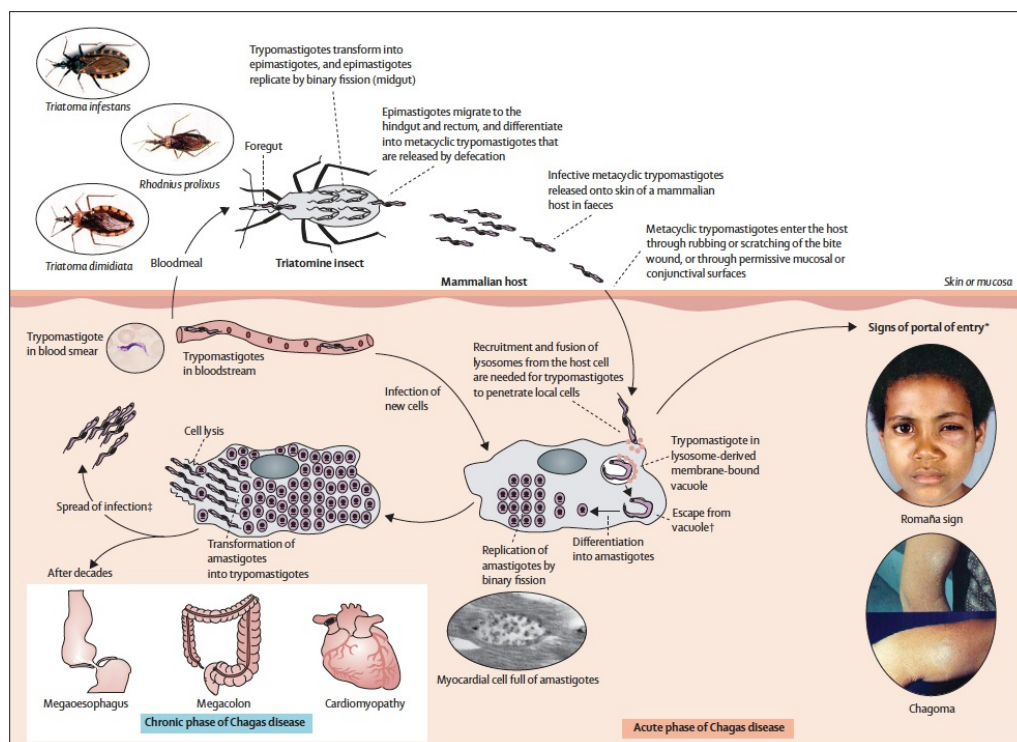


Figure 4. Vector-borne transmission and life cycle of *Trypanosoma cruzi*. Taken from *Rassi et al., 2010*.

4.2.2. Genetic diversity of *T cruzi*

T. cruzi belongs to a heterogeneous species consisting of a pool of strains, stocks, or isolates that circulate among mammalian hosts and insect vectors. The heterogeneity of the parasite has been extensively studied by biological, biochemical, and molecular

methods, and could explain the varying clinical manifestations of Chagas disease and the geographical differences in morbidity and mortality (*Macedo et al., 2004; Manoel-Caetano et al., 2007*). A wide range of genetic markers has been applied to analyse the genetic diversity of the parasite. In 2009, an expert committee reviewed the available knowledge and partitioned *T. cruzi* isolates into six subgroups or discrete typing units (DTUs) (*T. cruzi* I-VI) (*Zingales et al., 2009*). A comprehensive review of phylogeographical and eco-epidemiological features, and the correlation of DTU with natural and experimental infection, has been published (*Zingales et al., 2012*). In the Southern Cone region, TcII, TcV and TcVI are the main causes of Chagas disease. TcII predominates in eastern and central Brazil, TcV in Argentina, Bolivia, and Paraguay, and TcVI in the Gran Chaco. In the Southern Cone region, chagasic cardiomyopathy can be severe, and a proportion of cases may develop megaesophagus and megacolon. TcI is implicated with human disease in Amazonia, the Andean countries, Central America, and Mexico, and clinical presentations include chagasic cardiomyopathy. In these regions chagasic megaesophagus and megacolon are absent or very rare (*Zingales et al., 2012; Miles et al., 2009*). Methods for DTU genotyping are available for widespread use in endemic areas (*Zingales et al., 2012; Lewis et al., 2009*). **Figure 5** depicts the geographical distribution of *T. cruzi* DTUs in human infections and in the triatomine vector species of major epidemiological importance. The role of vector species as biological filters for DTU transmission has not been defined (*WHO, 2012*). Completion of the genome sequence of the *T. cruzi* CL Brener strain (a member of DTU VI) opens prospects for the development of novel therapeutic and diagnostic techniques, and could increase our understanding of the mechanisms of disease (*el Sayed et al., 2005*).

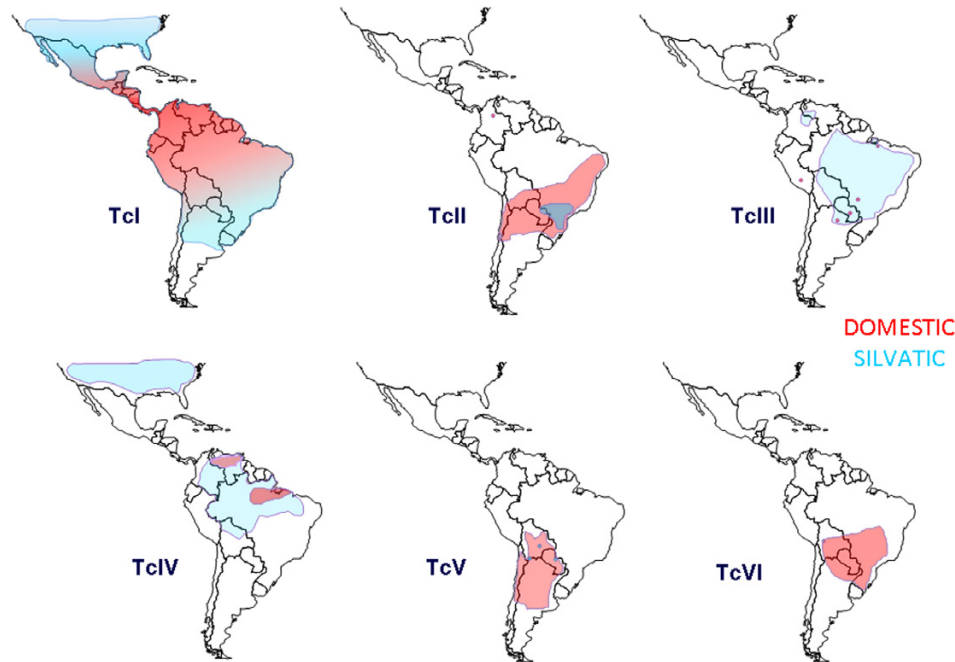


Figure 5. Geographical distribution of *T. cruzi* discrete typing units in human patients. Taken from Zingales *et al.*, 2012.

4.2.3. Metabolism

Studies on energy metabolism deal with the ways organisms produce ATP for their functioning and proliferation. Three different classes of substrates can, in principle, be used for the production of ATP: carbohydrates, fatty acids and amino acids. All eukaryotes, including trypanosomatids, can use carbohydrates if these are available. Many trypanosomatids live in carbohydrate-rich environments during their stay inside their non-insect host, vertebrates, or plants (Tielens *et al.*, 2009). So most, if not all, trypanosomatids depend on the available carbon sources present in their hosts for their energy metabolism. First, the trypomastigote forms *T. cruzi* use glucose, which is abundant in the fluids of its vertebrate host(s) (Cannata *et al.*, 1984; Fairlamb *et al.*, 1986). Second, hematophage insect vectors obtain their energy from L-proline and/or L-glutamine, the prominent constituent of their hemolymph and tissue fluids (Bursell, 1981). Consequently, the insect stages of trypanosomatids rely on amino acid catabolism, with a preference for L-proline. It is noteworthy that *T. cruzi* has the

[INTRODUCTION]

capacity to utilize D-proline, in addition to L-proline (expression of a proline racemase), and L-histidine (*Chamond et al., 2003*). Third and last, the carbon sources used by intracellular stages depend on the specific host compartment in which they live: *T. cruzi* amastigotes reside in the cytoplasm of the host cells with ready access to sugar phosphates and develop a glucose-based metabolism (*Cannata et al., 1984*). All trypanosomatid adaptive forms (exception *Leishmania*) prefer glucose when grown in rich medium, including those in which glucose is not the natural carbon source (**Table 2**). Since glucose-rich media are routinely used to grow these parasites, glucose metabolism has received most attention and relatively little is known about their aminoacid and fatty-acid metabolism, which are not known to be an important substrate used in the energy metabolism of trypanosomatids (*Bringaud et al., 2006*). Exceptions are probably the amastigotes of *Leishmania* and *T. cruzi*.

Table 2. End products of the metabolism of carbon sources by trypanosomatids cultured in glucose-rich media. Taken from *Bringaud et al. 2006*

Stage	Host	Carbon Source	Excreted end products in glucose-rich conditions.
Trypomastigote	Vertebrate	Glucose	CO ₂ , Suc, Ace
Amastigote	Vertebrate	Glucose	CO ₂ , Ace, Gly, Pyr, Suc
Epimastigote	Insect	Glucose	CO ₂ , Suc, L-Ala, Ace

4.3. Clinical forms and pathogenesis

The disease has the following three characteristic clinical phases: the acute phase, where around 5% of children die but can spontaneously resolve itself in 4–6 weeks; asymptomatic or indeterminate phase, where the patients do not present any clinical symptoms of the disease, but they can transmit the parasite to other humans; and the chronic symptomatic phase occurring in 10–30 % of the infected patients, where the

heart or the gastrointestinal tracts are affected (*Rodrigues et al, 2014*). Note that Chagas disease is one of the most important causes of cardiomyopathy worldwide. The acute phase of Chagas disease is recognized only in 1%–2% of infected individuals. This phase is usually asymptomatic or might present as a self-limiting febrile illness. Nevertheless, symptoms can develop at around 8–10 days after infection by vector-borne transmission; in the case of symptom development, an edema known as “chagoma” or Romaña signal appears in the palpebral and periocular regions, or up to a few months after transfusion of infected blood. (*Rodrigues et al, 2014*). This acute phase decline spontaneously after 4–8 weeks; treatment with an antiparasitic drug, such as benznidazole, will usually cure acute infection and prevent chronic manifestations. Death occurs occasionally in the acute phase (<5–10% of symptomatic cases) as a result of severe myocarditis or meningoencephalitis, or both. Manifestations of the acute disease resolve spontaneously in about 90% of infected individuals even if the infection is not treated with trypanocidal drugs (*Rassi et al., 2010*).

The chronic stage begins 2–3 months after initial infection and after resolution of the acute disease. In this phase, about 60–70% of these patients will never develop clinically apparent disease. These patients have the indeterminate form of chronic Chagas disease, which is characterised by positivity for antibodies against *T cruzi* in serum, a normal 12-lead electrocardiogram (ECG), and normal radiological examination of the chest, oesophagus, and colon. Circumscribed or necrotizing inflammatory injuries may also occur in the grey matter in the central nervous system (CNS). In addition, each year, 2%–3% of asymptomatic individuals evolve to the abovementioned symptomatic manifestations; the determinants of this conversion are unknown. The outcome of the infection in a particular individual is the result of a set of complex interactions between the genetic make-up of the parasite, the host immunogenetic background, and

[INTRODUCTION]

environmental factors. The remaining 30–40% of patients will subsequently develop a determinate form of chronic disease, ie, cardiac, digestive (megaesophagus and mega colon), or cardiodigestive, usually 10–30 years after the initial infection. A direct



Figure 6. Advanced cardiac disease. Taken from [Rassi et al., 2010](#).

progression from the acute phase to a clinical form of Chagas disease has been recorded in a few patients (5–10%) ([Rassi et al., 2010](#); [WHO, 2012](#)).

Chagas heart disease (CDC) is the most serious and frequent manifestation of chronic Chagas disease; it is the leading cause of abnormalities of the conduction system,

bradyarrhythmias and tachyarrhythmias, apical aneurysms, cardiac failure, thromboembolism, and sudden death. Episodes of non-sustained ventricular tachycardia are seen in about 40% of patients with mild wall motion abnormalities, and in virtually all patients with heart failure, which is more frequent than in other cardiomyopathies. For hence, heart failure is often a late manifestation of CDC. It is usually biventricular with a predominance of right-sided failure

(peripheral oedema, hepatomegaly, and ascites more prominent than pulmonary congestion) at advanced stages. Heart failure of chagasic aetiology is associated



Figure 7. Megaesophagus (groups I, II, III and IV). Taken from [Rassi Jr A. et al. 2010](#).

with higher mortality than is heart failure from other causes. Systemic and pulmonary embolisms arising from mural thrombi in the cardiac chambers are quite frequent. Clinically, brain is by far the most frequently recognised site of embolisms (followed by limbs and lungs), but at necropsy embolisms are found more frequently in the lungs,

kidneys, and spleen. Chagas disease is an independent risk factor for stroke in endemic countries. Sudden death is the main cause of death in patients with CDC, accounting for nearly two thirds of all deaths, followed by refractory heart failure (25–30%), and thromboembolism (10–15%). Sudden cardiac death can occur even in patients who were previously asymptomatic (*Rassi et al., 2010; WHO, 2012*).

The gastrointestinal manifestations are a progressive enlargement of the oesophagus or the colon and other parts of the intestine, caused by chronic inflammation and destruction of parasympathetic neurons. It develops in about 10–15% of chronically infected patients. The main gastro-intestinal symptoms are dysphagia and severe constipation. Oesophageal (mega oesophagus) disease can appear in infections in children and causes dysphagia with odynophagia, combined with epigastric pain, regurgitation, ptyalism, and malnutrition in severe cases.

Colonic disease evolves more slowly; megacolon often affects the sigmoid segment, rectum, or descending colon, or a combination, and produces prolonged obstipation, abdominal distension, and occasionally large bowel obstruction due to fecaloma or sigmoid volvulus.



Figure 8. Megacolon. Taken from *Rassi Jr A. et al. 2010.*

Although its clinical significance is not very clear, damage to the nervous system and striated muscle is manifested in the chronic stage as motor cell loss or degeneration in various muscles, with infiltration and demyelination areas in the nerves. Patients with mega oesophagus have an increased prevalence of cancer of the oesophagus. Conversely, an increased frequency of colorectal cancer has not been reported in patients with chagasic megacolon. Geographical differences in prevalence of the digestive form of Chagas disease have been reported, so, digestive form is seen almost exclusively south of the Amazon basin (mainly in Argentina, Brazil, Chile, and Bolivia),

and is rare in northern South America, Central America, and Mexico. This geographical distribution is probably due to differences in parasite strains (*Rassi et al., 2010; WHO, 2012*).

Congenital Chagas disease: T. cruzi can be transmitted from an infected mother to her child during pregnancy. Congenital transmission of Chagas disease in humans occurs less frequently than vector-borne and transfusion transmission. The incidence is estimated at more than 15,000 cases annually in the Americas. However, there is considerable uncertainty about congenital transmission rates since it receives no particular attention in endemic countries and perhaps even less in non-endemic countries where transmission does occur. The risk factors that determine the transmission of the parasite to the foetus are unknown. However, it is well established that treatment during the first year of a child's life is close to 100% effective in parasite elimination (*Rassi et al., 2010; WHO, 2012*).

Immunosuppressant therapies and HIV/AIDS: can bring about acute clinical manifestations, which lead to an increased risk of disease reactivation in patients with chronic *T. cruzi* infection. This suggests the need for routine assessment for the presence of *T. cruzi* infection in patients whose immune response is suppressed. Whenever a case is detected, it is necessary to monitor reactivation with tools offering fast and simple diagnosis, and prescribe specific treatment as early as possible. Although the effectiveness of etiological treatment for the control of reactivation episodes has been demonstrated, it is necessary to gather evidence as to whether preventive treatment is effective in patients with no signs of clinical reactivation who have altered immunological parameters. Some protocols also recommend treating organ

donors infected with *T. cruzi* to reduce the risk of transmission by transplantation (*Rassi et al., 2010; WHO, 2012*).

In conclusion, the association of heart disease with megaesophagus or megacolon, or both defines the cardiodigestive form of Chagas disease. In most countries the development of megaesophagus usually precedes heart and colon disease, but the exact prevalence of the cardiodigestive form is not known because of the scarcity of appropriate studies. Individuals with AIDS or receiving immunosuppressive treatment might experience an exacerbation of chronic infection, leading to increases in parasitaemia and intracellular parasite replication. Fever, myocarditis, panniculitis, and skin lesions are common in recipients of solid organ or bone marrow transplants, whereas in patients with AIDS the most common manifestations are meningoencephalitis and CNS lesions that resemble the lesions of cerebral toxoplasmosis (*Rassi et al., 2010; WHO, 2012*).

4.4. Diagnosis

The primary methods for diagnosing Chagas disease are serological, and the secondary tests are parasitological (*WHO, 2002*). Most Chagas cases are currently diagnosed during the chronic phase of the disease. Diagnostic tests for *T. cruzi* infection are used during epidemiological surveys, surveillance for vectorial transmission, blood screening, screening of pregnant women, and in individual patients, but the tests need to be improved (*WHO, 2012*).

Diagnosis of acute infection is based on the microscopic detection of trypomastigotes in blood (*Rassi et al., 2010*). During the chronic phase, because parasitaemia is scarce, the presence of Ig G antibodies against *T. cruzi* antigens needs to be detected by at least two different serological methods ((indirect haemagglutination

[INTRODUCTION]

(IHA), indirect immunofluorescence (IIF), and enzyme-linked immunosorbent assay (ELISA)) to confirm diagnosis (*WHO, 2012*). PCR is not helpful in routine diagnosis because of the need for specific laboratory facilities, poor standardisation, potential DNA cross-contamination, and variable results across laboratories and countries. However, because of its heightened sensitivity compared with other parasitological methods, PCR could be useful to confirm diagnosis in cases of inconclusive serology, and as an auxiliary method to monitor treatment. PCR is useful to identify treatment failure from positive detection of *T. cruzi* DNA, but not treatment success since even repeated negative PCR results do not necessarily indicate parasitological cure. At best, such results are indicative of the absence of parasite DNA at the time of the test (*Rassi et al., 2010; WHO, 2012*).

Parasitological diagnosis: Although parasitaemia is generally present in the acute phase, the initial infection is seldom detected except in cases where acute symptoms are severe. In such cases, microscopic observation of fresh blood or stained blood smears can reveal parasites (*WHO, 2002*).

Serology: three types of conventional test based on detection of parasite-specific antibodies are widely used for immunodiagnosis: IHA, IIF, and ELISA. The commercially available diagnostic tests employ crude antigenic *T. cruzi* preparations, semi-purified fractions, or recombinant antigens. Most of the tests have 94%–99.5% sensitivity and 94%–96% specificity (**Table 3**) (*WHO, 2012*). Rapid chromatography tests with a mixture of recombinant antigens for screening for anti-*T. cruzi* antibodies in whole blood and serum, and in umbilical cord blood of infected mothers at the time of delivery, have been assessed in Latin American countries and variable results were obtained (*Umezawa et al., 1999; Luquetti et al., 2003; Yun et al., 2009*).

Quantitative and qualitative detection of parasite DNA: Detection of parasite DNA by polymerase chain reaction (PCR) during the chronic phase of *T. cruzi* infection is less sensitive than serological tests (Britto, 2009). Recently an accurate real-time PCR strategy for monitoring clinical reactivation and etiological treatment outcome in Chagas disease patients has been proposed (Duffy *et al.*, 2009). In addition, a multicentric study to standardize PCR methods for detection of *T. cruzi* DNA in blood samples from Chagas disease patients was carried out under the coordination of the Special Programme for Research and Training in Tropical Diseases (TDR-WHO) (Schijman *et al.*, 2011). Four methods depicted the best performing parameters and await validation through prospective studies in different settings.

Table 3. Summary of characteristics of available diagnostics. ELISA, enzyme-linked immunosorbent assay; IHA, indirect haemagglutination; IIF, indirect immunofluorescence; PCR, polymerase chain reaction; RT-PCR, reverse transcriptase polymerase chain reaction. Taken from WHO, 2012

Parasite demonstration	Source	Blood
	Sensitivity	>70% when smear performed 15-30 days after onset of symptoms (only in the acute phase)
	Specificity	100%
Parasite DNA detection	Test	PCR, RT-PCR
	Sensitivity	≈ 60%(in children)
	Specificity	If properly done, can be 100%
Serology	Test	IHA, IIF, ELISA (chronic phase)
	Sensitivity	94%-99.5% (kit-dependent difference)
	Specificity	94%-96% (kit-dependent difference)

Diagnosis in newborns: direct examination for blood parasites using the microhaematocrit concentration method (MH) in capillary tubes is recommended as a first procedure for diagnosis of congenital *T. cruzi* transmission, because of its

[INTRODUCTION]

heightened sensitivity and the small amount of blood needed (*WHO, 2012*). Microscopic examination of cord blood or peripheral blood of the neonate by this technique is strongly recommended during the first month of life (*Freilij et al., 1995*). If the results are repeatedly negative or if the test is not done early in life, the infant should be tested for anti-*T. cruzi* Ig G antibodies at 6–9 months of age (preferentially at 9 months) when maternal antibodies are no longer present in the baby (*Gomes et al. 2009*). In specialised centres, assays based on amplification of *T. cruzi* DNA by PCR could also be used for early diagnosis of congenital infection, since in this context the sensitivity of PCR seems to be greater than that of microscopic examination (*Mora et al., 2005*).

Diagnosis of therapy efficacy and cure: currently successful cure of Chagas disease is assessed by the disappearance of anti-*T. cruzi* antibodies (seroconversion), employing the above-mentioned serological tests, while therapeutic failure is assigned by parasite persistence. However, serological markers may take up to 5 years to disappear. Accordingly, positive serology does not mean active infection, whereas negative serology indicates cure. Parasitological tests have limited sensitivity (xenodiagnosis, 30%–50%; PCR, 60%–90%); consequently a positive parasitological test means treatment failure, whereas a negative result does not indicate absence of parasites. Thus, a diagnostic technique for parasitological cure is urgently needed and necessary for the evaluation of new approaches to Chagas disease treatment. It is anticipated that the assessment of parasitological cure in patients with chronic disease, in whom parasitaemia is extremely low or undetectable, will be very challenging (*WHO, 2012*).

Diagnosis of drug resistant Chagas disease: therapeutic failures of benznidazole and nifurtimox (see section 1.5) are documented in Chagas disease. Therapeutic success

seems to depend on the interplay among drug susceptibility of *T. cruzi* strains, drug access and accumulation in different environments, and the host immune response. A test for screening of drug resistance of the infective strain is not available (*WHO, 2012*).

4.5. Current treatments & new compounds under study

According to recommendations in 2007 anti-trypanosomal treatment is strongly recommended for all cases of acute, congenital, and reactivated infection, for all children with infection, and for patients up to 18 years of age with chronic disease. Drug treatment should generally be offered to adults aged 19–50 years without advanced Chagas heart disease, and is optional for those older than 50 years because benefit has not been proven in this population (*Bern et al., 2007*). By contrast, anti-trypanosomal treatment is contraindicated during pregnancy and in patients with severe renal or hepatic insufficiency, and generally should not be offered to patients with advanced Chagas heart disease or megaesophagus with substantial impairment of swallowing (*Rassi et al., 2010*).

The goal of a specific treatment against *T. cruzi* infection is to eliminate the parasite from the infected individual and, accordingly, to decrease the probability of developing symptomatic Chagas disease, and hinder parasite transmission. The two registered drugs for Chagas disease treatment were introduced in the 1960's (nifurtimox, Bayer) and 1970's (benznidazole, Roche). Various clinical studies have shown that both drugs are effective in newborns (up to 99% cure) and in the acute phase (up to 80% cure, defined as seroconversion and negative parasitaemia) (*Sosa-Estani et al., 2006; Fabbro et al., 2007; WHO, 2012*). Benznidazole and nifurtimox are the only drugs with proven efficacy against Chagas disease. Benznidazole has the best safety and efficacy profile, and therefore is usually used for first-line treatment (*Viotti et al., 2009*). Children should

be treated with benznidazole (5–10 mg/kg daily) in two or three divided doses for 60 days, or with nifurtimox (15 mg/kg daily) in three divided doses for 60–90 days, preferably after meals for both drugs. For adults, daily treatment with 5 mg/kg benznidazole or 8–10 mg/kg nifurtimox is recommended for the same duration as for children (*Ministério da Saúde, 2005*). Nifurtimox and benznidazole require prolonged treatment (60 days) and have frequent side effects that can lead to discontinuation of treatment. Available data indicate that success in treatment reflects: the phase of infection in which treatment is administered, the age of the patient at the time he/she receives the treatment, and the region where the patient was infected (*WHO, 2012*). In fact, there are regional differences in the decline of antibody levels in treated patients, with reductions apparently occurring more rapidly in the northern region of South America and Central America than in the Southern Cone of South America or in the USA (*Yun et al., 2009*), probably due to differences in drug susceptibility among *T. cruzi* strains (*Filardi et al., 1987*). There are many basic limitations in the management of infected patients, including: low drug coverage of those already infected; limitations in demonstrating the efficacy of drugs in adult chronic patients, which is when first contact is made with most infected patients; lack of a proper diagnostic test for infants born to infected mothers; lack of a diagnostic test for treatment follow-up and cure.

New, effective, safe and affordable drugs, preferably oral, are needed for this trypanosomiasis. The drugs in current use for treatment of this disease have well known problems of toxicity, efficacy, administration or length of treatment (*Castro et al., 2006*). The side effects of these drugs, including allergic dermatitis, pruritus, fever, and gastrointestinal intolerance among others, are well documented and have limited their broader use, particularly in adult populations (*Castro et al., 2006; Viotti et al., 2009*).

Indeed, more than one new drug is needed so that combination therapy can be employed to avoid drug resistance and to provide back-up drugs when resistance emerges (*Nozaki et al., 1996; Murta et al., 1998; Nogueira et al., 2006; Wilkinson, 2008*). There are few new drugs or treatments in clinical trials. Research consortia have organized to provide the multidisciplinary requirements needed for drug development. However, resources are needed to enable the coordination of these researchers' activities and to incorporate the expertise of the for-profit drug development enterprises. Such activities have the ability to lead to the needed drugs. Overall, the priorities in Chagas disease research should be to produce new drugs that provide a shorter treatment course with fewer side effects, and to devise paediatric formulations.

Ten years ago, efforts to deliver new drug candidates for Chagas disease were very limited (*Clayton, 2010*), and the number of researchers involved in drug discovery, were few. Indeed, at the time, the activities ongoing worldwide were generally with low critical mass and working on only a few compounds. Moreover, the quality of the compounds that were available and assessed was clearly poor and very often associated with potential or demonstrated toxicity or druggability issues: these include naphthoquinones, diamidines, nitroimidazoles and related compounds, and ruthenium complexes (*Soeiro et al., 2009; Soeiro et al., 2011; Silva et al, 2010; Demoro et al., 2013; Buckner et al., 2013*). Both target-based and phenotypic approaches for screening were used, with the former concentrating on putative targets and pathways of potential importance for *T. cruzi* such as cysteine protease, trypanothione reductase, and ergosterol synthesis. Among these, the most promising approaches are (*WHO, 2012*):

- a. Ergosterol biosynthesis inhibitors, such as posaconazole and ravuconazole:

Two proof-of-concept phase II clinical studies with posaconazole for the specific treatment of Chagas disease are currently under way:

- The first was launched in October 2010 at the Vall d'Hebron Hospital in Barcelona (Spain), and patients began to be recruited into the second trial, sponsored by Merck & Co., in July 2011 in Argentina.
- The Drugs for Neglected Diseases Initiative (DNDi) and Eisai Co. are partnering in a phase II trial of a pro-drug of ravuconazole (E1224), which began in Bolivia in July 2011.
- b. Inhibitors of cruzipain, the main cysteine protease of *T. cruzi*: the vinyl sulphone K777 inhibitor of cruzipain is in pre-clinical development.
- c. Bisphosphonates, that inhibits the parasite's farnesyl-pyrophosphate synthase.
- d. Inhibitors of trypanothione synthesis.
- e. The pharmacokinetics of a new paediatric formulation of benznidazole is under evaluation for elimination of infection in newborns, and in children with recent chronic infection.
- f. Combinations of existing and new drugs are recommended to avoid drug resistance.
- g. Associations of compounds with different mechanisms of action have been mentioned as another way to look for new treatment alternatives.

While treatment of patients is still far from ideal, it would be valuable if international consensus could be reached on: who should be treated with the available drugs, the drug regimen, and how patients can be provided with access to the drugs and

supportive treatment (*WHO, 2012*). The following table summarizes the acceptable and ideal criteria of a target product profile:

Table 4. Summary of characteristics of Chagas disease target product profile. Taken from Chatelain, 2015

	ACCEPTABLE	IDEAL
Target population	Chronic	Chronic and acute (reactivation)
Strains	TcI, TcII, TcV, and TcVIa	All ^a
Distribution	All areas	All areas
Adult/children	Adult	All
Clinical efficacy	Noninferior to benznidazole in all regions (parasitological)	Superiority to benznidazole in different phases of the disease—acute and chronic (parasitological)
Safety	Superiority to benznidazole ^b 3 CE plus 2 standard LE or ECG during treatment	Superiority to benznidazole or nifurtimox. No CE or LE or ECG needed during treatment
Activity against resistant strains	Not necessary	Active against nitrofurans- and nitroimidazole-resistant <i>T. cruzi</i> strains
Contraindications	Pregnancy/lactation	None
Precautions	No genotoxicity; no proarrhythmic potential	No genotoxicity; no teratogenicity; no negative inotropic effect; no proarrhythmic potential
Drug-drug interactions	No clinically significant interaction with antihypertensive, antiarrhythmic, anticoagulant drugs	None
Presentation	Oral	Oral
Stability	3 years, climatic zone IV	5 years, climatic zone IV
Dosing regimen	Comparable to systemic antifungal treatments	Once daily/30 days

^aClassification according to *Zingales et al. 2009*; requires further research for definition of target strains for evaluation. ^bCE, clinical evaluation; LE, laboratory evaluation; ECG, electrocardiogram.

4.6. Vaccines against *Trypanosoma cruzi*

A good understanding of the interactions between *T. cruzi* and the immune system is key to the rational design and improvement of vaccines, and important advances have been made in recent years (*Quijano-Hernandez et al., 2011*). However, it is important to recall that *T. cruzi* vaccine research has been hindered for decades, due to the idea of a vaccine for Chagas disease was not even contemplated for fear that enhancement of anti-*T. cruzi* immunity by vaccination would only exacerbate the immunopathology that appears to be responsible for clinical disease (*Tarleton, 2003*).

With the realization that tissue damage in Chagas disease is tightly linked to the tenacious persistence of *T. cruzi* in tissues rather than to an over-exuberant immune response to self-antigens, the prospects for potentially using vaccines in Chagas disease improved (Tarleton, 2007). This potential has been further buoyed by great strides in understanding the immune effector mechanisms responsible for control of infection, as well as discovery of the targets of some of these responses.

T. cruzi infection is a lifelong infection controlled by a battery of host immune responses. Life-threatening disease in the early stages of the infection is relatively rare, except in cases of high-dose infections, or in the immune-compromised patient. A more frequent, although not universal, complication is chronic phase disease that emerges many years after the initial infection (WHO, 2012). Vaccine development efforts have been targeted primarily on the prevention of infection and acute phase disease and to a lesser extent on the amelioration of disease.

Naturally induced immunity to *T. cruzi* generally limits parasite load to very low, almost undetectable, levels in the vast majority of individuals but rarely results in sterile (parasite-free) cure. Several *T. cruzi* antigens have been tested as prophylactic vaccines in experimental models, but none of them proved to induce the sterile immunity that fully protects animals from becoming infected when challenged with virulent parasite strains. Some vaccines resulted in a milder acute phase disease (Camargo, 2009). A very wide range of vaccine formulations has been evaluated over the years, ranging from whole parasites, to purified or recombinant proteins, viral vectors and DNA vaccines (Quijano-Hernandez et al., 2011) (Table 5).

Table 5 Preventive vaccines against *T. cruzi* evaluated in mice. Taken from [Quijano-Hernandez et al., 2011](#). NR, not reported.

FORMULATION	ANTIGENS	IMMUNE RESPONSE	PARASITEMIA	HEART PARASITE BURDEN	HEART HISTOPATHOLOGY	SURVIVAL
WHOLE ORGANISM	Live attenuated <i>T. cruzi</i>	NR	Decreased	Decreased	NR	NR
	Live attenuated <i>T. rangeli</i>	NR	Decreased	Decreased	No change	Increased
RECOMBINANT PROTEIN	rASP-2+Alum or CpG ODN	Increased IFN γ	Decreased	NR	NR	Increased
	rTS(trans-sialidase)+CpG ODN	IgA, IgG and IFN γ	NR	Decreased	NR	Increased
	rCruzipain + CpG ODN	Humoral and cellular response, IFN γ and lytic activity	Decreased	NR	Decreased inflammation	NR
	rGP82 + CpG ODN	IFN γ	NR	NR	NR	Variable according to challenge route
	Adenovirus or vaccinia expressing TSSA CD8+ epitope	IFN γ	Decreased	NR	NR	Increased
VIRAL VECTOR	Adenovirus expressing TS and ASP-2	Antibodies and cytolytic activity	Decreased	NR	NR	Increased
	Sendai virus expressing ASP-2	IFN γ and CD8+	Decreased	NR	NR	Increased
	TSA-1, ASP-1 and ASP-2 with IL-12 and GM-CSF	Antibodies and cytolytic activity	Decreased	NR	Decreased inflammation	Increased
DNA	ASP-2 or UB-ASP-2	IFN γ , CD8+, cytolytic activity	Decreased	NR	NR	Increased
	TS+IL15	IFN γ and CD8+	NR	NR	NR	Increased
	TSA-1 and Tc24	NR	Decreased	NR	Decreased inflammation	NR
	TcVac2 (TcG1, TcG2, TcG4) + IL-12 + GM-CSF DNA and recombinant protein boost + saponin DNA + adenovirus expressing TS and ASP-2 clone 9 (Prime-Boost)	Humoral and cellular response, IFN γ and CD8+	Decreased	Decreased	Increased	NR
HETEROLOGOUS PRIME-BOOST	ASP-2 or UB-ASP-2	IFN γ , CD8+, cytolytic activity	Decreased	NR	NR	Increased

[INTRODUCTION]

In summary, development of a prophylactic or therapeutic human vaccine for *T. cruzi* infection may be feasible but may not necessarily be testable or practical to implement. Before substantial efforts to develop such a vaccine are undertaken, serious examination needs to be made of the ethical and practical issues involved. Currently there is no vaccine available.



5. OBJECTIVES/OBJETIVOS

"When you want to start something, there will be many people who will tell you not to do it, when they see they can not stop you, they will tell you how you have to do it, and when they finally see that what you have achieved, they will say they always believed in you"

("Cuando quieras emprender algo, habrá mucha gente que te dirá que no lo hagas, cuando vean que no te pueden detener, te dirán como lo tienes que hacer y cuando finalmente vean que lo has logrado, dirán que siempre creyeron en tí")

J. Maxwell

1. Determine the potential trypanocida activity, both *in vitro* and *in vivo*, of a series of different chemical families whose precursors and/or members have demonstrated previous antiprotozoal activity, or they could theoretically do it based on previous modeling studies.
2. Establish a reliable, reproducible, and as complete as possible methodology for the screening of compounds with activity *in vivo* against *Trypanosoma cruzi* infection in mouse model, according to the equipments that are available.
3. To compare the data obtained, with the reference drug (benznidazole) in order to know the advantages and disadvantages of the new compounds compared to it.
4. To elucidate the mechanism of action of the compounds with better expectations of future candidates for following preclinical phase.

-
1. Determinar la actividad trypanocida potencial, tanto *in vitro* como *in vivo*, de una serie de familias químicas de diferente origen cuyos precursores y/o miembros han demostrado capacidad antiprotozoaria previa o teóricamente podrían hacerlo en base a previos estudios de modelización.
 2. Establecer una metodología fiable, reproducible y lo mas completa posible para el cribado de compuestos con actividad *in vivo* frente a la infección por *Trypanosoma cruzi* en modelo murino, de acuerdo a los medios que se disponen.
 3. Comparar los datos obtenidos con la droga de referencia, el benznidazol, con objeto de conocer los pros y contras de los nuevos compuestos frente a ésta.
 4. Dilucidar el mecanismo de acción de los compuestos con mejores expectativas de futuros candidatos para la siguiente fase preclínica.



6. METHODOLOGY

"The civilized man is not in proportion to their disposition to believe, but it is in proportion to its ease to doubt "

("El hombre se hace civilizado no en proporción a su disposición para creer, sino en proporción a su facilidad para dudar.")

Henry Louis Mencken

6.1. Published techniques:

The following table summarizes the aggregate of publications (*see 7.1*), of which this thesis forms part, where the various assays performed are explained in detail.

Table 6. Publications where the techniques performed are explained in detail.

TECHNIQUE	REFERENCE IN 7.1
➤ Chemistry:	
○ Synthesis of compounds.	See 6.2
○ Molecular modelling.	[6]
➤ Cellular Cultures:	
○ Parasite cultures.	[2]
○ Mammalian cells cultures.	[2]
➤ <i>In vitro</i> activity:	
○ Cytotoxicity test.	[1]
○ Extracellular forms tests:	
▪ Epimastigotes assays.	[1]
▪ Trypomastigotes assays.	
○ Intracellular forms test: Amastigotes assays.	[1]
○ Infectivity Assays.	[1]
○ Drug-combination: Isobologram	See 6.3.2
➤ <i>In vivo</i> activity:	
○ <i>Trypanosoma cruzi</i> SN3 characterization and schedule set up.	See 6.3.1, [4]
○ Mice infection and treatment.	[3]
○ Cyclophosphamide-induced immunosuppression and assessment of cure.	[3]
○ ELISA test.	[3]
○ Toxicity tests by clinical chemistry measurements.	[3]
○ Drug-combination: <i>In vivo</i> bioluminescence imaging of <i>T. cruzi</i> expressing red-shifted luciferase	See 6.3.3
➤ Studies on the Mechanism of action:	
○ Metabolites excretion study.	[5]
○ Ultrastructural alterations.	[3]
○ Superoxide Dismutase (SOD) enzymatic inhibition studies.	[1]
○ Trypanothione reductase (TR) enzymatic inhibition studies.	[6]

6.2. Synthesis of compounds:

All the compounds tested in this study were supplied by different chemistry groups within the collaborations established previously by our group and the following groups:

Table 7. Families of chemical compounds, and publications where they can be found.

ORIGEN	CHEMICAL FAMILY	NAME IN THE THESIS	REFERENCE in 7.1
Departamento de Química, Facultad de Ciencias, Universidad de las Islas Baleares, Palma de Mallorca.	N,N'-Squaramides	Comp 1 – 18	[3]
Departamento de Química Orgánica, Facultad de Química, Universidad Complutense, Madrid / Instituto de Química Médica, Centro de Química Orgánica M. Lora-Tamayo, CSIC	Phthalazines	Comp 19 – 22	[1]
	Hydroxi-Phthalazines	Comp 23 – 24	[7]
Departamento de Química Orgánica, Universidad de Granada.	Abietic acid derivatives	Comp 25 – 29	[5]
QBIS Research Group, Institut de Química Computacional i Catalàlisi (IQCC) y Departament de Química, Universitat de Girona.	Tetradentated polyamines	Comp 30 – 34	[8]
		Comp 35 – 40	[9]
Instituto de Ciencia Molecular, Departamento de Química Inorgánica, Universidad de Valencia / Departamento de Química Orgánica, Universidad de Valencia	Scorpiand-like azamacrocycles	Comp 41 – 50	[2]
	Aza-scorpiand derivatives	Comp 51 – 63	[6]

6.3. Set up of techniques (unpublished):

6.3.1. Establishing of an *in vivo* model for Chagas disease:

In the literature it is described that the development of the *T. cruzi* infection in animal models depends on the host used (*Caldas et al., 2008*) and the parasite strain utilized (*Toledo et al., 2004; Santos et al., 2010*). In this case, the *Trypanosoma cruzi* strain used was isolated in Guajira, Colombia; the strain was identified as *T. cruzi* SN3

(IRHOD/CO/2008/SN3) *Téllez-Meneses et al., 2008*; it has been genetically characterized to be within the DTU-I (*Olmo et al., 2014*), according to the classification of *Zingales et al., 2012*. The animal model for the experiments was the murine model Balb/c, which appears in the literature as a widely used model for this parasitic infection (*Ferreira et al., 2011; Pellegrini et al., 2011; Henriques et al., 2014*). In order to know the curve of parasitemia that occurs in this model of *T.cruzi* SN3-Balb/c mice, a mouse, which was previously immunosuppressed with various doses of 200 mg/kg body mass of cyclophosphamide to facilitate the infection, was inoculated with a dose of about 10^5 trypanosomes/ml of which 45% were metacyclic forms obtained from a culture medium TAU, according to the method described by *Cardoso et al., 2010*. Once the parasitemia was detectable in the immunosuppressed mouse (5-7 days post-infection), a group of fifteen mice were infected by intraperitoneal injection with 100 μ l of PBS-diluted blood from the initial mouse at a concentration of 1000 blood trypomastigotes/100 μ l. Parasitemia levels in the blood of this group of mice were monitored by counting in a Neubauer chamber every 3 days using fresh blood obtained from the maxillary vein at dilutions 1:100 in PBS and 1:15 in Lysis/Citrate buffer (2M Tris-HCl, 1M MgCl₂, 100 mM C₆H₈O₇, 100 mM C₆H₇NaO₇).

Chart 1 shows the distribution of parasitaemia over time (days post infection). Whereas it can be seen that the peak of infection occurred around day 21 post-infection (p.i.), after this, the levels of trypomastigotes in the blood dropped progressively and by day 40 p.i. they were undetectable for the dilution in PBS method (detection limit of 10^7 parasites/ml). This allowed us to establish the criteria for the acute phase of *T. cruzi* SN3 strain of up to 40 days. The parasitemia count continued using the lysis/citrate buffer that allows a lower threshold to be detected (up to 10^6 parasites/ml). For the next 100 days in the chronic phase (42-150 p.i.) there was a discontinuity with intermittent parasitemia,

[METHODOLOGY]

involving alternating periods of parasite absence with small peaks of parasites, but always within stable limits, as shown in **chart 1**. There was also a high degree of variability from the standard deviation during this phase, demonstrating that the immune system's fight to contain the infection until it chronifies is different in each individual, although within a range. On day 150 p.i., the mice were immunosuppressed using a treatment of cyclophosphamide, according to the method described by *Caldas et al., 2008* (which will later be replaced by the same procedure but as described by *Cencig et al., 2011*, since this induces the same effect but it is less invasive for the mice).

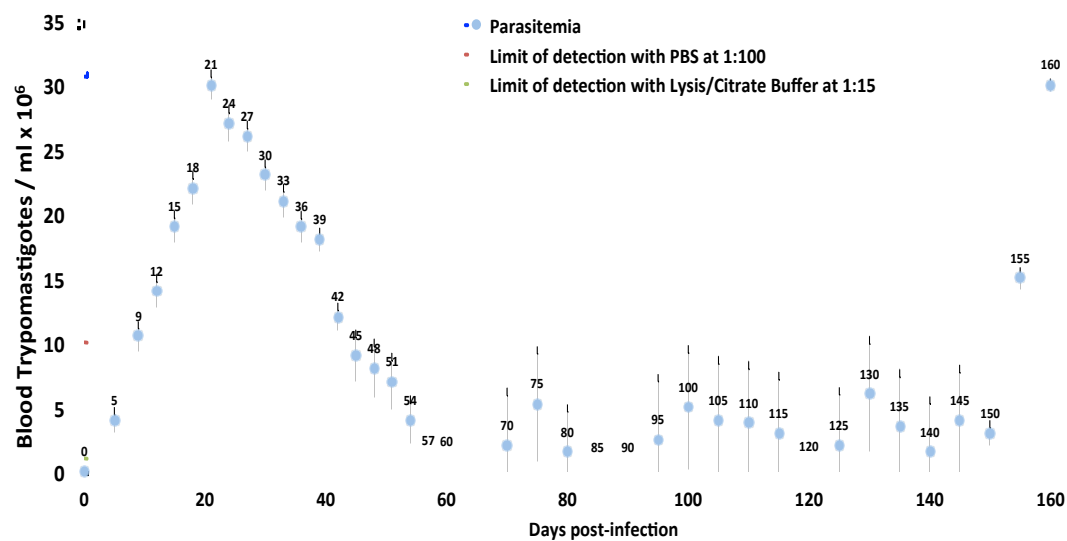


Chart 1. Parasitaemia levels during the establishment of *in vivo* mice models for *T. cruzi* SN3 infection.

During this entire procedure the serum of all fifteen mice was also obtained from whole blood (taken by maxillary puncture as explained above) in order to study the IgG response that causes the infection, to know more about the immune status of the mouse. To quantify the IgG concentration, the enzyme-linked immunosorbent assay (ELISA) was used according to the method described by our group (Mateo et al., 2010). **Chart 2** shows the total IgG levels obtained for two different serum dilutions 1:80 and 1:40, plus the

parasitemia curve during the time of infection. It was observed that there is a high production of total IgG at the onset of infection, followed by decreasing levels with no seroconversion at any time for either of the dilutions studied. Finally, after immunosuppressive treatment, there was a further increase in the levels; the data obtained agree with *El Bouhdidi et al., 1994*.

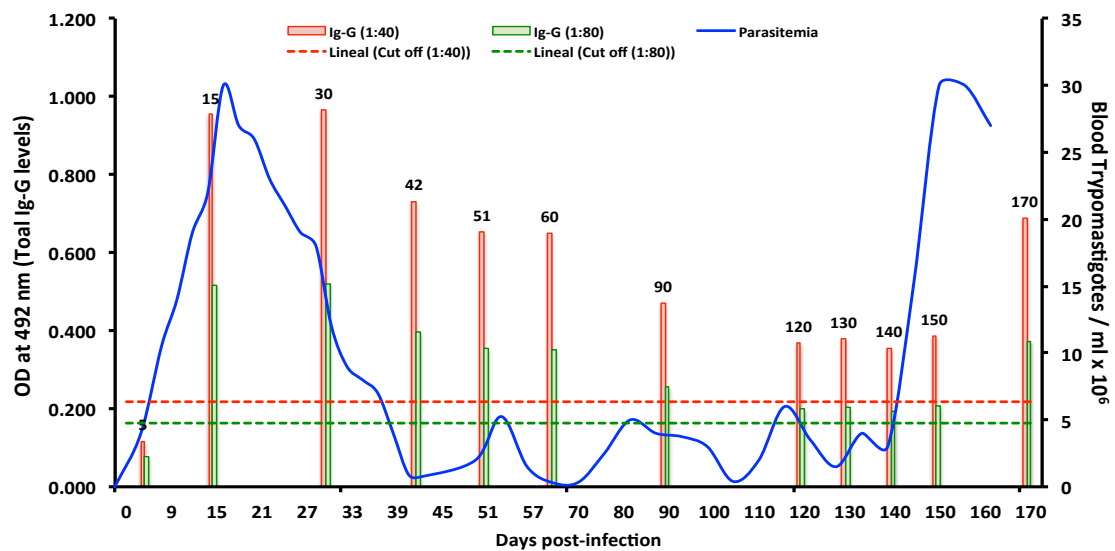


Chart 2. Parasitaemia levels and IgG levels (measured by ELISA) during the establishment of *in vivo* mice models for *T. cruzi* SN3 infection.

When the strain arrived at our lab, we were informed that it was likely it had cardiac tropism. By PCR we confirmed that this strain targeted the heart during the chronic phase, as after necropsy on day 170 the hearts of all mice tested positive in the PCR performed. The organs were extracted and perfused with warm PBS to remove the circulating blood. Then, the organs were ground using a Potter-Elvehjem grinder and total DNA was obtained using a commercial DNA extraction kit (Wizard® Genomic DNA Purification Kit), and a PCR was run using specific primers for gene b of the Fe-SOD designed in our laboratory (*Olmo et al., 2014*). All the mice contained parasites in their heart as shown in **Figure 9**. The criteria of curing in the absence of parasites in the target organ PCR has been widely used in the literature for the murine model (*Moser et*

[METHODOLOGY]

al., 1989; Vallejo *et al.*, 1999; Keenan *et al.*, 2012). Therefore, our aim was to obtain a treatment that prevented the settling of parasites in the target organ.

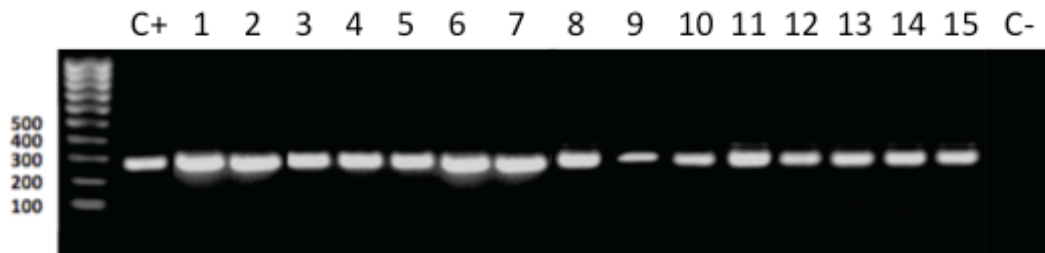


Figure 9. Picture of the agarose gel showing the amplification fragment of the 270 bp fragment within the *sod* gene *b* in *T. cruzi*, after a PCR using the total DNA extracted from the mice's hearts.

For this reason, after obtaining these results, we established the following guidelines for our *in vivo* experiments:

- The inoculation is to be made using infected blood, from an immunosuppressed mouse in the acute phase of the infection, diluted in PBS to inoculate 1000 trypomastigotes in 100 μ l.
- The treatment is to begin between the fifth and seventh day p.i., once the infection is confirmed. It will be performed by intraperitoneal injection for 5 consecutive or alternate days depending on the pharmacokinetics of the compound to be tested, and the dose will also depend on the results obtained during the *in vitro* assays.
- The parasitemia will be monitored in fresh blood by counting with the Neubauer chamber every three days until day 40 post-infection.
- The immunosuppression is to be induced after day 120 post-infection by administrating 4 intraperitoneal doses (200mg/kg of body mass) of cyclophosphamide, one every three days. We will consider a mouse cured if its target organ (heart) is negative in the PCR after treatment.

6.3.2. Drug-combination studies:

Combining drugs to increase the therapeutic effect, reduce toxicity and to minimize drug resistance is becoming increasingly important in the treatment of infectious diseases such as malaria (Co *et al.*, 2009), AIDS (Petropoulos *et al.* 2000), and tuberculosis (Ramón-García *et al.*, 2011), and can offer a favourable outcome. However, challenges exist in the design of *in vitro* combination studies that are not only appropriate to the mechanism of action of the compounds, but that can accurately quantify the drug interaction. There are two different, commonly employed methods used when studying drug combinations *in vitro*: the fold of potentiation index and the combination index (CI); The fold of potentiation method measures the shift in IC₅₀ to clearly show how one drug that has no effect on its own enhances the effect of another. However, this method cannot be used when both drugs display cytotoxicity as single agents. In this case the CI (Chow, 2006) method is more appropriate. This method allows three interaction types between drugs to be distinguished: antagonistic, additive and synergistic. In this case we used an *in vitro* screening method for compounds using the alamarBlue© viability reagent. The steps are:

- Set up a 96 well plate with 100 µl of compound (each concentration in triplicate) solubilized in the growth medium for epimastigotes.
- Add 100 µl of 10³ epimastigotes/100 µl to each well.
- Incubate for 72 hours at 28°C.
- After 48 hours incubating add 20 µl/well of alamarBlue © at 0.125 mg/ml in sterile PBS.
- Keep the culture in the incubator for the remaining 24 hours at 28°C

[METHODOLOGY]

- Add 5µl of 10% SDS and incubate for 15 minutes at room temperature.
- Measure in a plate reader at 570 nm, using a 600 nm as a reference wavelength.
- Calculate the cell viability compared to the control.

After the cell viability data were obtained we continued according to the procedures described by *Chou, 2006* for obtaining information about possible effects in the combinations of our best compounds against *T.cruzi*. In our case, the best compounds were assayed in pairs, because all the compounds selected for this assay are trypanocidal as single agents. Since the CI method is required for studying the combined effect, the CI values were calculated using the equation in **Figure 10**; where: **C(A)** and **C(B)** are the concentrations of drug A and B that in combination cause 50% inhibition. **IC₅₀(A)** and **IC₅₀(B)** are the concentrations of drug A and B that individually cause 50% inhibition.

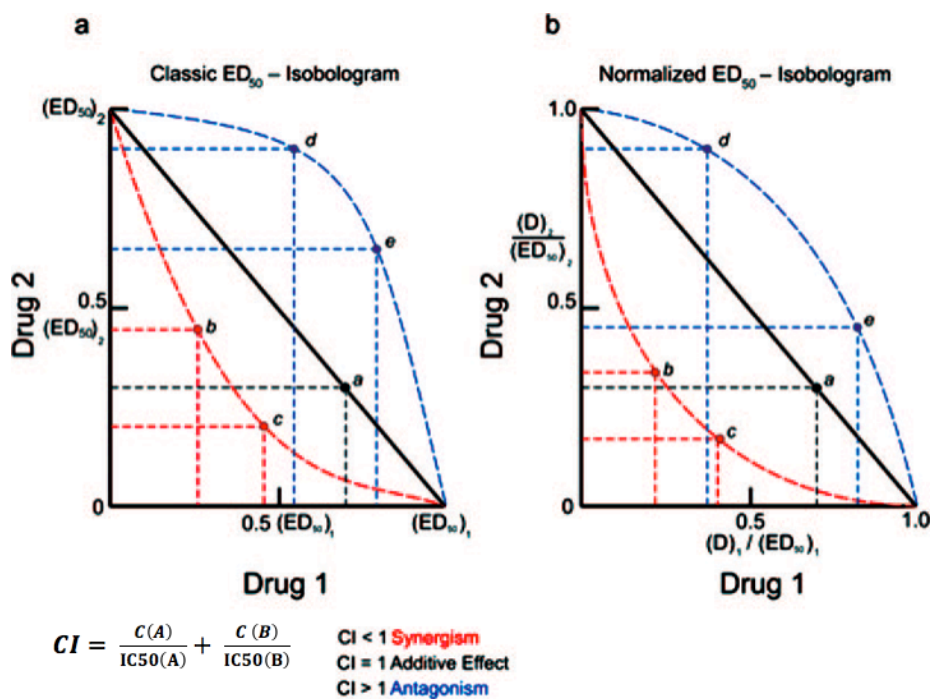


Figure 10 The ED50 isobologram. **A:** classic isobologram for two drugs with actual doses on the *x*- and *y*-axis. **B:** dose-normalized isobologram for two drugs with dose normalized with ED50 to unity on both *x*- and *y*-axis. Taken from *Chou, 2006*

A CI value of less than 1 indicates synergy, 1 indicates additivity, and a result of greater than 1 indicates antagonism. The CI data has been analyzed and displayed as an isobologram, which is a dose-orientated graphic that can be generated for any single effect level (in this case, 50% inhibition).

6.3.3. New, high sensitive, and advanced experimental murine model:

Once the best compounds were selected *in vivo* using the previously detailed model a last test was performed on them. This was carried out in the group of Professor John M. Kelly (Department of Pathogen Molecular Biology, Faculty of Infectious and Tropical Diseases, London School of Hygiene and Tropical Medicine) during a research stay. This last assay was possible thanks to the highly sensitive *in vivo* imaging system of *T. cruzi* expressing red-shifted luciferase that they have in their laboratory (Lewis *et al.*, 2014). Bioluminescence imaging is a non-invasive technique which can be used to monitor infections in real-time. However, its utility is restricted by difficulties in detecting pathogens in deep tissue. ‘Red-shifted’ luciferases, which emit light of longer wavelength than standard bioluminescence-generating proteins, greatly enhance sensitivity, and have wide applicability for studying parasite infections (Taylor and Kelly, 2014). As is shown in **Figure 11** the detection limit is remarkably low and treatment response versus non-treated can be perfectly quantified.

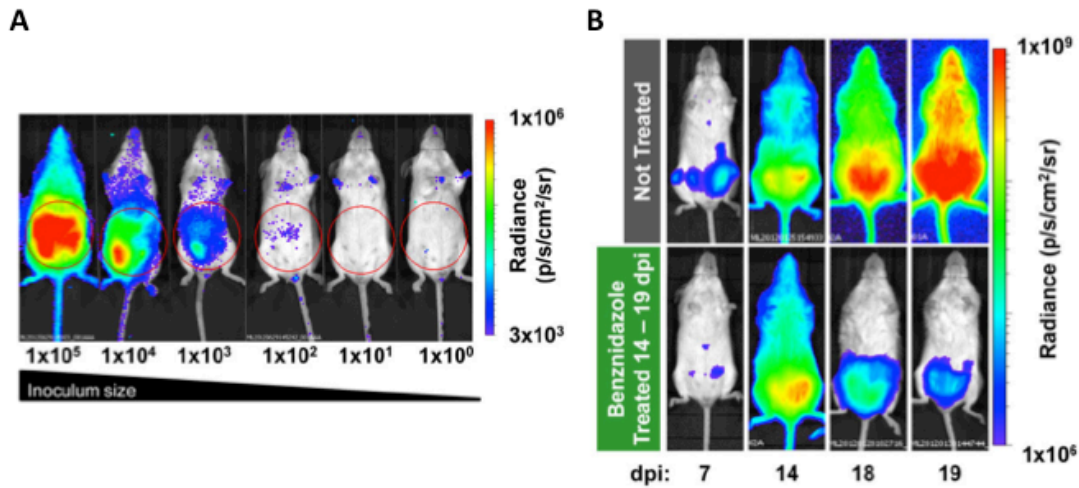


Figure 11. Evaluation of *T. cruzi* infection in SCID mice by *in vivo* bioluminescence imaging. A) Evaluation of *in vivo* limit of parasite detection. B) Example ventral view images of the same individual SCID mouse 7, 14, 18 and 19 days after i.p. injection with $1 \cdot 10^3$ BTs (upper panels) and comparison with an equivalent infected mouse treated with $100 \text{ mg kg}^{-1} \text{ day}^{-1}$ benznidazole (BZ) for 5 days starting at 14 dpi (lower panels). All images use the same log₁₀ scale heat-map with minimum and maximum radiance values as indicated. Taken from [Lewis et al., 2014](#)

Note that this new method has a number of differences compared with the method used in our lab, but has the advantage of being closer to a clinical situation and is therefore a good final indicator for screening compounds, the main objective of this study. The basic comparative differences are:

- The *Trypanosoma cruzi* strain used here is CLBrenner (DTU-VI) instead of *T. cruzi* SN3 (DTU-I).
- The treatment here is administered orally rather than intraperitoneally.
- In the treatment administered during the chronic phase a combination of two different compounds was used, while in our lab we always treated them during acute phase only and using a single compound each time.

This shows that the behaviour of the compound can vary from the results previously obtained using our method. Nevertheless, this new technique allowed us to once

again show that the parasitemia during the chronic phase is intermittent (**Figure 12**), even though the *T. cruzi* strain is different.

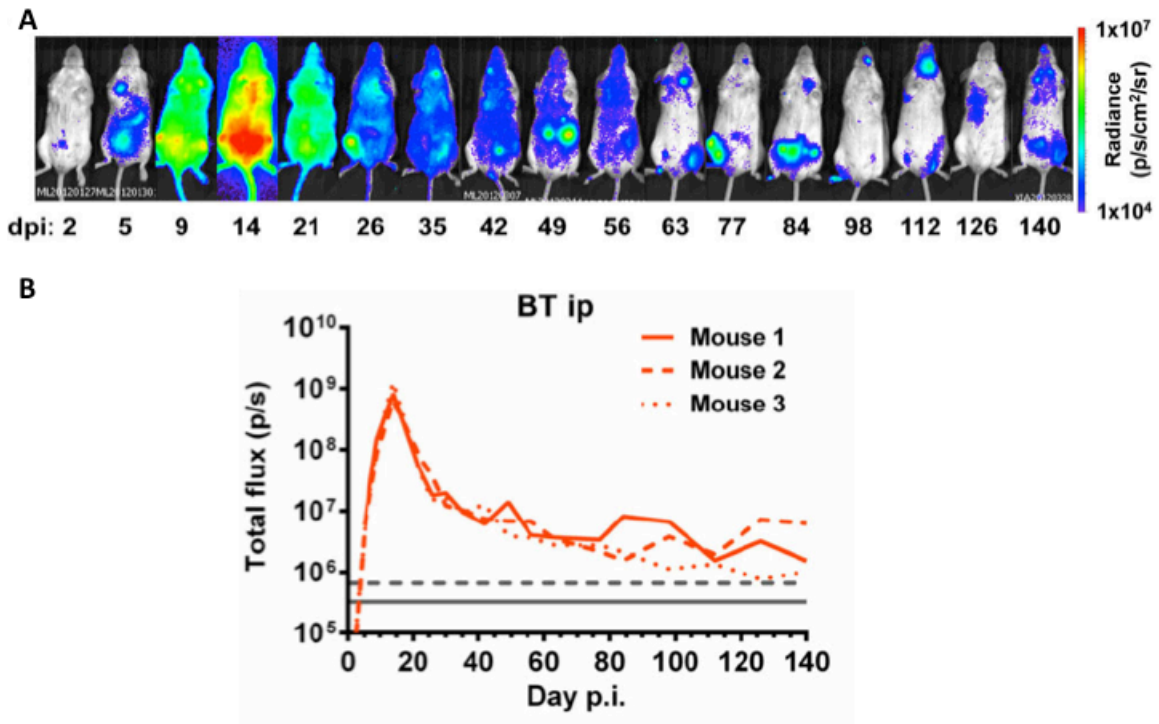
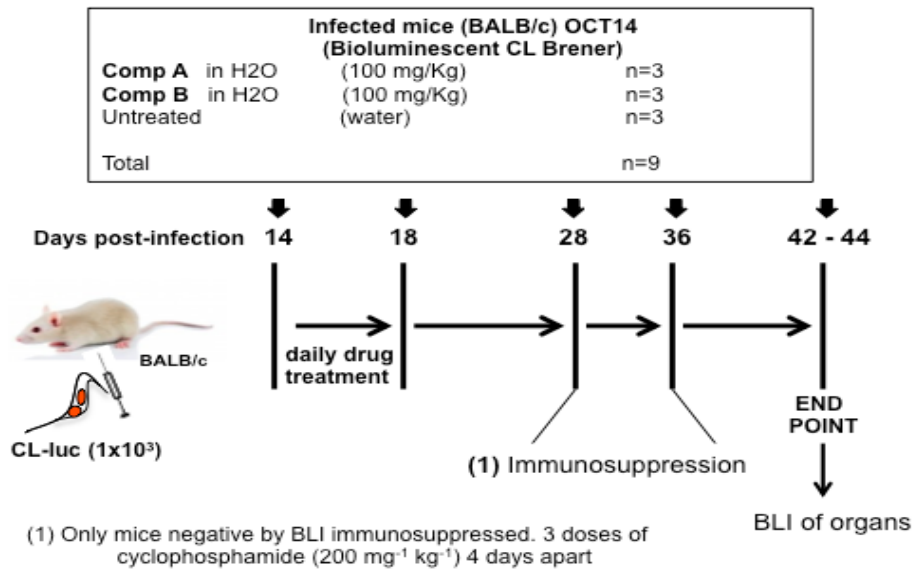


Figure 12. Chronic *T. cruzi* infection is highly dynamic in space and time. **A)** Representative ventral view images of the same BALB/c mouse taken at sequential time points over the course of 140 days after i.p. inoculation with $1 \cdot 10^3$ *PpyRE9h* luciferase-expressing *T. cruzi* CL Brener blood trypomastigotes (BT) (representative of $n = 3-6$ per experiment). Heat-maps are on log₁₀ scales and indicate intensity of bioluminescence from low (blue) to high (red); the minimum and maximum radiances for the pseudocolour scale are indicated. **B)** Quantification of whole animal total ventral bioluminescence for three individual mice from the experiment represented by the images in A. Grey lines indicate detection thresholds determined as the mean (solid line) and mean +2SD (dashed line) of background luminescence of control uninfected mice. Taken from [Lewis et al., 2014](#)

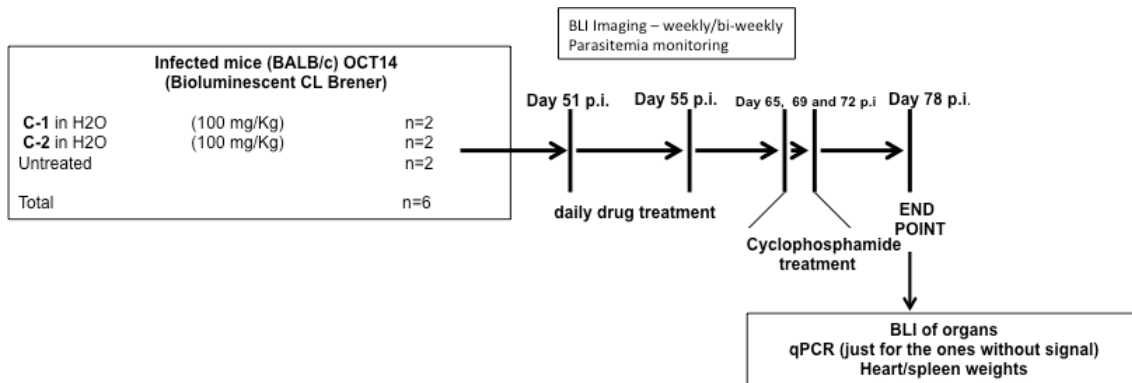
In consultation with Professor Kelly and Dr. Amanda Fortes we established the two schedules for acute and chronic phases as follows:

[METHODOLOGY]

Scheme 1. Screen line protocol” to test drug efficacy using acute phase model



Scheme 2. Screen line protocol” to test drug-combination efficacy using chronic phase model





7. RESULTS

"The world of these beings is finite and yet has no limits"

("El mundo de estos seres es finito y sin embargo no tiene límites")

Albert Einstein

7.1. Publications already published.

Publication	Journal (Impact Factor)	Category Name (Journal Rank in Category)	Quartile in Category
[1]. Sánchez-Moreno M, Gómez-Contreras F, Navarro P, Marín C, Olmo F, Yunta MJR, Sanz AM, Rosales MJ, Cano C, Campayo L. Phthalazine Derivatives Containing Imidazole Rings Behave as Fe-SOD Inhibitors and Show Remarkable Anti-T. cruzi Activity in Immunodeficient-Mouse Mode of Infection. <i>J Med Chem.</i> 2012 Oct 8.	Journal of Medicinal Chemistry (5.614)	CHEMISTRY, MEDICINAL (3)	Q1
[2]. Olmo F, Marin C, Clares MP, Blasco S, Albelda MT, Soriano C, Gutierrez-Sánchez R, Arrebola-Vargas F, García-España E, Sánchez-Moreno M. Scorpian-like azamacrocycles prevent the chronic establishment of <i>Trypanosoma cruzi</i> in a murine model. <i>Eur J Med Chem.</i> 2013. 70C, 189 - 198.	European Journal of Medicinal Chemistry (3.432)	CHEMISTRY, MEDICINAL (13)	Q1
[3]. Olmo F, Rotger C, Ramírez-Macías I, Martínez L, Marín C, Carreras L, Urbanová K, Vega M, Chaves-Lemaur G, Sampedro A, Rosales MJ, Sánchez-Moreno M, Costa A. Synthesis and biological evaluation of N,N'-squaramides with high in vivo efficacy and low toxicity: toward a low-cost drug against Chagas disease. <i>J Med Chem.</i> 2014 Feb 13; 57(3): 987-99.	Journal of Medicinal Chemistry (5.480)	CHEMISTRY, MEDICINAL (3)	Q1
[4]. Olmo F, Escobedo-Ortegón J, Palma P, Sánchez-Moreno M, Mejía-Jaramillo A, Triana O, Marín C. Specific primers design based on the superoxide dismutase b gene for <i>Trypanosoma cruzi</i> as a screening tool: Validation method using strains from Colombia classified according to their discrete typing unit. <i>Asian Pac J Trop Med.</i> 2014 Nov; 7(11):854-859.	Asian Pacific Journal of Tropical Medicine (0.926)	PUBLIC ENVIRONMENTAL & OCCUPATIONAL HEALTH (125)	Q4
		TROPICAL MEDICINE (11)	Q3
[5]. Olmo F, Guardia JJ, Marin C, Messouri I, Rosales MJ, Urbanová K, Chayboun I, Chahboun R, Alvarez-Manzaneda EJ, Sánchez-Moreno M. Prospects of an alternative treatment against <i>Trypanosoma cruzi</i> based on abietic acid derivatives show promising results in Balb/c mouse model. <i>Eur J Med Chem.</i> 2014 Nov 3; 89C: 683-690.	European Journal of Medicinal Chemistry (3.432)	CHEMISTRY, MEDICINAL (13)	Q1
[6]. Olmo F, Clares MP, Marín C, González J, Inclán M, Soriano C, Urbanová K, Tejero R, Rosales MJ, Krauth-Siegel RL, Sánchez-Moreno M, García-España E. Synthetic single and double aza-scorpian macrocycles acting as inhibitors of the antioxidant enzymes iron superoxide dismutase and trypanothione reductase in <i>Trypanosoma cruzi</i> with promising results in a murine model. <i>RSC Adv.</i> 2014; 4, 65108–65120.	RSC Advances (3.708)	CHEMISTRY, MULTIDISCIPLINARY (35)	Q1

Phthalazine Derivatives Containing Imidazole Rings Behave as Fe-SOD Inhibitors and Show Remarkable Anti-*T. cruzi* Activity in Immunodeficient-Mouse Mode of Infection

Manuel Sánchez-Moreno,^{*,†} Fernando Gómez-Contreras,^{*,‡} Pilar Navarro,^{*,§} Clotilde Marín,[†] Francisco Olmo,[†] María J. R. Yunta,[‡] Ana María Sanz,[‡] María José Rosales,[†] Carmen Cano,[‡] and Lucrecia Campayo[‡]

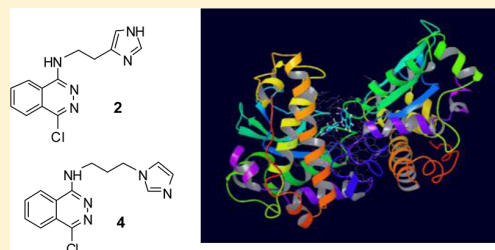
[†]Departamento de Parasitología, Facultad de Ciencias, Universidad de Granada, E-18071 Granada, Spain

[‡]Departamento de Química Orgánica, Facultad de Química, Universidad Complutense, E-28040 Madrid, Spain

[§]Instituto de Química Médica, Centro de Química Orgánica M. Lora-Tamayo, CSIC, E-28006 Madrid, Spain

S Supporting Information

ABSTRACT: A series of new phthalazine derivatives 1–4 containing imidazole rings were prepared. The monoalkylamino substituted derivatives 2 and 4 were more active in vitro against *T. cruzi* and less toxic against Vero cells than both their disubstituted analogues and the reference drug benznidazole. Compounds 2 and 4 highly inhibited the antioxidant parasite enzyme Fe-SOD, and molecular modeling suggested that they interact with the H-bonding system of the iron atom moiety. In vivo tests on the acute phase of Chagas disease gave parasitemia inhibition values twice those of benznidazole, and a remarkable decrease in the reactivation of parasitemia was found in the chronic phase for immunodeficient mice. Glucose metabolism studies showed that compounds 1–4 did not affect the succinate pathway but originated important changes in the excretion of pyruvate metabolites. The morphological alterations found in epimastigotes treated with 1–4 confirmed extensive cytoplasm damage and a high mortality rate of parasites.



■ INTRODUCTION

The protozoan parasite *Trypanosoma cruzi* is responsible for Chagas disease, which is a potentially fatal considerable health problem in Latin America due to inadequate therapy and the lack of an effective vaccine.^{1,2} Diverse factors, like increasing immigration, easy transmission via blood transfusion, pregnancy, and the consumption of contaminated food, have contributed to the spread of the disease all over the world, and it is also progressively becoming a threat of major concern to health authorities in Europe and North America.^{3,4} Many research groups have investigated the synthesis of molecules able to act efficiently on the amastigote forms of *T. cruzi*, but results obtained so far are unsatisfactory. The only two drugs currently used worldwide for the treatment of Chagas disease are the pentaheterocyclic derivatives nifurtimox and benznidazole. However, both drugs present significant side effects and limited efficacy, especially in the most lethal chronic phase of the disease. The most frequently prescribed is the imidazole derivative benznidazole (BZN), which is activated by nicotinamide adenine dinucleotide NADH-dependent trypanosomal reductases and forms reductive metabolites. Those metabolites supposedly cause a series of effects like DNA damage and inhibition of proteine synthesis, which breaks the respiratory chain in the amastigote forms of *T. cruzi*.^{5,6} However, in adults, BZN generates a considerable number of

adverse effects, mainly digestive (gastric upset, nausea, vomiting), hematologic (leukopenia, thrombocytopenia, agranulocytosis), dermatologic (erythema, dermatitis, Stevens–Johnson syndrome), and neurologic (dose-dependent polyneuropathies) alterations.^{5,7} Furthermore, BZN originates reactive metabolites that interact with fetal components and has also shown tumorigenic or carcinogenic effects in some cases.⁸ The effectiveness of BZN in the chronic phase is substantially lower than in the acute phase, and parasitological cure in the later chronic phase is only obtained in 10–20% of the patients.⁹

Another disturbing aspect of Chagas disease is the high reactivation ability of the parasitemia in immunocompromised individuals. It has been shown that apparently cured patients who had been further submitted to kidney or liver transplantation, diagnosed with acquired immunodeficiency syndrome (AIDS), or treated with anticancer chemotherapy experienced Chagas reactivation with a very aggressive clinical course leading to meningoencephalitis and/or acute myocarditis.^{10–14} When patients with chronic chagasic cardiopathy undergo cardiac transplant, reactivation of the trypanosomiasis occurs and treatment with benznidazole only leads to

Received: July 26, 2012

Published: October 8, 2012

temporary remission, while *T. cruzi* infection persists.^{15–17} From all of these facts it can be concluded that the design of new, less toxic drugs that are more effective against the chronic phase of Chagas disease and able to reduce reactivation in cases of immunodeficiency is urgently needed.

Antichagasic agent research mainly targets key metabolic biochemical pathways or crucial parasite-specific enzymes. Sterol metabolism, kinetoplast DNA sites, trypanothione reductase, cysteine proteinase, hypoxanthineguanine phosphoribosyltransferase, dihydrofolate reductase, and glyceraldehyde 3-phosphate dehydrogenase have fed the main lines of investigation in recent years.¹⁸ Among the trypanosomatid-specific enzymes, we have focused our attention on iron superoxide dismutase (Fe-SOD) because it is not found in mammals and it plays an essential role in the defense of the parasite against oxidation. It has been shown that parasitic protozoan survival is closely related to the ability of that enzyme for evading toxic free radical damage originated by their host.¹⁹ Because of the predominant role of the prosthetic groups, interaction with the active sites containing the metal ion of Fe-SOD could be an efficient way of deactivating the antioxidant effect of the enzyme.

In relation to this matter, we have described in previous work new mono- and bis(alkylamino) derivatives of the benzo[g]-phthalazine system functionalized at the end of the alkylamine side chains with amino groups or heterocyclic units such as pyridine, pyrazole, or imidazole (Figure 1, general structures I

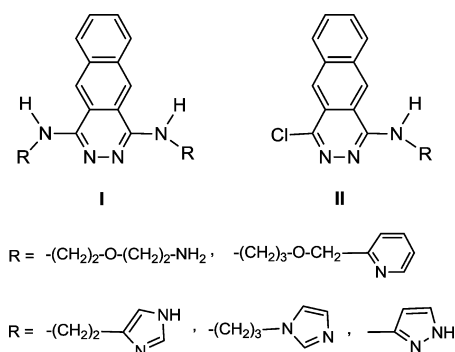


Figure 1. Benzo[g]phthalazine derivatives with potential antiparasitic activity.

and II).^{20–22} Some of these compounds have shown very low toxicity against Vero cells and remarkable in vivo activity in mice infected with *T. cruzi* in both the acute and the chronic phases of the disease.²² Activity results obtained for the chronic phase in parasitemia studies²² are especially valuable because that stage of the disease is highly resistant to commonly used drugs. Furthermore, we found recently that those compounds that contained pyrazole or imidazole rings also present a significant in vitro activity against *Leishmania braziliensis* and *Leishmania donovani* species.²³ Structural features significantly influence the antiparasitic activity, since results obtained with the monoalkylamino substituted compounds II are much better than those of their type I disubstituted counterparts, as well as for those found for BZN. On the other hand, histopathological studies concluded that the monosubstituted derivatives containing imidazole rings are less toxic to mice than those with the pyrazole system.²²

Another remarkable result of our previous work was that both the imidazole and pyrazole derivatives were shown to be

good inhibitors of the Fe-SOD antioxidant enzyme of the parasites, not only of *T. cruzi*²¹ but also of *Leishmania* sp. species.²³ Furthermore, their inhibitory ability of human CuZn-SOD was negligible and, interestingly, the monoalkylaminosubstituted derivatives type II were also more powerful inhibitors of Fe-SOD than the disubstituted analogues. As commented before, Fe-SOD plays a key role in the defense of trypanosomatids against oxidation and it is not present in humans, so these findings are probably related to the antiparasitic activity obtained. Molecular modeling studies suggest that imidazole derivatives of type II can penetrate between the strands of the enzyme and locate an sp^2 imidazole nitrogen near one of the active sites²² so that some kind of interaction with the environment of the iron atom could be responsible for the higher level of inhibition obtained in the assays performed.

On the basis of all of the results described above, we have prepared now structurally related imidazole derivatives in which the benzo[g]phthalazine moiety has been modified by the removal of one of the benzene rings (Figure 2, compounds 1–

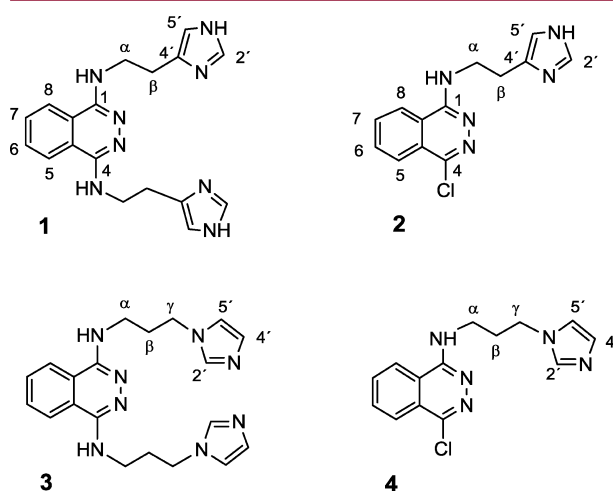


Figure 2. Imidazole-containing phthalazine derivatives tested against *T. cruzi* in this study.

4). That modification results in less bulky structures that could more easily approach the active sites of the enzyme. Removal of one aromatic ring should also reduce toxicity against the host and enhance solubility in aqueous media. This last feature makes synthesis and biological testing easier, but above all it has obvious pharmacological implications: an efficient trypanocidal agent must reach effective trypanocidal concentration levels in the blood plasma, biological fluids, and tissues of the host,²⁴ and its transport ability inside the parasite is also an essential feature.⁵

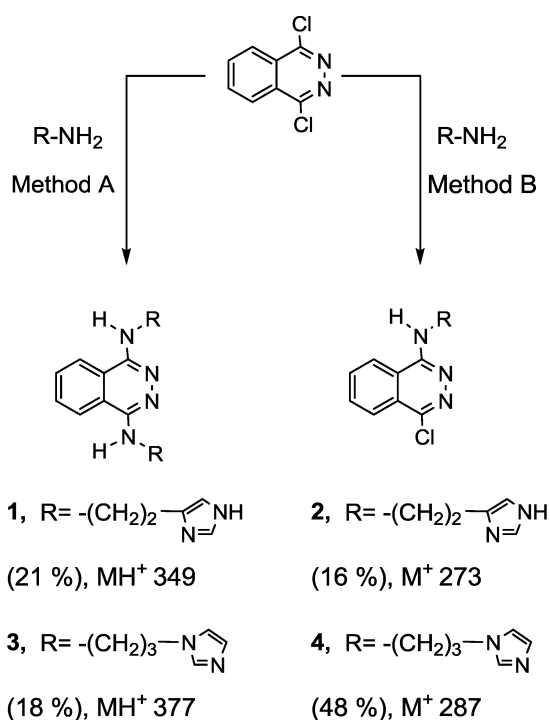
In this work, the synthesis and characterization of compounds 1–4 is described along with an evaluation of their effectiveness as selective inhibitors of Fe-SOD in relation to human CuZn-SOD. Their in vitro antiparasitic activity and toxicity against Vero cells are tested and compared with values obtained for the reference drug BZN, and on the basis of the results obtained, their in vivo trypanosomicidal activity on female BALB/c mice is measured in both the acute and chronic phases. As commented above, one of the major unresolved problems caused by drugs currently in use is the lethality of *T. cruzi* infection in immunocompromised patients, as well as its

failure to prevent the resurgence of the infection. The good activity results obtained with the benzo[*g*]phthalazine analogues in the chronic phase of the disease has prompted us to study, for the first time, the course of the infection in immunodeficient mice treated with *T. cruzi* and, thereafter, with compounds 1–4. The effects of compounds 1–4 on the ultrastructure of *T. cruzi* are also studied by transmission electronic microscopy (TEM) experiments in order to confirm the type of damage caused to the parasite cells. Finally, an NMR analysis of the nature and percentage of the metabolites excreted is performed in order to gain some information about the inhibitory effects of these compounds on the glycolytic pathway, since this represents the prime energy source of the parasite.

RESULTS AND DISCUSSION

Chemistry. The preparation of compounds 1–4 was performed from 1,4-dichlorophthalazine according to the methodology shown in Scheme 1, following conditions related

Scheme 1. Preparation of the Imidazole-Containing Phthalazine Derivatives



Method A: Et_3N /xylene, 120 °C, 6 h or 24 h

Method B: K_2CO_3 /MeCN/reflux, 72 h or 45 h

to those previously established by our group for the synthesis of I and II^{20–22} (Figure 1). The bis(alkylamino)substituted derivatives 1 and 3 were obtained with respective yields of 21% and 18% via simultaneous nucleophilic substitution at the C-1 and C-4 positions of the starting compound with 2-(imidazol-4-yl)ethylamine or 3-(imidazol-1-yl)propylamine under reflux of xylene for 6 or 24 h, using triethylamine as the chlorine acceptor (method A).²¹

Alternatively, the synthesis of the mono(alkylamino)-substituted compounds 2 and 4 was achieved using a different procedure in which the reaction was performed under reflux of acetonitrile over 72 or 45 h, and triethylamine was replaced by potassium carbonate (method B).²² That modification usually leads to better yields of the monosubstituted compounds in relation to the disubstituted analogues, and in this case, yields of 16% and 48% were found for compounds 2 and 4, respectively. Isolation of the compounds from the crude reaction mixtures was performed by column flash chromatography with a chloroform/methanol mixture of increasing polarity.

All of the newly synthesized compounds were unequivocally identified by their analytical, MS-ESI, IR, ¹H NMR, and ¹³C NMR spectroscopic data, as shown in the Experimental Section. Scheme 1 displays the molecular ions obtained from the electrospray mass spectra, which agree in all cases with the proposed structures. For an accurate assignment of the ¹H and ¹³C NMR spectra signals, registered in deuterated dimethylsulfoxide ($\text{DMSO}-d_6$), heteronuclear multiple quantum coherence (gHMQC) experiments were performed, and results were especially useful.

The mono- and bis(alkylamino) substitution products were easily differentiated in both ¹H and ¹³C NMR spectra on the basis of signals corresponding to the ring atoms of the phthalazine system. Protons H-5 and H-8 (see numbering in Figure 2), which appeared as a unique singlet in the ¹H NMR spectra of 1 and 3, lost their equivalence in the monosubstituted compounds 2 and 4, with their chemical shifts differing by 0.28 and 0.18 ppm, respectively. The H-8 proton, close to the alkylamino chain, was deshielded with respect to the proton neighboring the chlorine atom (H-5). Accordingly, the carbon atom attached to the alkylamino substituent (C-1) was always deshielded with respect to the carbon neighboring the chlorine atom in the ¹³C NMR spectra: carbons C-1 and C-4, identical in 1 and 3, showed variations of 10.05 and 9.99 ppm in 2 and 4, respectively. The carbon pairs C-4a/8a and C-5/8 also followed the same pattern, although the chemical shift differences were lower.

In Vitro Trypanosomicidal Evaluation. In order to get preliminary information, the in vitro activity of compounds 1–4 were evaluated against extracellular epimastigote and axenic amastigote forms of *T. cruzi* obtained from an SN3 strain isolated from Colombian *R. prolixus*, as described in the Experimental Section. More indicative data were found when the compounds were also tested on intracellular amastigotes, since extracellular forms are not the developed form of the parasite in vertebrate hosts. Therefore, Vero cells were infected with metacyclic forms of *T. cruzi* that were transformed into amastigotes within 1 day of infection and treated with 1–4. Finally, the phthalazine derivatives were tested against blood trypomastigotes, since these forms of the parasite are responsible for the chronic phase of Chagas disease. Table 1 shows the IC_{50} values obtained after 72 h of exposure and at 1–100 μM when compounds 1–4 were assayed against the four parasite forms mentioned above. Values obtained for the reference drug BZN were included in all cases for comparison. Results obtained for all the *T. cruzi* forms studied were very homogeneous. As happened with the benzo[*g*]phthalazine analogues, the monoalkylamino substituted compounds 2 and 4 were always more active than their bis(alkylamino) substituted counterparts 1 and 3, so the structural influences upon activity proposed in previous studies^{21,22} were confirmed. Differences

Table 1. In Vitro Activity and Toxicity Found for the Phthalazine Derivatives 1–4 against Extra- and Intracellular Forms of *T. cruzi*^a

compd	activity, IC ₅₀ (μM) ^b				toxicity Vero cells IC ₅₀ (μM) ^c
	epimastigote form	axenic amastigote form	intracellular amastigote form	blood trypomastigote form	
BZN	15.9 ± 1.1	18.9 ± 1.5	23.3 ± 4.6	16.4 ± 3.2	13.6 ± 0.9
1	13.0 ± 0.8	15.2 ± 1.2	18.1 ± 1.5	22.5 ± 3.7	323.6 ± 14.3
2	8.7 ± 1.1	10.1 ± 0.7	9.4 ± 1.2	9.2 ± 0.7	427.3 ± 17.3
3	17.4 ± 2.0	12.4 ± 0.9	16.6 ± 0.8	16.9 ± 4.0	301.5 ± 11.8
4	8.8 ± 0.5	10.6 ± 0.4	8.9 ± 0.6	10.2 ± 1.2	436.7 ± 20.1

^aThe results are averages of three separate determinations. ^bIC₅₀ = the concentration required to give 50% inhibition, calculated by linear regression analysis from the K_c values at concentrations employed (1, 10, 25, 50, and 100 μM). ^cAgainst Vero cells after 72 h of culture.

in activity between 2 and 4 were not significant and remained below the experimental error in all cases. When comparing with the reference drug, it was evident that the monosubstituted compounds were substantially more effective than BZN in the four cases considered.

The cytotoxicity of compounds 1–4 was evaluated using mammalian Vero cells as the cellular model (Table 1). Toxicity data were highly interesting because they confirmed that all of the phthalazine derivatives were substantially less cytotoxic than the corresponding compounds containing the benzo[g]-phthalazine moiety, in accordance with the previously outlined hypothesis that the elimination of one of the benzene rings should lead to lower toxicity levels. For instance, the monosubstituted compounds 2 and 4 showed IC₅₀ values of 427.3 and 436.7 μM, whereas values of 213.0 and 145.8 μM had been found for their respective benzo[g]phthalazine analogues.²¹ On the other hand, the most active monosubstituted compounds 2 and 4 were less toxic than 1 and 3, and all of them were much less toxic than BZN, for which an IC₅₀ value as small as 13.6 μM was obtained.

From the in vitro data shown above, the more informative selectivity index (SI) values were calculated and are shown in Table 2. When the number of times that the SI of each

Table 2. Selectivity Index Found for the Phthalazine Derivatives 1–4 against Extra- and Intracellular Forms of *T. cruzi*

compd	SI ^a			
	epimastigote form	axenic amastigote form	intracellular amastigote form	blood trypomastigote form
BZN	0.8	0.7	0.6	0.8
1	24.9 (31)	21.3 (30)	17.9 (30)	14.4 (18)
2	49.1 (61)	42.3 (60)	45.5 (75)	46.5 (58)
3	17.3 (22)	24.2 (34)	18.2 (30)	17.8 (22)
4	49.6 (62)	41.2(59)	49.1 (82)	42.8 (53)

^aSelectivity index = (IC₅₀ of cell Vero)/(IC₅₀ of extracellular and intracellular forms of parasite). In parentheses are the number of times that a compound SI exceeds the reference drug SI.

compound exceeded the SI of BZN (in parentheses) were calculated, very good results were found for the monosubstituted derivatives: the SI values of 2 and 4 exceeded those of BZN by 61-, 60-, 75-, and 58-fold and by 62-, 59-, 82-, and 53-fold, respectively. The best comparative results (75- and 82-fold) were obtained when the compounds were tested against the most significant intracellular amastigote forms. These data support the convenience of carrying out in vivo assays in order

to confirm the apparent advantages found in vitro for compounds 2 and 4 with respect to BZN.

Going one step further in the activity study, the effect of the four compounds on the infectivity, intracellular replication of amastigotes, and further transformation of these in trypomastigotes was determined. For these assays, the IC₂₅ of each product was used as the test concentration, with BZN as the reference drug. Vero cells were cultured for 2 days and then infected with epimastigote forms in the stationary phase. The parasites invaded the cells and underwent morphological conversion to amastigotes within 2 days of infection. On day 10, the rate of host cell infection reached its maximum in the control experiment (Figure 3A). When the imidazole derivatives 1–4 were added to the infected Vero cells, the infection rate significantly decreased with respect to the control for all of the compounds tested, leading to inhibition values varying from 51.5% to 83.3%. The four compounds were more effective than BZN, which showed a 39.4% inhibition, and the monosubstituted derivatives 2 and 4 were by far the most efficient of all (80.3% and 83.3% inhibition, respectively).

On the other hand, data on the mean number of amastigotes per infected Vero cell (Figure 3B) led to similar but even more compelling conclusions, since the four compounds were found to be much more effective than BZN, which only achieved 12.5% inhibition on day 10. Concerning the mean number of trypomastigotes detected (Figure 3C), although differences with BZN were less significant on the whole, inhibition values as high as 85.1% and 73.9% were found for the monosubstituted derivatives 2 and 4, respectively, doubling the inhibition obtained for BZN (41.6%). Finally, compound 2 appeared to be a better inhibitor of parasitemia than 4 in the three cases (83.9%, 62.9%, and 85.1% against 80.3%, 55.8%, and 73.9%, respectively). The same thing happened with the couple 1 and 3, where compound 1 was always more active than 3. We think that the presence of an NH group in the imidazole rings of 1 and 2 could be related to the differences found with respect to 3 and 4.

Inhibitory Effect on the *T. cruzi* Fe-SOD Enzyme. In previous work we had found that benzo[g]phthalazine derivatives containing sp² or sp³ nitrogen atoms in the side chains and other pyrazole-containing related structures were able to inhibit the activity of the Fe-SOD enzyme of the parasite, and the inhibiting features had been related to the high complexing potentiality of the polyaminic structures assayed, since the environment of the active site could be modified by complexation.^{20–23,25}

Therefore, the effects of compounds 1–4 on *T. cruzi* Fe-SOD were assayed at concentrations ranging from 1 to 100 μM. Epimastigote forms of *T. cruzi* which excreted Fe-SOD when cultured in a medium lacking inactive fetal calf serum (FCS)

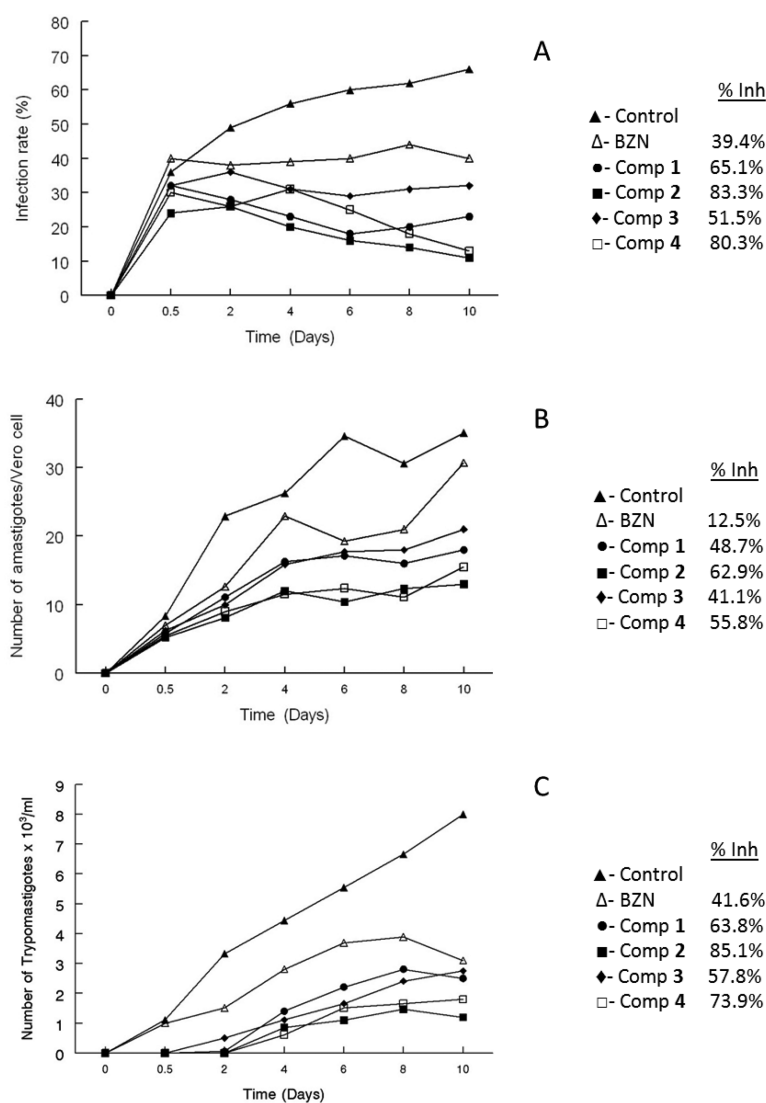


Figure 3. Effect of the imidazole-containing phthalazine derivatives 1–4 on the infection rate and growth of *T. cruzi*: (A) rate of infection; (B) mean number of amastigotes per infected Vero cell; (C) number of trypomastigotes in the culture medium for (▲) control, (△) BZN, (●) 1, (■) 2, (◆) 3, (□) 4. Measured at IC₂₅. Values are the means of three separate experiments.

were used.²⁶ The inhibition data obtained are shown in Figure 4A, and the corresponding IC₅₀ values are included in order to make the interpretation of results easier. For comparison, Figure 4B shows the effect of the same compounds on CuZn-SOD obtained from human erythrocytes. A simple visual comparison of Figure 4A and Figure 4B revealed that Fe-SOD was clearly inhibited, whereas the inhibition of human CuZn-SOD was substantially lower. Results were especially noteworthy for the monosubstituted compounds 2 and 4 (which also showed the best in vitro activity results), since both of them reached 100% inhibition of Fe-SOD even at 50 μ M. Concerning the IC₅₀ data, the four compounds showed lower values for Fe-SOD than for CuZn-SOD, and 2 and 4 were 5.5-fold and 5.8-fold more inhibitory against Fe-SOD than against human SOD, respectively, whereas much lower differences were found for 1 and 3 (2.6-fold and 1.6-fold, respectively). On the other hand, when the monosubstituted derivatives were assayed against Fe-SOD, lower IC₅₀ values were obtained than in the case of their disubstituted counterparts (12.89 μ M

against 48.03 μ M for the couple 2 and 1, and 14.36 μ M against 41.66 μ M for 4 and 3).

In order to obtain more information on the activity shown by the tested compounds over Fe-SOD, a tentative molecular modeling study on their mode of interaction with the enzyme was performed. It is known that Fe-SOD enzymes are formed by two monomers, both of which contain a non-heme iron as a five-coordinated active site ligated by three histidine units, an aspartate group, and an axial H₂O or HO⁻ ligand supported by an essential conserved H-bonding network comprising amino acids and extending across the interface to the other monomer of the Fe-SOD dimer.²⁷ Specifically, the coordinated solvent engages in a H-bond with the Asp160 ligand and another engages with the conserved active site Gln69²⁸ (Figure 5A). Several studies have emphasized the importance of that ligand and its hydrogen-bonding partners in tuning the antioxidant activity of Fe-SOD.²⁹ It acts as a proton donor/acceptor, thereby facilitating the release of peroxide generated in the reduction of the substrate,²⁸ and it also plays a critical role in

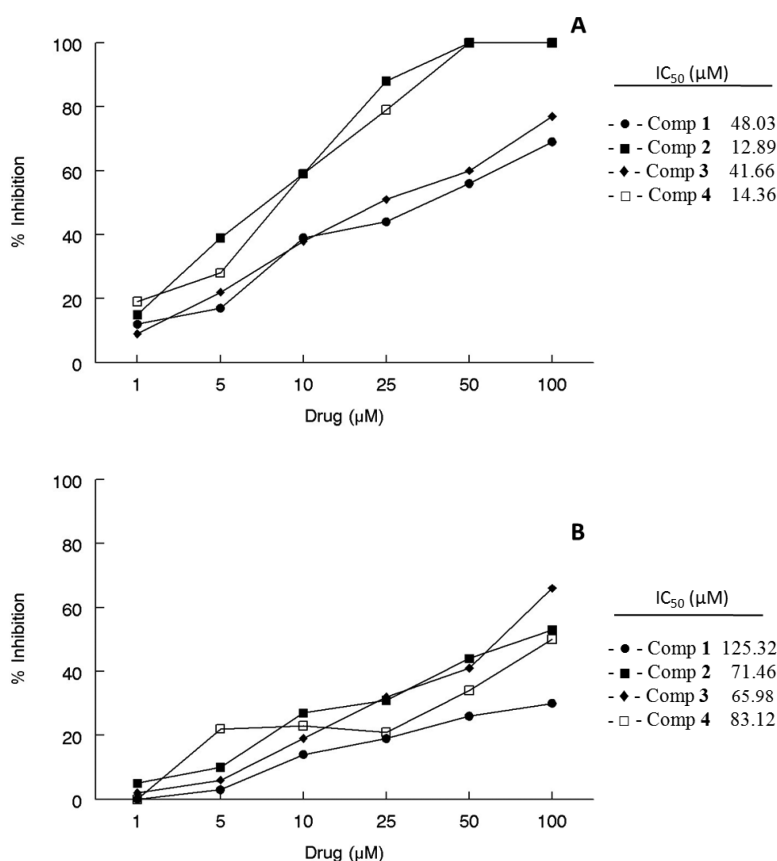


Figure 4. (A) In vitro inhibition (%) of Fe-SOD in *T. cruzi* epimastigotes for compounds 1–4 (activity, 20.77 ± 3.18 U/mg). (B) In vitro inhibition of CuZn-SOD in human erythrocytes for compounds 1–4 (activity, 23.36 ± 14.21 U/mg). Values are the average of five separate determinations. Differences between the activities of the control homogenate and those incubated with compounds 1–4 were obtained according to the Newman–Keuls test. IC₅₀ was calculated by linear regression analysis from the K_c values at concentrations used (1, 10, 25, 50, and 100 μM).

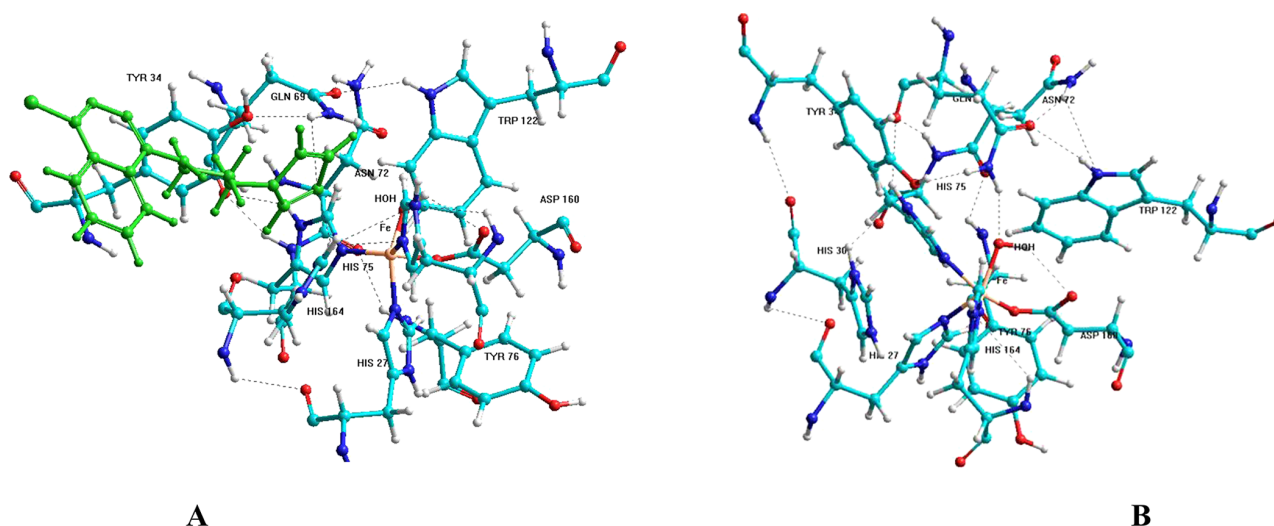


Figure 5. Molecular models of the free Fe-SOD enzyme active site with the supporting network of hydrogen bonds (A) and the same active site with compound 4 embedded in the proximity of the iron atom with the hydrogen-bonding network modified (B).

modulating the reduction potential of the iron center.²⁹ It is believed that a turnover mechanism takes place between the Fe³⁺/HO⁻ and Fe²⁺/H₂O pairs, since uptake of an electron is coupled to the acquisition of a proton, and the proton released upon reoxidation of iron contributes to the product

formation.³⁰ In that scheme, the protonation state of the coordinated solvent is supposed to be strongly influenced by H-bonding with Gln69, which in turn H-bonds to a network including Tyr34, Asn72, and Trp122, among others. On that basis, it has been proposed that enzyme inhibition could take

place by modification of the H-bonding system induced by the presence of a different ligand.³¹

The ability of related benzo[*g*]phthalazine derivatives to interact with a single strand of Fe-SOD had been previously tested by us using the AMBER force field implemented in Hyperchem 8.0,²² so the methodology was applied to the complete structure of the Fe-SOD enzyme obtained from the Brookhaven Proteine Data Bank 2gpc entry. Figure 5A shows the active site moiety of the Fe-SOD enzyme obtained as specified in the Experimental Section, with the hydrogen-bonding system outlined above displayed as dashed lines and the solvent ligand in the foreground linked to the iron atom. The interactions with Gln69 and Asp160 are clearly seen. When introducing the monoalkylamino substituted compound 4 (with a side chain that is longer than that of 2), approaching the active site took place through the interface between the two monomers of the enzyme, and the side chain was buried into one monomer and located between the tyrosine residue and the iron atom, with the imidazole *sp*² nitrogen N-3' pointing toward the metal ion in the most favored disposition (Figure 5B). As a consequence, the hydroxyl ligand was displaced a little apart from its initial position, and the H-bonding pattern seemed to be completely distorted, with Gln69 located too far from the HO⁻ group to form a stable hydrogen bond and interacting instead with the imidazole nitrogen. We think that these findings could explain in part the enzyme deactivation found experimentally.

In order to complement the molecular modeling results commented above, the most favored distance between the iron atom and the imidazole nitrogen atom N-3' for compounds 1–4 was also calculated. It was shown that the N-3' nitrogen of the dialkylamino substituted compounds 1 and 3 was located further away than that of the respective monoalkylamino substituted analogues 2 and 4: 0.409 and 0.368 nm for 1 and 3 against 0.394 and 0.343 nm for 2 and 4, suggesting that the less bulky (and more active) compounds 2 and 4 are inserted deeper into the active site. On the other hand, compound 4, with the longest side chain, is located closer to the iron atom than 2, so the chain length could be a factor favoring approach to the active site core. According to this, the synthesis of a series of phthalazine derivatives with variable chain lengths is planned in order to more accurately evaluate the effect of that modification on anti-*T. cruzi* activity.

In Vivo Anti-*T. cruzi* Activity in the Acute Phase of Chagas Disease. Since the monosubstituted compounds 2 and 4 showed remarkable SI values with respect to BZN in the *in vitro* experiments and were also the best inhibitors of the parasitic Fe-SOD enzyme, they were selected for performing further *in vivo* studies in the chosen murine model. Their trypanocidal activity during the acute phase of Chagas disease [until 40 days postinfection (pi)] was first investigated. Different groups of female Balb/c mice were inoculated with 5×10^5 metacyclic blood trypomastigotes of SN3 *T. cruzi*, and the infection started. We opted for the intraperitoneal doping route, which usually leads to lower mortality rates than the intravenous procedure,³² and testing compounds doses of 5 and 15 mg/kg body weight were administered every day from the seventh day of infestation until day 12 pi. The 5 mg/kg dose was selected in order to allow comparison of the parasitemia data with those obtained previously for related structures.²² The 15 mg/kg dose had the purpose of pondering the effect of an increment of the dose on the parasitemia levels and the mortality of mice. Parasite counting was performed on 5 μ L

blood samples obtained from the mandibular vein. None of the animals treated with either the control or compounds 2 and 4 died during the treatment. However, similar assays performed in the presence of BZN always led to mice mortality values of about 20%. As shown in Figure 5, the reduction of parasitemia in mice treated with compounds 2 and 4 was evident as early as the very beginning of treatment and was maintained until days 15–20 pi. A decrease in the trypomastigote numbers per infected cell was more intense in assays performed with the highest dose of the testing compounds (15 mg/kg body weight). However, on day 15 pi the four assays provided very similar trypomastigote numbers, resulting in parasitemia reduction values between 59% and 64% with respect to the control experiment. Although benznidazole graphic data have not been included in Figure 6 for easier visualization, it must be

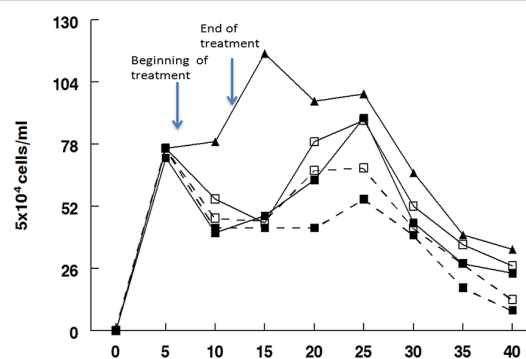


Figure 6. Parasitemia in the murine model of acute Chagas disease: control (▲) and dose receiving 5 mg/kg (continuous lines) and 15 mg/kg (dashed lines) of compound 2 (■) and compound 4 (□).

noted that parasitemia reductions originated by BZN at the 5 mg/kg body weight dose were much smaller (15.3% on day 15 pi and 16.7% on day 40 pi). After day 25 pi, the parasitemia levels began to decrease again rapidly in all cases, and when the highest dose was used, low numbers of the parasitic trypomastigotes were found at day 40 pi for the two compounds. On the whole, the behavior of 2 and 4 was similar and both of these compounds were effective in the acute phase at the concentrations selected. However, compound 2 was, in general, more efficient in the reduction of parasitemia than compound 4, especially when the 15 mg/kg concentration was tested (with a parasitemia reduction value on day 40 pi as high as 74%, in contrast with the 61% reduction found for compound 4 on the same day).

The next step was to evaluate the behavior of compounds 2 and 4 in the chronic phase, in which the positive effect of the current drugs is under much discussion.⁹ Above it is stated that the high reactivation ability of the parasitemia in immunocompromised individuals cured of Chagas disease with apparent success was a major problem. Therefore, the mice treated as described above were taken up to day 120 pi (advanced chronic phase) and were subsequently divided into two subgroups: one of them was maintained under the same conditions without further treatment, while the other was subjected to three successive cycles of immunosuppression with cyclophosphamide monohydrate for 3 consecutive weeks, as described in the Experimental Section.³³ In order to evaluate the immune status and the disease extent of the mice at that stage, blood samples were extracted for determining the parasitemia and immunoglobulin G (IgG) levels in comparison with the corresponding

nonimmunosuppressed (control) subgroup of mice. Concerning the parasitemia assay, the number of parasites was counted from blood extracted on the day after finishing the three immunosuppression cycles, and the same procedure used in the acute phase was followed. The enzyme-linked immunosorbent assay (ELISA) was used for the detection of IgG levels,³⁴ and the antigen source was the Fe-SOD enzyme isolated in our laboratory. The detection of total IgG allows the evaluation of the immune status of the mice, since that protein indicates the level of protection that should be attributed to the tested compounds, as well as the innate protection that mice have naturally. It has been described that the IgG levels are stable in the chronic phase and close to the baseline.³⁵ Table 3 (column

Table 3. OD Values Obtained in the ELISA Experiment for Compounds 2 and 4 on Day 150 pi for the Different Groups of Mice Assayed^a

	A	B	Δ_{B-A}
control	0.1089	0.1306	0.0217
2 (5 mg/kg)	0.1019	0.1130	0.0103
4 (5 mg/kg)	0.1027	0.1162	0.0143
2 (15 mg/kg)	0.1080	0.1150	0.0067
4 (15 mg/kg)	0.1083	0.1176	0.0096
mean \pm SD	0.1060 \pm 0.0030	0.1185 \pm 0.0062	

^aA = Group of non-immunocompromised mice; B = Group of immunocompromised mice; Δ_{B-A} = Differences between the OD values of the two groups. Values were obtained as an average of three independent experiments.

A) shows that the stability of IgG levels was achieved in the nonimmunosuppressed mice, with the control optical density (OD) values falling inside the calculated standard deviation (SD) of the group. However, the control OD, measured for the immunosuppressed mice, was much higher than the corresponding mean plus the calculated SD, confirming a greater presence of the parasite. If the Δ_{B-A} values obtained for compounds 2 and 4 are compared, it is clear that they led to a decrease in the infection revival. As expected, the best results were obtained with the higher 15 mg/kg dose, and it was also shown that compound 2 was more effective than 4 for the two concentrations tested, in accordance with the results obtained in the acute phase.

Results obtained from the ELISA experiments were confirmed by the parasitemia assay performed as indicated above. Figure 7 shows a very illustrative tridimensional graph indicating the percentage of parasitemia reactivation for compounds 2 and 4 at 5 and 15 mg/kg weight, in comparison with the control mice. Very low percentages were obtained in the four cases, with values ranging from 4% to 21%, whereas a reactivation of 63% was found in the control mice. BZN data obtained from the 80% mice that survived after treatment gave a substantially higher parasitemia reactivation of 36% at a weight of 5 mg/kg, indicating that the two tested compounds were clearly more efficient than the reference drug. In concordance with the ELISA test, compound 2 was more effective than 4 at both the lowest and highest doses assayed (9% and 4% reactivation for 2 against 21% and 8% for 4, respectively).

Metabolite Excretion Study. Trypanosomatids are unable to completely degrade glucose to CO₂, so they excrete part of the hexose skeleton into the medium as partially oxidized fragments, whose nature and percentage depend on the

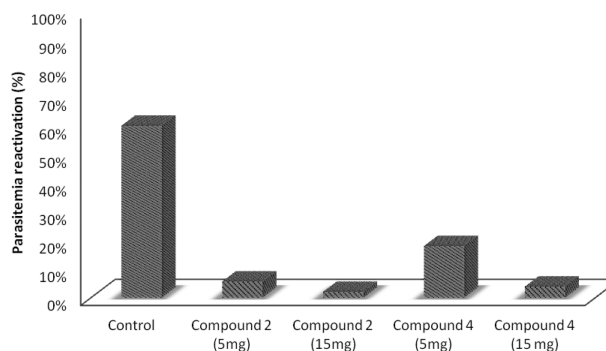


Figure 7. Reactivation percentage in mice after immunosuppression. Each group was compared with the nonimmunosuppressed group treated with the same compound and dosage. Values were obtained as an average of three independent experiments.

pathway used for glucose metabolism.³⁶ The catabolism products in *T. cruzi* are mainly succinate, acetate, L-lactate, L-alanine, and ethanol.³⁷ In order to obtain some information about the effects of compounds 1–4 on the glucose metabolism of the parasite, the ¹H NMR spectra of *T. cruzi* epimastigotes treated with the testing compounds (spectra are included in the Supporting Information data sheet for consideration by the reader) were registered, the final excretion products were identified qualitatively and quantitatively, and the results obtained were compared with those found for untreated control epimastigotes. Table 4 shows the differences found in

Table 4. Variation in the Height of the Peaks Corresponding to Catabolites Excreted by *T. cruzi* Epimastigotes in the Presence of Compounds 1–4 with Respect to the Control Test^a

compd	Eth	Lac	Ala	A	S
1	=	-15%	=	-10%	=
2	-12%	-33%	-13%	-21%	=
3	=	-24%	=	-21%	=
4	-16%	-38%	-27%	-54%	=

^aEth, ethanol; Lac, L-lactate; Ala, L-alanine; A, acetate; S, succinate; (–) peak decreasing; (=) no difference detected.

every case with respect to the control. Excretion of succinate was not affected in the presence of any of the four compounds with respect to the nontreated epimastigotes. However, the formation of acetate and L-lactate was substantially reduced in all cases, and the amounts of L-alanine and ethanol decreased in the most active monosubstituted compounds 2 and 4 but remained unaltered in their disubstituted analogues 1 and 3. Even more, excretion of acetate and L-lactate decreased by a greater extent in 2 and 4 than in their respective disubstituted counterparts. On the basis of these data, it seems that the succinate pathway is not modified by the compounds assayed, but the acetate pathway is apparently affected, especially in the case of the most active compounds, which should interfere more effectively with the enzymes involved in the production of the corresponding metabolites. As described in recent studies, succinate is produced in both the glycosome and the mitochondrion from phosphoenolpyruvate (PEP) via malate and fumarate,³⁸ and the tested compounds do not seem to interact with either of those pathways. On the other hand, acetate, L-lactate, L-alanine, and ethanol originate from the

transformation of PEP in pyruvate in the presence of pyruvate kinase or pyruvate phosphate dikinase.³⁹ With the only exception of the more elaborate acetate pathway, the other three catabolites are formed directly from pyruvate in the cytosol. On the basis of data shown in Table 4, it would be possible that compounds 2 and 4 were interacting with the pyruvate kinase enzymes and modifying the glucose metabolism of the parasite at the pyruvate stage.

Ultrastructural Alterations. The remarkable trypanosomicidal activity shown by compounds 1–4 should cause important damage in the parasite cells. Therefore, the morphological alterations caused in *T. cruzi* Maracay epimastigotes were analyzed using TEM, in order to obtain some information about the way in which the cell structure was affected. The most significant variations compared to the control cells are shown in Figure 8 for parasites treated with 1–

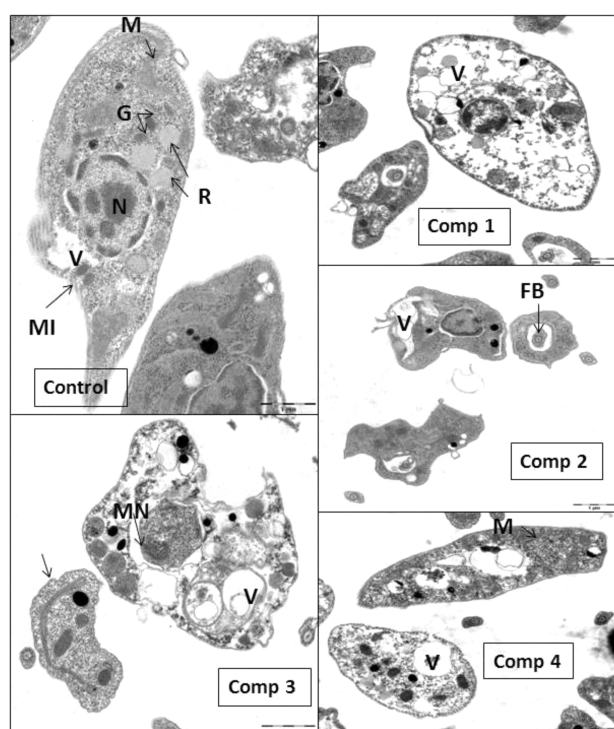


Figure 8. Ultrastructural alterations by TEM in epimastigotes of *T. cruzi* Maracay that were either untreated (control) or treated with compounds 1–4, showing organelles with their characteristics: parasite nucleus (N), reservosomes (R), vacuoles (V), mitochondrion (M), glycosomes (G), cytoskeleton microtubules (MI), large flagellar pockets (FB), parasite size reduction (arrow), altered nuclear membrane (MN): (control) untreated parasites, bar 1 μm ; (Comp 1) parasites treated with compound 1, bar 1 μm ; (Comp 2) parasites treated with compound 2, bar 1 μm ; (Comp 3) parasites treated with compound 3, bar 1 μm ; (Comp 4) parasites treated with compound 4, bar 1 μm .

4. As expected, highly significant alterations were shown by all four compounds tested. A large number of parasites died, and deep modifications were evident in most of the rest. As a general rule, many cytoplasm were completely filled with vacuoles, and many other were electron dense. The shape of many parasites was heavily distorted, with some reduced in size and others very swollen (second to fifth panels in Figure 8). In particular, parasites treated with compound 2 also showed large

flagellar pockets (third panel in Figure 8), and those assayed with 3 were characterized by nuclear membranes that were fully altered and separated into two units with a significant space between them (fourth panel in Figure 8). In the case of compound 4, mitochondria were frequently swollen, and epimastigotes with granular and membranous cytoplasm and bulky vacuoles were common. The cytoplasm were extremely disorganized (fifth panel in Figure 8). The disubstituted derivative 1 appeared to affect the cells to a lesser extent than the other compounds, but even in that case nearly 50% of the parasites still died, and many empty zones were observed in the cytoplasm (second panel in Figure 8). All of these observations regarding essential damage in the parasite cells agree with the significant activity found for compounds 1–4.

From the results of this work, it can be concluded that the imidazole-based monoalkylaminophthalazine derivatives 2 and 4 showed remarkable *in vitro* and *in vivo* trypanosomicidal activity, being especially active against the acute phase of Chagas disease. These compounds also showed a much lower level of toxicity in Vero cells than BZN, and they were almost inactive against human SOD but active against the Fe-SOD of the parasite. Furthermore, both of these compounds substantially decreased the parasitemia reactivation in immunocompromised mice, and reactivation at the higher dose was negligible in the case of 4, which is an unusual characteristic in most of the commonly prescribed drugs against Chagas disease. These tentative results suggest the convenience of performing further histopathological studies on target organs, which will be the object of a next publication. On this basis, we believe that both compounds fulfill the requirements for performing a more detailed study of the nature of the mechanisms involved in their activity patterns and, furthermore, that they are serious candidates for studying antiparasitical activity at a higher level.

EXPERIMENTAL SECTION

Chemistry. The starting amines 3-(imidazol-1-yl)propylamine and 2-(imidazol-4-yl)ethylamine (histamine) were purchased from Sigma-Aldrich and used without further purification. 1,4-Dichlorophthalazine was obtained from commercial phthalhydrazide (Sigma-Aldrich) following a standard method.⁴⁰ Solvents were dried using standard techniques.⁴¹ All of the reactions were monitored using thin layer chromatography (TLC) on precoated aluminum sheets of silica gel 60PF₂₅₄ (Merck, layer thickness 0.2 mm). Compounds were detected with UV light (254 nm). Chromatographic separations were performed on columns in the indicated solvent system using flash chromatography on silica gel (particle size 0.040–0.063 mm). Melting points were determined in a Gallenkamp apparatus and were uncorrected. ¹H NMR spectra were recorded on a Bruker 300 and a Variant XL 300 at 300 MHz, and ¹³C NMR spectra were recorded at 75 MHz at room temperature employing DMSO-*d*₆ as the solvent. Chemical shifts were reported in ppm (δ scale) from tetramethylsilane (TMS). All assignments were performed on the basis of ¹H–¹³C heteronuclear multiple quantum coherence experiments (gHMQC). IR spectra were recorded on a Perkin-Elmer 257 spectrometer (4000–400 cm^{-1} range). Electrospray mass spectra were recorded with a Hewlett-Packard 1100 MSD apparatus. Elemental analyses were performed in a Perkin-Elmer 2400-CHN instrument by the CAI of Microanalysis, Universidad Complutense, Madrid, Spain. Elemental analysis was used to ascertain a purity higher than 95% for all the biologically tested compounds.

Synthesis of 1 and 3 (Method A). A solution of 1,4-dichlorophthalazine, the corresponding aminoalkylimidazole, and triethylamine in xylene was heated at 120 °C for several hours. The reaction mixture was cooled to room temperature and the solvent removed under reduced pressure. The solid residue was purified by

column chromatography with a polarity-increasing chloroform/methanol/ammonium hydroxide mixture as the eluent to obtain the desired product.

1,4-Bis[2-(imidazol-4-yl)ethylamino]phthalazine (1). This compound was prepared by heating 1,4-dichlorophthalazine (450 mg, 2.26 mmol), 2-(imidazol-4-yl)ethylamine (500 mg, 4.50 mmol), and triethylamine (1.36 g, 13.5 mmol) in 45 mL of xylene during 6 h. Further workup and purification of the reaction mixture afforded 200 mg (21%) of a solid which was identified as 1·2HCl ($R_f = 0.52$, $\text{CHCl}_3/\text{MeOH}/\text{NH}_4\text{OH}$, v/v 8/2/1), mp 198–200 °C. IR (KBr) = 3722, 3169, 1928, 1742, 1636, 1545, 1482, 1359, 1223, 945, 775 cm^{-1} . ^1H NMR (DMSO- d_6): δ 8.44 (m, 2H, H-5, H-8), 8.03 (m, 2H, H-6, H-7), 7.81 (s, 2H, H-2'), 6.99 (s, 2H, H-5'), 3.66 (t, 4H, Ha), 2.97 (t, 4H, H β) ppm. ^{13}C NMR (DMSO- d_6): δ 148.02 (C-1, C-4), 134.54/134.42 (C-2', C-4'), 134.02 (C-6, C-7), 124.04 (C-5, C-8), 121.25 (C-4a, C8a), 116.31 (C-5'), 42.33 (C α), 25.14 (C β) ppm. MS-ESI (MeOH): m/z (%): 349 ($\text{MH}^+ - 2\text{HCl}$, 100). Anal. ($\text{C}_{18}\text{H}_{20}\text{N}_8 \cdot 2\text{HCl} \cdot 5\text{H}_2\text{O}$) C, H, N.

1,4-Bis[3-(imidazol-1-yl)propylamino]phthalazine (3). This compound was prepared by heating 1,4-dichlorophthalazine (1.45 g, 7.28 mmol), 3-(imidazol-1-yl)propylamine (1.90 g, 14.52 mmol), and triethylamine (1.37 g, 13.8 mol) in 60 mL of xylene during 24 h. Further workup and purification of the reaction mixture afforded 525 mg (16%) of a solid which was identified as 3·2HCl ($R_f = 0.11$, $\text{CHCl}_3/\text{MeOH}/\text{NH}_4\text{OH}$, v/v 8/2/1), mp 190–192 °C. IR (KBr) = 3669, 3405, 3213, 3107, 2960, 1641, 1562, 1515, 1371, 1342, 1235, 1091, 662 cm^{-1} . ^1H NMR (DMSO- d_6): δ 8.89 (m, 2H, H-5, H-8), 8.17 (m, 2H, H-6, H-7), 7.75 (s, 2H, H-2'), 7.22 (s, 2H, H-5'), 6.96 (s, 2H, H-4'), 4.25 (t, 4H, H γ), 3.53 (t, 4H, Ha), 2.31 (m, 4H, H β) ppm. ^{13}C NMR (DMSO- d_6): δ 148.43 (C-1, C-4), 137.50 (C-2'), 132.67 (C-6, C-7), 128.15 (C-4'), 124.03 (C-5, C-8), 121.12 (C-5'), 119.80 (C-4a, C-8a), 43.99 (C γ), 38.77 (C α), 29.52 (C β) ppm. MS-ESI (MeOH): m/z (%): 377 ($\text{MH}^+ - 2\text{HCl}$, 100). Anal. ($\text{C}_{20}\text{H}_{24}\text{N}_8 \cdot 2\text{HCl} \cdot \text{H}_2\text{O}$) C, H, N.

Synthesis of 2 and 4 (Method B). A solution of 1,4-dichlorophthalazine, the corresponding aminoalkylimidazole, and sodium carbonate in acetonitrile was heated to reflux for several hours. The reaction mixture was cooled to room temperature, and a solid containing the reaction products and potassium carbonate was separated by filtration and extracted three times with chloroform. The organic solution was evaporated under reduced pressure and the residue was purified by flash column chromatography with a polarity increasing chloroform/methanol mixture as eluent to obtain the desired product.

1-[2-(imidazol-4-yl)ethylamino]-4-chlorophthalazine (2). This compound was prepared by heating 1,4-dichlorophthalazine (895 mg, 4.50 mmol), 2-(imidazol-4-yl)ethylamine (500 mg, 4.50 mmol), and potassium carbonate (3.10 g, 29.2 mmol) in 70 mL of acetonitrile during 72 h. Further workup and purification of the reaction mixture afforded 200 mg (16%) of a solid which was identified as free 2 ($R_f = 0.45$, $\text{CHCl}_3/\text{MeOH}$, v/v 8/2), mp 158–160 °C. IR (KBr) = 3219, 3102, 2886, 2932, 1731, 1576, 1525, 1484, 1362, 1181, 981, 769 cm^{-1} . ^1H NMR (DMSO- d_6): δ 8.33 (m, 1H, H-8), 8.05 (m, 1H, H-5), 8.02 (m, 2H, H-6, H-7), 7.59 (s, 1H, H-2'), 6.88 (s, 1H, H-5'), 3.79 (t, 2H, Ha), 2.95 (m, 2H, H β) ppm. ^{13}C NMR (DMSO- d_6): δ 154.01 (C-1), 143.96 (C-4), 134.59 (C-2'/C-4'), 132.59/132.50 (C-6/C-7), 125.26 (C-4a), 124.48 (C-8), 122.76 (C-5), 120.00 (C-8a), 116.70 (C-5'), 41.35 (C α), 25.97 (C β) ppm. MS-ESI (MeOH): m/z (%): 273 (M^+ , 100). Anal. ($\text{C}_{13}\text{H}_{12}\text{N}_5\text{Cl} \cdot \text{H}_2\text{O}$) C, H, N.

1-[3-(imidazol-1-yl)propylamino]-4-chlorophthalazine (4). This compound was prepared by heating 1,4-dichlorophthalazine (200 mg, 0.995 mmol), 3-(imidazol-1-yl)propylamine (124 mg, 0.995 mmol), and potassium carbonate (1.37 g, 12.9 mmol) in 70 mL of acetonitrile during 45 h. Further workup and purification of the reaction mixture afforded 138 mg (48%) of a solid which was identified as free 4 ($R_f = 0.52$, $\text{CHCl}_3/\text{MeOH}$, v/v 8/2), mp 183–185 °C. IR (KBr) = 3666, 3216, 3107, 2964, 2932, 1679, 1574, 1520, 1416, 1286, 1178, 1106, 799, 660 cm^{-1} . ^1H NMR (DMSO- d_6): δ 8.68 (m, 1H, H-8), 8.50 (m, 1H, H-5), 8.17 (m, 2H, H-6, H-7), 7.65 (s, 1H, H-

2'), 7.21 (s, 1H, H-5'), 6.95 (s, 1H, H-4'), 4.22 (t, 2H, H γ), 3.64 (t, 2H, Ha) 2.30 (m, 2H, H β) ppm. ^{13}C NMR (DMSO- d_6): δ 154.13 (C-1), 144.14 (C-4), 137.60 (C-2'), 132.90/132.49 (C-6/C-7), 128.4 (C-4'), 125.25 (C-4a), 124.49 (C-8), 122.88 (C-5), 120.00 (C-8a), 119.50 (C-5'), 44.01 (C γ), 38.46 (C α), 29.84 (C β) ppm. MS-ESI (MeOH), m/z (%): 287 (M^+ , 100). Anal. ($\text{C}_{14}\text{H}_{14}\text{N}_5\text{Cl}$) C, H, N.

Parasite Strain, Culture. *Trypanosoma cruzi* SN3 strain of IRHOD/CO/2008/SN3 was isolated from domestic *Rhodnius prolixus*; biological origin is Guajira (Colombia).⁴² Epimastigote forms were grown in axenic Grace's insect medium (Gibco) supplemented with 10% inactivated fetal bovine serum (FBS) at 28 °C in tissue-culture flasks. In order to obtain the parasite suspension for the trypanocidal assay, the epimastigote culture (in the exponential growth phase) was concentrated by centrifugation at 400g for 10 min and the number of flagellates was counted in a hemocytometric chamber.

Transformation of Epimastigotes to the Metacyclic Form. Metacyclogenesis was induced by culturing the parasites at 28 °C in modified Grace's medium (Gibco) for 12 days, as described previously.⁴³ Twelve days after cultivation at 28 °C, metacyclic forms were counted in a Neubauer hemocytometric chamber. The proportion of metacyclic forms was around 40% at this stage.

Cell Culture and Cytotoxicity Tests. Vero cells (Flow) were grown in Roswell Park Memorial Institute (RPMI) medium (Gibco), supplemented with 10% inactivated FBS, in a humidified 95% air, 5% CO_2 atmosphere at 37 °C for 2 days. For the cytotoxicity testing, cells were placed in 25 mL Colie-based bottles (Sterling) and centrifuged at 100g for 5 min. The culture medium was removed, and fresh medium was added to a final concentration of 1×10^5 cells/mL. This cell suspension was distributed in a culture tray (with 24 wells) at a rate of 100 μL /well and incubated for 2 days at 37 °C in a humidified atmosphere enriched with 5% CO_2 . The medium was removed, and fresh medium was added together with each test compound (at concentrations of 100, 50, 25, 10, and 1 μM). After 72 h of treatment, cell viability was determined by flow cytometry according to a methodology described by us.⁴⁴

In Vitro Activity Assays: Extracellular Forms. Epimastigote Assay. Epimastigotes were collected in the exponential growth phase and distributed in culture trays (with 24 wells) at a final concentration of 5×10^4 parasites/well. The compounds to be tested and benznidazole were dissolved in medium trypanosomes liquid (MTL) and were tested at 100, 50, 25, 10, and 1 μM . The effects of the different concentrations of each compound against the epimastigotes were tested for 72 h using a Neubauer hemocytometric chamber. The trypanocidal effect is expressed as IC_{50} , i.e., the concentration required to result in 50% inhibition, as calculated by linear-regression analysis from the K_c of the concentrations used.

In Vitro Activity Assays: Intracellular forms. Axenic Amastigotes Assay. Axenic amastigotes of *T. cruzi* were cultured following the methodology described previously by Moreno et al.⁴⁵ Thus, the epimastigote transformation to amastigotes was achieved after 3 days of culture in M199 medium (Invitrogen, Leiden, The Netherlands) supplemented with 10% heat-inactivated FCS, 1 g/L β -alanine, 100 mg/L L-asparagine, 200 mg/L saccharose, 50 mg/L sodium pyruvate, 320 mg/L malic acid, 40 mg/L fumaric acid, 70 mg/L succinic acid, 200 mg/L α -ketoglutaric acid, 300 mg/L citric acid, 1.1 g/L sodium bicarbonate, 5 g/L 4-morpholinoethanesulfonic acid (MES), 0.4 mg/L hemin, and 10 mg/L gentamicine, pH 5.4, at 37 °C. The effect of each compound against the axenic amastigotes was tested for 48 h using a Neubauer hemocytometric chamber. The trypanocidal effect is expressed as IC_{50} , i.e. the concentration required to result in 50% inhibition, as calculated by linear-regression analysis from the K_c of the concentrations used.

Amastigotes Assay. Vero cells were cultured in RPMI medium in a humidified 95% air and 5% CO_2 atmosphere at 37 °C. The cells were seeded at a density of 1×10^4 cells/well in 24-well microplates (Nunc) with rounded coverslips on the bottom and then cultivated for 2 days. Afterward, adhered Vero cells were infected in vitro with metacyclic forms of *T. cruzi* at a ratio of 10:1 and maintained for 24 h at 37 °C in 5% CO_2 in air. The extracellular parasites were removed by washing,

and the infected cultures were incubated with the compounds (1, 10, 25, 50, and 100 μM) and cultured for 72 h in RPMI and 10% inactivated fetal bovine serum. The activity of the compounds was determined from the percentage reduction in the number of amastigotes in the treated and untreated cultures in methanol-fixed and Giemsa-stained preparations. The values are the mean of four separate determinations.⁴⁶ The trypanocidal effect was expressed as IC_{50} .

Blood Trypomastigotes Assay. Compounds 1–4 were also evaluated on blood trypomastigote forms of *T. cruzi*. BALB/c mice infected with *T. cruzi* were used 7 days after infection. Blood was obtained by cardiac puncture using 3.8% sodium citrate as anticoagulant in a 7:3 blood/anticoagulant ratio. The parasitemia in the infected mice was about 1×10^5 parasites/mL. The compounds were diluted in phosphate-buffered saline solution (PBS) to give a final concentration 10, 25, and 50 μM for each product. Aliquots (20 μL) of each solution were mixed in cultures trays (96 wells) with 55 μL of infected blood containing the parasites at a concentration near 1×10^6 parasites/mL. Infected blood with PBS, at the same concentrations as the products, was used as control. The plates were shaken for 10 min at room temperature and kept at 4 $^\circ\text{C}$ for 24 h. Each solution was examined microscopically (Olympus CX41) for parasite counting using the Neubauer hemocytometric chamber (a dilution of 1:100 in PBS was necessary to get into the range of counting). The activity (percent of parasites reduction) was compared with that of the control.

Infectivity Assay. Vero cells were cultured in RPMI medium as described above. Afterward, the cells were infected in vitro with metacyclic forms of *T. cruzi* at a ratio of 10:1. The test compounds (IC_{25} concentrations) were added immediately after infection and incubated for 12 h at 37 $^\circ\text{C}$ in a 5% CO_2 atmosphere. The extracellular parasites and the test compounds were removed by washing, and the infected cultures were grown for 10 days in fresh medium. Fresh culture medium was added every 48 h. The activity of each compound tested was determined from the percentage of infected cells and the number of amastigotes per infected cell in treated and untreated cultures in the methanol-fixed and Giemsa-stained preparations. The percentage of infected cells and the mean number of amastigotes per infected cell were determined by analyzing more than 100 host cells distributed throughout randomly chosen microscopic fields. The values are the mean of four separate determinations. The number of trypomastigotes in the medium was determined as previously described.⁴³

SOD Enzymatic Inhibition. The parasites cultured as described above were centrifuged. The pellet was suspended in 3 mL of sodium chloride-Tris-EDTA (STE) buffer [0.25 M sucrose, 25 mM Tris-HCl, 1 M ethylenediaminetetraacetic acid (EDTA), pH 7.8] and disrupted by three cycles of sonic disintegration, 30 s each at 60 V. The sonicated homogenate was centrifuged at 1500g for 5 min at 4 $^\circ\text{C}$, and the pellet was washed three times in ice-cold STE buffer. This fraction was centrifuged (2500g for 10 min at 4 $^\circ\text{C}$), and the supernatant was collected. The protein concentrations were determined using the Bradford method.⁴⁷ Iron and copper–zinc superoxide dismutase (Fe-SOD and CuZn-SOD) activities were determined using the method described by Beyer and Fridovich,⁴⁸ which measures the reduction in nitroblue tetrazolium (NBT) by superoxide ions. Into each bucket, an amount of 845 μL of stock solution [3 mL of L-metionine (300 mg, 10 mL^{-1}), 2 mL of NBT (1.41 mg, 10 mL^{-1}), and 1.5 mL of Triton X-100 1% (v/v)] was added, along with 30 μL of the parasite homogenate fraction, 10 μL of riboflavin (0.44 mg, 10 mL^{-1}), and an equivalent volume of the different concentrations of the compounds tested. Five different concentrations were used for each product: 1, 2.5, 5, 12.5, and 25 μM (equivalent to 5, 12.5, 25, 62, and 125 μL , respectively, of the Stock solution). In the control experiment the volume was made up to 1000 μL with 50 mM potassium phosphate buffer (pH 7.8, 3 mL), whereas 30 μL of the parasite homogenate fraction was added to the mixtures containing the compounds. Then the absorbance (A_0) was measured at 560 nm in a spectrophotometer. Following this, each bucket was illuminated with UV light for 10 min under constant stirring and the absorbance (A_1) was measured. The human CuZn-SOD, coenzymes, and substrates used in these assays were obtained

from Sigma Chemical Co. The data obtained were analyzed using the Newman–Keuls test.

Molecular Modeling. Molecular modeling studies were carried out using the AMBER method implemented in the HyperChem Professional 8.0 package,⁴⁹ modified by the inclusion of appropriate parameters.⁵⁰ Starting structures for compounds 1–4 were built by using HyperChem capabilities. Its geometry was minimized to a maximum energy gradient of 0.1 kcal/mol with the AMBER force field, using the Polak–Ribiere (conjugate gradient) minimizer, and a “simulated annealing” procedure was used to cover all conformational space. The most stable extended geometry was always used in all calculations of interaction with the enzyme. To mimic the conditions used in the activity measurements, i.e., water as solvent, all calculations were carried out in vacuo with a distance dependent dielectric constant. Charge assignments for all atoms were done by means of ab initio calculations using STO-3G basis set, as it is compatible with AMBER force field, prior to energy minimization using AMBER. The *T. cruzi* Fe-SOD enzyme structure was obtained from the Brookhaven Protein Data Bank (2gpc) and its energy minimized in the same way. Interaction studies were performed starting from structures with the compound positioned in the border of the enzyme cavity. Entering the cavity was forced using a restraint to the N–Fe distance, slowly decreasing this distance, and letting the complex achieve the minimum energy conformation with no restraints, for all the small driving steps, using the same conditions mentioned above.

In Vivo Trypanosomicidal Activity Assay. This experiment was performed using the rules and principles of the international guide for biomedical research in experimental animals and with the approval of the ethical committee of the University of Granada, Spain. Groups of six BALB/c albino female mice (6–8 weeks old, 25–30 g weight), maintained under standard conditions, were inoculated via the intraperitoneal route (bloodstream) with 5×10^5 metacyclic *T. cruzi* trypomastigotes obtained from previously infected mice blood. The animals were divided as follows: I, positive control group (mice infected but not treated); II, study group (mice infected and treated with two different concentrations of the compounds under study, one subplot per every concentration tested). An assessment of the effect of the compounds on the level of parasitemia after treatment (in acute and chronic phases) was performed by counting, as was an ELISA experiment (also comparing acute and chronic phases). For the acute phase assays, the administration of the testing compounds was begun on the seventh day of infestation once the infection was confirmed, and doses of 5 and 15 mg/kg body weight/day were used for 5 consecutive days (7–12 days postinfection). Peripheral blood was obtained from the mandibular vein of each treated mouse (5 μL samples) and dissolved in 495 μL of a PBS solution at a dilution of 1:100. The circulating parasite numbers were quantified with a Neubauer’s chamber for counting blood cells. This counting was performed every 3 days during 40 days (acute phase). The number of metacyclic forms was expressed as parasites/mL. After day 60, the animals entered the chronic phase of the experiment, and on day 120 the mice were submitted to successive cycles of immunosuppression with cyclophosphamide monohydrate. The immunosuppression protocol was maintained for 3 weeks and consisted of three cycles of 50 mg cyclophosphamide/kg body weight for 4 consecutive days, with an interval of 3 days between each cycle.³³ Parasitemia at that stage was evaluated from the next day after finishing the third cycle, according to the procedure described for the acute phase. After that, the animals were sacrificed. Animals were considered cured when, after inoculation with *T. cruzi* and further treatment with the testing compounds, reappearance of parasitemia after three cycles of immunosuppression was not found³¹ and/or the presence of amastigote nests or other forms of parasites in histological sections was not observed.

ELISA.³⁴ Fe-SOD excreted from the parasite, cultured and processed as described in the corresponding section, was used as the antigen fraction. The total homogenate and purified protein fractions were coated onto polystyrene microtiter plates (Nunc, Denmark) at 5 and 1.5 μg , respectively, in carbonate buffer (pH 8.2) for 2 h at 37 $^\circ\text{C}$. The antigen remaining on the plate was eliminated by washing three

times with 0.05% PBS-Tween 20 (washing buffer). Free adsorption sites were taken by incubation (2 h at 37 °C) with blocking buffer [0.2% PBS-Tween 20, 1% bovine serum albumin (BSA)]. After the mixture was washed as described previously, the plates were incubated (45 min at 37 °C) with a serum dilution of 1:100 in washing buffer. After a second wash, the plates were incubated in darkness for 20 min with 100 μ L of an enzyme-conjugated antibody (anti-IgG peroxidase) at a dilution of 1:1000. The enzyme reaction was developed with the chromogenic substrate *o*-phenylenediamine dihydrochloride (OPD, Sigma) and 10 μ L of 30% H₂O₂ per 25 mL for 20 min in the dark. The reaction was stopped by the addition of 50 μ L of HCl, 3 N. Absorbance was read at 492 nm in a microplate reader (Sunrise, TECAN). All of the samples were analyzed in triplicate in polystyrene microtiter plates. Mean and standard deviations of the optical densities of the negative control sera were used to calculate the cutoff value.

Metabolite Excretion. Cultures of *T. cruzi* epimastigotes (initial concentration of 5×10^5 cells/mL) received IC₂₅ of the compounds (except for the control cultures). After incubation for 96 h at 28 °C, the cells were centrifuged at 400g for 10 min. The supernatants were collected in order to determine the excreted metabolites through ¹H NMR, and the chemical shifts were expressed in parts per million (ppm), using sodium 2,2-dimethyl-2-silapentane-5-sulfonate as the reference signal. The chemical displacements used to identify the respective metabolites were consistent with those described previously by us.⁵²

Ultrastructural Alterations. The parasites were cultured at a density of 5×10^5 cells/mL in each corresponding medium containing the compounds tested at the concentration of IC₂₅. After 96 h, these cultures were centrifuged at 400g for 10 min, and the pellets produced were washed in PBS before being then mixed with 2% (v/v) paraformaldehyde/glutaraldehyde in 0.05 M cacodylate buffer (pH 7.4) for 4 h at 4 °C. Following this, the pellets were prepared for transmission electron microscopy study using a technique described by us.⁵³

■ ASSOCIATED CONTENT

🔗 Supporting Information

Results from combustion analysis, molecular modeling of interactions with the Fe-SOD enzyme, and NMR spectra obtained from the metabolite excretion studies. This material is available free of charge via the Internet at <http://pubs.acs.org>.

■ AUTHOR INFORMATION

Corresponding Author

*For M.S.-M.: phone, +34-958-242-369; fax, +34-958-243-862; e-mail, msanchem@ugr.es. For F.G.-C.: phone, +34-91-394-4229; fax, +34-91-394-4103; e-mail, fercon@quim.ucm.es. For P.N.: phone, +34-91-258-7572; fax, +34-91-564-4853; e-mail, pnmnt38@iqm.csic.es.

Notes

Conflict of Interest Disclosure. The authors declare no competing financial interest.

■ ACKNOWLEDGMENTS

The authors thank the MCINN Projects: Consolider Ingenio CSD2010-00065 and CTQ2009-14288-C04-01 for financial support. We are also grateful to the NMR and elemental analysis by CAI of the Universidad Complutense (Madrid, Spain) and also to the transmission electron microscopy and nuclear magnetic resonance spectroscopy services of the CIC-University of Granada, Spain.

■ DEDICATION

This paper is dedicated to the memory of Prof. Mercedes Pardo Criado, without whose contribution and enthusiasm the

synthetic branch of this research group would not have evolved as it has. She is sorely missed.

■ ABBREVIATIONS USED

SOD, superoxide dismutase; BZN, benzimidazole; NADH, nicotinamide adenine dinucleotide; AIDS, acquired immunodeficiency syndrome; TEM, transmission electron microscopy; HMQC, heteronuclear single quantum coherence experiment; SI, selectivity index; dpi, days postinfection; IgG, immunoglobulin G; ELISA, enzyme-linked immunosorbent assay; OD, optical density; SD, standard deviation; PEP, phosphoenolpyruvate; TLC, thin-layer chromatography; HMBC, heteronuclear multiple-bond correlation spectroscopy; TMS, tetramethylsilane; DMSO, dimethylsulfoxide; MS-ESI, electrospray ionization mass spectrometry; FBS, fetal bovine serum; RPMI, Roswell Park Memorial Institute; MES, 4-morpholinoethanesulfonic acid; PBS, phosphate buffered saline solution; FCS, fetal calf serum; MTL, medium trypanosomes liquid; EDTA, ethylenediaminetetraacetic acid; STE, sodium chloride-Tris-EDTA; NBT, nitroblue tetrazolium; BSA, bovine serum albumin; OPD, *o*-phenylenediamine dihydrochloride

■ REFERENCES

- (1) Mc Kerrow, J. H.; Doyle, P. S.; Engel, J. C.; Podust, L. M.; Robertson, S. A.; Ferreira, R.; Saxton, T.; Arkin, M.; Kerr, I. D.; Brinen, I. S.; Craik, C. S. Two approaches to discovering and developing new drugs for Chagas disease. *Mem. Inst. Oswaldo Cruz* **2009**, *104*, 263–269.
- (2) Rassi, A., Jr.; Rassi, A.; Marin-Neto, J. A. Chagas disease. *Lancet* **2010**, *375*, 1388–1402.
- (3) Gascon, J.; Bern, C.; Pinazo, M. J. Chagas disease in Spain, the United States and other non-endemic countries. *Acta Trop.* **2010**, *115*, 22–27.
- (4) Bern, C.; Montgomery, S. P.; Katz, L.; Caglioti, S.; Stramer, S. L. Chagas disease and the US blood supply. *Curr. Opin. Infect. Dis.* **2008**, *21*, 476–482.
- (5) Apt, W.; Zulantay, I. Estado actual en el tratamiento de la enfermedad de Chagas. *Rev. Med. Chile* **2011**, *139*, 247–257.
- (6) Hall, B. S.; Wilkinson, S. R. Activation of benzimidazole by trypanosomal type I nitroreductases results in glyoxal formation. *Antimicrob. Agents Chemother.* **2012**, *56* (1), 115–123.
- (7) Viotti, R.; Vigliano, C.; Lococo, B.; Alvarez, M. G.; Petti, M.; Bertocchi, G.; Armenti, A. Side-effects of benzimidazole as treatment in chronic Chagas disease: fears and realities. *Expert Rev. Anti-Infect. Ther.* **2009**, *7*, 157–163.
- (8) Castro, J. A.; de Mecca, J. J.; Bartel, L. C. Toxic side effects of drugs used to treat Chagas disease. *Hum. Exp. Toxicol.* **2006**, *25* (8), 471–479.
- (9) Coura, J. R.; de Castro, S. L. A critical review on Chagas disease chemotherapy. *Mem. Inst. Oswaldo Cruz* **2002**, *97*, 3–24.
- (10) Le Loup, G.; Ibrahim, K.; Malvy, D. Chagas disease and immunodeficiency: HIV infection and transplantation. *Bull. Soc. Pathol. Exot.* **2009**, *102* (5), 310–318.
- (11) Rivera, J.; Hillis, L. D.; Levine, B. D. Reactivation of cardiac Chagas disease in acquired immune deficiency syndrome. *Am. J. Cardiol.* **2004**, *94*, 1102–1103.
- (12) Gallerano, V.; Consigli, J.; Pereyra, S.; Gomez-Zanni, S.; Daniello, C.; Gallerano, R. H.; Guidi, A. Chagas disease reactivation with skin symptoms in a patient with kidney transplant. *Int. J. Dermatol.* **2007**, *46*, 607–610.
- (13) Center for Disease Control and Prevention. Chagas disease after organ transplantation. *Morbidity Mortality Wkly. Rep.* **2001**, *51*, 210–212.
- (14) Corti, M.; Yampolski, C. Prolonged survival and immune reconstitution after chagasic meningoencephalitis in a patient with

acquired immunodeficiency syndrome. *Rev. Soc. Bras. Med. Trop.* **2006**, *39*, 85–88.

(15) Ferreira, M. S. Chagas disease and immunosuppression. *Mem Inst. Oswaldo Cruz* **1999**, *94*, 325–327.

(16) Campos, S. V.; Strabelli, T. M. V.; Neto, V. A.; Silva, C. P.; Bacal, F.; Bocchi, E. A.; Stolf, N. A. G. Risk factors for Chagas disease reactivation after heart transplantation. *J. Heart Lung Transplant.* **2008**, *27* (6), 597–602.

(17) Doyle, P. S.; Zhou, Y. M.; Engel, J. M.; McKerrow, J. H. A cysteine protease inhibitor cures Chagas disease in an immunodeficient-mouse model of infection. *Antimicrob. Agents Chemother.* **2007**, *51* (11), 3932–3939.

(18) Soeiro, M. N.; de Castro, S. L. *Trypanosoma cruzi* targets for new chemotherapeutic approaches. *Expert Opin. Ther. Targets* **2009**, *13* (1), 105–121.

(19) (a) Mehlotra, R. K. Antioxidant defense mechanisms in parasitic protozoa. *Crit. Rev. Microbiol.* **1996**, *22* (4), 295–314. (b) Atwood, J. A., 3rd; Weatherly, D. B.; Minning, T. A.; Bundy, B.; Cavola, C.; Opperdoes, F. R.; Orlando, R.; Tarleton, R. L. The *Trypanosoma cruzi* proteome. *Science* **2005**, *309*, 473–476.

(20) Rodríguez-Ciria, M.; Sanz, A. M.; Yunta, M. J. R.; Gomez-Contreras, F.; Navarro, P.; Sanchez-Moreno, M.; Booutaleb-Charki, S.; Osuna, A.; Castiñeiras, A.; Pardo, M.; Cano, C.; Campayo, L. 1,4-Bis(alkylamino)benzo[g]phthalazines able to form complexes of Cu(II) which as free ligands behave as SOD inhibitors and show efficient in vitro activity against *Trypanosoma cruzi*. *Bioorg. Med. Chem.* **2007**, *15*, 2081–2091.

(21) Sanz, A. M.; Gomez-Contreras, F.; Navarro, P.; Sánchez-Moreno, M.; Boutaleb-Charki, S.; Campuzano, J.; Pardo, M.; Osuna, A.; Cano, C.; Yunta, M. J. R.; Campayo, L. Efficient inhibition of Fe-SOD and of *Trypanosoma cruzi* growth by benzo[g]phthalazine derivatives functionalized with one or two imidazole rings. *J. Med. Chem.* **2008**, *51*, 1962–1966.

(22) Sánchez-Moreno, M.; Sanz, A. M.; Gómez-Contreras, F.; Navarro, P.; Marín, C.; Ramírez-Macias, I.; Rosales, M. J.; Olmo, F.; García-Aranda, I.; Campayo, L.; Cano, C.; Arrebola, F.; Yunta, M. J. R. In vivo trypanosomicidal activity of imidazole- or pyrazole-based benzo[g]phthalazine derivatives against acute and chronic phases of Chagas disease. *J. Med. Chem.* **2011**, *54*, 970–979.

(23) Sánchez-Moreno, M.; Gómez-Contreras, F.; Navarro, P.; Marín, C.; Ramírez-Macias, I.; Olmo, F.; Sanz, A. M.; Campayo, L.; Cano, C.; Yunta, M. J. R. In vitro leishmanicidal activity of imidazole- or pyrazole-based benzo[g]phthalazine derivatives against *L. infantum* and *L. braziliensis* species. *J. Antimicrob. Chemother.* **2012**, *67*, 387–397.

(24) López-Antuñano, F. J. Quimioterapia de las infecciones producidas por *Trypanosoma cruzi*. *Salud Publica Mex.* **1997**, *39* (5), 463–471.

(25) Sánchez-Moreno, M.; Marín, C.; Navarro, P.; Lamarque, L.; García-España, E.; Miranda, C.; Huertas, O.; Olmo, F.; Gómez-Contreras, F.; Pitarch, J.; Arrebola, F. In vitro and in vivo trypanosomicidal activity of pyrazole-containing macrocyclic and macrobicyclic polyamines: their action on acute and chronic phases of Chagas disease. *J. Med. Chem.* **2012**, *55* (9), 4231–4243.

(26) Villagran, M. E.; Marín, C.; Rodríguez-González, I.; de Diego, J. A.; Sanchez-Moreno, M. Use of an iron superoxide dismutase excreted by *T. cruzi* in the diagnosis of Chagas disease: seroprevalence in rural zones of the state of Queretaro, Mexico. *Am. J. Trop. Med. Hyg.* **2005**, *73*, 510–516.

(27) Miller, A. F.; Sorkin, D. L.; Padmakumar, K. Anion binding properties of reduced and oxidized iron-containing superoxide dismutase reveal no requirement for tyrosine 34. *Biochemistry* **2005**, *44*, 5969–5981.

(28) Yikilmaz, E.; Rodgers, D. W.; Miller, A. F. The crucial importance of chemistry in the structure–function link: manipulating hydrogen bonding in iron-containing superoxide dismutase. *Biochemistry* **2006**, *45*, 1151–1161.

(29) (a) Vance, C. K.; Miller, A. F. Specificity and phenetic relationships of iron- and manganese-containing superoxide dismutases on the basis of structure and sequence comparisons. *Biochemistry*

2001, *40*, 13079–13087. (b) Yikilmaz, E.; Xie, J.; Brunold, T. C.; Miller, A. F. Hydrogen-bond-mediated tuning of the redox potential of the non-heme Fe site of superoxide dismutase. *J. Am. Chem. Soc.* **2002**, *124*, 3482–3483. (c) Vance, C. K.; Miller, A.-F. A simple proposal that can explain the inactivity of metal-substituted superoxide dismutases. *J. Am. Chem. Soc.* **1998**, *120*, 461–467. (d) Stallings, W. C.; Metzger, A. L.; Patridge, K. A.; Fee, J. A.; Ludwig, M. L. Structure–function relationships in iron and manganese superoxide dismutases. *Free Radical Res. Commun.* **1991**, *12–13*, 259–268.

(30) Han, W. G.; Lovell, T.; Noodleman, L. Coupled redox potentials in manganese and iron superoxide dismutases from reaction kinetics and density functional/electrostatics calculations. *Inorg. Chem.* **2002**, *41*, 205–218.

(31) Muñoz, I. G.; Moran, J. F.; Becana, M.; Montoya, G. The crystal structure of a eukaryotic iron superoxide dismutase suggests intersubunit cooperation during catalysis. *Protein Sci.* **2005**, *14*, 387–394.

(32) Da Silva, C. F.; Batista, M. M.; Batista, D. G. J.; de Souza, E. M.; da Silva, P. B.; de Oliveira, G. M.; Meuser, A. S.; Shareef, A. R.; Boykin, D. W.; Soeiro, M. N. C. In vitro and in vivo studies of the trypanocidal activity of a diarylthiophene diamidine against *Trypanosoma cruzi*. *Antimicrob. Agents Chemother.* **2008**, *9*, 3307–3314.

(33) Caldas, S.; Santos, F. M.; de Lana, M.; Diniz, L. F.; Machado-Coelho, G. L.; Veloso, V. M.; Bahia, M. T. *Trypanosoma cruzi*: acute and long-term infection in the vertebrate host can modify the response to benzimidazole. *Exp. Parasitol.* **2008**, *118* (3), 315–323.

(34) Lopez-Céspedes, A.; Villagran, E.; Briceño-Alvarez, K.; de Diego, J. A.; Hernandez-Montiel, H. L.; Saldaña, C.; Sanchez-Moreno, M.; Marín, C. *Trypanosoma cruzi*: seroprevalence detection in suburban population of Santiago de Queretaro (Mexico). *Sci. World J.* **2012**, DOI: 10.1100/2012/914129.

(35) El Bouhdidi, A.; Truyens, C.; Rivera, M. T.; Bazin, H.; Carlier, Y. *Trypanosoma cruzi* infection in mice induces a polyisotopic hypergammaglobulinemia and parasite-specific response involving high IgG2a concentrations and highly avid IgG1 antibodies. *Parasite Immunol.* **1994**, *16* (2), 69–76.

(36) Ginger, M. Trypanosomatid biology and euglenozoan evolution: new insights and shifting paradigms revealed through genome sequencing. *Protist* **2005**, *156* (4), 377–392.

(37) Cazzulo, J. J. Aerobic fermentation of glucose by trypanosomatids. *FASEB J.* **1992**, *6* (13), 3153–3161.

(38) Costou, V.; Besteiro, S.; Riviere, L.; Biran, M.; Biteau, N.; Franconi, J. M.; Boshart, M.; Baltz, T.; Bringaud, F. A mitochondrial NADH-dependent fumarate reductase involved in the production of succinate excreted by procyclic *Trypanosoma brucei*. *J. Biol. Chem.* **2005**, *280* (17), 16559–16570.

(39) Bringaud, F.; Riviere, L.; Coustou, V. Energy metabolism of trypanosomatids: adaptation to available carbon sources. *Mol. Biochem. Parasitol.* **2006**, *149*, 1–9.

(40) Hirsch, A.; Orphanos, D. Quantitative preparation of chloro- and bromophthalazines. *Can. J. Chem.* **1965**, *43*, 2708–2710.

(41) Perrin, D. D.; Armarego, W. L. F.; Perrin, D. R. *Purification of Laboratory Chemicals*; Pergamon Press: Oxford, U.K., 1980.

(42) Téllez-Meneses, J.; Mejía-Jaramillo, A. M.; Triana-Chávez, O. Biological characterization of *Trypanosoma cruzi* stocks from domestic and sylvatic vectors in Sierra Nevada of Santa Marta, Colombia. *Acta Trop.* **2008**, *108*, 26–34.

(43) Osuna, A.; Adroher, F. J.; Lupiáñez, J. A. Influence of electrolytes and non-electrolytes on growth and differentiation of *Trypanosoma cruzi*. *Cell Differ. Dev.* **1990**, *30*, 89–95.

(44) Marín, C.; Ramírez-Macias, I.; López-Céspedes, A.; Olmo, F.; Villegas, N.; Diaz, J. G.; Rosales, M. J.; Gutiérrez-Sánchez, R.; Sánchez-Moreno, M. In vitro and in vivo trypanocidal activity of flavonoids from *Delphinium staphisagria* against Chagas disease. *J. Nat. Prod.* **2011**, *74*, 744–750.

(45) Moreno, D.; Plano, D.; Baquedano, Y.; Jiménez-Ruiz, A.; Palop, J. A.; Sanmartín, C. Antileishmanial activity of imidothiocarbamates and imidoselenocarbamates. *Parasitol. Res.* **2011**, *108*, 233–239.

(46) González, P.; Marín, C.; Rodríguez-González, I.; Hitos, A. B.; Rosales, M. J.; Reina, M.; Díaz, J. G.; Gonzalez-Coloma, A.; Sanchez-Moreno, M. In vitro activity of C₂₀-diterpenoid alkaloid derivatives in promastigotes and intracellular amastigotes of *Leishmania infantum*. *Int. J. Antimicrob. Agents* **2005**, *25*, 136–141.

(47) Bradford, M. M. A refined and sensitive method for the quantification of microquantities of protein–dye binding. *Anal. Biochem.* **1976**, *72*, 248–252.

(48) Beyer, W. F.; Fridovich, I. Assaying for superoxide dismutase activity: some large consequences of minor changes in conditions. *Anal. Biochem.* **1987**, *161*, 559–566.

(49) *HyperChem Professional 8.0*; Hypercube, Inc. (1115 NW 4th Street, Gainesville, FL 32601, U.S.).

(50) Miranda, C.; Escartí, F.; Lamarque, L.; Yunta, M. J. R.; Navarro, P.; García-España, E.; Jimeno, M. L. New 1*H*-pyrazole-containing polyamine receptors able to complex L-glutamate in water at physiological pH values. *J. Am. Chem. Soc.* **2004**, *126*, 823–833.

(51) Santos, D. M.; Martins, T. A. F.; Caldas, I. S.; Diniz, L. F.; Machado-Coelho, G. L. L.; Carneiro, C. M.; Oliveira, R. P.; Talvani, A.; Lana, M.; Bahia, M. T. Benznidazole alters the pattern of cyclophosphamide-induced reactivation in experimental *Trypanosoma cruzi*-dependent lineage infection. *Acta Trop.* **2010**, *113* (2), 134–138.

(52) Fernandez-Becerra, C.; Sánchez-Moreno, M.; Osuna, A.; Opperdoes, F. R. Comparative aspects of energy metabolism in plant trypanosomatids. *J. Eukaryotic Microbiol.* **1997**, *44* (5), 523–529.

(53) González, P.; Marín, C.; Rodríguez-González, I.; Hitos, A. B.; Rosales, M. J.; Reina, M.; Díaz, J. G.; Gonzalez-Coloma, A.; Sanchez-Moreno, M. In vitro activity of C₂₀-diterpenoid alkaloid derivatives in promastigotes and intracellular amastigotes of *Leishmania infantum*. *Int. J. Antimicrob. Agents* **2005**, *25*, 136–141.



Original article

Scorpiand-like azamacrocycles prevent the chronic establishment of *Trypanosoma cruzi* in a murine model

Francisco Olmo^a, Clotilde Marín^a, M. Paz Clares^b, Salvador Blasco^b, M. Teresa Albelda^b, Conxa Soriano^c, Ramón Gutiérrez-Sánchez^d, Francisco Arrebola-Vargas^e, Enrique García-España^{b,**}, Manuel Sánchez-Moreno^{a,*}

^a Departamento de Parasitología, Facultad de Ciencias, Universidad de Granada, E-18071 Granada, Spain

^b Instituto de Ciencia Molecular, Departamento de Química Inorgánica, Universidad de Valencia, E-46980 Paterna, Valencia, Spain

^c Departamento de Química Orgánica, Universidad de Valencia, E-46100 Burjassot, Valencia, Spain

^d Department of Statistics, University of Granada, Severo Ochoa s/n, E-18071 Granada, Spain

^e Departamento de Histología, Facultad de Medicina, Universidad de Granada, E-18071 Granada, Spain

ARTICLE INFO

Article history:

Received 3 June 2013

Received in revised form

27 September 2013

Accepted 29 September 2013

Available online 9 October 2013

Keywords:

Trypanosoma cruzi

Synthetic aza-scorpiand

Trypanocidal activity

In vivo activity

ABSTRACT

Chagas disease is today one of the most important neglected diseases for its upcoming expansion to non-endemic areas and has become a threat to blood recipients in many countries. In this study, the trypanocidal activity of ten derivatives of a family of aza-scorpiand like macrocycles is evaluated against *Trypanosoma cruzi* *in vitro* and *in vivo* murine model in which the acute and chronic phases of Chagas disease were analyzed. The compounds **4**, **3** and **1** were found to be more active against the parasite and less toxic against Vero cells than the reference drug benznidazole, **4** being the most active compound, particularly in the chronic phase. While all these compounds showed a remarkable degree of inhibition of the Fe-SOD enzyme of the epimastigote forms of *T. cruzi*, they produced a negligible inhibition of human CuZn-SOD and Mn-SOD from *Escherichia coli*. The modifications observed by ¹H NMR and the amounts of excreted catabolites by the parasites after treatment suggested that the mechanism of action could be based on interactions of the side chains of the compounds with enzymes of the parasite metabolism. The ultrastructural alterations observed in treated epimastigote forms confirmed that the compounds having the highest activity are those causing the largest cell damage. A complementary histopathological analysis confirmed that the compounds tested were significantly less toxic to mammals than the reference drug.

© 2013 Elsevier Masson SAS. All rights reserved.

1. Introduction

Chagas disease (CD) is a chronic, systemic, parasitic infection caused by the protozoan *Trypanosoma cruzi* and is recognized by the WHO as one of the world's 13 most neglected tropical diseases [1]. This disease represents one of the main public health concerns in 22 developing countries of Latin America where every year about 8–15 million people are currently infected with *T. cruzi* [2]. Presently, CD is becoming an emerging health problem in non-endemic areas because with population movements, the *T. cruzi* parasite is traveling outside the Americas (North America, Pacific region and

Europe). This parasite is becoming a new worldwide epidemiological, economic, social and political challenge, which can have severe consequences for human health.

The main drugs currently used to treat Chagas disease are two nitroaromatic heterocycles: the furane-based nifurtimox and the imidazole-based benznidazole [3]. Both drugs are effective in the acute phase of the disease, although benznidazole shows a better safety and efficacy profile [4], the efficacy of both is very low in the chronic phase [5]. Furthermore, these compounds have severe side effects including anorexia, vomiting, peripheral polyneuropathy, and allergic dermatopathy. The presence of nitro groups attached to the heterocyclic rings suggests that these drugs act on the parasite by nitro reduction, originating reduced intermediates that covalently modify biomolecules. However, their mode of action is currently disputed [6,7]. The high level of toxicity of these drugs toward humans is probably a result of oxidative or reductive tissue

* Corresponding author. Tel.: +34 958 242 369; fax: +34 958 243 862.

** Corresponding author. Tel.: +34 963 544879; fax: +34 96 354 3274.

E-mail addresses: enrique.garcia-es@uv.es (E. García-España), msanchem@ugr.es, cmaris@ugr.es (M. Sánchez-Moreno).

damage and it is inextricably linked to their antiparasitic activity [3]. Therefore, less toxic and more selective drugs are urgently needed [8].

One promising target for new drugs against CD is iron superoxide dismutase (Fe-SOD). It has been shown that parasitic protozoan survival is closely related to the ability of some enzymes to evade toxic free-radical damage [9,10]. One of the main protective mechanisms involves Fe-SOD, a specific enzyme of trypanosomatids that acts as a scavenger of superoxide ions and hydroxyl radicals [11]. Since prosthetic groups are essential in all enzymatic processes, modifications in the enzyme active site of Fe-SOD by dissociation of the metal ion or by changes in the coordination sphere of the metal may be effective ways to deactivate its antioxidant features that will be presumably affecting both the growth and survival of parasite cells.

In relation to this matter, our research group has designed in recent years a new family of polyamine compounds that consists of a macrocyclic pyridinophane core to which side chains containing additional donor atoms are appended [12]. Structures are shown in Fig. 1. These macrocycles are termed scorpion ligands since the side chain can fold towards the macrocyclic core following the binding of target guest species such as protons, anions or metal ions [12,13]. Recently, we have studied ten of these compounds *in vitro*

against *Leishmania infantum* and *Leishmania braziliensis* and the results showed that the synthetic aza-scorpion like macrocyclic derivatives are potentially promising agents for the treatment of *Leishmania* infection [14].

In this work, we evaluate the effectiveness of 10 polyamine compounds as selective inhibitors of Fe-SOD in relation to human CuZn and Mn-SOD. The *in vitro* antiparasitic activity and toxicity against Vero cells was tested and compared with the values obtained for the reference drug benznidazole (BZN). The compounds with the best selectivity indexes were chosen for performing *in vivo* trypanocidal activity tests on female BALB/c mice, in the acute and chronic phases. The effect of the compounds on the ultrastructure of *T. cruzi* was also studied by transmission electronic microscopy (TEM) experiments to confirm the type of damage caused to the parasite cells. A ^1H NMR analysis of the nature and percentage of the metabolites excreted was performed to gain information about the inhibitory effect of our compounds on the glycolytic pathway since this represents the prime energy source of the parasite. Finally, a histopathological analysis was carried out in order to get of a better insight into the toxicity and cure levels obtained.

2. Materials and methods

2.1. Chemistry. Synthesis of ligands

The synthesis of the ligands (**1**, **2**, **3** and **4**) was accomplished as described in references [12,14,15] following a modification of the Richman–Atkins procedure by reaction of the pertosylated polyamine tris(2-aminoethyl)amine with 2,6-bis(bromomethyl) pyridine in 1:1 molar ratio using K_2CO_3 as a base in refluxing CH_3CN . Detosylation was carried out with $\text{HBr}/\text{HAc}/\text{PhOH}$, obtaining the final product (**1**) as a hydrobromide salt. Compounds **2**, **3** and **4** were obtained by reacting **1**, in its free amine form, with 1-naphthaldehyde, 2- or 3-pyridinecarboxaldehyde, respectively, in dry ethanol followed by *in situ* reaction with sodium borohydride. The compounds were finally precipitated as the hydrochloride salts.

5 was obtained by reaction of the pertosylated polyamine **1** with N-(3-bromopropyl) phthalimide in 1:1 molar ratio using K_2CO_3 as a base in refluxing CH_3CN . Deprotection and detosylation is carried out with hydrazine monohydrate and $\text{HBr}/\text{HAc}/\text{PhOH}$ respectively, and the final product (**5**) is obtained as the hydrobromide salt [16]. Structures are shown in Fig. 1.

2.2. Parasite strain and culture

Culture *T. cruzi* SN3 strain of IRHOD/CO/2008/SN3 was isolated from domestic *Rhodnius prolixus* captured in Guajira (Colombia) [17]. Epimastigote forms were grown in axenic Grace's Insect Medium (Gibco®) supplemented with 10% inactivated fetal bovine serum (FBS) at 28 °C in tissue-culture flasks. In order to obtain the parasite suspension for the trypanocidal assay, the epimastigote culture in the exponential growth phase was concentrated by centrifugation at 400 g for 10 min and the number of flagellates was counted in a hemocytometric chamber.

2.3. Cell culture and cytotoxicity tests

Vero cells (Flow) were grown in RPMI (Gibco®), supplemented with 10% inactivated fetal bovine serum, in a humidified 95% air, 5% CO_2 atmosphere at 37 °C for two days. For the cytotoxicity testing, cells were placed in 25 mL Conical Skirted Bottom Universal Sample Tube and centrifuged at 100 g for 5 min [18]. The culture medium was removed, and fresh medium was added to a

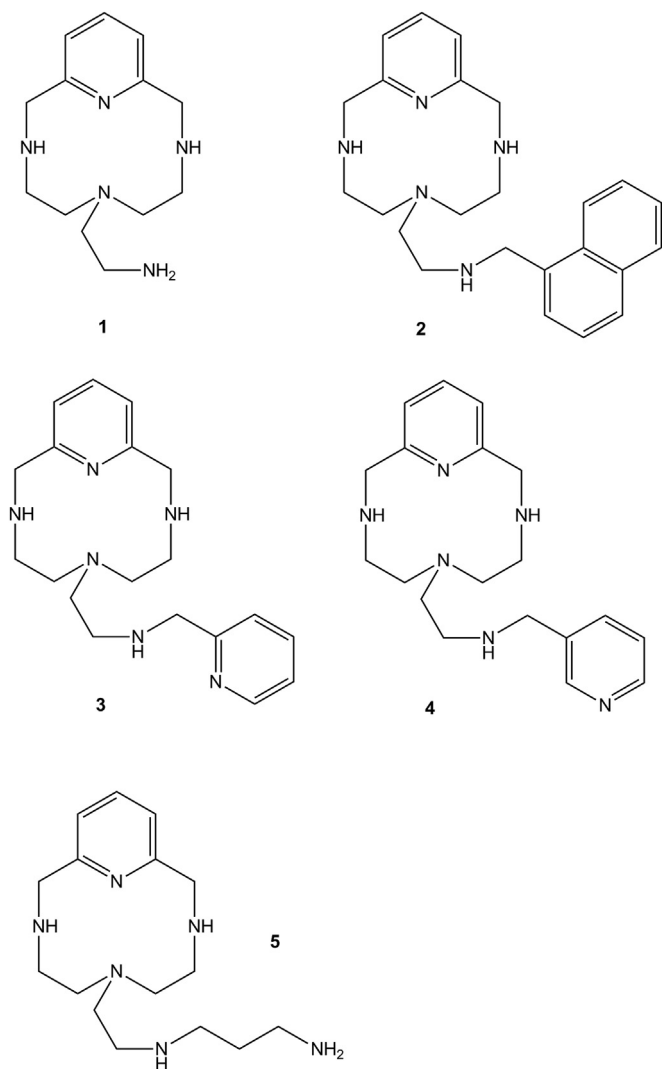


Fig. 1. Structure of the compounds.

final concentration of 1×10^5 cells/mL. This cell suspension was distributed in a culture tray (with 24 wells) at a rate of 100 μ L/well and incubated for two days at 37 °C in a humidified atmosphere enriched with 5% CO₂. The medium was removed, and fresh medium was added together with each test compound (at concentrations of 100, 50, 25, 10, and 1 μ M). After 72 h of treatment, cell viability was determined by flow cytometry according to a methodology described by us [19].

2.4. *In vitro* activity assays: extracellular forms

2.4.1. Epimastigote assay

Epimastigotes were collected in the exponential growth phase and distributed in culture trays (with 24 wells) at a final concentration of 5×10^4 parasites/well. The compounds to be tested and benznidazole were dissolved in medium trypanosomes liquid (MTL) and were tested at 100, 50, 25, 10, and 1 μ M. The effects of the different concentrations of each compound against the epimastigotes were tested for 72 h using a Neubauer hemocytometric chamber [20]. The trypanocidal effect is expressed as IC₅₀ values, i.e. the concentration required to result in 50% inhibition, as calculated by linear-regression analysis from the Kc values of the concentrations used.

2.4.2. Transformation of epimastigotes into metacyclic forms

Metacyclogenesis was induced by culturing a 5-day-old culture of epimastigotes that was harvested by centrifugation at 7000 g for 10 min at 10 °C. The parasites were then incubated for 2 h at 28 °C at a density of 5×10^8 cells/mL in TAU medium (190 mM NaCl, 17 mM KCl, 2 mM MgCl₂, 2 mM CaCl₂, 8 mM phosphate buffer, pH 6.0). Thereafter, the parasites were incubated at a 1:100 dilution (final epimastigotes concentration: 5×10^6 cells/mL) for 96 h at 28 °C in TAU3AAG medium (TAU supplemented with 10 mM L-proline, 50 mM L-sodium glutamate, 2 mM L-sodium aspartate and 10 mM D-glucose) in 25 mL culture flasks with a layer of culture medium that was not more than 1 cm in depth [21].

2.4.3. Trypomastigote forms

The activity (% of parasites reduction) was compared with the control following the methodology described in Ref. [22] with some modifications implemented in our laboratory. The assay of drug activity against *T. cruzi* was carried out using blood from Balb/c albino mice collected during the parasitemia peak (7th day) after infection with the SN3 strain of *T. cruzi*. The infected blood was diluted with non-infected murine blood to the concentration of 4×10^6 trypomastigotes/mL then, diluted to 1:2 in RPMI 1640 medium – GIBCO (2×10^6 trypomastigotes/mL). Stock solutions of the compounds were prepared in dimethylsulfoxide (DMSO). In order to calculate the IC₅₀ values, samples of infected blood and each one of the drug were added to the wells of a 96-microwell plate providing a final volume of 200 μ L and drug concentrations of 1, 10, 25, 50 and 100 μ M. Plates were incubated at 4–8 °C for 24 h. The experiments were repeated three times. Each solution was examined microscopically (OLYMPUS CX41) for parasite counting using the Neubauer chamber.

2.5. *In vitro* activity assays: intracellular forms

2.5.1. Amastigotes assay

Vero cells were cultured in RPMI medium in a humidified 95% air and 5% CO₂ atmosphere at 37 °C. The cells were seeded at a density of 1×10^4 cells/well in 24-well microplates (Nunc) with rounded coverslips on the bottom and then cultivated for 2 days. Afterward, adhered Vero cells were infected *in vitro* with metacyclic forms of *T. cruzi* [21], at a ratio of 10:1 and maintained for 24 h at

37 °C in 5% CO₂ in air. The extracellular parasites were removed by washing, and the infected cultures were incubated with s (1, 10, 25, 50 and 100 μ M concentrations) and cultured for 72 h in RPMI and 10% inactivated fetal bovine serum. The activity of the compounds was determined from the percentage of reduction in the number of amastigotes in the treated and untreated cultures in methanol-fixed and Giemsa-stained preparations. The values are the means of four separate determinations. The trypanocidal effect was expressed as IC₅₀ values [23].

2.5.2. Infectivity assay

The Vero cells were cultured in RPMI medium as described above. Afterward, the cells were infected *in vitro* with metacyclic forms of *T. cruzi* at a ratio of 10:1. The test compounds (IC₂₅ concentrations) were added immediately after infection and incubated for 12 h at 37 °C in a 5% CO₂ atmosphere. The extracellular parasites and the test compounds were removed by washing and the infected cultures were grown for 10 days in fresh medium. Fresh culture medium was added every 48 h. The activity of each compound tested was determined from the percentage of infected cells and the number of amastigotes per infected cell in treated and untreated cultures in the methanol-fixed and Giemsa-stained preparations. The percentage of infected cells and the mean number of amastigotes per infected cell were determined by analyzing more than 200 host cells distributed throughout randomly chosen microscopic fields. The values are the means of four separate determinations. The number of trypomastigotes in the medium was determined as previously described [18].

2.6. *In vivo* trypanocidal activity assay

Experimental tests performed during the *in vivo* stage were carried out for the following purposes: i) assessment of the effect of the compounds on the levels of parasitemia after treatment by counting in a Neubauer chamber activity as a marker of acute phase; ii) measure the reactivation of the parasitemia after immunosuppression submission as a marker of chronic phase; iii) ELISA test as an indicator of immune response to compare the acute and chronic phases levels of Ig-G; iv) detection of the presence of the parasite by PCR in organs and v) study of damage level in cardiac tissue by histopathology.

Groups of three BALB/c female mice (6–8 weeks old; 20–25 g), maintained under standard conditions, were infected via the intraperitoneal route with 1×10^5 bloodstream forms of *T. cruzi*. The animals were divided into the following groups: (I) group 1: uninfected (not infected and not treated); (II) group 2: untreated (infected with *T. cruzi* but not treated); (III) group 3: treated (infected and treated with 1 mg/kg body weight/day, for 5 consecutive days, 5–10 days post-infection, via the intraperitoneal route with the test compounds and benznidazole). A blood sample (5 μ L) was drawn from the mandibular vein of each mouse and then it was diluted at a ratio of 1:100 with PBS. The number of blood trypomastigote forms of *T. cruzi* was recorded every 2 days from 5 to 60 days post-infection by counting using the Neubauer chamber. The number of parasites was expressed as parasites/mL.

Circulating antibodies in serum against *T. cruzi*, on days 40 and 120 post-infection, were quantitatively evaluated using an ELISA. The serum was obtained from whole blood by centrifugation and then diluted to 1:80 in PBS. The antigen was composed of an excreted isoform of the enzyme Fe-SOD of *T. cruzi* epimastigotes. The results were expressed as the ratio of the absorbance of each sample at 490 nm to the cut-off value. The cut-off point for each reaction was the mean of the values determined for the negative controls plus three times the standard deviation.

Table 1

In Vitro activity, toxicity and selectivity index found for the studied compounds on extracellular and intracellular forms of *Trypanosoma cruzi*.

Compounds	Activity IC ₅₀ (μM) ^a			Toxicity Cells Vero IC ₅₀ ^b	SI ^c		
	Epimastigote forms	Amastigote forms	Trypomastigote forms		Epimastigote forms	Amastigote forms	Trypomastigote forms
BZN	16 ± 1	23 ± 5	22.6 ± 0.6	13.6 ± 0.9	0.8	0.6	0.6
1	6.5 ± 0.8	7.8 ± 0.7	16.3 ± 0.9	269.5 ± 16.1	41.4 (52)	34.5 (57)	16.5 (27)
1*	13 ± 1	17 ± 2	nd	234.9 ± 20.6	18.1 (23)	13.8 (23)	nd
3	9 ± 2	10 ± 1	18.0 ± 1	366.2 ± 14.7	42.2 (53)	36.4 (61)	20.3(34)
3*	15 ± 2	18.2 ± 2	nd	261.4 ± 21.1	17.6 (22)	14.4 (24)	nd
2	10 ± 1	16.1 ± 2	19.5 ± 0.8	324.9 ± 23.7	31.2 (39)	20.2 (34)	16.7(28)
2*	15 ± 2	22.3 ± 2	nd	271.3 ± 23.1	18.0 (22)	12.2 (20)	nd
4	8 ± 1	9.5 ± 0.6	19.7 ± 0.6	425.2 ± 29.6	52.7 (66)	44.8 (75)	21.6(36)
4*	21 ± 2	22 ± 1	nd	271.9 ± 22.3	13.0 (16)	12.6 (21)	nd
5	21 ± 2	20 ± 2	27.6 ± 1.6	167.3 ± 22.6	8.0 (10)	8.3 (14)	6.1(10)
5*	21 ± 2	20 ± 2	nd	214.3 ± 31.0	10.1 (13)	10.6 (18)	nd

Results are averages of four separate determinations.

^a IC₅₀ = the concentration required to give 50% inhibition, calculated by linear-regression analysis from the Kc values at concentrations employed (1, 10, 25, 50 and 100 μM).

^b Towards Cell Vero after 72 h of culture.

^c Selectivity index = IC₅₀ Cell Vero/IC₅₀ extracellular and intracellular form of parasite. In brackets: number of times that compound SI exceeds the reference drug SI. Nd = non determined.

After day 150 post-infection, those groups of mice treated whose parasitemia levels were significantly decreased were submitted to three cycles of immunosuppression with cyclophosphamide monohydrate as described in Ref. [24]. The experiment ended with the complete mouse bleeding out and removal of target organs (heart and liver). As mentioned above in order to know the antigen level change patterns associated to the presence of the parasite in blood, the blood collected was used to check the percentage of reactivation in the parasitemia levels and to figure out the Ig-G concentration in serum by ELISA. Finally, after removing the hearts and livers they were cut longitudinally; one piece was used to obtain total DNA and then PCR was performed for a fragment in the SOD gene from *T. cruzi* according to a pair of primer designed by our group that allow the detection of *T. cruzi* DNA in different biological samples (unpublished results). In the case of livers, the other part of the organ was used for histopathological analysis, so it was rinsed in ice-cold PBS, and fixed in 10% buffered formalin. The tissues were dehydrated and embedded in paraffin. Sections were cut at a thickness of 4–5 μm and stained with Masson's trichrome staining protocol (Trichrome). The slides were coded for a blinded analysis. Histological examinations were done using a conventional light microscope; each slide was visualized in at least 30 fields (total magnifications: ×40, ×100, ×200, and ×400). The histological alterations were ranked from (–) to 5 (+++++), with 0 representing a complete absence of alterations and 5 representing the most severe alterations [20].

Those animals inoculated with *T. cruzi* and treated whose parasitemia did not reappear after cycles of immunosuppression and whose histological sections did not present amastigote nests or other forms of parasites were consider as a definition of cure [25]. These animal experiments were performed with the approval of the Ethical Committee of the University of Granada.

2.7. Studies on the mechanism of action

2.7.1. Metabolite excretion

Cultures of *T. cruzi* epimastigotes (initial concentration 5 × 10⁵ cells/mL) received IC₂₅ of the compounds (except for the control cultures). After incubation for 96 h at 28 °C, the cells were centrifuged at 400 g for 10 min. The supernatants were collected to determine the excreted metabolites through ¹H NMR, and the chemical shifts were expressed in parts per million (ppm), using

sodium 2,2-dimethyl-2-silapentane-5-sulfonate as the reference signal. The chemical displacements used to identify the respective metabolites were consistent with those described by us [18].

2.7.2. Ultrastructural alterations

The parasites were cultured at a density of 5 × 10⁵ cells/mL in a medium containing the compounds tested at the IC₂₅ concentration. After 96 h, these cultures were centrifuged at 400 g for 10 min, and the pellets produced were washed in PBS and then mixed with 2% (v/v) p-formaldehyde/glutaraldehyde in 0.05 M cacodylate buffer (pH 7.4) for 4 h at 4 °C. The pellets were then prepared for transmission electron microscopy study using a procedure already described by us [23].

2.7.3. SOD enzymatic inhibition

The parasites cultured as described above were centrifuged. The pellet was suspended in 3 mL of STE buffer (0.25 M sucrose, 25 mM Tris–HCl, 1 M EDTA, pH 7.8) and disrupted by three cycles of sonic disintegration, 30 s each at 60 W. The sonicated homogenate was centrifuged at 1500 g for 5 min at 4 °C, and the pellet was washed three times in ice-cold STE buffer. This fraction was centrifuged (2500 g for 10 min at 4 °C) and the supernatant was collected. The protein concentrations were determined using the Bradford method [26]. Iron and copper–zinc superoxide dismutases (Fe-SOD and CuZn-SOD) activities were determined using the method described by Beyer and Fridovich [27], which measures the reduction of nitrobluetetrazolium (NBT) by superoxide ions. Into each cuvette, 845 μL of Stock solution [3 mL of L-methionine (300 mg, 10 mL⁻¹), 2 mL of NBT (1.41 mg, 10 mL⁻¹) and 1.5 mL of Triton X-100 1% (v/v)] were added, along with 30 μL of the parasite homogenate fraction, 10 μL of riboflavine (0.44 mg, 10 mL⁻¹), and an equivalent volume of the different concentrations of the compounds tested. Five different concentrations were used for each product: 1–100 μM. In the control experiment the volume was taken up to 1000 μL with 50 mM potassium phosphate buffer (pH 7.8, 3 mL), whereas 30 μL of the parasite homogenate fraction was added to the mixtures containing the compounds. Then, the absorbance (A₀) was measured at 560 nm in a spectrophotometer. Every cuvette was illuminated with UV light for 10 min under constant stirring and the absorbance (A₁) was measured. The human CuZn-SOD, coenzymes and substrates used in these assays were obtained from Sigma Chemical Co. The data obtained were analyzed using the Newman–Keuls test.

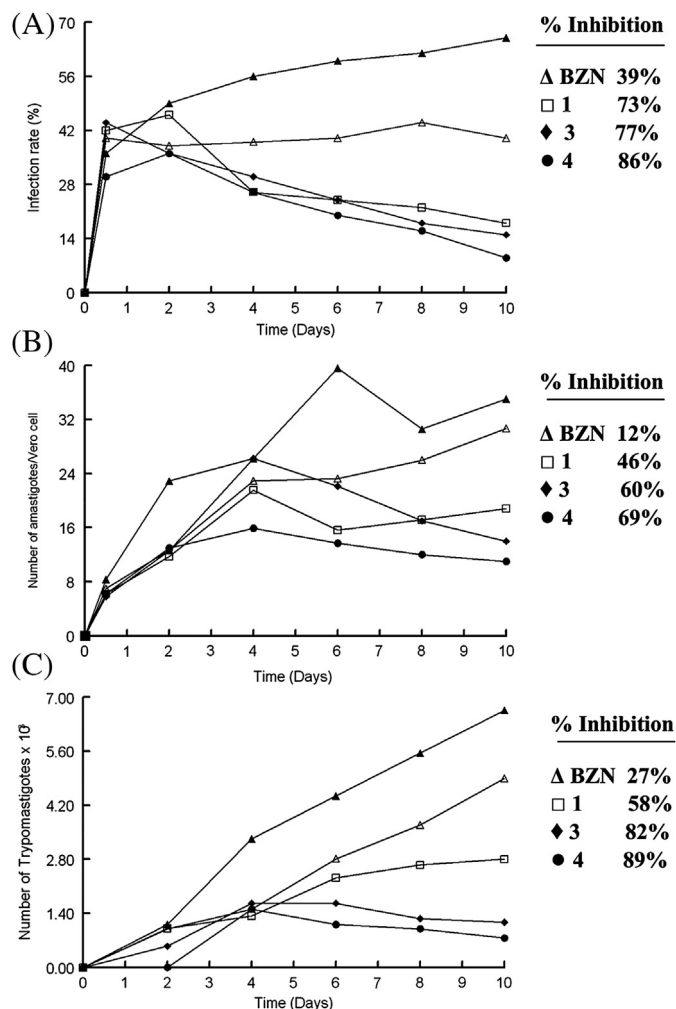


Fig. 2. Effect of activity of the different compounds on the infection rate and *T. cruzi* growth. (A) Rate of infection, (B) mean number of amastigotes per infected Vero cell, (C) number of trypomastigotes in the culture medium. (A-1): Control (-▲-); BZN (-Δ-); 1 (-□-); 3 (-◆-); 4 (-●-). Measured at IC₂₅ concentration. The values are means of three separate experiments.

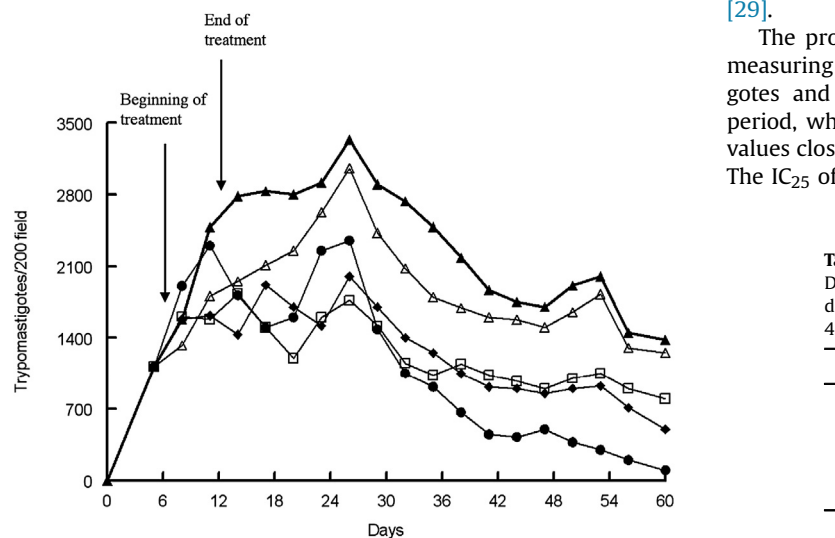


Fig. 3. Parasitemia in the murine model of acute Chagas disease: Control (-▲-) and dose receiving 5 mg/kg dose of: BZN (-Δ-); 1 (-□-); 3 (-◆-); 4 (-●-).

3. Results

3.1. In vitro studies

The IC₅₀ values obtained for the epimastigote, trypomastigote and amastigote forms for the tested compounds at concentrations ranging from 1 to 100 μM are shown in the first three columns of Table 1, which also include the results obtained for the reference drug benznidazole. Toxicity values against mammalian Vero cells were calculated, and the selectivity indexes (SI, IC₅₀Vero cells toxicity/IC₅₀ activity of extracellular or intracellular forms of the parasite) are also shown in the last three columns of Table 1. The number of times that the compound SI exceeded the SI of benznidazole is shown in brackets, since this value is very illustrative of the *in vitro* potentiality of the compounds tested with respect to the reference drug.

If we consider now the results displayed in Table 1 for activity against *T. cruzi*, the trypanocidal activity in both extra- and intracellular forms was similar or, in most cases, higher than that found for benznidazole, the best results were achieved by compounds 4 > 3 > 1 > 2 > 5. However, when we checked the Mn²⁺ complexes of these compounds (1*, 3*, 2*, 4* and 5*) a lower effect was observed. This can be probably attributed to the protective effect that the Mn²⁺ complexes of these ligands can exert over free radicals generated in the oxidative metabolism [28]. It can be seen that the 1, 3 and 4 were the most active of the 10 compounds tested in the three assays completed. Furthermore, they were much more active than benznidazole against both the extra- and intracellular forms of the parasite. Although showing an interesting activity, the rest of compounds were less active. Regarding the cytotoxicity evaluation against Vero cells, all the compounds were with IC₅₀ values over 200 μM substantially less toxic than the reference drug benznidazole (IC₅₀ = 13.6 μM). 5 having a longer side chain with an additional nitrogen atom proved to be slightly more toxic (IC₅₀ 167.3 μM). Considering now the more illustrative selectivity index values, compounds 1, 3 and 4 were again the potentially most interesting, since their SI values were 52, 53 and 66 times higher than that of benznidazole in the case of 1, 53, 51 and 61 times higher in the case of 3 and 66, 65 and 75 times higher in the case of 4. The rest of the compounds also have higher SI values than the reference drug. However, according to some authors, only those with SI values exceeding 50-times the SI value of benznidazole are good enough to be considered interesting as antiparasitic drugs [29].

The propagation of the parasite in Vero cells was studied by measuring the infection rates and the average number of amastigotes and trypomastigotes present during a 10-day treatment period, where the rate of host cell infection gradually increased: values close to 70% percent cells were infected on day 10 (Fig. 2A). The IC₂₅ of the compounds were used as the test dosage in these

Table 2

Difference in the level of anti-*T. cruzi* antibodies between day 40 and day 120 post-infection for compounds: 1; 3 and 4, expressed in absorbance unit (abs).

Treatment ^a	ΔA ^b
Control (untreated)	0.687
BZN	0.516
1	-0.022
3	0.325
4	-0.113

^a Dose of 5 mg/(kg day), administered by the intraperitoneal route for five days (See *In vivo studies section*).

^b ΔA = absorbance at 490 nm on day 120 p.i. – absorbance at 490 nm on day 40 p.i.

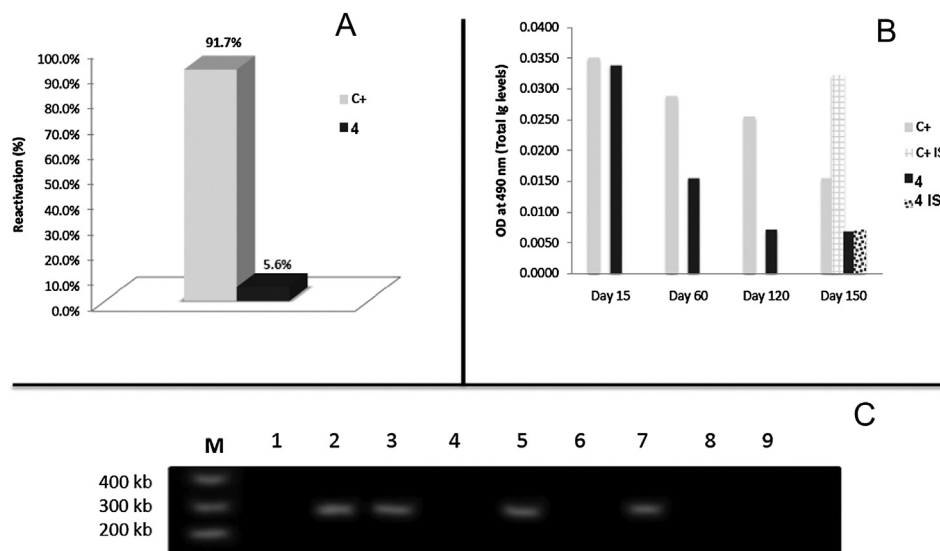


Fig. 4. *In vivo* effect of **4** in late chronic phase after immunosuppression. A, shows the percentage of reactivation in the parasitemia levels after the cycles of immunosuppressor treatment for control and treated groups. B, shows the total Ig-G level of anti-*T. cruzi* antibodies, expressed in absorbance units (OD), between control and treated groups of mice at different days post-infection. For day 150 groups are divided into two subgroups: immunosuppressed and non-immunosuppressed. C, Results of PCR amplification of different organs with the SOD gene primers at day 150 pi. Lanes: (M) marker, (1) PCR negative control, (2) PCR positive control, (3) infection control heart, (4) **4** treated heart, (5) infection control liver, (6) **4** treated liver, (7) infection control immunosuppressed heart, (8) **4** treated and immunosuppressed heart, (9) **4** treated and immunosuppressed liver.

assays and benznidazole was the reference drug. The decrease in the infection rate for the compounds **1**, **3** and **4** was always greater than 70%, making them much more effective than benznidazole (39%). The average number of amastigotes increased to a peak on the sixth day of culture and decreased thereafter (Fig. 2B). At the end of treatment, the three tested compounds had decreased the number of amastigotes present in the cells by 46%, 60%, and 69% respectively for **1**, **3** and **4**, whereas **BZN** only showed a reduction of 12%. Regarding the number of trypomastigote forms released in the medium (Fig. 2C), the maximum was reached in the control on day 10 (7.3×10^3 parasites/mL), but this value was substantially reduced in the presence of compounds **4** and **3** with a drop in the presence of trypomastigote forms of 89% and 82%, respectively. **1** and the reference drug although still active with a reduction of 58% and 27%, respectively, were again less effective.

3.2. *In vivo* studies

Parasitemia counting (Fig. 3) shows the number of trypomastigote forms found in blood until day 60 post-infection (pi). On the days of maximum parasitic burden (peak days, 22–25 post-infection) all the tested compounds greatly reduced the number of circulating parasites. Furthermore, this reduction lasted until day 60 and was more significant for the groups treated with the compounds under study than for those treated with benznidazole. Concerning the activity in the chronic phase, Table 2 shows the differences found in the level of anti-*T. cruzi* antibodies between days 120 and 40 pi. It can be seen that **1** and **4** significantly reduce the levels of antibodies with respect to the control. The order of *in vivo* decreasing activity in the chronic phase was found to be: **4** > **1** >> **3** > **BZN**.

Since **4** showed the best activity, a last test was done immunosuppressing the mice treated with this compound. Results are shown in Fig. 4. In Fig. 4A showing the reactivation of parasitemia after immunosuppression, it can be perceived that the control group recovered almost their initial peak of parasitemia with a 91.7% of reactivation, while in the treated group the parasitemia load only experienced a 5.6% of reactivation. As mentioned before,

another way to check the effect in chronic phase of the treatment was by ELISA. Fig. 4B shows the total Ig-G levels of anti-*T. cruzi* at different days of infection, interesting result can be seen specially attending to day 150 (already after immunosuppression), since the control's level of Ig-G resemble to the initial at day 15, attaining the level of Ig-G to values close to those found in the acute phase. Finally, to confirm the curative effect of the compound Fig. 4C shows the PCR results where organs of treated mice were clean of parasites while the control ones were positive.

In order to get a better insight into the toxicity level induced by our compound on the liver, an organ so important in many vital functions, we have performed an histopathological analysis on mice infected with the parasite and treated with **4** (Table 3). This compound was selected because of their especially good activity results both in the *in vivo* and *in vitro* tests. It was shown that mice infected, but not treated, developed after 150 days several alterations undoubtedly due to the action of the parasite during the chronic phase. Among them, lymphocytic infiltration with formation of many microgranulomas (+++++), delocalized hepatic destruction (++++) and, to a lesser extent, lymphocytic infiltration in the portal tracts (++) and also interstitial hemorrhage (++) were observed. When parasited mice were treated with the reference drug (**BZN**), lymphocytic infiltration and granulomas formation

Table 3
Degree of histopathological alterations found liver mice infected with *Trypanosoma cruzi*.

	Control ^a	Bzn ^b	Treated ^c
Granuloma with lymphocytic infiltrate	+++++	++	++
Delocalized hepatic destruction	+++	++++	+
Vessels with thickened walls	+	–	+
Lymphocytic infiltration in the portal tracts	++	–	+++
Interstitial hemorrhage	++	–	–
Hepatic destruction in the portal space	–	+++++	–
Centrilobular destruction of the hepatic vein	–	–	–
Presence of necrotic cells in the portal space	–	+++	–

^a Mice infected but untreated after 150 d.pi.

^b Mice infected and treated with 5 mg/kg w of benznidazole.

^c Mice infected and treated with 5 mg/kg w of **4**.

diminished (++) due to the lesser parasite numbers remaining after the drug action. On the contrary, a significant increase in the delocalized hepatic destruction (++++), a very severe hepatic destruction in the portal tracts (+++++), and presence of necrotic cells in those tracts (++++) were found caused by the BZN toxicity. Treatment of the infected mice with the compound also showed some hepatic damage 150 d.p.i. However, alterations were never as severe as those ones commented above for BZN, indicating a lesser toxicity for the compound tested. Only a very small formation of granulomas with lymphocytic infiltration (++) and slight delocalized hepatic parenchyma destruction (+) could be detected after treatment with **4**. Also a very slight thickening of the blood vessel walls was also observed. Some lymphocytic infiltration in the portal tracts (+++) was present in the livers, while no interstitial hemorrhage was shown (-). We can conclude that, in the hepatic level, our compound was much less toxic for the host than BZN.

All the results revealed that **4** is the most effective stopping *T. cruzi* from setting down as a chronic disease. Future studies could profile this compound as a preclinical drug. A patent application regarding this family of compound has been already filed (P201132035).

3.3. Studies on the mechanism of action

We accomplished several experiments to elucidate a possible mechanism of action for the aza-scorpianid like macrocycles **1**, **3** and **4** which showed a SI number 50 times higher than that of benznidazole.

3.3.1. Metabolite excretion effect

In the untreated group, the major metabolites excreted by *T. cruzi* were acetate and succinate, with smaller percentages of L-alanine and D-lactate, in agreement with the data in the literature [30]. When the trypanosomatids were treated with the tested scorpianids the excretion of some of these catabolites was neatly altered at the dosage used, whereas the presence of benznidazole did not lead to significant alterations in fuel metabolism (data not shown). Variation percentages in the height of the signals corresponding to the significant catabolites are shown in Fig. 5. It can be seen that the excretion, of both succinate and acetate, was strongly inhibited by **1** and **3** compounds, while **4** does not affect the succinate production, the acetate was moderately inhibited. Alanine and lactate excretion, were inhibited by the three compounds, while the production of ethanol was activated as an adaptive response to keep the NAD⁺/NADH balance. Since the less bulky compounds showed greater alterations of the level of glucose metabolism of the parasite, and taking into account the relevant role of mitochondria in the formation of the catabolic end products [31], it could be possible that its smaller size allows it to more easily penetrate the cristae (tubular invaginations of the inner mitochondrial membrane) [32] leading to subsequent changes in the metabolic pathway.

3.3.2. Ultrastructural alterations

The morphological alterations of *T. cruzi* epimastigotes caused by the three compounds were analyzed with transmission electron microscopy (TEM), in order to determine the way in which the compounds affected parasite survival. The most significant variations in comparison to the control cells are shown in Fig. 6.1. The three tested compounds were responsible for the death of a high percentage of parasites and other abnormalities such as vacuolization, disintegration of the cell cytoplasm and rupture of the parasites. Scorpianid **1** was one of the most effective compounds being responsible for the lyses of the epimastigotes (Fig. 6.2), which also killed almost all parasites after a process of cytoplasmic

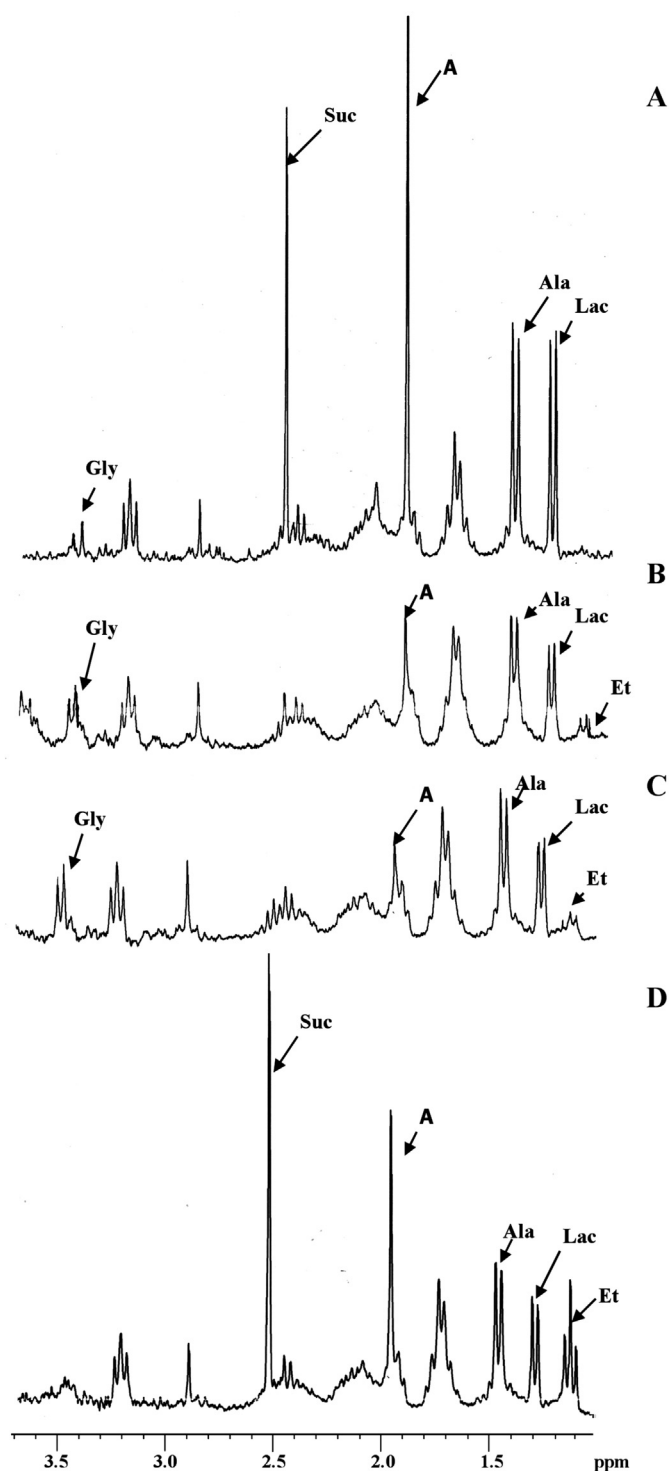


Fig. 5. ¹H NMR spectra epimastigote forms of *T. cruzi* treated against polyamine compounds (at a concentration of IC₂₅): (A) Control (untreated), (B) **1**, (C) **3** and (D) **4**.

vacuolization and disintegration. The epimastigotes cytoplasm had a disorganized electron-dense rather than granular appearance and unrecognizable cytoplasmic organelles in most of the parasites. Other less affected parasites also showed alterations such as excessive dilation of the kinetoplast or loss of plasma membrane integrity. Similar alterations were produced by **3** (Fig. 6.3), in which dead parasites and other profoundly altered parasites with a disorganization of the cytoplasm were seen. Mitochondria were

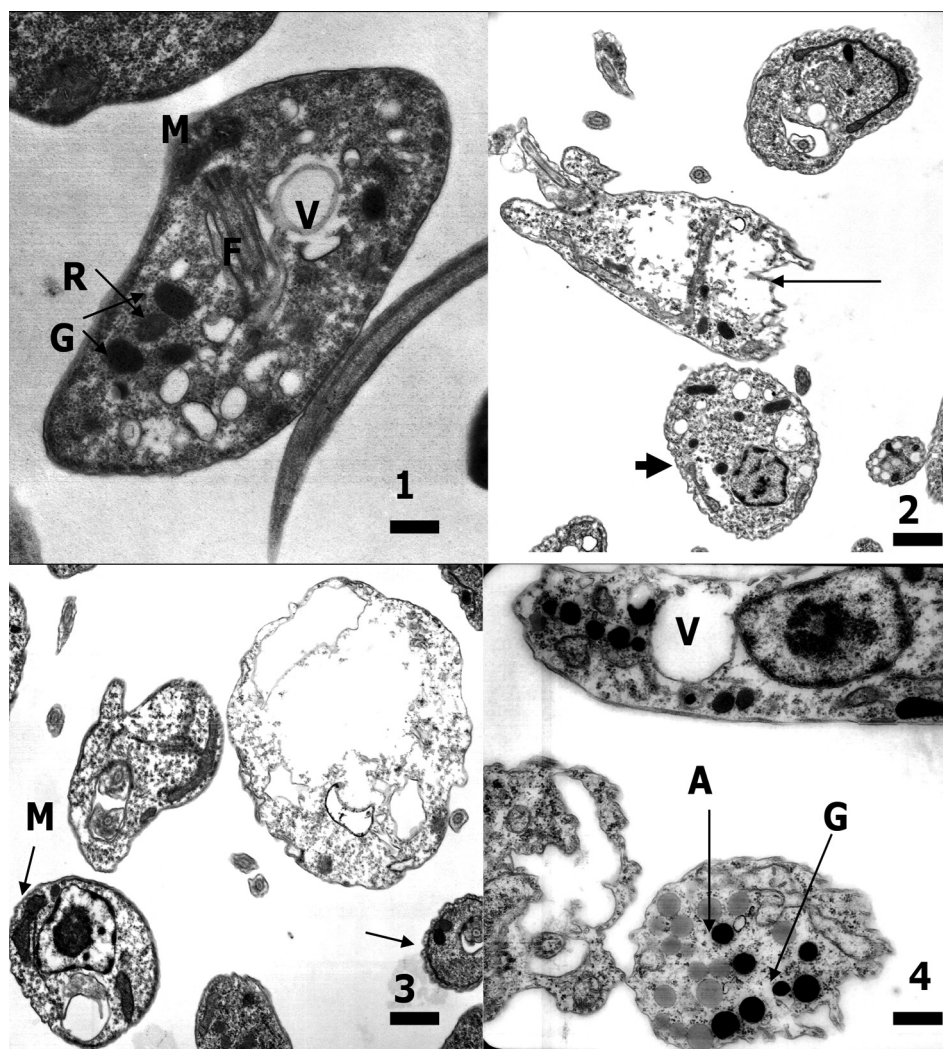


Fig. 6. Ultrastructural alterations by TEM in epimastigotes of *Trypanosoma cruzi* treated with the studied compounds. 6-1. Control parasites of *T. cruzi* showing organelles with their characteristic aspect, such as reservosomes (R), mitochondrion (M), glycosomes (G), microtubules (MT) and flagellum (F). (Bar: 0.583 μm). 6-2. Epimastigote forms of *T. cruzi* treated with **1** that were found disrupted (arrow) and showed cytoplasm slightly electron-dense and with granular aspect (arrowhead) (Bar: 1.00 μm). 6-3. *T. cruzi* treated with **3** with swollen mitochondria (M) and the cytoplasmic membrane disorganized (arrow) (Bar: 1.00 μm). 6-4. Epimastigotes of *T. cruzi* treated with **4** with abundant acidocalcisomes (A), huge glycosomes strongly electron-dense (G) and large vacuoles (V) (Bar: 0.583 μm).

found swollen and the cytoplasmic membrane was fenestrated. Compound **4** was also very effective (Fig. 6.4). In this case, we could observe the culture full of debris while those parasites that remained viable had large vacuoles and strongly electron-dense glycosomes, some of them showing abundant larger than normal acidocalcisomes and empty mitochondria. All parasites treated with this product also presented a dispersed cytoplasm.

So in summary, all the compounds tested showed a wide range of ultrastructural alterations of the epimastigote forms of the treated *T. cruzi*, which mainly took place at the mitochondrial and cytoplasmic levels. These alterations could be related to the metabolic changes mentioned above concerning the production of succinate and acetate, which might originate from a disturbance in the enzymes involved in pyruvate metabolism inside the cells.

3.3.3. Inhibitory effect on the *T. cruzi* Fe-SOD enzyme

These results prompted us to evaluate the inhibitory effect of the **1**, **3** and **4** on SOD activity to test their potential as enzyme inhibitors.

The results obtained are shown in Fig. 7 with the corresponding IC_{50} values that were calculated and included in the same figure.

Significant inhibitory values of Fe-SOD activity were found for the three compounds tested (Fig. 7A). All compounds showed values close to 100% inhibition at the 12.5–25 μM , with IC_{50} values between 8.2 and 12.5 μM . The design of an effective drug able to inhibit the parasite Fe-SOD without inhibiting the human SOD is an interesting goal. Therefore, we have also assayed the effect of compounds on Cu/Zn-SOD and Mn-SOD of human erythrocytes (Fig. 7B and C). The results obtained showed that the inhibition percentages for human CuZn-SOD and Mn-SOD were lower than for the Fe-SOD. So, IC_{50} values of 381.1, 178.5 and 641.0 μM were reached on Cu–Zn-SOD for **1**, **3** and **4**, respectively; and values of 111.4; 62.5 and 63.6 μM were obtained on Mn-SOD for the same compounds.

It should be noted that, as mentioned above, these compounds not only showed greater alterations in glucose catabolism, but also led to greater levels of Fe-SOD inhibition. Since the Fe-SOD present in mitochondria is an essential part of the whole enzyme excreted by epimastigotes in the inhibition tests [33], this fact would agree with the hypothesis that compounds having the pyridine nitrogen of the side chain better disposed for getting closer to the active center of the enzyme, as is the case of **4**, might have a greater

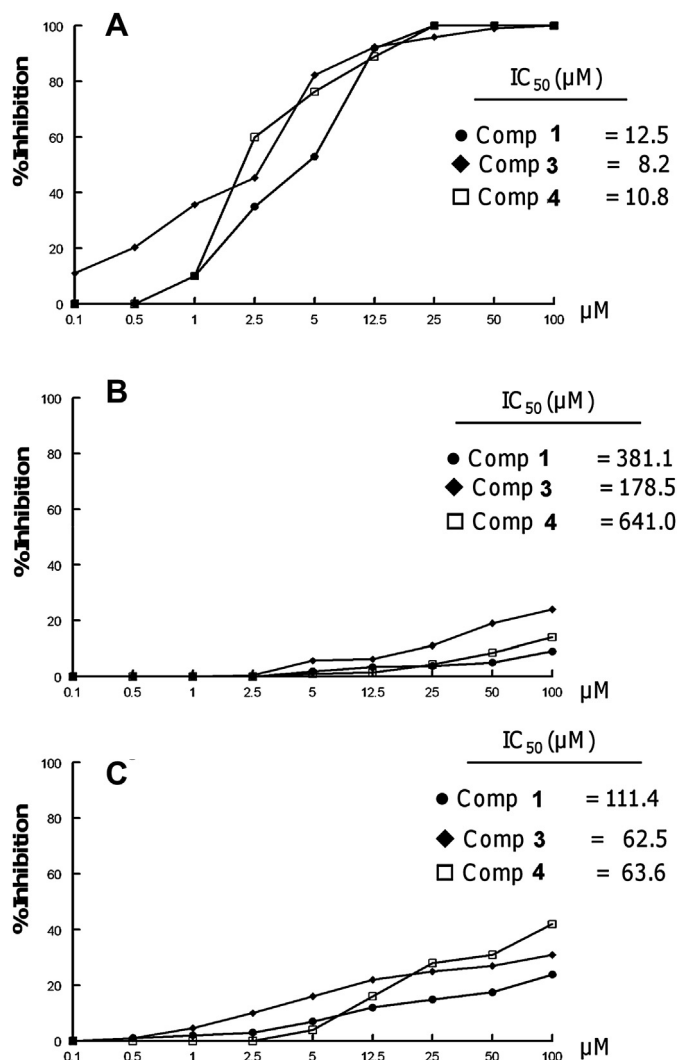


Fig. 7. (A) *In vitro* inhibition (%) of Fe-SOD from *T. cruzi* epimastigotes for compounds (activity 20.77 ± 3.18 U/mg). (B) *In vitro* inhibition (%) of CuZn-SOD from human erythrocytes for compounds (activity 23.36 ± 4.21 U/mg). (C) *In vitro* inhibition (%) of Mn-SOD from *Escherichia coli* for compounds (activity 18.12 ± 5.32 U/mg). Differences between the activities of the control homogenate and those ones incubated with compounds were obtained according to the Newman–Keuls test. A IC_{50} = the concentration required to give 50% inhibition was calculated by linear-regression analysis from the K_c values at concentrations employed (0.1–100 μM). Values are the average of three separate determinations.

activity. Modeling studies will be carried out to obtain clues about this point.

Acknowledgments

Financial support by the Spanish Ministerio de Ciencia e Innovación and FEDER funds of the E.U. (CONSOLIDER INGENIO 2010 CSD2010-00065), GeneralitatValenciana (PROMETEO 2011/008) is gratefully acknowledged. F.O. is grateful for a FPU Grant from the Ministry of Education of Spain.

Appendix A. Supplementary data

Supplementary data related to this article can be found at <http://dx.doi.org/10.1016/j.ejmech.2013.09.048>.

References

- [1] C. Huppertz, D.N. Durrheim, Control of neglected tropical diseases, *N. Engl. J. Med.* 357 (2007) 2407–2408.
- [2] J. Clayton, Chagas disease: pushing through the pipeline, *Nature* 465 (2010) S12–S15.
- [3] J.A. Urbina, Chemotherapy of Chagas disease, *Curr. Pharm. Des.* 8 (2002) 287–295.
- [4] R. Viotti, C. Vigliano, B. Lococo, M.G. Alvarez, M. Petti, G. Bertocchi, A. Armenti, Side effects of benznidazole as treatment in chronic Chagas disease: fears and realities, *Expert Rev. Anti Infect. Ther.* 7 (2009) 157–163.
- [5] C.J. Schofield, J. Jannin, R. Salvatella, The future of Chagas disease control, *Trends Parasitol.* 22 (2006) 583–588.
- [6] J.D. Maya, D.K. Cassels, P. Iturriaga-Vasquez, J. Ferreira, M. Faúndez, N. Galanti, A. Ferreira, A. Morello, Mode of action of natural and synthetic drugs against *Trypanosoma cruzi* and their interaction with the mammalian host, *Comp. Biochem. Physiol. A* 146 (2007) 601–620.
- [7] S.R. Wilkinson, C. Bot, J.M. Kelly, B.S. Hall, Trypanocidal activity of nitro-aromatic prodrugs: current treatments and future perspectives, *Curr. Top. Med. Chem.* 11 (2011) 2072–2084.
- [8] A.M. Strosberg, K. Barrio, V.H. Stinger, J. Tashker, J.C. Wilbur, L. Wilson, K. Woo, Chagas Disease: a Latin American Nemesis. Technical report, Institute for One World Health (IOWH), 2007, pp. 1–110.
- [9] R.K. Mehlotra, Antioxidant defense mechanisms in parasitic protozoa, *Crit. Rev. Microbiol.* 22 (1996) 295–314.
- [10] J.A. Atwood, D.B. Weatherly, T.A. Minning, B. Bundy, C. Cavola, F.R. Opperdoes, R. Orlando, R.L. Tarleton, The *Trypanosoma cruzi* proteome, *Science* 309 (2005) 473–476.
- [11] S. Ghosh, S. Goswami, S. Adhya, Role of superoxide dismutase in survival of *Leishmania* within the macrophage, *Biochem. J.* 369 (2003) 447–452.
- [12] B. Verdejo, A. Ferrer, S. Blasco, C.E. Castillo, J. González, J. Latorre, M.A. Máñez, M.G. Basallote, C. Soriano, E. García-España, Hydrogen and copper ion-induced molecular reorganizations in scorpionand-like ligands. A potentiometric, mechanistic, and solid-state study, *Inorg. Chem.* 46 (2007) 5707–5719.
- [13] V. Amendola, L. Fabbri, C. Mangano, P. Pallavicini, Molecular machines based on metal ion translocation, *Acc. Chem. Res.* 34 (2001) 488–493.
- [14] C. Marín, M.P. Clares, I. Ramírez-Macías, S. Blasco, F. Olmo, C. Soriano, B. Verdejo, M.J. Rosales, D. Gómez-Herrera, E. García-España, M. Sánchez-Moreno, *In vitro* activity of scorpionand-like azamacrocyclic derivatives in promastigotes and intracellular amastigotes of *Leishmania infantum* and *Leishmania braziliensis*, *Eur. J. Med. Chem.* 62 (2013) 466–477.
- [15] S. Blasco, B. Verdejo, M.P. Clares, C.E. Castillo, A.G. Algarra, J. Latorre, M.A. Máñez, M.G. Basallote, C. Soriano, E. García-España, Hydrogen and copper ion induced molecular reorganizations in two new scorpionand-like ligands appended with pyridine rings, *Inorg. Chem.* 49 (2010) 7016–7027.
- [16] M. Inclán, M.T. Albelda, J.C. Frías, S. Blasco, B. Verdejo, C. Serena, C. Salat-Canela, M.L. Díaz, A. García-España, E. García-España, Modulation of DNA binding by reversible metal-controlled molecular reorganizations of scorpionand-like ligands, *J. Am. Chem. Soc.* 134 (2012) 9644–9656.
- [17] J. Téllez-Meneses, A.M. Mejía-Jaramillo, O. Triana-Chávez, Biological characterization of *Trypanosoma cruzi* stocks from domestic and sylvatic vectors in Sierra Nevada of Santa Marta, Colombia, *Acta Trop.* 108 (2008) 26–34.
- [18] M. Sánchez-Moreno, C. Marín, P. Navarro, L. Lamarque, E. García-España, C. Miranda, O. Huertas, F. Olmo, F. Gómez-Contreras, J. Pitarch, F. Arrebola, *In vitro* and *in vivo* trypanosomicidal activity of pyrazole-containing macrocyclic and macrobicyclic polyamines: their action on acute and chronic phases of Chagas disease, *J. Med. Chem.* 55 (2012) 4231–4243.
- [19] C. Marín, I. Ramírez-Macías, A. López-Céspedes, F. Olmo, N. Villegas, J.G. Díaz, M.J. Rosales, R. Gutiérrez-Sánchez, M. Sánchez-Moreno, *In vitro* and *in vivo* trypanocidal activity of flavonoids from *Delphinium staphisagria* against Chagas disease, *J. Nat. Prod.* 74 (2011) 744–750.
- [20] I. Ramírez-Macías, C. Marín, R. Chahboun, I. Messouri, F. Olmo, M.J. Rosales, R. Gutiérrez-Sánchez, E. Álvarez-Manzaneda, M. Sánchez-Moreno, *In vitro* and *in vivo* studies of the trypanocidal activity of four terpenoid derivatives against *Trypanosoma cruzi*, *Am. J. Trop. Med. Hyg.* 87 (2012) 481–488.
- [21] J. Cardoso, M.J. Soares, *In vitro* effects of citral on *Trypanosoma cruzi* metacyclogenesis, *Mem. Inst. Oswaldo Cruz* 5 (2010) 1026–1032.
- [22] C.O. Júnior, R.O. Alves, C.A. Rezende, C.F. da Costa, H. Silva, M. Le Hyaric, A.P. Fontes, R.J. Alves, A.J. Romanha, M.V. de Almeida, Trypanocidal activity of lipophilic diamines and amino alcohols, *Biomed. Pharmacother.* 64 (2010) 624–626.
- [23] C. Fernández-Becerra, M. Sánchez-Moreno, A. Osuna, F.R. Opperdoes, Comparative aspects of energy metabolism in plant trypanosomatids, *J. Eukaryot. Microbiol.* 44 (1997) 523–529.
- [24] S. Caldas, F.M. Santos, M. de Lana, L.F. Diniz, G.L. Machado-Coelho, V.M. Veloso, M.T. Bahia, *Trypanosoma cruzi*: acute and long-term infection in the vertebrate host can modify the response to benznidazole, *Exp. Parasitol.* 118 (2008) 315–323.
- [25] D.M. Santos, T.A. Martins, I.S. Caldas, L.F. Diniz, G.L. Machado-Coelho, C.M. Carneiro, Rde P. Oliveira, A. Talvani, M. Lana, M.T. Bahia, Benznidazole alters the pattern of cyclophosphamide-induced reactivation in experimental *Trypanosoma cruzi*-dependent lineage infection, *Acta Trop.* 113 (2010) 134–138.

- [26] M.M. Bradford, A refined and sensitive method for the quantification of microgram quantities of protein utilizing the principle of protein-dye binding, *Anal. Biochem.* 72 (1976) 248–254.
- [27] W.F. Beyer, I. Fridovich, Assaying for superoxide dismutase activity: some large consequences of minor changes in conditions, *Anal. Biochem.* 161 (1987) 559–566.
- [28] M.P. Clares, S. Blasco, M. Inclán, L. del Castillo Agudo, B. Verdejo, C. Soriano, A. Doménech, J. Latorre, E. García-España, Manganese(II) complexes of scorpion-like azamacrocycles as MnSOD mimics, *Chem. Commun.* 47 (2011) 5988–5990.
- [29] S. Nwaka, A. Hudson, Innovative lead discovery strategies for tropical diseases, *Nat. Rev. Drug Discov.* 5 (2006) 941–955.
- [30] J. Turrens, More differences in energy metabolism between trypanosomatidae, *Parasitol. Today* 15 (1999) 346–348.
- [31] H. McBride, M. Neuspiel, S. Wasiak, Mitochondria: more than just a powerhouse, *Curr. Biol.* 16 (2006) R551–R560.
- [32] K. Von der Malsburg, J.M. Müller, M. Bohnert, S. Oeljeklaus, P. Kwiatkowska, T. Becker, A. Loniewska-Lwowska, S. Wiese, S. Rao, D. Milenkovic, D.P. Hutu, R.M. Zerbes, A. Schulze-Specking, H.E. Meyer, J.C. Martinou, S. Rospert, P. Rehling, C. Meisinger, M. Veenhuis, B. Warscheid, I.J. van der Klei, N. Pfanner, A. Chacinska, M. van der Laan, Dual role of mitoflin in mitochondrial membrane organization and protein biogenesis, *Dev. Cell* 21 (2011) 694–707.
- [33] L. Piacenza, F. Irigoín, M.N. Alvarez, F. Irigoín, M.N. Alvarez, G. Peluffo, M.C. Taylor, J.M. Kelly, S.R. Wilkinson, R. Radi, Mitochondrial superoxide radicals mediate programmed cell death in *Trypanosoma cruzi*: cytoprotective action of mitochondrial iron superoxide dismutase overexpression, *Biochem. J.* 403 (2007) 323–334.

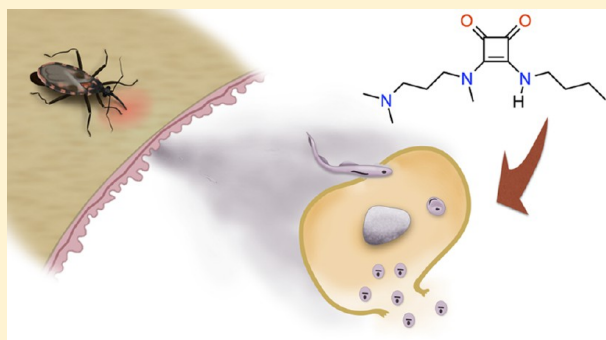
Synthesis and Biological Evaluation of *N,N'*-Squaramides with High in Vivo Efficacy and Low Toxicity: Toward a Low-Cost Drug against Chagas Disease

Francisco Olmo,^{†,§} Carmen Rotger,^{‡,§} Inmaculada Ramírez-Macías,[†] Luis Martínez,[‡] Clotilde Marín,[†] Lucas Carreras,[‡] Kristína Urbanová,[†] Manel Vega,[‡] Guillermo Chaves-Lemaur,[†] Angel Sampetro,[‡] María Jose Rosales,[†] Manuel Sánchez-Moreno,^{*,†} and Antonio Costa^{*,‡}

[†]Departamento de Parasitología, Facultad de Ciencias, Universidad de Granada, E-18071 Granada, Spain

[‡]Departamento de Química, Facultad de Ciencias, Universidad de las Islas Baleares, E-07122 Palma de Mallorca, Baleares, Spain

ABSTRACT: Access to basic drugs is a major issue in developing countries. Chagas disease caused by *Trypanosoma cruzi* is a paradigmatic example of a chronic disease without an effective treatment. Current treatments based on benznidazole and nifurtimox are expensive, ineffective, and toxic. *N,N'*-Squaramides are amide-type compounds that feature both hydrogen bond donor and acceptor groups and are capable of multiple interactions with complementary sites. When combined with amine and carboxylic groups, squaramide compounds have increased solubility and therefore make suitable therapeutic agents. In this work, we introduce a group of Lipinski's rule of five compliant squaramides as candidates for treating Chagas disease. The in vivo studies confirmed the positive expectations arising from the preliminary in vitro studies, revealing compound 17 to be the most effective for both acute and chronic phases. The activity, stability, low cost of starting materials, and straightforward synthesis make amino squaramides appropriate molecules for the development of an affordable anti-Chagasic agent.



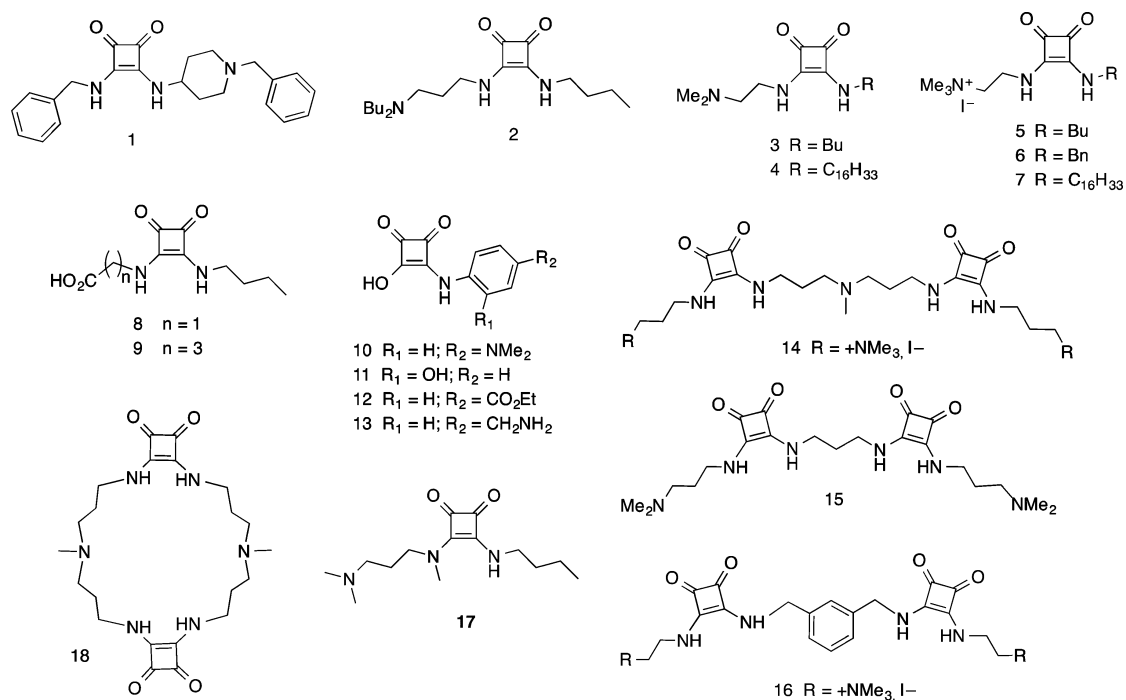
■ INTRODUCTION

Trypanosomatid protozoa are the etiological agents of several major insect transmitted parasitic illnesses such as Chagas disease (*Trypanosoma cruzi*), sleeping sickness (*Trypanosoma brucei* subsp. *rhodesiense* and subsp. *gambiense*) and leishmaniasis (*Leishmania* spp.). These infections are concentrated in the poorest areas of the planet and are considered the three “neglected tropical diseases” (NTDs) with the highest death rates.¹ Existing drug treatments for these diseases are far from satisfactory, and the development of a vaccine is a goal yet to be achieved. Current therapies are inadequate because of several factors such as low therapeutic indexes leading to high toxicities and unacceptable side effects, the emergence of resistant parasites, the difficulty of treatment compliance due to complex protocols, high prices that are unaffordable for the affected countries, etc. These drawbacks of current therapy meant that the discovery of new drugs is an immediate necessity. Nevertheless, owing to the low income of the affected population, investment in the development of new drugs to combat these diseases has not been financially attractive for pharmaceutical companies, and the interest of academic institutions is rather limited. This bleak picture is changing in recent years because of the financial backing from not-for-profit organisations and the participation of public–private partnerships.² Several illuminating articles covering different aspects of Chagas disease have recently been published.³ The main drugs currently

used to treat Chagas disease are two nitroaromatic heterocyclic compounds: the furane-based nifurtimox and the imidazole-based benznidazole.⁴ Both drugs are effective in the acute phase of the disease, although benznidazole has the better safety and efficacy profile,⁵ whereas both have a very low efficacy in the chronic phase.⁶ Furthermore, these compounds have severe side effects including anorexia, vomiting, peripheral polyneuropathy, and allergic dermatopathy. The presence of nitro groups attached to the heterocyclic rings suggests that these drugs act on the parasite by nitro reduction, producing reduced intermediates that covalently modify biomolecules. However, their action mechanism is currently under discussion.⁷ The high human toxicity level of these drugs is probably a result of oxidative or reductive tissue damage and is inextricably linked to their antiparasitic activity.⁴ Newer drugs, such as allopurinol and itraconazole, are yet to be verified in clinical trials.⁸ Therefore, less toxic and more selective drugs are urgently needed.⁹ More importantly, most of the drugs available require administration for extended periods of time, and their supply in the amounts required in underdeveloped endemic countries is not always guaranteed and may result in prohibitive financial burdens.

Received: November 4, 2013

Published: January 13, 2014

Chart 1. *N,N'*-Disubstituted Squaramides Evaluated against *T. cruzi*

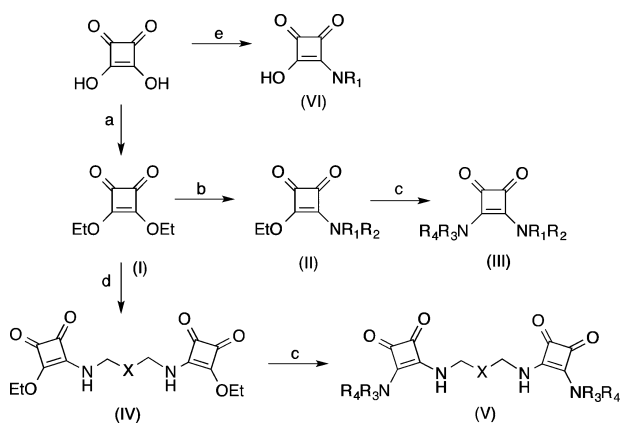
During the course of our program, aimed at exploring the potential of squaramide-based compounds as therapeutic agents, we have already described a series of oligomeric cyclosquaramides as kinase inhibitors with antitumor activity.¹⁰ A recent report about squaramides with antimalarial activity¹¹ and our promising results on the antichagasic activity of a series of cyclic polyamines¹² have fueled our interest in the potential of squaramides as antiparasitic agents. In this regard, herein we have explored the antichagasic properties of a selected group of minimalist squaramide-based compounds (acidic, basic, neutral, and amphoteric; Chart 1). Our selection criteria placed emphasis on the molecular properties that determine druggability but also on the commercial availability and affordability of the starting reagents and the production process. These factors coupled with a short synthesis and simple purification steps are relevant economic issues for developing drugs that address the NTDs that affect less developed countries.

The antichagasic properties and cellular toxicity of squaramide compounds have been evaluated on epimastigote and amastigote forms of *T. cruzi*. Our study includes infectivity assays performed on Vero cells with compounds that demonstrate higher activities. Using a murine model, we have determined the trypanocidal activity of the squaramide compounds in vivo on acute and chronic phases of Chagas disease. Furthermore, to follow the glycolytic pathway of parasites, we have analyzed changes in metabolite excretion by ¹H NMR, and finally the ultrastructural alterations of parasites treated with our compounds have been observed using transmission electron microscopy (TEM).

RESULTS AND DISCUSSION

Chemistry. Besides the cost and commercial availability of the starting chemicals, a drastic reduction in the number and complexity of synthetic operations contributes in decreasing the production costs of drugs. Consequently, all compounds

depicted in Chart 1 were synthesized from diethyl squarate or squaric acid itself by condensation with the corresponding amines of commercial origin. Most reactions were performed at room temperature using ethyl ether and ethanol as solvents according to well established methods (Scheme 1).¹³

Scheme 1. Synthesis of Squaramides 1–18^a

^aEtOH, reflux, 12 h; (b) amine 1 (R₁R₂NH, 1.1 equiv), Et₂O or EtOH, rt, 3–10 h; (c) amine 2 (R₃R₄NH, 1.1 equiv), EtOH, rt, 1–12 h; (d) diamine (H₂NCHXCHNH₂, 0.4 equiv), Et₂O (high dilution) rt, 12 h; (e) arylamine (ArNH₂, 0.5 equiv), reflux or microwave heating.^{16b}

Synthetic work with squaramides has advantages over syntheses involving carboxylic acid amides. As opposed to carboxylic acid esters, dialkyl esters of squaric acid are active enough to condense with primary and secondary amines, usually at room temperature, without the need for auxiliary reagents or catalysts.¹³ Hence, the diethyl squarate (I), used here as a precursor for the synthesis of squaramides, was prepared on a multigram scale by refluxing the cheapest commercial squaric acid

in ethanol.¹⁴ Squaramides **1–4** and **17**, all substituted with extra amino groups, were synthesized with 60–90% yields by sequential condensation of diethyl squarate and the corresponding amines, as described in the general method. Ammonium substituted squaramides **5–7** were prepared by exhaustive methylation of the corresponding squaramides.¹⁵ Squaramides **8** and **9**, containing a carboxylic acid group, amidosquaric acids **10–13**, and cyclosquaramide **18** were synthesized as recently described by our group.^{16,13b} Bissquaramides **14–16** were synthesized by a slightly modified method that involved the synthesis of mixed squaramide esters (Scheme 1, structure IV).¹⁷

Druglikeness was qualitatively evaluated by computing the relevant molecular properties. Among others, partition coefficients ($\log P$) and polar surface areas (PSAs) are particularly informative about cell penetrability of the squaramides (Table 1). In general,

Table 1. Molecular Properties of Squaramide Derivatives

compd	MW ^a	$\log P$ ^b	PSA ^c (Å ²)	HBD ^d	HBA ^e
1	389.5	2.61	52.8	2	3
2	337.5	2.70	49.3	2	3
3	239.3	-0.06	48.4	2	3
4	407.6	4.94	48.4	2	3
5	254.3	-0.04	48.3	2	2
6	288.3	0.45	47.3	2	2
7	422.7	4.97	49.8	2	2
8	226.2	-0.8	80.4	3	4
9	254.3	-0.2	79.9	3	4
10	232.2	0.76	59.3	2	4
11	205.2	0.09	75.8	3	4
12	261.2	0.63	60.7	2	5
13	218.2	-0.48	83.3	4	4
14	535.7	-1.68	91.5	4	5
15	434.5	-2.01	98.7	4	6
16	498.6	-0.57	94.5	4	4
17	267.4	0.59	36.3	1	3
18	446.5	-1.98	89.2	4	6

^aTabulated molecular weight (MW) of tetralkylammonium squaramides **5–7**, **14**, and **16** refers to the cationic portion. ^b $\log P$, partition coefficient. ^cPSA, polar surface area. ^dHBD, hydrogen-bond donor count. ^eHBA, hydrogen-bond acceptor count excluding positively charged nitrogens and squaramide nitrogens.

all of the selected compounds are Lipinski's rule of five (Ro5) compliant and with PSA values of <100 Å²; therefore, we anticipated good oral bioavailability for the selected group of compounds.¹⁸

In Vitro Biological Activity. In vitro activity of squaramides derivatives on epimastigotes and amastigotes of *T. cruzi*, the unspecific cytotoxicity against Vero cells, and the corresponding selectivity indexes (SI) are gathered in Table 2. Most studies on the in vitro activity of new compounds against *T. cruzi* are performed on epimastigote forms (extracellular insect vector stage) because it is much easier to work with these forms in vitro. However, since extracellular forms are not the developed forms of the parasite in vertebrate hosts, evaluations made with these forms are merely indicative of the potential trypanocidal activity of the compounds tested. Consequently, a preliminary test using extracellular epimastigote forms should always be complemented by a subsequent evaluation using intracellular forms (amastigotes in vertebrate host cells) to improve the interpretation of the activity results.¹⁹ First, we prepared an epimastigotes culture and in another step infected

Vero cells with metacyclic forms, which were converted into amastigotes (mainly intracellular mammalian host forms) using the aforementioned *T. cruzi* strain. All the compounds, as well as the standard drug benznidazole, were assayed at concentrations of 0.1–100 μM, and IC₅₀ values, shown in Table 2, were calculated from the data produced.

The IC₅₀ values obtained for the epimastigotes and intracellular amastigotes of the tested compounds are shown in the first two columns of Table 2, which also includes the results obtained from the reference drug benznidazole. Toxicity values against mammalian Vero cells, after 72 h of culture, were also calculated, and the selectivity indexes (SI = (IC₅₀, Vero cells toxicity)/(IC₅₀, activity of extracellular or intracellular forms of the parasite)) are shown in the last two columns of Table 2. We added the number of times, in parentheses, that the compound SI exceeded the benznidazole SI, since this value indicates the in vitro potentiality of the test compounds with respect to the reference drug.

Analysis of the activity data presented in Table 2 reveals that squaramides featuring permanent positively charged tetraalkylammonium groups **5–7** had poor activity against both forms of *T. cruzi*. Similar results were obtained with acidic squaramides **8** and **9** and also with amidosquaric acids **10–13**. On the contrary, simple aminosquaramides were of good activity. It can be seen that squaramide derivatives **2**, **3**, **14**, and **17** were the more active among all compounds tested in the two trypanocide assays. Furthermore, they had greater activity than benznidazole against both extra- and intracellular parasite forms. Regarding the cytotoxicity evaluation against Vero cells, these compounds were substantially less toxic than the reference drug (IC₅₀ values were 147.8, 260.2, 300.7, and 453.1 μM for **2**, **3**, **14**, and **17**, respectively, compared to 13.6 μM for benznidazole). Now, considering the more illustrative SI values, compound **17** is of potential interest, since its SI values were 60 and 89 times higher than those of benznidazole for epimastigote and amastigote forms, respectively. Overall, these results appeared to establish squaramide **17** as the optimal structure among the tested compounds.

A close examination of the structures in Chart 1 reveals that the squaramides of highest activity all include at least one tertiary amine group separated from the squaramide units by a two- to three-carbon aliphatic chain segment of two or three methylenes. This arrangement is particularly well suited to inducing conformational transitions of the squaramides from extended (*Z,Z*) to (*Z,E*) forms, which are significantly favored by intramolecular hydrogen bonding between the basic amine group and the squaramide NH group (Scheme 2).^{13b,20} The chameleonic character of amine derivatives of squaramides is further enhanced by ionization. The pK_a of **17**, determined by ¹H NMR titration, is 8.8 in aqueous solution. Thus, at physiological pH, both acid and basic forms coexist in solution.

Squaramide **17** also has distinctive properties: low molecular mass (267.4 Da), only one hydrogen bond donor, and remarkably, the smallest (36.3 Å²) of the polar surface areas computed. These parameters exceed the standard values for drug absorption including brain penetration.²¹ In addition, the high activity and low toxicity measured to date for **17** and other related amine squaramides fulfill the criteria for investigating their in vivo antichagasic activity.²²

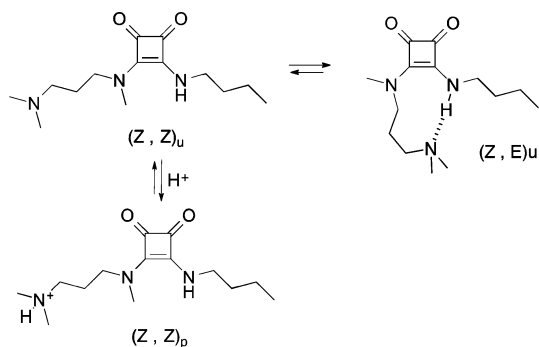
***T. cruzi* in Vitro Infection Assays.** In order to obtain more accurate information concerning the in vitro activity of squaramides **2**, **3**, **14**, and **17** in comparison with benznidazole, the propagation of the parasite in Vero cells was studied by measuring the infection rates and the average number of

Table 2. In Vitro Activity, Toxicity, and Selectivity Index Found for the Squaramide Derivatives on Extracellular and Intracellular Forms of *Trypanosoma cruzi*^a

compd	IC ₅₀ (μM) ^b		toxicity IC ₅₀ Vero cell (μM) ^c	SI ^d	
	epimastigote forms	intracellular amastigote forms		epimastigote form	intracellular amastigote form
benznidazole	15.9 ± 1.1	23.3 ± 4.6	13.6 ± 0.9	0.8	0.6
1	96.9 ± 4.2	34.7 ± 1.3	337.5 ± 18.5	3.5 (4)	9.7 (16)
2	21.1 ± 3.8	6.0 ± 0.4	147.8 ± 8.4	13.3 (17)	24.6 (41)
3	10.5 ± 7.0	9.3 ± 6.4	260.2 ± 11.3	24.8 (31)	28.0 (47)
4	49.8 ± 2.7	22.4 ± 1.7	90.1 ± 6.2	1.8 (2)	3.4 (6)
5	107.2 ± 6.3	38.5 ± 5.7	57.6 ± 6.8	0.5 (1)	1.5 (2)
6	60.8 ± 1.4	39.2 ± 2.0	74.2 ± 3.2	1.2 (1)	1.9 (3)
7	44.9 ± 3.0	26.3 ± 1.5	151.4 ± 7.4	3.4 (4)	5.7 (10)
8	35.7 ± 1.1	23.8 ± 2.5	54.8 ± 3.4	1.5 (2)	2.3 (4)
9	17.3 ± 2.0	66.9 ± 1.2	21.6 ± 3.1	1.2 (2)	0.3 (1)
10	15.9 ± 0.3	10.1 ± 1.0	12.9 ± 1.2	0.8 (1)	1.3 (2)
11	50.8 ± 4.1	44.0 ± 1.9	228.3 ± 12.5	4.5 (6)	5.2 (9)
12	26.3 ± 2.0	18.4 ± 0.8	21.5 ± 1.2	0.8 (1)	1.2 (2)
13	89.1 ± 4.5	72.6 ± 5.3	36.6 ± 3.0	0.4 (0)	0.5 (0)
14	18.5 ± 1.1	17.1 ± 0.4	300.7 ± 22.7	16.2 (20)	17.5 (29)
15	96.2 ± 7.2	46.0 ± 2.6	11.4 ± 0.5	0.1 (1)	0.2 (1)
16	118.9 ± 7.8	43.9 ± 2.7	73.1 ± 5.3	0.6 (1)	1.7 (3)
17	9.4 ± 0.4	8.5 ± 0.4	453.1 ± 22.6	48.2 (60)	53.3 (89)
18	21.8 ± 0.8	31.2 ± 0.8	110.6 ± 10.4	5.1 (6)	3.5 (6)

^aResults are averages of four separate determinations. ^bIC₅₀ = the concentration required to give 50% inhibition, calculated by linear regression analysis from the K_c values at concentrations employed (0.1–100 μM). ^cToward Vero cell after 72 h of culture. ^dSelectivity index = IC₅₀(Vero cell)/IC₅₀(extracellular and intracellular forms of parasite). In parentheses: number of times that compound exceeds the reference drug SI (on extracellular and intracellular forms of *T. cruzi*).

Scheme 2. Conformational Transitions between (Z,Z) and (Z,E) Rotamers of Aminosquaramide 17^a



^aThe subscripts “u” and “p” indicate neutral and protonated forms, respectively.

amastigotes and trypomastigotes present during a 10-day treatment period (Figure 1). Vero cells were incubated for 2 days and then infected with metacyclic forms of *T. cruzi*. The cells were invaded, and then progressive morphological conversion to the amastigote forms took place. During days 1–10 the rate of host cell infection gradually increased: 96% percent of cells were infected on day 10 (Figure 1A,B). The experiment was performed again in the presence of each of the four compounds assayed and also in the presence of the reference drug (at the concentration of IC₂₅). It was found that by the end of the experiment the infection rate was lower in all cases with respect to the control but not to the same extent. The decrease in the infection rate for compound 17 was a 67%, making it much more effective than the other derivatives and benznidazole (20%).

The average number of amastigotes per Vero cell (Figure 1C,D) was also consistent with the data mentioned above for infection

rates. After treatment, compound 17 significantly reduced the number of amastigotes per cell to 52% less than the control culture, while benznidazole showed a reduction of only 15%.

In relation to the number of trypomastigotes per milliliter found in the culture medium (Figure 1E,F), a maximum was reached on day 10 of the control run. This number was reduced by 21% by the reference drug but was particularly reduced by compound 17 (75% reduction). In summary, the results for parasite spreading in Vero cells agree with those for the trypanocidal activity reported in Table 2 for intracellular and extracellular forms of *T. cruzi*.

In Vivo Activity of Squaramide Derivatives. The positive results obtained for the in vitro tests prompted us to study the in vivo activity of compounds 2, 3, 14, and 17 on female BALB/c mice.

Since the effectiveness of drugs currently in use against Chagas disease varies widely between the acute and chronic phases, we decided to evaluate the impact of our compounds on both phases. For acute phase experiments, we considered the first 40 days after infection whereas the effect on the chronic phase was studied between days 40 and 120 after infection, both using the ELISA technique (Chart 2).

The intraperitoneal administration route was preferred over the intravenous procedure because intraperitoneal treatment substantially reduces animal mortality.²³ In fact, none of the mice died in any of our experiments performed either with the control or with compounds 2, 3, 14, and 17 at the concentrations used (25 mg/kg of body mass). Female mice were inoculated with trypomastigotes using the method described in the Experimental Section. Treatment, via the ip route, with the compounds of interest began 7 days postinfection and was maintained for 5 days. A group of mice were also treated in the same manner but with only the vehicle (control). During the study of acute phase activity, the level of parasitemia was determined every 2 days.

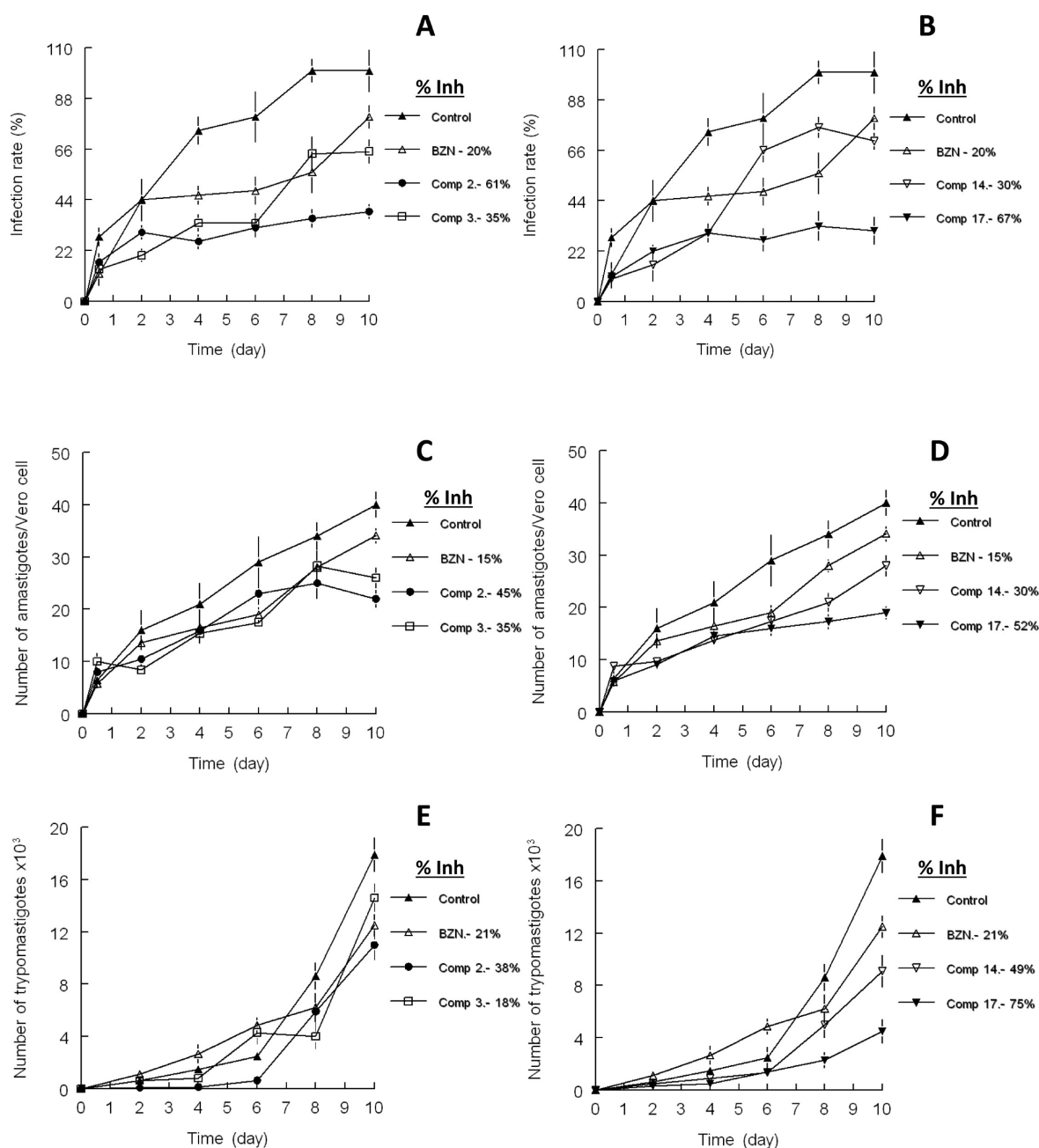


Figure 1. Reduction of the infectivity of *T. cruzi* in Vero cells treated with squaramide derivatives **2**, **3**, **14**, and **17** and benznidazole (BNZ): (A, B) rate of infection, (C, D) mean number of amastigotes per infected Vero cell, and (E, F) number of trypomastigotes in the culture medium for (▲) control, (△) BZN, (●) compound **2**, (□) compound **3**, (▽) compound **14**, and (▼) compound **17**; measured at IC₂₅. Values are the mean of three separate experiments, and error bars represent the mean ± standard deviation.

Figure 2 shows the number of trypomastigotes against days of treatment until day 40. On the day of maximum parasitic burden (day 14 pi), all tested compounds produced a reduction in the number of trypomastigotes compared to the untreated control, but squaramide **17** was the most effective causing a reduction of 67% at the end of the experiment on day 40.

Since compound **17** showed the best activity (parasitemia reduction of greater than 50% by the end of the acute phase), a new group of mice was incorporated, this time increasing the dosage up to 40 mg/kg of body mass but following the same assay schedule as previously. On this occasion the experiment

was concluded with an immunosuppression test on the treated mice after day 150 pi (late chronic phase, in which there are no parasites remaining in the bloodstream). The results are given in Figure 3, where Figure 3A shows the reactivation of parasitemia after immunosuppression. It can be appreciated that the control group recovers its initial peak of parasitemia almost entirely with a reactivation of 98.1%. In contrast, the treated group showed a parasitemia load of only 3.1%. ELISA assays offer an alternative method for verifying the effectiveness of squaramide **17** in the chronic phase. Figure 3B shows the total Ig-G levels of anti *T. cruzi* after immunosuppression in the

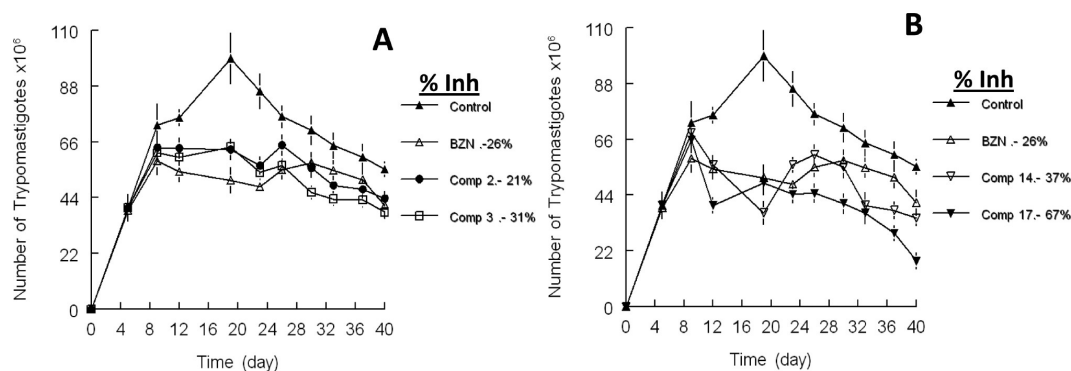
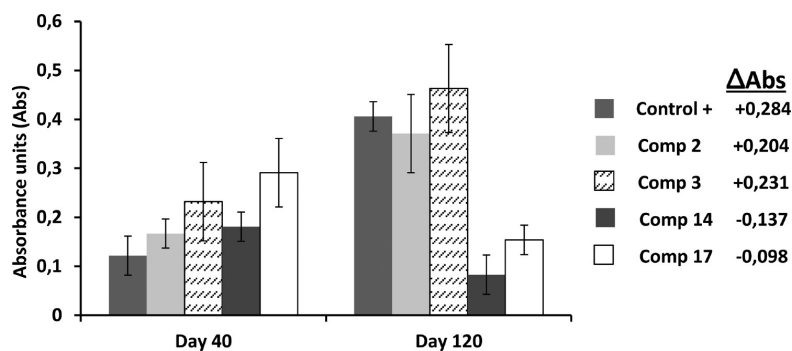
Chart 2. Level of Anti *T. cruzi* Antibodies on Days 40 and 120 Postinfection (pi) for Squaramides, Expressed in Absorbance Units (Abs)

Figure 2. Parasitemia in the murine model of acute Chagas disease: (\blacktriangle) control and dose receiving 25 mg/(kg-w) dose of (\triangle) BZN, (\bullet) compound 2, (\square) compound 3; (∇) compound 14, and (\blacktriangledown) compound 17. All the compounds were administered by the i.p. route. Values are the mean of three separate experiments, and error bars represent the mean \pm standard deviation.

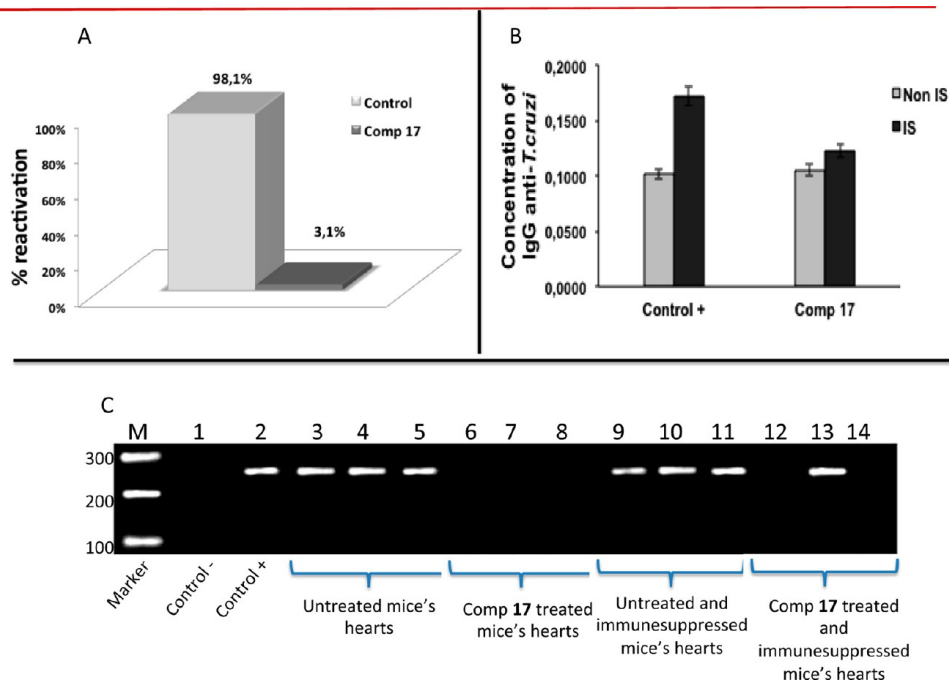


Figure 3. Immunosuppression experiment on a mouse model. (A) Reactivation of parasitemia after immunosuppression. (B) Total Ig-G levels of anti-*T. cruzi*. Values are the mean of three separate experiments, and error bars represent the mean \pm standard deviation. (C) Polymerase chain reaction (PCR) analysis of heart tissue on day 150 after infection.

chronic phase. In the control group, Ig-G levels resemble those of the initial acute phase, with the level of Ig-G increasing.

However, in the treated group the differences between immunosuppressed and nonimmunosuppressed groups were

not as significant. Finally, Figure 3C shows the PCR results after necropsy. After removal of the hearts, total DNA extraction, and amplification of a fragment within the parasite SOD gene, the hearts of control animals showed the ubiquitous presence of the parasite. In striking contrast, hearts in mice treated with compound 17 were relatively free from parasites (83.3%), thus confirming the curative effect of squaramide 17.

In order to check for metabolic disturbances or abnormalities associated with the treatment, representative biochemical parameters were measured for all groups of mice. Table 3 shows the changes observed in representative parameters between infected and uninfected mice during the acute and chronic phases of the infection. The significant changes were as follows: (i) a slight increase in the levels of both urea and creatine kinase (CK-MB) which were maintained throughout the infection and stabilized during the chronic phase; (ii) a considerable decrease in the total bilirubin in the acute phase followed by a gradual decay throughout the course of the infection; (iii) an initial increase of alkaline phosphatase levels that eventually stabilized and even tended to decrease because of physiological reasons. Compound 17, as can be seen in Table 3, did not show any toxicity effect compared with the control at 25 or 40 mg/kg of body mass, where the variation of the parameters is no more than 10%. When the dosage applied was 25 mg/kg of body mass, compounds 2, 3, and 14 showed some toxicity, since the AST/GOT and LDH values increased, both related to cell destruction prior to cell death in the liver and heart.

Metabolites Excretion Study. It is well-known that trypanosomatids are unable to completely degrade glucose to CO₂ under aerobic conditions. Consequently, they excrete a considerable part of the hexose skeleton into the medium as partially oxidized fragments in the form of fermented metabolites. The nature and percentage of the partially oxidized fragments depend on the pathway used for glucose metabolism by each of the species considered.²⁴ *T. cruzi* consumes glucose at a high rate, thereby acidifying the culture medium because of incomplete oxidation to acids.²⁴ Usually, the final products of glucose catabolism in *T. cruzi* are CO₂, succinate, acetate, D-lactate, pyruvate, and L-alanine.²⁵ Succinate is important because its main role is to maintain the glycosomal redox balance that facilitates the reoxidation of NADH produced in the glycolytic pathway. Succinic fermentation has the advantage of requiring only half of the phosphoenolpyruvate produced to maintain the NAD⁺/NADH balance, while the remaining pyruvate is converted inside the mitochondrion and the cytosol converted into acetate, D-lactate, or L-alanine, depending on the degradation pathway.²⁶

When epimastigotes from *T. cruzi* were treated with compound 17, the excretion of D-lactate, L-alanine, acetate, and succinate decreased by 28.3%, 18.5%, 18.6%, and 26.9%, respectively, and the excretion of pyruvate increased by 81.5% (Table 4 and Figure 4C). These squaramide-induced modifications of the *T. cruzi* glycolysis cycle suggest that squaramide 17 and, although in minor degree, squaramides 2, 3, and 14 (Table 4) produced cytoplasmic and mitochondrial alterations.

Ultrastructural Alterations. Structural alterations induced in *T. cruzi* epimastigotes by squaramide derivatives were also studied by transmission electron microscopy (TEM). Figure 5 shows the ultrastructural alterations produced by squaramides 3, 14, and 17 compared to control samples (Figure 5A).

Table 3. Biochemical Clinical Parameters Measured at Different Experimental Situations in Groups of Balb/c Mice Infected with *Trypanosoma cruzi*^a

	kidney marker profile			heart marker profile			liver marker profile		
	urea (mg/dL)	uric acid (mg/dL)	CK-MB (U/L)	LDH (U/L)	AST/GOT (U/L)	ALT/GPT (U/L)	total bilirubin (mg/dL)	alkaline phosphatase (U/L)	
uninfected mice (n = 15)	39 [36–43]	5 [4.3–5.5]	453 [215–690]	3086 [2108–4064]	126 [103–148]	46 [37–54]	0.23 [0.17–0.28]	133 [104–161]	
infected mice, acute phase (n = 15)	49 [39–60]	4.5 [3.7–5.5]	681 [400–950]	2910 [1589–4232]	129 [100–157]	48 [38–58]	0.15 [0.12–0.18]	231 [161–300]	
120 days after infection of mice (n = 6)	44	4.4	730	3012	140	43.5	0.13	178	
120 days after infection of mice and 2, 25 mg/(kg·w), treated (n = 6)	=	=	--	=	+++	=	++	=	
120 days after infection of mice and 3, 25 mg/(kg·w), treated (n = 6)	=	++	=	+++	+++	=	+++	=	
120 days after infection of mice and 14, 25 mg/(kg·w), treated (n = 6)	=	++	++	=	+++	=	=	=	
120 days after infection of mice and 17, 25 mg/(kg·w), treated (n = 6)	=	++	=	+	+	=	+	=	
150 days after infection of mice and 17, 40 mg/(kg·w), treated (n = 6)	=	=	=	+	+	=	++	--	
lethal dosage with 17, 500 mg/(kg·w) (n = 5)	++	=	++++	=	=	=	+++	++++	

^aKey: =, variation no larger than 10%; +, up to 10% increase over the range; ++, up to 30% increase over the range; +++, up to 40% increase over the range; ++++, more than 50% increase over the range; --, up to 10% decrease over the range; ---, up to 30% decrease over the range; ----, up to 40% decrease over the range; ----, more than 50% decrease over the range.

Table 4. Variation Percentages in the Height of the Peaks Corresponding to Catabolites Excreted by *T. cruzi* Epimastigotes in the Presence of Squaramide Derivatives at Their IC₂₅ Compared to a Control Sample^a

compd	Lac (%)	Ala (%)	A (%)	Pyr (%)	S (%)
2	-22.3 ± 2.2	-7.9 ± 2.0	+8.5 ± 5.2	-12.0 ± 4.7	-21.6 ± 5.1
3	-23.9 ± 3.0	-11.1 ± 3.0	-18.6 ± 3.5	-11.1 ± 3.8	-28.3 ± 3.9
14	-20.6 ± 1.6	-13.3 ± 1.7	-12.0 ± 2.4	+37.4 ± 4.8	-21.2 ± 4.7
17	-28.3 ± 0.9	-18.5 ± 1.1	-18.6 ± 1.8	+81.5 ± 5.6	-26.9 ± 4.6

^aLac = lactate; Ala = alanine; A = acetate; Pyr = pyruvate; S = succinate; (-) and (+) = ¹H NMR peak intensity reduction and increase, respectively, with ±SD presented with the values.

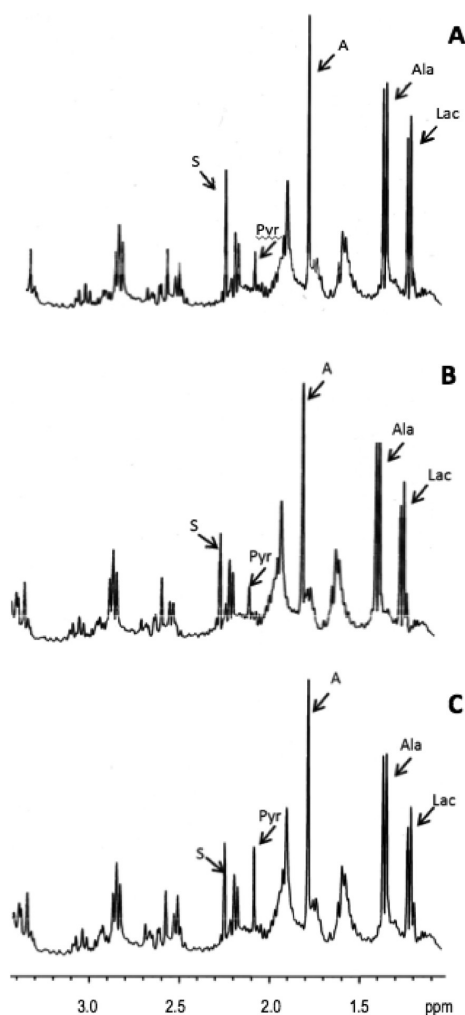


Figure 4. ¹H NMR spectra of the excretion products obtained after centrifugation of *T. cruzi* culture supernatants of epimastigotes: (A) control untreated; (B) treated with squaramide 14; (C) treated with squaramide 17.

Squaramide 3 induced a complete breakdown of parasites characterized by significant modifications to the cytoplasmic organelles. Mitochondrial swelling with rupture of the membrane was evident in a number of epimastigotes (Figure 5B and Figure 5C). In addition, the outer membrane of the parasite appeared to be discontinued, partially scalloped (Figure 5B, arrow), and lacking microtubular structures (Figure 5C), thus compromising the natural development of the parasite. In this regard, the effects of squaramides 14 and 17 on the epimastigotes were even more severe than those described earlier in this work. These compounds caused the death to the majority of the

epimastigotes, and the surviving parasites appeared swollen, filled with empty vacuoles (V) and enormous reservosomes (R) (Figure 5D and Figure 5E). For all of these cases, the formation of electron-dense vacuoles (VE) of different sizes was also characteristic (Figure 5B and Figure 5E).

In summary, these structurally simple aminosquaramide compounds appear to be promising candidates for in vivo assays. The in vitro and in vivo results indicate that squaramide derivative 17 is the most effective of the compounds we prepared, in both the acute and chronic phases of Chagas disease. The latest results obtained in vivo reveal a very promising candidate for treatment of Chagas disease, since the key organs are free of parasites after PCR amplification. This result is concordant with the minimal reactivation of parasitemia already observed probably because the residual number of parasites are unable to nest and keep the infection running. The ELISA technique (Figure 3B) confirmed this theory, since the level of anti *T. cruzi* Ig-G was comparatively low for treated mice irrespective of their immunosuppressive state.

Overall, the results obtained here allow us to consider that amino squaramide 17 stops *T. cruzi* from settling down as a chronic disease because it is very effective against the intracellular forms, as all testing revealed. This, together with its minimalist molecular structure and relatively simple synthesis, makes compound 17 an ideal candidate as a preclinical drug. A patent (P201330699) has already been filed for this family of compounds.

EXPERIMENTAL SECTION

Materials and Measurements. The various chemicals were of commercial origin (Aldrich or Scharlau) and used as received. All reactions were carried out under argon atmosphere. Melting and decomposition points were determined on a Dr. Tottoli (Büchi) apparatus and are uncorrected. ¹H and ¹³C NMR spectra were recorded at 300(75) MHz, on a Bruker Avance-300 NMR spectrometer. The ¹H and ¹³C NMR spectra and 2D correlation experiments were performed at 298 K using a 5 mm broadband inverse probe. All spectra were recorded with Bruker standard pulse programs, and the ¹H/¹³C chemical shifts are referenced to the solvent residual hydrogen signal of deuterated solvents at 7.26/77.16 ppm for chloroform or 2.50/39.52 for dimethyl sulfoxide. Electrospray high-resolution mass spectra were recorded in positive ion monitoring mode on a Micromass Autospec3000 spectrometer provided with an electrospray module. RP-HPLC analysis and purity check were performed on a Gilson modular system equipped with a 321 pump and a UV-visible diode array detector, using a X-Bridge (150 mm × 4.6 mm, 5 μm) C18 column with the use of H₂O–MeCN (10–90) in buffered solutions at pH 4 or 9. All evaluated compounds 1–22 were ≥95% pure by HPLC analysis. For biological evaluation, stock solutions of squaramides were prepared at millimolar concentration by dissolving the appropriate amount of the compound in 5% DMSO–H₂O (pH 5–7).

Synthesis. Compounds 5, 6, 8–13, 14, 16, and 18 were described previously in the literature.^{15,16,19}

General Synthetic Procedure for the Synthesis of Squaramides. For compounds 1–4 and 17, a solution of the appropriate amine (amine 1, 6.4 mmol) in diethyl ether (30 mL) was added dropwise to a solution of diethyl squarate (I) (5.8 mmol) in 10 mL of

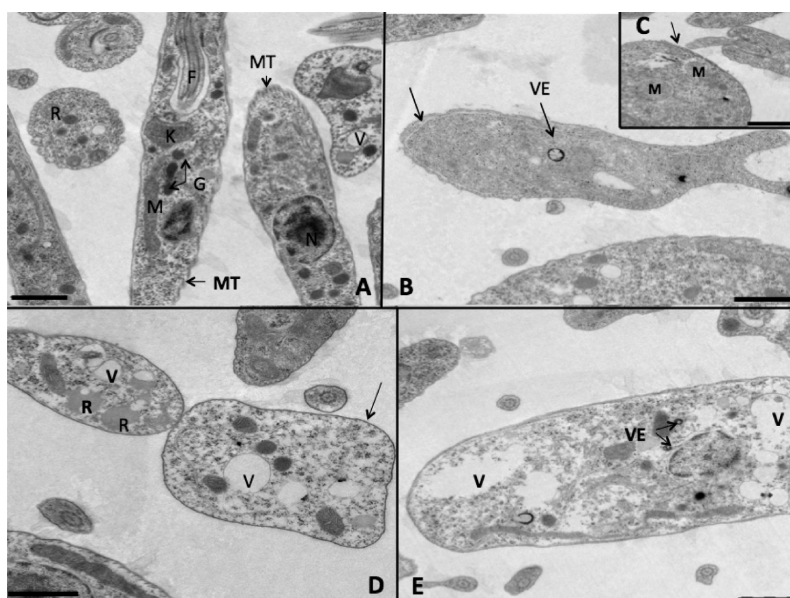


Figure 5. Ultrastructural alterations shown by TEM in epimastigotes of *T. cruzi* treated with squaramides **3** and **14** and **17**: (A) control parasite showing typical organelles such as nucleus (N), mitochondrion (M), glycosomes (G), microtubules (MT), vacuoles (V), reservosomes (R), kinetoplast (K), and flagellum (F); (B, C) treatment with squaramide **3**; (D) treatment with squaramide **17**; (E) treatment with squaramide **14**, at IC_{25} concentration. Scale bar is 1 μm .

diethyl ether, and the reaction mixture was stirred at room temperature for 12 h. In most cases during this period the mixed squaramide ester appeared as a precipitate. Thereafter, the solution was filtered and the remaining solid washed with ethyl ether ($3 \times 10 \text{ mL}$) and dried in vacuo. NMR pure monosquaramides (**II**) were obtained in 60–90% yield and were used without further purification in the next step. Alternatively, when the product of condensation remained in solution, the solvent was evaporated and the crude solid was purified by column chromatography (SiO_2 , AcOEt – EtOH 1%).

N,N'-Disubstituted squaramides were synthesized by dropwise addition of the appropriate amine (amine 2, 1.1 mmol) in EtOH (30 mL) to the above squaramide ester (1.0 mmol) in EtOH (10 mL). The solution was stirred at room temperature for 12 h. Afterward, solid squaramides were isolated by filtration and then triturated with *n*-pentane ($3 \times 10 \text{ mL}$). The resulting squaramides were dried, and their purity was checked by HPLC. For squaramides soluble in EtOH the solvent was previously evaporated at vacuo.

3-(Benzylamino)-4-((1-benzylpiperidin-4-yl)amino)cyclobut-3-ene-1,2-dione (1). Diethyl squarate was condensed first with aniline (amine 1) at reflux for 12 h and then reacted with 1-benzylpiperidin-4-amine (amine 2) as described in the general procedure (Scheme 1, routes b and c). White powder (75%): mp 240°C (dec). ^1H NMR (300 MHz, $\text{DMSO}-d_6$) δ : 7.65 (br, 1H), 7.2–7.5 (m, 11H), 4.68 (br, 2H), 3.74 (br, 1H), 3.73 (br, 2H), 2.70 (br, 2H), 2.03 (m, 2H), 1.81 (m, 2H), 1.45 (m, 2H). ^{13}C NMR (75 MHz, $\text{DMSO}-d_6$) δ : 188.0, 187.9, 172.8, 144.5, 143.9, 134.5, 134.3, 133.8, 133.3, 131.1, 132.5, 67.6, 56.8, 56.1, 52.4, 38.6. ESI-HRMS calcd for $\text{C}_{23}\text{H}_{26}\text{N}_3\text{O}_2$ m/z $[\text{M} + \text{H}]^+$ 376.2025, found 376.2023.

3-(Butylamino)-4-((3-(dibutylamino)propyl)amino)cyclobut-3-ene-1,2-dione (2). Diethyl squarate was condensed first with *n*-butylamine (amine 1) and then with *N,N*-dibutylpropane-1,3-diamine (amine 2) as described in the general procedure (Scheme 1, routes b and c). Off-white powder (80%): mp 116 – 118°C . ^1H NMR (300 MHz, CDCl_3) δ : 7.87 (br, 1H), 7.50 (br, 1H), 3.65 (m, 4H), 2.52 (t, $J = 6.8 \text{ Hz}$, 2H), 2.39 (t, $J = 7.11 \text{ Hz}$, 4H), 1.78 (m, 2H), 1.62 (m, 2H), 1.34 (m, 10H), 0.92 (m, 9H). ^{13}C NMR (75 MHz, CDCl_3) δ : 182.5, 182.4, 168.2, 168.1, 53.9, 51.5, 44.6, 43.5, 33.4, 29.2, 28.4, 20.9, 19.8, 14.3, 13.9. ESI-HRMS calcd for $\text{C}_{19}\text{H}_{36}\text{N}_3\text{O}_2$ m/z $[\text{M} + \text{H}]^+$ 338.2808, found 338.2795.

3-(Butylamino)-4-((2-(dimethylamino)ethyl)amino)cyclobut-3-ene-1,2-dione (3). Diethyl squarate was condensed with *n*-butylamine (amine 1) then with *N,N*-dimethylethane-1,2-diamine (amine 2) as described in the general procedure (Scheme 1, routes b and c). White solid (84%): mp 224°C (dec). ^1H NMR (300 MHz, $\text{DMSO}-d_6$) δ : 7.58 (br, 1H), 7.43 (br, 1H), 3.70 (d, $J = 5.3 \text{ Hz}$, 2H), 3.61 (m, 2H), 2.49 (t, $J = 5.9 \text{ Hz}$, 2H), 2.27 (s, 6H), 1.56 (m, 2H), 1.41 (m, 2H), 0.99 (t, $J = 7.3 \text{ Hz}$, 3H). ^{13}C NMR ($\text{DMSO}-d_6$) δ : 182.4, 167.7, 167.5, 59.2, 45.0, 42.8, 41.0, 32.8, 19.0, 13.5. ESI-HRMS calcd for $\text{C}_{12}\text{H}_{21}\text{N}_3\text{O}_2\text{Na}$ m/z $[\text{M} + \text{Na}]^+$ 262.1531, found 262.1540.

3-(Hexadecylamino)-4-((2-(dimethylamino)ethyl)amino)cyclobut-3-ene-1,2-dione (4). Diethyl squarate was condensed with *n*-hexadecylamine (amine 1), then with *N,N*-dimethylethane-1,2-diamine (amine 2) as above (Scheme 1, routes b and c). Off-white solid (65%): mp 171 – 173°C . ^1H NMR (300 MHz, CDCl_3) δ : 7.46 (br, 1H), 7.31 (br, 1H), 3.6–3.58 (br, 2H), 3.48–3.46 (br, 2H), 2.38 (m, 2H), 2.16 (s, 6H), 1.49 (br, 2H), 1.23 (br, 26H), 0.84 (m, 3H). ^{13}C NMR (CDCl_3 , 75 MHz): 182.6, 182.3, 168.2, 168.1, 59.8, 45.6, 44.9, 42.4, 32.1, 31.4, 29.9, 29.5, 26.8, 22.8, 14.2. ESI-HRMS calcd. for $\text{C}_{24}\text{H}_{46}\text{N}_3\text{O}_2$ m/z $[\text{M} + \text{H}]^+$ 408.3590, found 408.3583.

2-((2-Hexadecylamino)-3,4-dioxocyclobut-1-en-1-yl)amino-*N,N,N*-trimethylammonium iodide (7). Squaramide **4** (0.5 g, 1.2 mmol) and methyl iodide (0.5 g, 3.6 mmol) suspended in a mixture of dry acetone (20 mL) and dry DMF (10 mL) were refluxed under argon for 12 h. The resulting white solid was filtered and washed with acetone ($5 \times 10 \text{ mL}$) to afford 0.49 g of **7** (90%): mp 225 – 228°C . ^1H NMR (300 MHz, $\text{DMSO}-d_6$) δ : 7.52 (br, 1H), 7.40 (br, 1H), 3.95–3.93 (br, 2H), 3.5 (br, 4H), 3.11 (m, 9H), 1.49 (s, 2H), 1.23 (br, 26 H), 0.84 (br, 3H). ^{13}C NMR ($\text{DMSO}-d_6$, 75 MHz): 182.9, 182.3, 168.4, 166.9, 65.0, 52.7, 43.3, 37.4, 31.2, 30.6, 29.0, 28.6, 25.8, 22.0, 13.9. ESI-HRMS calcd for $\text{C}_{25}\text{H}_{48}\text{N}_3\text{O}_2$ m/z $[\text{M} - \text{I}]^+$ 422.3759, found 422.3747.

4,4'-Propane-1,3-diylbis(azanediyl)bis(3-((3-dimethylamino)propylamino)cyclobut-3-en-1,2-dione (15). Diethyl squarate (1.0 g, 5.9 mmol) in ethyl ether (5 mL) was condensed with 1,3-diaminopropane (163 μL , 1.96 mmol) in ether (50 mL) as described (Scheme 1, routes d and c). The resulting solid was filtered and washed with ether ($3 \times 20 \text{ mL}$) to leave after drying the mixed squaramide ester (IV, $\text{X} = \text{CH}_2$) as a white solid (80%): mp 143 – 147°C . ^1H NMR (300 MHz, $\text{DMSO}-d_6$) δ : 8.84 (br, 1H), 8.65 (br, 1H), 4.68 (q, $J = 7.1 \text{ Hz}$, 4H), 3.62 (t, 6.9 Hz, 4H), 1.87 (m, 2H), 1.41 (t, 7.2 Hz, 6H). ^{13}C NMR ($\text{DMSO}-d_6$, 75 MHz): δ : 189.2,

181.3, 172.6, 168.9, 68.8, 46.3, 30.5, 15.6. ESI-HRMS calc. for $C_{15}H_{18}N_2O_6Na$ m/z $[M + Na]^+$ 345.1063, found 345.1075. For the subsequent condensation, 3-(dimethylamino)-1-propylamine (824 μ L, 6.5 mmol, amine 2) was added via syringe to a solution of the squaramide ester (700 mg, 2.18 mmol) in dry ethanol (150 mL) as described in the general procedure. Squaramide 15 ($V, X = CH_2$) was obtained as an off-white solid (76%): mp 281–284 °C. 1H NMR (300 MHz, DMSO- d_6) δ : 7.46 (br, 4H), 3.63 (br, 8H), 2.34 (t, $J = 6.9$ Hz, 4H), 2.21 (s, 12H), 1.90 (m, 2H), 1.76 (m, 4H). ^{13}C NMR (DMSO- d_6 , 75 MHz): δ : 182.9, 168.5, 168.1, 56.5, 45.6, 42.1, 32.9, 29.2. ESI-HRMS calcd for $C_{21}H_{34}N_6O_4Na$ m/z $[M + Na]^+$ 457.2539, found 457.2537.

3-(Butylamino)-4-((3-(dimethylamino)propyl)(methylamino)cyclobut-3-en-1,2-dione) (17). To a solution of diethyl squarate (1.0 g, 5.9 mmol) in acetonitrile (10 mL) was added N^1,N^1,N^3 -trimethyl-1,3-propanediamine (5.1 g, cc 5.9 mmol, amine1) in acetonitrile (2 mL). After 2 h at room temperature, the solvent was evaporated and crude squaramide ester (II) was purified by column chromatography (SiO_2 , CH_2Cl_2 –EtOH 10%). The corresponding mixed squaramide ester (II, $R_1 = Me$, $R_2 = 3$ -(dimethylamino)propyl) was obtained as a colorless thick oil (90%). 1H NMR ($CDCl_3$) δ : 4.76 (q, $J = 7.2$ Hz, 2H), 3.72 (t, $J = 6.9$ Hz, 1H), 3.45 (q, $J = 7.2$ Hz, 1H), 3.34 (s, 1.5H), 3.16 (s, 1.5 H), 2.37 (t, $J = 6.6$, 2H), 2.28 (s, 3H), 2.23 (s, 3H), 1.85 (m, 2H), 1.50 (t, $J = 6.3$ Hz, 3H). ^{13}C NMR ($CDCl_3$, 75 MHz) δ : 188.3, 188.0, 181.5, 175.6, 175.5, 171.6, 171.3, 68.7, 55.4, 49.7, 49.0, 44.4, 36.0, 35.6, 25.0, 24.8, 15.2. Squaramide 17 was obtained from the squaramide ester (II) and *n*-butylamine (amine 2) as described in the general procedure (Scheme 1, routes b and c). Off-white solid (75%): mp 54–56 °C. 1H NMR (300 MHz, $CDCl_3$) δ : 8.36 (br, 1H), 3.67 (AB, $J = 6.9$ Hz, 2H), 3.34 (s, 3H), 3.30 (m, 2H), 2.37 (m, 2H), 2.23 (s, 6H), 1.75 (m, 2H), 1.55 (m, 2H), 1.37 (m, 2H), 0.95 (t, $J = 7.2$ Hz, 3H). ^{13}C NMR (DMSO- d_6) δ : 183.7, 183.6, 169.4, 168.8, 54.5, 48.66, 45.2, 44.9, 36.5, 34.0, 24.1, 20.2, 14.2. ESI-HRMS calcd. for $C_{14}H_{26}N_3O_3$ m/z $[M + H]^+$ 268.2025, found 268.2022.

Calculation of Molecular Properties. Low-energy conformations for each molecule were obtained from Monte Carlo (MC) automatic searching using the MMFF94 force field. The MC geometries were used as starting point for the quantum mechanical geometry optimizations at the B3LYP/6-31G* level of theory. The polar surface area (PSA) and the calculated partition coefficients ($\log P$), among others, were calculated with the QSAR module using MacSpartan10 program (Spartan¹⁰, Wavefunction, Inc., Irvine, CA).

Parasite Strains Culture. Epimastigote and Trypomastigote Forms. Epimastigotes of *T. cruzi* SN3 strain (IRHOD/CO/2008/SN3) isolated from domestic *Rhodnius prolixus* from Guajira (Colombia)²⁷ were cultivated in vitro in medium trypanosomes liquid (MTL) with 10% inactivated fetal bovine serum and were kept in an air atmosphere at 28 °C in Roux flasks (Corning, USA) with a surface area of 75 cm², according to a previously described methodology.²⁸ Transformation of epimastigotes into metacyclic forms was achieved by metacyclogenesis induced by culturing a 5-day-old culture of epimastigotes that was harvested by centrifugation at 7000g for 10 min at 10 °C. The parasites were then incubated for 2 h at 28 °C at a density of 5×10^8 cells/mL in TAU medium (190 mM NaCl, 17 mM KCl, 2 mM $MgCl_2$, 2 mM $CaCl_2$, 8 mM phosphate buffer, pH 6.0). Thereafter, the parasites were incubated at a 1:100 dilution (final epimastigotes concentration, 5×10^6 cells/mL) for 96 h at 28 °C in TAU3AAG medium (TAU supplemented with 10 mM L-proline, 50 mM L-sodium glutamate, 2 mM L-sodium aspartate, and 10 mM D-glucose) in 25 mL culture flasks with a layer of culture medium that was not more than 1 cm in depth.²⁹

Cell Culture and Cytotoxicity Tests. Vero cells (EACC number 84113001) originally obtained from monkey kidney were grown in RPMI (Gibco) and supplemented with 10% inactivated fetal bovine serum in a humidified 95% air, 5% CO_2 atmosphere at 37 °C for 2 days. The cytotoxicity test for Vero cells was performed according to a previously described methodology.²⁸ After 72 h of treatment, cell viability was determined by flow cytometry. Thus, 100 μ L/well of propidium iodide solution (100 mg/mL) was added and incubated for 10 min at 28 °C in darkness. Afterward, 100 μ L/well of fluorescein diacetate (100 ng/mL) was added and incubated under the same

conditions. Finally, the cells were recovered by centrifugation at 400g for 10 min and the precipitate was washed with phosphate buffered saline (PBS). Flow cytometric analysis was performed with a FACSVantage flow cytometer (Becton Dickinson). The percentage viability was calculated in comparison with the control culture. The IC_{50} was calculated using linear regression analysis from the K_c values of the concentrations employed (0.1–100 μ M).

In Vitro Activity. Epimastigotes Assays (Extracellular Forms). The obtained compounds and the reference drug (benznidazole) were dissolved in DMSO (Panreac, Barcelona, Spain) at a concentration of 0.01% and were afterward assayed as nontoxic and without inhibitory effects on parasite growth, according to a reported procedure.²⁸ The compounds were added to the culture medium at dosages of 100, 50, 25, 10, 1, 0.5, 0.25, and 0.1 μ M. The effects of each compound against epimastigotes of *T. cruzi* were tested at 72 h using a Neubauer hemocytometric chamber. The antitrypanosomatid effect is expressed as the IC_{50} , i.e., the concentration required to give 50% of growth inhibition, calculated by linear regression analysis from the K_c values of the concentrations employed.

Amastigotes Assays (Intracellular Forms). Vero cells were grown as described above in RPMI medium (Gibco). Cells were seeded at a density of 1×10^4 cells/well in 24-well microplates (Nunc) with rounded coverslips on the bottom and cultured for 2 days. Afterward the cells were infected in vitro with metacyclic forms, at a ratio of 10:1 during 24 h. The nonphagocytosed parasites were removed by washing, and then the drugs (at 100, 50, 25, 10, 1, 0.5, 0.25, and 0.1 μ M) were added. Vero cells with the drugs were incubated for 72 h at 37 °C in 5% CO_2 . Drug activity was determined on the basis of number of amastigotes in treated and untreated cultures in methanol-fixed and Giemsa-stained preparations. The number of amastigotes was determined by analyzing 200 host cells distributed in randomly chosen microscopic fields. The antitrypanosomatid effect is expressed as the IC_{50} .

Infection Assays. Vero cells were grown under the same conditions expressed during 2 days. Afterward, the cells were infected in vitro with metacyclic forms of *T. cruzi*, at a ratio of 10:1. The drugs (IC_{25} concentrations) were added immediately after infection and were incubated for 12 h at 37 °C in 5% CO_2 . The nonphagocytosed parasites and the drugs were removed by washing, and then the infected cultures were grown for 10 days in fresh medium. Fresh culture medium was added every 48 h. The drug activity was determined from the percentage of infected cells, the number of amastigotes per infected cell, and the number of trypomastigotes in the medium,³⁰ in treated and untreated cultures and in methanol-fixed and Giemsa-stained preparations. The percentage of infected cells and the mean number of amastigotes per infected cell were determined by analyzing 200 host cells distributed in randomly chosen microscopic fields every 48 h. The number of trypomastigotes in the medium was determined using a Neubauer hemocytometric chamber every 48 h.

In Vivo Trypanosomocidal Activity Assay. Mice Infection and Treatment. This experiment was performed using the rules and principles of the international guide for biomedical research in experimental animals and with the approval of the ethical committee of the University of Granada, Spain. Groups of six BALB/c albino female mice (6–8 weeks old, 25–30 g weight), maintained under a 12-h dark/light cycle (lights on at 07:30 h) at a temperature of 22 ± 3 °C and provided with water and standard chow ad libitum, were inoculated via the intraperitoneal route with 5×10^5 metacyclic trypomastigotes of *T. cruzi* obtained from previously infected mice blood. The animals were divided as follows: I, positive control group (mice infected but not treated); II, study group (mice infected and treated with the compounds under study). The administration of the tested compounds was begun on the seventh day of infestation once the infection was confirmed, and doses of 25 mg/kg body weight per day were administered for 5 consecutive days (7–12 days post-infection) by intraperitoneal route. Peripheral blood was obtained from the mandibular vein of each mouse (5 μ L samples) and dissolved in 495 μ L of a PBS solution at a dilution of 1:100. The circulating parasite numbers were quantified with a Neubauer's chamber for counting blood cells. This counting was performed every 3 days during

40 days (acute phase). The number of bloodstream forms found was expressed as parasites/mL.

Cyclophosphamide-Induced Immunosuppression and Assessment of Cure. After day 60, the mice entered the chronic phase of the experiment where levels of parasitemia decreased progressively, independent of the treatment. So on day 120 the parasitemia was checked to be undetectable by fresh blood microscopic examination. Then the mice received four ip injections of 200 mg/(kg-w) cyclophosphamide monohydrate (CP) (ISOPAC) on alternate days as previously described.³¹ The efficacy of such an immunosuppression procedure to assess cryptic infection was verified by the high parasitemias under microscopic examination and/or mortality close to the 100% of chronically untreated mice having received the immunosuppression treatment. Within 1 week after the last CP injection parasitemia was evaluated according to the procedure described for acute phase to quantify the presence of blood trypomastigote forms as reactivation rate. Finally, mice were bled out, under gaseous anesthesia (CO₂), via heart puncture and blood was collected. Blood was incubated for 2 h at 37 °C and then overnight at 4 °C in the order to allow the clotting. Then the serum was obtained from the samples after centrifuging the supernatant twice at 1000g and 2700g, consecutively. The serum was aliquoted and used for ELISA and biochemical analysis, as explained below. Hearts were harvested and immediately flushed free of blood by gentle infusion of 10 mL of prewarmed PBS through the left ventricle,³² in order to avoid contamination of collected tissue with blood parasites. Afterward, they were frozen at -80 °C and stored until their use for DNA extraction.

ELISA Tests. Fe-SOD excreted from the parasite, cultured, and processed as described by Lopez-Céspedes et al.³³ was used as the antigen fraction. The partially purified protein fraction was coated onto polystyrene microtiter plates (Nunc, Denmark) at 1.5 µg in carbonate buffer (pH 8.2) for 2 h at 37 °C. The antigen remaining on the plate was eliminated by washing three times with 0.05% PBS-Tween 20 (washing buffer). Free adsorption sites were taken by incubation (2 h at 37 °C) with blocking buffer [0.2% PBS-Tween 20, 1% bovine serum albumin (BSA)]. After the mixture was washed as described previously, the plates were incubated (45 min at 37 °C) with a serum dilution of 1:80 in washing buffer. After a second wash, the plates were incubated in darkness for 20 min with 100 µL of an enzyme-conjugated antibody (anti-IgG peroxidase) at a dilution of 1:1000. The enzyme reaction was developed with the chromogenic substrate *o*-phenylenediamine dihydrochloride (OPD, Sigma) and 10 µL of 30% H₂O₂ per 25 mL for 20 min in the dark. The reaction was stopped by the addition of 50 µL of HCl, 3 N. Absorbance was read at 492 nm in a microplate reader (Sunrise, TECAN). All of the samples were analyzed in triplicate in polystyrene microtiter plates. Mean and standard deviations of the optical densities of the negative control sera were used to calculate the cutoff value.

DNA Extraction and Quantitative PCR. Hearts were thawed and then ground using a Potter-Elvehjem to follow the purification procedure of Wizard genomic DNA purification kit (Promega). The PCR was performed according to two primers designed in our laboratory (unpublished data), based on the published sequence of the enzyme superoxide dismutase *T. cruzi* CL Brenner (GenBank accession no. XM_808937), which amplify a fragment of approximately 300 bp belonging to superoxide dismutase gene b of *T. cruzi*. The PCR was run in a total volume of 20 µL. The reaction mixture was 1 µL of DMSO, 200 nM iSODd, 200 nM iSODr, 10 mM Tris-HCl (pH 9.0), 1.5 mM MgCl₂, 50 mM KCl, 0.01% gelatin, 0.1% Triton X-100, 100 mM of each dNTP, 0.5 U of Taq DNA polymerase, 0.5–1 µg of DNA, and HPLC water, with a final volume of 20 µL. The amplification was done in a MyCycler thermocycler (BioRad) with the following routine: 95 °C/3 min, 30 cycles of 95 °C/30 s, 55.5 °C/45 s, 72 °C/30 s, and 72 °C/7 min. Next, the amplification products were subjected to electrophoresis on 1.6% agarose gel containing 1:10000 of GelRed nucleic acid gel stain, during 90 min at 90 V.

Toxicity Tests by Clinical Chemistry Measurements. A fraction of the serum obtained as was indicated above was sent to the Biochemical Service at the University of Granada where a series of parameters were

measured, according to their commercial kits acquired from Cromakit, by BS-200 chemistry analyzer, Shenzhen Mindray Bio-Medical Electronics Co., Ltd. With the levels obtained for different populations of sera ($n = 15$, $n = 6$) we calculated the mean value and standard deviation. Finally we also calculated the confidence interval for the mean normal populations based on a confidence level of 95% ($100 \times (1 - \alpha) = 100 \times (1 - 0.05)$). These ranges obtained are shown in Table 4, which allows comparison and analysis of sera studied in this work.

Studies on the Mechanism of Action. Metabolites Excretion Study. Cultures of *T. cruzi* epimastigotes (initial concentration of 5×10^5 cells/mL) received IC₂₅ concentrations of the compounds under study (except for control cultures). After incubation for 96 h at 28 °C, the cells were centrifuged at 400g for 10 min. The supernatants were collected to determine the excreted metabolites using ¹H NMR. Chemical shifts were expressed in parts per million (ppm, δ scale), using sodium 2,2-dimethyl-2-silapentane-5-sulfonate as the reference signal. The chemical displacements used to identify the respective metabolites were consistent with those previously described.³⁴

Ultrastructural Alterations. The epimastigotes of *T. cruzi* were cultured at a density of 5×10^5 cells/mL in each corresponding medium containing the compounds tested at their IC₂₅ concentrations. After 72 h, these cultures were centrifuged at 400g for 10 min, and the pellets produced were washed in PBS and then mixed with 2% (v/v) paraformaldehyde/glutaraldehyde in 0.05 M cacodylate buffer (pH 7.4) for 4 h at 4 °C. Following this, the pellets were prepared for transmission electron microscopy (TEM) study using a previously described technique.³⁵

AUTHOR INFORMATION

Corresponding Authors

*M.S.-M.: phone, +34-958-242-369; fax, +34-958-243-862; e-mail, msanchem@ugr.es.

*A.C.: phone, +34-971-173-266; fax, 34-971-173-426; e-mail, antoni.costa@uib.es.

Author Contributions

§F.O. and C.R. contributed equally.

Notes

The authors declare no competing financial interest.

ACKNOWLEDGMENTS

Financial support from the Spanish Ministry of Economy and Competitiveness (MINECO) (Grants CTQ2011-27512/BQU and CONSOLIDER-INGENIO 2010 CSD2010-00065, FEDER funds) and the "Direcció General de Recerca, Desenvolupament Tecnològic i Innovació del Govern Balear" (CAIB, Project 23/2011, FEDER funds) are gratefully acknowledged. L.M. thanks MICINN for a predoctoral fellowship. F.O. is grateful for a FPU Grant from the Ministry of Education of Spain.

ABBREVIATIONS USED

T. cruzi, *Trypanosoma cruzi*; BNZ, benzimidazole; Ro5, Lipinski's rule of five; SI, selectivity index; SOD, superoxide dismutase; NADH, nicotinamide adenine dinucleotide; AIDS, acquired immunodeficiency syndrome; TEM, transmission electron microscopy; dpi, days postinfection; IgG, immunoglobulin G; ELISA, enzyme-linked immunosorbent assay; OD, optical density; SD, standard deviation; PEP, phosphoenolpyruvate; TLC, thin-layer chromatography; DMSO, dimethyl sulfoxide; FBS, fetal bovine serum; RPMI, Roswell Park Memorial Institute; MES, 4-morpholinoethanesulfonic acid; PBS, phosphate buffered saline solution; FCS, fetal calf serum; MTL, medium trypanosomes liquid; EDTA, ethylenediamine-tetraacetic acid; STE, sodium chloride-Tris-EDTA; NBT, nitroblue tetrazolium; BSA, bovine serum albumin; OPD,

o-phenylenediamine dihydrochloride; CK-MB, creatinphosphokinase-MB; LDH, lactate deshydrogenase; AST/GOT, aspartate aminotransferase; ALT/GPT, alanine aminotransferase

REFERENCES

- (1) (a) Cavalli, A.; Bolognesi, M. L. Neglected tropical diseases: multi-target-directed ligands in the search for novel lead candidates against *Trypanosoma* and *Leishmania*. *J. Med. Chem.* **2009**, *52*, 7339–7359. (b) Espuelas, S.; Plano, D.; Nguewa, P.; Font, M.; Palop, J. A.; Irache, J. M.; Sanmartín, C. Innovative lead compounds and formulation strategies as newer kinetoplastid therapies. *Curr. Med. Chem.* **2012**, *19*, 4259–4288.
- (2) Dujardin, J. C.; González-Pacanowska, D.; Croft, S. L.; Olesen, O. F.; Späth, G. F. Collaborative actions in anti-trypanosomatid chemotherapy with partners from disease endemic areas. *Trends Parasitol.* **2010**, *26*, 395–403.
- (3) (a) Guedes, P. M. M.; Silva, G. K.; Gutierrez, F. R. S.; Silva, J. S. Current status of Chagas disease chemotherapy. *Expert Rev. Anti-Infect. Ther.* **2011**, *9*, 609–620. (b) Urbina, J. A. Specific chemotherapy of Chagas disease: relevance, current limitations and new approaches. *Acta Trop.* **2010**, *115*, 55–68. (c) Cerecetto, H.; González, M. Synthetic medicinal chemistry in Chaga's disease: compounds at the final stage of "hit-to-lead" phase. *Pharmaceuticals* **2010**, *3*, 810–838. (d) Sánchez-Sancho, F.; Campillo, N. E.; Páez, J. A. Chagas disease: progress and new perspectives. *Curr. Med. Chem.* **2010**, *17*, 423–452. (e) Soeiro, M. N. C.; de Castro, S. L. *Trypanosoma cruzi* targets for new chemotherapeutic approaches. *Expert Opin. Ther. Targets* **2009**, *13*, 105–121.
- (4) Urbina, J. A. Chemotherapy of Chagas disease. *Curr. Pharm. Des.* **2002**, *8*, 287–295.
- (5) Viotti, R.; Vigliano, C.; Lococo, B.; Alvarez, M. G.; Petti, M.; Bertocchi, G.; Armenti, A. Side effects of benznidazole as treatment in chronic Chagas disease: fears and realities. *Expert. Rev. Anti-Infect. Ther.* **2009**, *7*, 157–163.
- (6) Schofield, C. J.; Jannin, J.; Salvatella, R. The future of Chagas disease control. *Trends Parasitol.* **2006**, *22*, 583–588.
- (7) (a) Maya, J. D.; Cassels, D. K.; Iturriaga-Vasquez, P.; Ferreira, J.; Faúndez, M.; Galanti, N.; Ferreira, A.; Morello, A. Mode of action of natural and synthetic drugs against *Trypanosoma cruzi* and their interaction with the mammalian host. *Comp. Biochem. Physiol., Part A* **2007**, *146*, 601–620. (b) Wilkinson, S. R.; Bot, C.; Kelly, J. M.; Hall, B. S. Trypanocidal activity of nitroaromatic prodrugs: current treatments and future perspectives. *Curr. Top. Med. Chem.* **2011**, *11*, 2072–2084.
- (8) (a) Guerin, P. J.; Olliaro, P.; Sundar, S.; Boelaert, M.; Croft, S. L.; Desjeux, P.; Wasunna, M. K.; Bryceson, A. D. M. *Lancet Infect. Dis.* **2002**, *2*, 494–501. (b) Urbina, J. A.; Docampo, R. Specific chemotherapy of Chagas disease: controversies and advances. *Trends Parasitol.* **2003**, *19*, 495–501.
- (9) (a) Barrio, K.; Stinger, V. H.; Tashker, J.; Wilbur, J. C.; Wilson, L.; Woo, K. Chagas Disease: A Latin American Nemesis. Technical Report; Institute for OneWorld Health (IOWH): San Francisco, CA, 2007; pp 1–110. (b) Clayton, J. Chagas disease: pushing through the pipeline. *Nature* **2010**, *465*, S12–S15.
- (10) Villalonga, P.; Fernandez de Mattos, S.; Ramis, G.; Obrador-Hevia, A.; Sampedro, A.; Rotger, C.; Costa, A. Cyclosquaramides as kinase inhibitors with anticancer activity. *ChemMedChem* **2012**, *7*, 1472–1480.
- (11) Kumar, S. P.; Glória, P. M. C.; Gonçalves, L. M.; Gut, J.; Rosenthal, J.; Moreira, R.; Santos, M. M. M. Squaric acid: a valuable scaffold for developing antimalarials. *Med. Chem. Commun.* **2012**, *3*, 489–493.
- (12) Sánchez-Moreno, M.; Marín, C.; Navarro, P.; Lamarque, L.; García-España, E.; Miranda, C.; Huertas, O.; Olmo, F.; Gómez-Contreras, F.; Pitarch, J.; Arrebola, F. In vitro and in vivo trypanosomycidal activity of pyrazole-containing macrocyclic and macrobicyclic polyamines: their action on acute and chronic phases of Chagas disease. *J. Med. Chem.* **2012**, *55*, 4231–4243.
- (13) (a) Tietze, W. F.; Arlt, M.; Beller, M.; Glüsenkamp, K.-H.; Jähde, E.; Rajewsky, M. F. Squaric acid diethyl ester: a new coupling reagent for the formation of drug biopolymer conjugates. *Chem. Ber.* **1991**, *124*, 1215–1221. (b) Rotger, M. C.; Piña, M. N.; Frontera, A.; Martorell, G.; Ballester, P.; Deyà, P. M.; Costa, A. Conformational preferences and self-template macrocyclization of squaramide-based foldable modules. *J. Org. Chem.* **2004**, *69*, 2302–2308.
- (14) Yum, J.-H.; Walter, P.; Huber, S.; Rentsch, D.; Geiger, T.; Nüesch, F.; De Angelis, F.; Grätzel, M.; Nazeeruddin, M. K. Efficient near-IR sensitization of nanocrystalline TiO₂ films by an asymmetrical squaraine dye. *J. Am. Chem. Soc.* **2007**, *129*, 10320–10321.
- (15) Prohens, R.; Rotger, M. C.; Piña, M. N.; Deyà, P. M.; Morey, J.; Ballester, P.; Costa, A. Thermodynamic characterization of the squaramide-carboxylate interaction in squaramide receptors. *Tetrahedron Lett.* **2001**, *42*, 4933–4936.
- (16) (a) Martínez, L.; Sampedro, A.; Sanna, E.; Costa, A.; Rotger, C. Synthesis and conformational studies of peptido-squaramide foldable modules: a new class of turn-mimetic compounds. *Org. Biomol. Chem.* **2012**, *10*, 1914–1921. (b) López, C.; Vega, M.; Sanna, E.; Rotger, C.; Costa, A. Efficient microwave-assisted preparation of squaric acid monoamides in water. *RSC Adv.* **2013**, *3*, 7249–7253.
- (17) (a) Piña, M. N.; Rotger, C.; Soberats, B.; Ballester, P.; Deyà, P. M.; Costa, A. Evidence of anion-induced dimerization of a squaramide-based host in protic solvents. *Chem. Commun.* **2006**, 963–965. (b) Tomás, S.; Prohens, R.; Deslongchamps, G.; Ballester, P.; Costa, A. An effective fluorescent sensor for choline-containing phospholipids. *Angew. Chem., Int. Ed.* **1999**, *38*, 2208–2211.
- (18) (a) Lipinski, C. A.; Lombardo, F.; Dominy, B. W.; Feeney, P. J. Experimental and computational approaches to estimate solubility and permeability in drug discovery and development settings. *Adv. Drug Delivery Rev.* **1997**, *46*, 3–26. (b) Veber, D. F.; Johnson, S. R.; Cheng, H.-Y.; Smith, B. R.; Ward, K. W.; Kopple, K. D. Molecular properties that influence the oral bioavailability of drug candidates. *J. Med. Chem.* **2002**, *45*, 2615–2623.
- (19) (a) González, P.; Marín, C.; Rodríguez-González, I.; Hitos, A. B.; Rosales, M. J.; Reina, M.; Diaz, J. G.; González-Coloma, A.; Sánchez-Moreno, M. In vitro activity of C20-diterpenoid alkaloid derivatives in promastigotes and intracellular amastigotes of *Leishmania infantum*. *Int. J. Antimicrob. Agents* **2005**, *25*, 136–41. (b) Sánchez-Moreno, M.; Gómez-Contreras, F.; Navarro, P.; Marín, C.; Ramírez-Macías, I.; Olmo, F.; Sanz, A. M.; Campayo, L.; Cano, C.; Yunta, M. J. R. In vitro leishmanicidal activity of imidazole- or pyrazole-based benzo[g]phthalazine derivatives against *Leishmania infantum* and *Leishmania braziliensis* species. *J. Antimicrob. Chemother.* **2012**, *67*, 387–397.
- (20) Rotger, C.; Piña, M. N.; Vega, M.; Ballester, P.; Deyà, P. M.; Costa, A. Efficient macrocyclization of preorganized palindromic oligosquaramides. *Angew. Chem., Int. Ed.* **2006**, *45*, 6844–6848.
- (21) Ursu, O.; Rayan, A.; Goldblum, A.; Oprea, T. I. Understanding drug-likeness. *Wiley Interdiscip. Rev.: Comput. Mol. Sci.* **2011**, *1*, 760–781.
- (22) Nwaka, S.; Besson, D.; Ramirez, B.; Maes, L.; Matheussen, A.; Bickle, Q.; Mansour, N. R.; Yousif, F.; Townson, S.; Gokool, S.; Chongwa, F.; Samje, M.; Misra-Bhattacharya, S.; Murthy, P. K.; Fakorede, F.; Paris, J. M.; Yeates, C.; Ridley, R.; Van Voorhis, W. C.; Geary, T. Integrated dataset of screening hits against multiple neglected disease pathogens. *PLoS Neglected Trop. Dis.* **2011**, *5*, e1412.
- (23) Da Silva, C. F.; Batista, M. M.; Batista, D. G. J.; de Souza, E. M.; da Silva, P. B.; de Oliveira, G. M.; Meuser, A. S.; Shareef, A. R.; Boykin, D. W.; Soeiro, M. N. C. In vitro and in vivo studies of the trypanocidal activity of a diarylthiophene diamidine against *Trypanosoma cruzi*. *Antimicrob. Agents Chemother.* **2008**, *52*, 3307–3314.
- (24) (a) Bringaud, F.; Rivière, L.; Coustou, V. Energy metabolism of trypanosomatids: adaptation to available carbon sources. *Mol. Biochem. Parasitol.* **2006**, *149*, 1–9. (b) Turens, J. More differences in energy metabolism between Trypanosomatidae. *Parasitol. Today* **1999**, *15*, 346–347.
- (25) Cazzulo, J. J. Aerobic fermentation of glucose by trypanosomatids. *FASEB J.* **1992**, *6*, 3153–3161.

(26) Michels, P. A.; Bringaud, F.; Herman, M.; Hannaert, V. Metabolic functions of glycosomes in trypanosomatids. *Biochim. Biophys. Acta* **2006**, *1763*, 1463–1477.

(27) Téllez-Meneses, J.; Mejía-Jaramillo, A. M.; Triana-Chávez, O. Biological characterization of *Trypanosoma cruzi* stocks from domestic and sylvatic vectors in Sierra Nevada of Santa Marta, Colombia. *Acta Trop.* **2008**, *108*, 26–34.

(28) Marín, C.; Clares, M. P.; Ramírez-Macías, I.; Blasco, S.; Olmo, F.; Soriano, C.; Verdejo, B.; Rosales, M. J.; Gomez-Herrera, D.; García-España, E.; Sánchez-Moreno, M. In vitro activity of scorpian-like azamacrocyclic derivatives in promastigotes and intracellular amastigotes of *Leishmania infantum* and *Leishmania braziliensis*. *Eur. J. Med. Chem.* **2013**, *62*, 466–477.

(29) Cardoso, J.; Soares, M. J. In vitro effects of citral on *Trypanosoma cruzi* metacyclogenesis. *Mem. Inst. Oswaldo Cruz* **2010**, *5*, 1026–32.

(30) Sánchez-Moreno, M.; Sanz, A. M.; Gómez-Contreras, F.; Navarro, P.; Marín, C.; Ramírez-Macías, I.; Rosales, M. J.; Olmo, F.; Garcia-Aranda, I.; Campayo, L.; Cano, C.; Arrebola, F.; Yunta, M. J. R. In vivo trypanosomicidal activity of imidazole- or pyrazole-based benzo[g]phthalazine derivatives against acute and chronic phases of Chagas disease. *J. Med. Chem.* **2011**, *54*, 970–979.

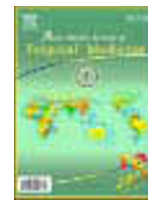
(31) Cencig, S.; Coltel, N.; Truyens, C.; Carlier, Y. Parasitic loads in tissues of mice infected with *Trypanosoma cruzi* and treated with AmBisome. *PLoS Neglected Trop. Dis.* **2011**, *5*, e1216.

(32) Ye, X.; Ding, J.; Zhou, X.; Chen, G.; Liu, S. F. Divergent roles of endothelial NF- κ B in multiple organ injury and bacterial clearance in mouse models of sepsis. *J. Exp. Med.* **2008**, *205*, 1303–1315.

(33) Lopez-Cespedes, A.; Villagran, E.; Briceño-Alvarez, K.; de Diego, J. A.; Hernandez-Montiel, H. L.; Saldaña, C.; Sanchez-Moreno, M.; Marin, C. *Trypanosoma cruzi*: seroprevalence detection in suburban population of Santiago de Queretaro (Mexico). *Sci. World J.* **2012**, DOI: 10.1100/2012/914129.

(34) Fernández-Becerra, C.; Sánchez-Moreno, M.; Osuna, A.; Opperdoes, F. R. Comparative aspects of energy metabolism in plant trypanosomatids. *J. Eukaryotic Microbiol.* **1997**, *44*, 523–529.

(35) Ramírez-Macías, I.; Marín, C.; Chahboun, R.; Messouri, I.; Olmo, F.; Rosales, M. J.; Gutierrez-Sánchez, R.; Alvarez-Manzaneda, E.; Sánchez-Moreno, M. In vitro and in vivo studies of the trypanocidal activity of four terpenoid derivatives against *Trypanosoma cruzi*. *Am. J. Trop. Med. Hyg.* **2012**, *87*, 481–488.



Document heading doi: 10.1016/S1995-7645(14)60149-8

Specific primers design based on the superoxide dismutase b gene for *Trypanosoma cruzi* as a screening tool: Validation method using strains from Colombia classified according to their discrete typing unit

Francisco Olmo¹, Javier Escobedo–Ortegón², Patricia Palma¹, Manuel Sánchez–Moreno¹, Ana Mejía–Jaramillo³, Omar Triana³, Clotilde Marín^{1*}

¹Grupo de Parasitología Molecular, Departamento de Parasitología; Universidad de Granada, Severo Ochoa s/n, E-18071 Granada (España)

²Laboratorio de Zoonosis y ETV's, C.I.R. Dr. Hideyo Noguchi, Universidad Autónoma de Yucatán, Ave. Itzaes #490 x 59, 97000 Mérida, Yucatan (Mexico)

³Grupo Biología y Control de Enfermedades Infecciosas BCEI – SIU, Instituto de Biología, Universidad de Antioquia, Medellín, Colombia

ARTICLE INFO

Article history:

Received 10 April 2014

Received in revised form 15 May 2014

Accepted 15 July 2014

Available online 20 November 2014

Keywords:

Trypanosoma cruzi

Polymerase chain reaction

Colombia

Superoxide dismutase gene b - based primers

Discrete typing unit

ABSTRACT

Objective: To classify 21 new isolates of *Trypanosoma cruzi* (*T. cruzi*) according to the Discrete Typing Unit (DTU) which they belong to, as well as tune up a new pair of primers designed to detect the parasite in biological samples. **Methods:** Strains were isolated, DNA extracted, and classified by using three Polymerase Chain Reactions (PCR). Subsequently this DNA was used along with other isolates of various biological samples, for a new PCR using primers designed. Finally, the amplified fragments were sequenced. **Results:** It was observed the predominance of DTU I in Colombia, as well as the specificity of our primers for detection of *T. cruzi*, while no band was obtained when other species were used. **Conclusions:** This work reveals the genetic variability of 21 new isolates of *T. cruzi* in Colombia. Our primers confirmed their specificity for detecting the presence of *T. cruzi*.

1. Introduction

Chagas disease, also called American Trypanosomiasis, is a tropical parasitic disease caused by the flagellate protozoan *Trypanosoma cruzi* (*T. cruzi*). It is commonly transmitted to humans and other mammals by an insect vector [1, 2], the blood-sucking bugs of the subfamily Triatominae (family Reduviidae) and with the most of its commonly species belonging to the *Triatoma*, *Rhodnius*,

and *Panstrongylus genera*. The disease may also be spread through blood transfusion and organ transplantation and from a mother to her fetus. This disease is an endemic zoonosis in the Americas [3] and it is considered as the most important parasitic disease in Latin America, because the morbidity and the economic losses that it can produce. Currently, about 8 million people are infected with this systemic disease and another 28 million are currently at risk of acquiring the infection. In America, the incidence of infection is approximately 41 200 new cases, and an average of 12 500 deaths occur annually [4]. The nomenclature of *T. cruzi* has been recently modified and six DTUs have been proposed within *T. cruzi* being: *T. cruzi* I (Tc I), *T. cruzi* II (Tc II), *T. cruzi* III (Tc III), *T. cruzi* IV (Tc IV), *T. cruzi* V (Tc V) and *T. cruzi* VI (Tc VI) to reflect the high genetic variability of the species [5]. Since this classification is one of the

*Corresponding author: Clotilde Marín, Grupo de Parasitología Molecular, Departamento de Parasitología; Universidad de Granada, Severo Ochoa s/n, E-18071 Granada (España).

Tel: +34 958 248886

Fax: +34 958 243174

E-mail: cmaris@ugr.es

Foundation project: This project is funded by a FPU a grant from the Ministry of Education of Spain.

most currently accepted, we decided to follow it in order to homogenize the knowledge albeit to have performed some other analysis as biochemical and Restriction Fragment Length Polymorphism of the same group of trypanosomes (data not shown).

The proper characterization of the isolates of *T. cruzi* is essential to determine the possible role that the different strains play in the disease evolution, the geographic variability, the clinic stage, disease evolution or prognosis and the morbidity caused by the disease but also the resistance to specific drug chemotherapy. The introduction of new techniques, have increased the ability to characterize the parasites through isoenzymatic analysis, chromosomes migration, restriction enzymes, sequencing, DNA synthesis, DNA probes and the PCR[6]. The kDNAminicircles are a very useful target for PCR since there are present in 10–20 000 copies/parasite, so assays based on the PCR in amplification of these minicircles are especially sensitive[7]. Another advantageous strategy is the amplification of the conserved sequence that includes a hyper variable region that can be used to typify strains[8].

Superoxide dismutases (SOD) are a group of metalloenzymes that have a central component in antioxidant defense in most organisms by their ability of removes excess of superoxide radicals (O_2^-) by converting them to oxygen (O_2) and hydrogen peroxide (H_2O_2). According to their metal cofactor, SODs can be classified into four isoform types: iron (FeSOD), copper/zinc (Cu/ZnSOD), manganese (MnSOD) and nickel (NiSOD)[9]. However, in a number of protozoan organisms, only FeSOD has been found[10]. The enzymatic activity of the FeSOD in *T. cruzi* was detected first by Boveris and Stoppani[11]. Two SOD genes, Fesod–A and Fesod–B, were later cloned and characterized[12, 13]. Recently, new FeSOD–C and two closely related FeSOD–B genes (FeSOD–B1 and FeSOD–B2) have been identified in *T. cruzi* and in other trypanosomatids[10, 14].

The purpose of this work is to classify 21 new isolates in Colombia according to DTU to which they belong, this will be done based on the three molecular markers by PCR: SL, 24S rDNA[15, 16] and 18S rDNA[17]. Once classified, these strains were used for the tuning of a pair of primers designed according with the superoxide dismutase (sod–b) nucleotide sequence of the parasite to detect the presence of parasite DNA in biological samples no matter which strain of *T. cruzi* the sample has. Finally, the amplified fragments were studied by sequencing to obtain more complete information about them specially to let us know which are the differences at this level.

2. Material and methods

2.1. *T. cruzi* new stocks isolation and in vitro culture

The new 21 stocks from different biologic origins and geographical areas from Colombia and 3 different *T. cruzi* reference strains from South America. Epimastigotes were grown in the biphasic culture NNN (Novy–McNeal–Nicole), supplemented with minimal essential medium, and 20% of Foetal Bovine Serum Inactivated (FBSI) at 56 °C for 30 minutes. The isolates were then seed and cultured in vitro using Grace's insect medium supplemented with 10% of FBSI in 75 cm² flask (Roux) starting with a concentration of 5×10^4 parasites/mL at 28 °C. The parasites were removed by centrifugation at 600 g for 10 min at room temperature.

Eleven other trypanosomatids, 6 species belonging to *Leishmania* genera [*Leishmania amazonensis* (*L. amazonensis*), *Leishmania braziliensis* (*L. braziliensis*), *Leishmania guyanensis* (*L. guyanensis*), *Leishmania infantum* (*L. infantum*), *Leishmania mexicana* (*L. Mexicana*) and *Leishmania peruviana* (*L. peruviana*)] and 5 different *Trypanosoma rangeli* (*T. rangeli*) strains (*T. rangeli* 605, *T. rangeli* 606, *T. rangeli* 706, *T. rangeli* Pa and *T. rangeli* Pe) were cultured in similar conditions as described above at 28 °C in tissue–culture flasks until the cultures reached a density of approximately 2×10^7 parasites/mL. Cells were collected at the logarithmic growth phase by centrifugation (600 g for 10 min at room temperature). Similarly, mammalian cells (J774.2 macrophage stable cell line from mouse) were grown in a humidified 95% air, 5% CO₂ atmosphere at 37 °C, using in Minimal Essential Medium plus glutamine (2 mM) and 20% of FBSI. Finally the cells are collected by centrifugation at 100 g for 10 min and washed twice with phosphate buffered saline and about 10 mg of fresh or thawed pellet was used to isolate the DNA of each sample, following the manufacturer instructions of the kit mentioned below.

2.2. DNA extraction and purification

Trypanosomatids were collected by centrifugation of 300 mL of culture medium, when their concentrations had reached about 2×10^7 cells/mL, after about 5 days. They were washed twice in 50 mL of 0.15 M NaCl, 0.015 M sodium citrate, and once with SE buffer (0.15M NaCl, 0.1M EDTA, pH 8.0). Trypanosomatids, genomic DNA from cultured mammalian cells and human cells obtained by scraping the buccal mucosa were isolated following the purification procedure of Wizard® Genomic DNA Purification Kit (Promega).

2.3. PCR–fragments to DTU analysis

Once the DNA has been extracted and purified, the different samples were amplified for certain sequences using PCR. Firstly, the three primer reaction mix used were able to amplify the non–transcribed spacer of the minixon genes (SL) of the *T. cruzi* DNA, the primer sequences were: Tc1 (5′–GTGTCCGCCACCTCCTCGGGCC–3′), Tc2 (5′–CCTGCAGGCACACGTGTGTGTG–3′) and TcC (5′–CCCCCTCCCAGGCCACACTG–3′). These primers amplified a fragment of 350 bp for the group *T. cruzi* I, 300 bp for the groups *T. cruzi* II, V and VI and no band was obtained for the groups *T. cruzi* III and IV[5]. Then, the amplification products were subjected to electrophoresis on 1.5% agarose gel containing 1:10000 of GelRed™ Nucleic Acid Gel Stain, during 90 minutes at 90 V. Finally the results were visualized in a UV–transilluminator and photographed with a digital camera Olympus Camedia, C–4000 Zoom.

The next PCR performed was done over a divergent domain from 24S α ribosomal RNA gene. The corresponding fragment was achieved with the primers: D71 (5′–AAGGTCCGTCGACAGTGTGG–3′) and D72 (5′–TTTTCAGAAATGGCCGAACAGT–3′). The amplification products of these pair of primers was a fragment of 110 bp for the group *T. cruzi* I, II and V, 120 bp for the group *T. cruzi* IV or 125 bp length for the group *T. cruzi* VI[15,16]. Once again, the amplification products were subjected to electrophoresis on 3.0% agarose gel containing 1:10000 of GelRed™ Nucleic Acid Gel Stain, during 120 minutes at 80 V and carried out as described above.

The last PCR was performed over the small subunit ribosomal DNA (18S rDNA), so the primers used were: V1 (5′–CAAGCGGCTGGGTGTTATTCCA–3′) and V2 (5′–TTGAGGGAAGGCATGACACATGT–3′). The amplification products of these pair of primers were fragment of 155 bp for the group *T. cruzi* IV, 165 bp for the group *T. cruzi* II, III and V or 175 bp for the group *T. cruzi* I, while no band was detected for DTU VI[17]. Further observation and documentation of the products was done equally as above.

2.4. Sod gene PCR

Finally, two primers were designed in our laboratory, based on the published sequence of the enzyme superoxide dismutase *T. cruzi* CL Brenner (GenBank accession No. XM_808937): iSODTc–r (5′–GTTGTCGATGGCAACCTCTT–3′) and iSODTc–d (5′–ATGAGCTTCGTCATTCTCC –3′). These two nucleotide sequences have been deposited in the GenBank database with accession number DQ441589.

This pair of primers amplify a fragment of approximately 270 bp belonging to superoxide dismutase gene b in all strains of *T. cruzi*. The PCR was performed in a total volume of 20 μ L. The reaction mixture: 10% of DMSO, 200 nM of iSODd, 200 nM of iSODr, 10 mM Tris–HCl (pH 9.0), 1.5 mM MgCl₂, 50 mM KCl, 0.01% gelatin, 0.1% triton X–100, 10 mM of each dNTP, 0.5 U of *Taq* DNA polymerase, 1–20 ng of kDNA and HPLC water to complete a final volume of 20 μ L. The amplification was done in Thermal Cycler™ MyCyclerthermocycler (BioRad) with the following routine temperature: 95 °C/3 min, 30 cycles of 95 °C/30 s, 55.5 °C/45 s, 72 °C/30 s and 72 °C/7 min. Next, the amplification products were subjected to electrophoresis on 1.5% agarose gel containing 1:10 000 of GelRed™ Nucleic Acid Gel Stain, during 90 minutes at 90 V.

2.5. Sequencing

The fragments amplified by PCR–SOD of the 24 strains, were migrated in low melting point agarose gel and then purified with a column (Wizard SV gel purification system; Promega, Madison, USA) and then sequenced. The sequencing was carried out, for the 300 bp fragments, using a capillary electrophoresis sequencer ABI3100 Avant (AppliedBiosystems). Finally, the chromatograms obtained were treated with the program MEGA4 getting a size sequence approximately 270 bp for each strain after removing the primers, where the variable nucleotides or polymorphism in the sequence were observed of each strain.

3. Results

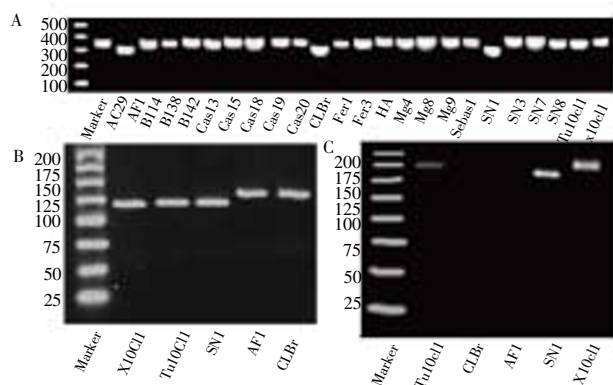
After performing the above three PCRs mentioned, a series of bands of the *T. cruzi* strains were obtained that allowed us to identify those DTUs which the new isolates belong to. Table 1 lists the identification names of the strains together with their geographical origin and the species from they were isolated. The next three columns show the results according to the three PCRs: SL, 24S α 18S ribosomal RNA gene and rDNA (Figure 1). The classification could be sufficiently clear only through PCR#1: SL (Figure 1A), with exception of AF1, SN1 and CLBr isolates which were submitted to PCR#2: 24S α rDNA (Figure 1B) and PCR#3: 18S rDNA (Figure 1C). The last column shows the final results obtained by assigning the DTU to which each strain belongs. As reference strains were selected two DTU I: Tu10cl1 and X10cl1[19], also one of the most studied strains, CLBr, representative of the DTU VI[20]. All new isolated belong to DTU I except for AF1 and SN1

Table 1Origin and classification of isolates studied of *T. cruzi*.

Code	Geographical origin	Biological origin	PCR#1:SL	PCR#2: 24S rDNA	PCR#3: 18S rDNA	DTU
AC 29	Acandí–Choco (Colombia)	<i>Rhodnius pallescens</i>	350	–	–	Tc I
AF 1	Amalfi–Antioquia (Colombia)	<i>Panstrongylus geniculatus</i>	300	125	no band	Tc VI
B 114	Cordoba (Colombia)	<i>Triatoma dimidiata</i>	350	–	–	Tc I
B 138	Cordoba (Colombia)	<i>Triatoma dimidiata</i>	350	–	–	Tc I
B 142	Cordoba (Colombia)	<i>Triatoma dimidiata</i>	350	–	–	Tc I
Cas 13	Casanare (Colombia)	<i>Rhodnius prolixus</i>	350	–	–	Tc I
Cas 15	Casanare (Colombia)	<i>Rhodnius prolixus</i>	350	–	–	Tc I
Cas 18	Casanare (Colombia)	<i>Didelphis marsupialis</i>	350	–	–	Tc I
Cas 19	Casanare (Colombia)	<i>Rhodnius prolixus</i>	350	–	–	Tc I
Cas 20	Casanare (Colombia)	<i>Rhodnius prolixus</i>	350	–	–	Tc I
*CL Br	Brazil	<i>Triatoma infestans</i>	300	125	no band	Tc VI
Fer 1	Bolivar (Colombia)	<i>Rhodnius pallescens</i>	350	–	–	Tc I
Fer 3	Bolivar (Colombia)	<i>Rhodnius pallescens</i>	350	–	–	Tc I
HA	Casanare (Colombia)	<i>Homo sapiens</i>	350	–	–	Tc I
Mg 4	Magdalena (Colombia)	<i>Rhodnius pallescens</i>	350	–	–	Tc I
Mg 8	Magdalena (Colombia)	<i>Triatoma dimidiata</i>	350	–	–	Tc I
Mg 9	Magdalena (Colombia)	<i>Triatoma dimidiata</i>	350	–	–	Tc I
Sebas 1	Magdalena (Colombia)	<i>Rhodnius pallescens</i>	350	–	–	Tc I
SN 1	Guajira (Colombia)	<i>Rhodnius prolixus</i>	300	110	165	Tc V
SN 3	Guajira (Colombia)	<i>Rhodnius prolixus</i>	350	–	–	Tc I
SN 7	Guajira (Colombia)	<i>Triatoma dimidiata</i>	350	–	–	Tc I
SN 8	Guajira	<i>Rhodnius prolixus</i>	350	–	–	Tc I
*Tu10cl 1	Bolivia	<i>Triatoma infestans</i>	350	110	175	Tc I
*X10cl 1	Brazil	<i>Homo sapiens</i>	350	110	175	Tc I

*Reference strains

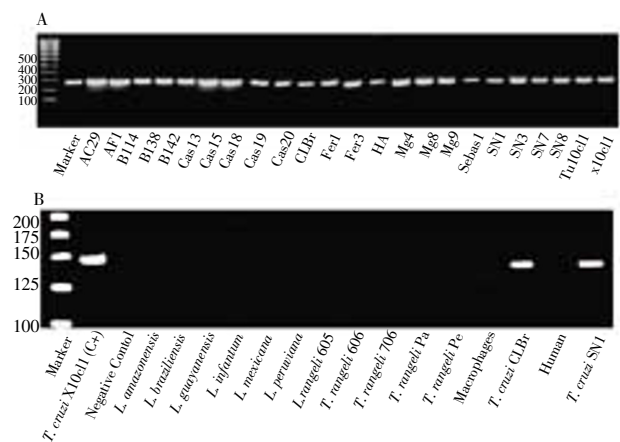
that belong to DTU VI and V, respectively.

**Figure 1.** DNA fragments obtained by the different PCR assays.

A, Shows fragment obtained after SL PCR; B, Shows fragment obtained after 24S rDNA PCR and C, Shows fragment obtained after 18S rDNA PCR.

Then the pair of primers designed in our laboratory was set up, using the same set of DNA samples. As it can be seen in Figure 2A, all strains originate a band near the 300 bp that corresponds to a fragment within the *sod* gene of the parasite. After obtaining these fragments, they were purified and sequenced as it has been described above; Table 2 shows the variations that appear within this fragment,

and the positions where the variations occur. Within the sequence of 270 bp, the variable positions were 20. All these DNA sequences were deposited into the NCBI/GeneBank database under the Accession numbers ET064919 to ET064942 (GSS category).

**Figure 2.** Tune up of new primers designed based on *sod* gene primers.

A, Result of PCR amplification of different strains with the *T. cruzi*. B, Result of PCR amplification of DNA samples belonging to different species.

In order to confirm the *T. cruzi* *sod*-PCR specificity, this pair of primers was assayed with several DNA isolates of

Table 2Variable positions within a sequence of 270 bp belonging to the *sod*-b gene of the *T. cruzi* strains studied.

STRAIN CODE	Variable positions																				
	20	110	122	143	146	155	186	188	189	190	191	218	219	220	221	222	224	226	230	242	
CLBr	C	C	C	T	C	G	T	C	T	T	G	-	G	A	G	A	G	C	-	A	
AF1	G	A	-	-	.
Tu10cl 2	G	T	N	G	A	.	.	T	.	G	-	T	-	.	
AC29	G	T	T	G	A	.	.	G	A	.	.	-	-	.	
B114	G	T	T	G	A	.	.	-	T	.	
B138	G	T	T	T	.	.	.	-	-	.	
B142	G	T	T	T	.	.	.	-	-	.	
Cas13	G	T	T	T	.	.	.	-	-	.	
Cas15	G	T	T	.	.	.	-	-	.	
Cas18	G	T	N	T	.	.	.	G	A	G	A	G	C	T	-	.	
Cas19	G	T	N	T	.	.	.	T	-	.	
Cas20	G	T	N	T	.	.	.	T	-	.	
Fer1	G	T	T	T	.	.	.	-	-	.	
Fer3	G	T	T	T	.	.	.	-	-	.	
HA	G	T	T	T	.	.	.	T	-	.	
Mg4	G	T	T	T	.	.	.	-	-	.	
Mg8	G	T	T	T	.	.	.	-	-	.	
Mg9	G	T	T	T	.	.	.	T	-	.	
Sebas1	G	T	T	G	.	.	.	-	-	-	
SN1	G	T	T	T	.	.	.	-	-	.	
SN3	G	T	T	T	.	.	.	T	-	.	
SN7	G	T	.	G	A	.	G	T	G	G	.	T	-	.	
SN8	G	T	T	T	.	.	.	-	-	.	
X10cl1	G	T	T	G	A	.	.	T	A	.	.	T	-	.	

Key: G, guanidine; C, cytosine; A, adenine; T, thymine; -, Gap; N, any nucleotide; •, repetition

different species of kinetoplastids (*Trypanosoma rangeli* and *Leishmania* spp.) and three mammals (mice, monkeys and humans). The results are shown in Figure 2B, which display only the expected band of around 300 bp in the samples corresponding to *T. cruzi* but not in any other non-*T. cruzi* DNA.

4. Discussion

As its has known, the clonal evolution of this parasite and its several forms found in a lot of mammal reservoirs, arthropod vector and humans has an important role in the behavior of a particular variety of a strain. The correct positioning and identification of its origin is very important for the comprehension and understanding of the epidemiological pattern that a particular clone of this

parasite may represent for a local environment, not only for the human impact in health but also for the economy (cost of treatment or work disabilities).

Thus, the results of this work show a clear representation of *T. cruzi* DTU I in Colombia, saving an isolate identified as DTU V and another as DTU VI. This result confirm the previous reports which showed the high prevalence of DTU I in north of the Amazon where is located Colombia^[19].

The PCR designed based on the sequence of the *sod* gene of *T. cruzi* allows to identify the strains of the parasite in different samples. After more extensive studies, including other kind of samples of different origin, it could become in a new tool to perform epidemiological surveys and genotyping studies, since it is a highly specific technique capable of discriminating the parasite DNA compared to other DNA samples from different species. It also would allow establish a criteria for cure after observing the disappearance of the

parasite DNA in chemotherapy experiments and new drugs design against *T. cruzi* as observed in preliminary studies currently being carried on in our lab (data not shown).

Conflict of interest statement

The authors declare that there are no conflicts of interest.

Acknowledgements

The authors thank the member of the Department of Physical Chemistry of the University of Granada for their technical support. Also we must thank the Sequencing service of the CIC–University of Granada and especially to Dr. Francisca Robles of Department of Genetics for her help and support. F.O. is grateful for a FPU Grant from the Ministry of Education of Spain.

References

- [1] Miles MA, Feliciangeli MD, Arias AR. American trypanosomiasis (Chagas' disease) and the role of molecular epidemiology in guiding control strategies. *BMJ* 2003; **326**: 1444–1448.
- [2] Moncayo A. Chagas disease: current epidemiological trends after the interruption of vectorial and transfusional transmission in the Southern Cone countries. *Mem Inst Oswaldo Cruz* 2003; **98**: 577–591.
- [3] Villagran ME, Marin C, Hurtado A, Sanchez–Moreno M, de Diego JA. Natural infection and distribution of triatomines (Hemiptera: Reduv [i] dae) in the state of Queretaro, Mexico. *Trans R Soc Trop Med Hyg* 2008; **102**: 833–838.
- [4] Guedes PM, Silva GK, Gutierrez FR, Silva JS. Current status of Chagas disease chemotherapy. *Expert Rev Anti Infect Ther* 2011; **9**: 609–620.
- [5] Zingales B, Miles MA, Campbell DA, Tibayrenc M, Macedo AM, Teixeira MMG, et al. The revised *Trypanosoma cruzi* subspecific nomenclature: Rationale, epidemiological relevance and research applications. *Infect Genet Evol* 2012; **12**: 240–253.
- [6] Desquesnes M, Dávila AM. Applications of PCR–based tools for detection and identification of animal trypanosomes: a review and perspectives. *Vet Parasitol* 2002; **109**: 213–231.
- [7] Dorn PL, Engelke D, Rodas A, Rosales R, Melgar S, Brahney B, et al. Utility of the polymerase chain reaction in detection of *Trypanosoma cruzi* in Guatemalan Chagas' disease vectors. *Am J Trop Med Hyg* 1999; **60**: 740–745.
- [8] Zingales B, Andrade SG, Briones MR, Campbell DA, Chiari E, Fernandes O, et al. A new consensus for *Trypanosoma cruzi* intraspecific nomenclature: second revision meeting recommends TcI to TcV]. Second Satellite Meeting. *Mem Inst Oswaldo Cruz* 2009; **104**:1051–1054.
- [9] Miller AF. Superoxide dismutases: active sites that save, but a protein that kills. *Curr Opin Chem Biol* 2004; **8**: 1–7.
- [10] Dufernez F, Yernaux C, Gerbod D, Noël C, Chauvenet M, Wintjens R, et al. The presence of four iron–containing superoxide dismutase isozymes in Trypanosomatidae: characterization, subcellular localization, and phylogenetic origin in *Trypanosoma brucei*. *Free Radic Biol Med* 2006; **40**: 210–225.
- [11] Boveris A, Stoppani AO. Hydrogenperoxide generation in *Trypanosoma cruzi*. *Experientia* 1977; **33**: 1306–1308.
- [12] Ismail SO, Paramchuk W, Skeiky YAW, Reed SG, Bhatia A. Molecular cloning and characterization of two iron superoxide dismutase cDNAs from *Trypanosoma cruzi*. *Mol Biochem Parasitol* 1997; **86**: 187–197.
- [13] Temperton NJ, Wilkinson SR, Kelly JM. Cloning of a Fe–superoxide dismutase gene homologue from *Trypanosoma cruzi*. *Mol Biochem Parasitol* 1996; **76**: 339–343.
- [14] Wilkinson SR, Prathalingam SR, Taylor MC, Ahmed A, Horn D, Kelly JM. Functional characterisation of the iron superoxide dismutase gene repertoire in *Trypanosoma brucei*. *Free Radic Biol Med* 2006; **40**: 198–209.
- [15] Souto RP, Zingales B. Sensitive detection and strain classification of *Trypanosoma cruzi* by amplification of a ribosomal RNA sequence. *Mol Biochem Parasitol* 1993; **62**: 45–52.
- [16] Souto RP, Fernandes O, Macedo AM, Campbell DA, Zingales B. DNA markers define two major phylogenetic lineages of *Trypanosoma cruzi*. *Mol Biochem Parasitol* 1996; **83**: 141–152.
- [17] Clark CG, Pung OJ. Host specificity of ribosomal DNA variation in sylvatic *Trypanosoma cruzi* from North America. *Mol Biochem Parasitol* 1994; **66**: 175–179.
- [18] Gonçalves AM, Nehme N, Morel CM. Trypanosomatids characterization by schizodeme analysis. In: Morel CM, editors. *Genes and antigens of parasites–A laboratory manual*. Rio de Janeiro: Fundação Oswaldo Cruz 1984, p. 95–109.
- [19] Franzén O, Ochaya S, Sherwood E, Lewis MD, Llewellyn MS, Miles MA, et al. Shotgun sequencing analysis of *Trypanosoma cruzi* I Sylvio X10/1 and comparison with *T. cruzi* V] CL Brener. *PLoS Negl Trop Dis* 2011; **5**: e984.
- [20] Andersson B. The *Trypanosoma cruzi* genome; conserved core genes and extremely variable surface molecule families. *Res Microbiol* 2011; **162**: 619–625.



Original article

Prospects of an alternative treatment against *Trypanosoma cruzi* based on abietic acid derivatives show promising results in Balb/c mouse model

F. Olmo^a, J.J. Guardia^b, C. Marin^a, I. Messouri^b, M.J. Rosales^a, K. Urbanová^a,
I. Chayboun^b, R. Chahboun^b, E.J. Alvarez-Manzaneda^b, M. Sánchez-Moreno^{a,*}

^a Department of Parasitology, Instituto de Investigación Biosanitaria ibs, University of Granada, Severo Ochoa s/n, E-18071 Granada, Spain

^b Department of Organic Chemistry, University of Granada, Severo Ochoa s/n, E-18071 Granada, Spain

ARTICLE INFO

Article history:

Received 26 February 2014

Received in revised form

29 October 2014

Accepted 1 November 2014

Available online 3 November 2014

Keywords:

Anti-chagasic

Abietic acid

Chemotherapy

Trypanosomiasis

ABSTRACT

Chagas disease, caused by the protozoa parasite *Trypanosoma cruzi*, is an example of extended parasitaemia with unmet medical needs. Current treatments based on old-featured benznidazole (Bz) and nifurtimox are expensive and do not fulfil the criteria of effectiveness, and a lack of toxicity devoid to modern drugs. In this work, a group of abietic acid derivatives that are chemically stable and well characterised were introduced as candidates for the treatment of Chagas disease. *In vitro* and *in vivo* assays were performed in order to test the effectiveness of these compounds. Finally, those which showed the best activity underwent additional studies in order to elucidate the possible mechanism of action. *In vitro* results indicated that some compounds have low toxicity (i.e. >150 µM, against Vero cell) combined with high efficacy (i.e. <20 µM) against some forms of *T. cruzi*. Further *in vivo* studies on mice models confirmed the expectations of improvements in infected mice. *In vivo* tests on the acute phase gave parasitaemia inhibition values higher those of Bz, and a remarkable decrease in the reactivation of parasitaemia was found in the chronic phase after immunosuppression of the mice treated with one of the compounds. The morphological alterations found in treated parasites with our derivatives confirmed extensive damage; energetic metabolism disturbances were also registered by ¹H NMR. The demonstrated *in vivo* activity and low toxicity, together with the use of affordable starting products and the lack of synthetic complexity, put these abietic acid derivatives in a remarkable position toward the development of an anti-Chagasic agent.

© 2014 Elsevier Masson SAS. All rights reserved.

1. Introduction

American trypanosomiasis is a potentially life-threatening parasitic disease caused by *Trypanosoma cruzi*. There are more than 10–20 million people infected worldwide, mostly in Latin America. Although not a uniform death sentence, *T. cruzi* infection is far from innocuous, as an estimated 30–40% of infected individuals develop debilitating and chronic disease, and this infection accounts for 20,000–50,000 deaths per year [1]. Currently, the available drugs used for the treatment of this infection, Benznidazole (Bz) or nifurtimox, show limited therapeutic potential and are associated with serious side effects, such as skin rashes, leucopenia, neurotoxicity, fever, articular and muscular pain, peripheral

neuropathy, lymphadenopathy, agranulocytosis, and thrombocytopenic purpura [2,3]. Thus, there is an urgent need for the development of new anti-trypanosomal agents with lower toxicity and greater activity, especially for the chronic phase of the disease. To date, no vaccine has been developed against *T. cruzi* [4]. Therefore, the search for new targets for chemotherapy and vaccines is a major challenge. Among the targets, the parasite antioxidant system has attracted attention due to its uniqueness in the trypanosomatids.

Antiprotozoal activity has been reported for some abietane diterpenoids. Thus, 5,6-didehydro-7-hydroxy-taxodone showed remarkable activity with acceptable selectivity against *Plasmodium falciparum* (IC₅₀ 9.2 µM, SI 10.4 µM) and *Trypanosoma brucei* (IC₅₀ 1.9 µM, SI 50.5 µM) [5]. 7-Hydroxy-12-methoxy-20-nor-abieta-1,5(10),7,9,12-pentaen-6,14-dione and abieta-8,12-dien-11,14-dione (12-deoxy-royleanone) showed appreciable *in vitro* anti-leishmanial activity against intracellular amastigote forms of both *Leishmania donovani* (IC₅₀ values of 170 and 120 nM, respectively)

* Corresponding author.

E-mail address: msanchem@ugr.es (M. Sánchez-Moreno).

and *Leishmania major* (IC₅₀ values of 290 and 180 nM, respectively) [6]. 12-Methoxycarnosic acid showed antiprotozoal activity against axenically grown *L. donovani* amastigotes with an IC₅₀ of 0.75 μM with marginal cytotoxicity against the L6-cells (IC₅₀, 17.3 μM) [7]. The 20-nor-abietane diterpene komariviquinone showed strong trypanocidal activity against epimastigotes of *T. cruzi*, the causative agent of American Trypanosomiasis [8].

Taking into account this need for new drugs to combat *T. cruzi* parasites, we considered studying the activity of the abietic acid derivatives 1–5 against the causing agent of Chagas disease to be of great interest. These compounds are quite interesting, since their synthesis starts from cheap substrates and the procedures are not very complicated in most of the cases. In this work, their anti-proliferative activity and unspecific mammalian cytotoxicity in the species considered were evaluated *in vitro*, and these measures were complemented by infectivity assays on Vero cells. Furthermore, those in whom *in vitro* activity showed remarkable effects were tested *in vivo*. Finally, the parasites were submitted to a thorough study of the possible mechanisms of action of the compounds assayed, as follows: (i) an ¹H NMR study concerning the nature and percentage of metabolite excretion was performed in order to obtain information on the inhibitory effect of the phenolic derivatives 1–5 on the glycolytic pathway, since it represents the primary source of energy for the parasite, (ii) alterations caused in the cell ultrastructure of the parasites were recorded using transmission electronic microscopy (TEM), and (iii) an enzymatic study of inhibition over the iron superoxide dismutase (Fe-SOD), which represent one of the many mechanisms of antioxidant defence in trypanosomatids.

2. Materials and methods

2.1. Chemistry

The abietane type diterpenes 1–4 and the podocarpane derivative 5 were synthesized starting from commercial abietic acid (Fig. 1). 1 (11-bromoferruginol), not yet found in nature, was obtained after bromination of ferruginol (12-hydroxy-abieta-8,11,13-triene), previously synthesized from abietic acid. 2, (+)-sugiol is a natural terpene widely distributed in nature, which was isolated for the first time from *Juniperus communis* L. [9].

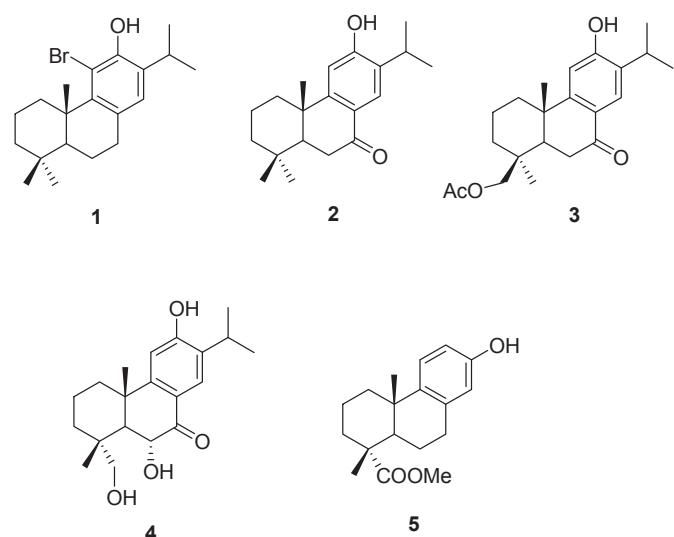


Fig. 1. Chemical structure of the 5 different compounds assayed: Phen 1–5.

It has been prepared after a Friedel–Crafts acetylation of 8,11,13-abietatriene, Baeyer–Villiger oxidation of the resulting methyl ketone, benzylic oxidation of the obtained acetyloxy derivative and further deacetylation. The natural terpene 3 and the abietane derivative 4, (+)-fortunin E, isolated from *Cladonia fortunei* [10], have been synthesized starting from methyl 12-hydroxydehydroabietate, prepared from abietic acid [11]. 5, the methyl ester of 13-hydroxypodocarpa-8,11,13-trien-18-oic acid, a constituent of the *Pinus massoniana* resin [12], has also been synthesized from abietic acid, via methyl 15-hydroxydehydroabietate [13].

2.2. Parasite strain culture

T. cruzi SN3 strain of IRHOD/CO/2008/SN3 was isolated from domestic Rhodnius prolixus; biological origin is Guajira (Colombia) [14]. Epimastigote forms were grown in axenic Grace's insect medium (Gibco) supplemented with 10% inactivated foetal bovine serum (FBS) at 28 °C in tissue-culture flasks, Roux flasks (Corning, USA) with a surface area of 75 cm², as described by Ref. [15].

2.3. Transformation of epimastigotes to metacyclic forms

Metacyclogenesis was induced by culturing a 5-day-old culture of epimastigote forms of *T. cruzi* that was harvested by centrifugation at 7000 g for 10 min at 10 °C according to [16].

2.4. Cell culture and cytotoxicity tests

Vero cells (Flow) were grown in RPMI and MEM (Gibco), supplemented with 10% iFBS and the procedure followed was as in Ref. [17].

2.5. In vitro activity assays, extracellular forms

2.5.1. Epimastigotes assay

T. cruzi epimastigotes were collected in the exponential growth phase and distributed in culture trays (with 24 wells) at a final concentration of 5×10^4 parasites/well. The effects on the parasite growth were tested according to [17].

2.5.2. Blood trypomastigote forms assay

Compounds 4–5 were also evaluated in blood trypomastigote forms of *T. cruzi*. BALB/c female mice infected with *T. cruzi* were used 7 days after infection. Blood was obtained by cardiac puncture using 3.8% sodium citrate as an anticoagulant in a 7:3 blood:anticoagulant ratio. The parasitaemia in the infected mice was about 1×10^5 parasites/mL. The compounds were diluted in phosphate-buffered saline solution (PBS) to give a final concentration 10, 25, and 50 μM for each product. Aliquots (20 μL) of each solution were mixed in culture trays (96 wells) with 55 μL of infected blood containing the parasites at a concentration of approximately 1×10^6 parasites/mL. Infected blood with PBS, at the same concentrations as the products, was used as control. The plates were shaken for 10 min at room temperature and kept at 4 °C for 24 h. Each solution was examined microscopically (Olympus CX41) for parasite counting using the Neubauer haemocytometric chamber (a dilution of 1:100 in PBS was necessary to get into the range of counting). The activity (percent of parasites reduction) was compared with that of the control.

2.6. In vitro activity assays, intracellular forms: amastigotes assay

Vero cells were cultured in RPMI medium supplemented with 10% iFBS, in a humidified 95% air and 5% CO₂ atmosphere at 37 °C. Then the cells were infected and treated as in Ref. [15].

2.7. Infectivity assay

Vero cells were cultured in RPMI medium supplemented with 10% iFBS as described above. Afterward, the cells were infected *in vitro* with metacyclic trypomastigote forms of *T. cruzi* at a ratio of 10:1. The assay was performed as in Ref. [15].

2.8. In vivo trypanosomicidal activity assay

2.8.1. Mice infection and treatment

This experiment was performed using the rules and principles of the International Guide for Biomedical Research in Experimental Animals and with the approval of the ethical committee of the University of Granada, Spain. Groups of six BALB/c albino female mice (6–8 weeks old, 25–30 g weight), maintained under a 12-h dark/light cycle (lights on at 07:30 h) at a temperature of 22 ± 3 °C and provided with water and standard chow *ad libitum*, were inoculated via the intraperitoneal route with 5×10^5 blood trypomastigotes of *T. cruzi* obtained from previously infected mice blood. The animals were divided as follows: I, positive control group (mice infected but not treated); II, study group (mice infected and treated with the compounds under study). The administration of the testing compounds was begun on the seventh day of infestation once the infection was confirmed, and doses of 5 mg/kg body mass per day were used for 5 consecutive days (7–12 days post-infection). Peripheral blood was obtained from the mandibular vein of each mouse (5 μ L samples) and dissolved in 495 μ L of a PBS

solution at a dilution of 1:100. The circulating parasite numbers were quantified with a Neubauer's chamber for counting blood cells. This counting was performed every 3 days during a 40 day period (acute phase). The number of bloodstream forms was expressed as parasites/mL.

2.8.2. Cyclophosphamide-induced immune suppression and assessment of cure

After day 60, the animals entered the chronic phase of the experiment where parasitaemia showed progressively decreasing levels independent of the treatment. Therefore, on day 120, parasitaemia was shown to be undetectable by fresh blood microscopic examination, and the mice received 4 intraperitoneal injections of 200 mg/kg of body mass of cyclophosphamide monohydrate (CP) (ISOPAC[®]) on alternate days, as previously described [18]. Within 1 week of the last CP injection, parasitaemia was evaluated according to the procedure described for acute phase to quantify the presence of blood trypomastigote forms as reactivation rate. Finally, mice were bled out, under gaseous anaesthesia (CO₂), via heart puncture and blood was collected. Blood was incubated for 2 h at 37 °C and then over night at 4 °C in order to allow clotting and then the serum was obtained from samples after centrifuging the supernatant twice at 1000 and 2700 g, consecutively. The serum was aliquoted and used for ELISA and biochemical analysis, as explained below. Hearts were harvested and immediately flushed free of blood by gentle infusion of 10 mL of pre-warmed PBS through the left ventricle [19] in order to avoid contamination of the collected tissue

Table 1

In vitro activity, toxicity and selectivity index found for Phen 1–5 and the reference drug on extracellular and intracellular forms of *Trypanosoma cruzi*.

Compounds	IC ₅₀ (μ M) ^a			Toxicidad IC ₅₀ Vero cell (μ M) ^b	IS ^c		
	Epimastigote forms	Intracellular amastigote forms	Trypomastigote forms		Epimastigote forms	Intracellular amastigote forms	Trypomastigote forms
Bz	15.9 \pm 1.1	23.3 \pm 4.6	16.4 \pm 3.2	13.6 \pm 0.9	0.8	0.6	0.8
1	49.7 \pm 3.5	41.9 \pm 8.1	nd	183.6 \pm 12.2	3.69 (5)	4.38 (7)	nd
2	33.1 \pm 3.6	24.6 \pm 2.2	nd	45.4 \pm 6.1	1.37 (2)	1.84 (3)	nd
3	26.3 \pm 1.9	25.5 \pm 1.6	nd	72.7 \pm 7.7	2.8 (3)	2.8 (5)	nd
4	18.7 \pm 0.9	7.1 \pm 0.3	59.88 \pm 0.7	221.6 \pm 13.5	11.85 (15)	31.4 (52)	3.7 (5)
5	39.2 \pm 3.8	27.1 \pm 1.1	89.3 \pm 1.1	473.6 \pm 22.1	12.1 (15)	17.46 (29)	5.3 (7)

^a IC₅₀ = the concentration required to give 50% inhibition, calculated by linear regression analysis from the K_c values at concentrations employed (1, 10, 25, 50 and 100 μ M).

^b Towards cell Vero after 72 h of culture.

^c Selectivity index = IC₅₀ cell Vero/IC₅₀ extracellular and intracellular form of parasite. In brackets: number of times that compound SI exceeds the reference drug SI. Results are averages of three separate determinations.

Table 2

Summarizes the biochemical clinical parameters tested in different groups of Balb/c mice infected with *Trypanosoma cruzi* at different experimental situations.

	Kidney markers profile		Heart markers profile		Liver markers profile			
	Urea (mg/dL)	Uric acid (mg/dL)	CK-MB (U/L)	LDH (U/L)	AST/GOT (U/L)	ALT/GPT (U/L)	Total bilirubin (mg/dL)	Alkalyne phosphatase (U/L)
Uninfected mice (n = 15)	39 [36–43]	5 [4.3–5.5]	453 [215–690]	3086 [2108–4064]	126 [103–148]	46 [37–54]	0.23 [0.17–0.28]	133 [104–161]
Infected mice-acute phase (n = 15)	49 [39–60]	4.5 [3.7–5.5]	681 [400–950]	2910 [1589–4232]	129 [100–157]	48 [38–58]	0.15 [0.12–0.18]	231 [161–300]
120 days post-infection mice (n = 6)	49 \pm 12	4.3 \pm 1.1	800 \pm 45	2536 \pm 765	148 \pm 18	53 \pm 9	0.12 \pm 0.04	186 \pm 45
120 days post-infection mice and 4 25 mg/kg of body mass treated (n = 6)	=	=	=	+	+	=	=	=
120 days post-infection mice and 5 25 mg/kg of body mass treated (n = 6)	=	-	--	=	=	=	=	=

Key: =, variation no larger than 10%; +, up to 10% of increasing over the range; ++, up to 30% of increasing over the range; +++, up to 40% of increasing over the range; +++++, more than 50% of increasing over de range; -, up to 10% of decreasing over the range; --, up to 30% of decreasing over the range; ---, up to 40% of decreasing over the range; ---, more than 50% of decreasing over de range.

with blood parasites. After this, samples were frozen at -80°C and stored until used for DNA extraction.

2.8.3. ELISA tests

Fe-SOD excreted from the parasite, cultured and processed as described in Ref. [20], was used as the antigen fraction. The ELISA test to measure the antibodies against *T. cruzi* used was performed as in Ref. [21].

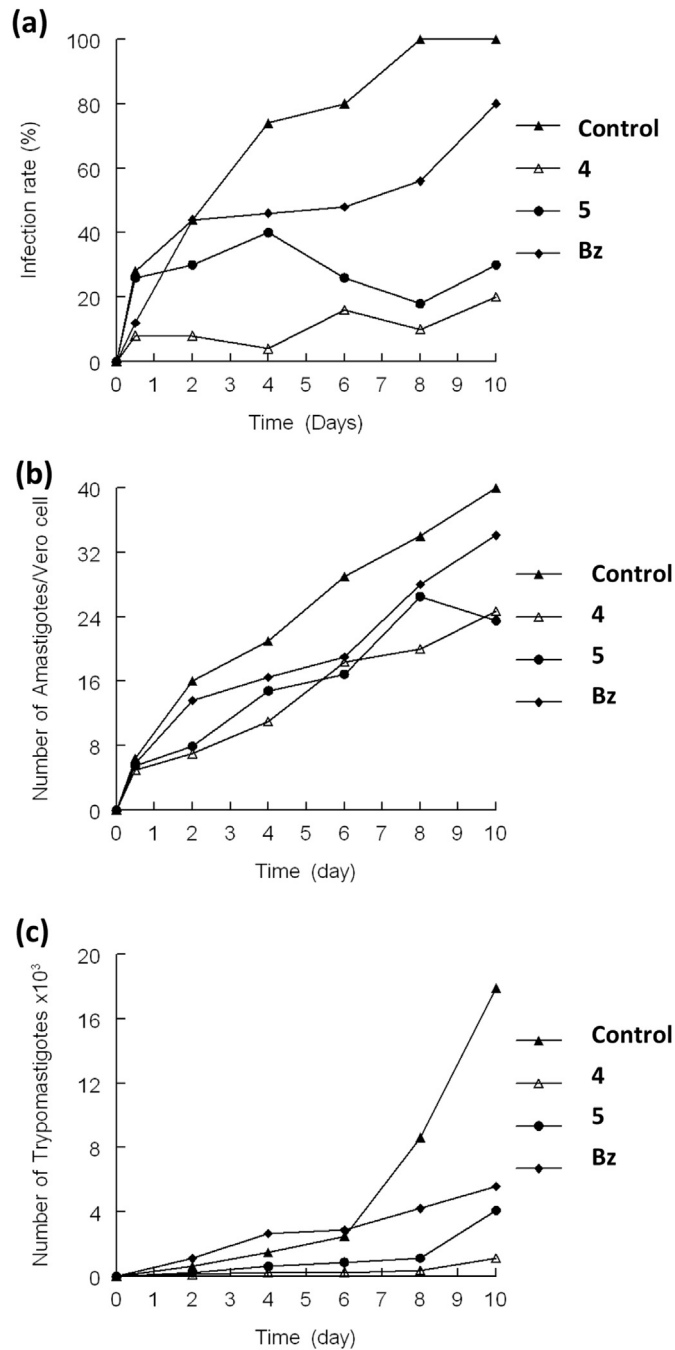


Fig. 2. Reduction of the infectivity of *T. cruzi* in Vero cells treated with 4, 5 and Bz. (a) Rate of infection, (b) mean number of amastigotes per infected Vero cell and (c) number of trypomastigotes in the culture medium. Control group is represented with filled triangles; filled rhombuses represent Bz; open triangles represent 4; 5 is represented by filled circles. Measured at IC₂₅. Values are the means of three separate experiments.

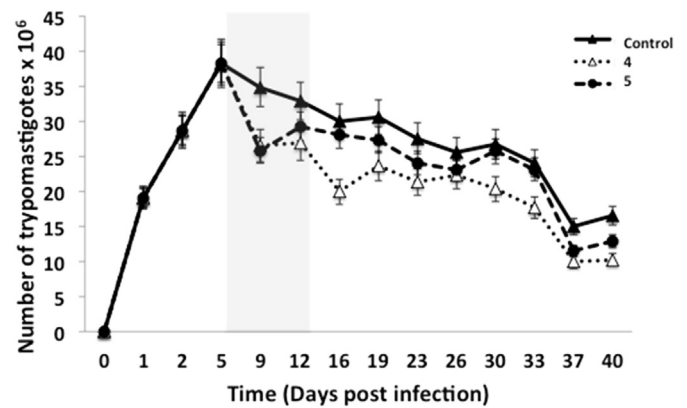


Fig. 3. Parasitaemia in the murine model of acute Chagas disease: filled triangles represent control, open triangles and filled circles represent group treated with 4 and 5, respectively, with a final dose received of 25 mg/kg of body mass administered by the intraperitoneal route. Grey shade represents the treatment days.

2.8.4. DNA extraction and PCR

Hearts were defrosted and then ground using a Potter-Elvehjem to follow the purification procedure of the Wizard[®] Genomic DNA Purification Kit (Promega). PCR was performed using two primers designed in our laboratory (unpublished data), based on the published sequence of the enzyme superoxide dismutase *T. cruzi* CL Brenner (GenBank accession No. XM_808937), which amplifies a fragment of approximately 300 bp belonging to the superoxide dismutase gene b of *T. cruzi*. The PCR was run in a total volume of 20 μL . Next, the amplification products were subjected to electrophoresis on 1.6% agarose gel containing 1:10,000 GelRed[™] Nucleic Acid Gel Stain, for 90 min at 90 V.

2.8.5. Toxicity tests by clinical chemistry measurements

A fraction of the serum obtained as it was shown above was sent to the Biochemical service in the University of Granada where a series of parameters were measured according to their commercial kits

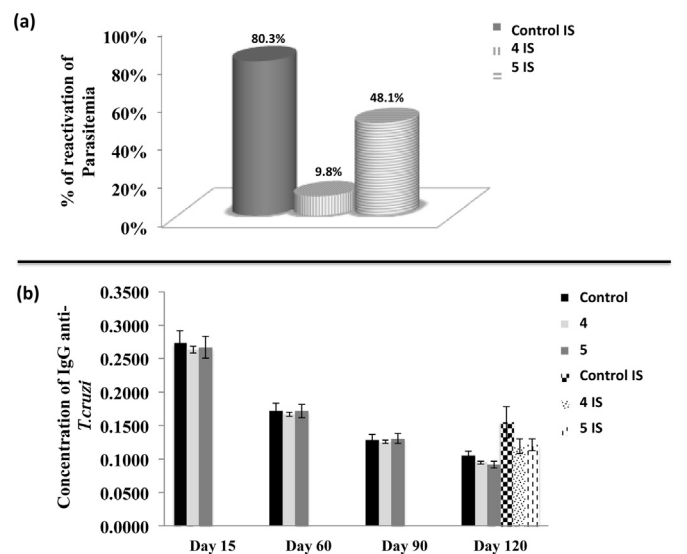


Fig. 4. Immunosuppression *in vivo* assay for mice untreated and treated with 25 mg/kg of body mass of 4 and 5. (a) Shows the reactivation of blood parasitaemia after the immunosuppression cycles by fresh blood counting comparing to the peak day of parasitemia during acute phase. (b) Shows differences in the Ig G levels measured by ELISA at different day post-infection for immunosuppressed and non-immunosuppressed group of mice.

acquired from Cromakit[®] by BS-200 Chemistry Analyzer Shenzhen Mindray (Bio-medical Electronics Co., LTD). With the levels obtained for different populations of sera ($n = 15$, $n = 6$) we calculated the mean value and standard deviation. Finally, we also calculated the confidence interval for the mean normal populations based on a confidence level of 95% ($100 \times (1 - \alpha) = 100 \times (1 - 0.05)\%$). The ranges obtained are shown in Table 2, which allows comparison and analysis of the sera studied in this work.

2.9. Assays to figure out the mechanism of action

2.9.1. Metabolite excretion

Cultures of *T. cruzi* epimastigote forms (initial concentration of 5×10^5 cells/mL) received IC₂₅ of the compounds (except for the control cultures). After incubation for 96 h at 28 °C, the cells were centrifuged at 400 g for 10 min. The supernatants were collected in order to determine the excreted metabolites through ¹H NMR, and the chemical shifts were expressed in parts per million (ppm), using dimethyl sulphoxide (DMSO) as the reference signal. One-dimensional ¹H NMR spectra were acquired on VARIAN DIRECT DRIVE 400 MHz Bruker spectrometer with AutoX probe using D₂O. The assignments of metabolites were based on 1D NMR spectrum. The chemical shifts used to identify the respective metabolites were consistent with those described previously by our group [22]. In addition, the human metabolome database (<http://www.hmdb.ca/>) was also used for this purpose. The spectral region of 1.0–5.5 ppm was bucketed into a frequency window of 0.1 ppm. The region corresponding to water (4.5–5.5 ppm) was excluded during binning to avoid artefacts due to pre-saturation of water, and the region corresponding to glucose (3.4–3.8 ppm) was also excluded. The aromatic region was excluded because the signal to noise ratio in this region was poorer compared to that of the aliphatic region. The peak (2.6 ppm) corresponding to DMSO was removed before binning. The resulting integrals were normalised to the working region (1.0–3.4) ppm of the spectrum to correct for inter-sample differences in dilution. The binning and normalisations were achieved using Mestrenova 9.0 software. The matrix obtained in Mestrenova was imported to Microsoft Excel for further data analyses.

2.9.2. Ultrastructural alterations

The parasites were cultured at a density of 5×10^5 cells/mL in each corresponding medium containing the compounds tested at the concentration of IC₂₅. After 96 h, these cultures were centrifuged at 400 g for 10 min and the pellets produced were washed in PBS before being mixed with 2% (v/v) paraformaldehyde/glutaraldehyde in 0.05 M cacodylate buffer (pH 7.4) for 24 h at 4 °C. Following this, the pellets were prepared for transmission electron microscopy study using a technique described by our group [15].

2.9.3. Superoxide dismutase inhibition assay

The parasites cultured as described above were centrifuged. The pellet was suspended in 3 mL of STE buffer (0.25 M sucrose, 25 mM Tris–HCl, 1 M EDTA, pH 7.8) and disrupted by three cycles of sonic disintegration, 30 s each at 60 W. The sonicated homogenate was centrifuged at 1500 g for 5 min at 4 °C, and the pellet was washed three times in ice-cold STE buffer. This fraction was centrifuged (2500 g for 10 min at 4 °C) and the supernatant was collected. The protein concentrations were determined using the Bradford method [23]. Iron and copper–zinc superoxide dismutases (Fe-SOD and CuZn-SOD) activities were determined using the method described by Beyer and Fridovich [24].

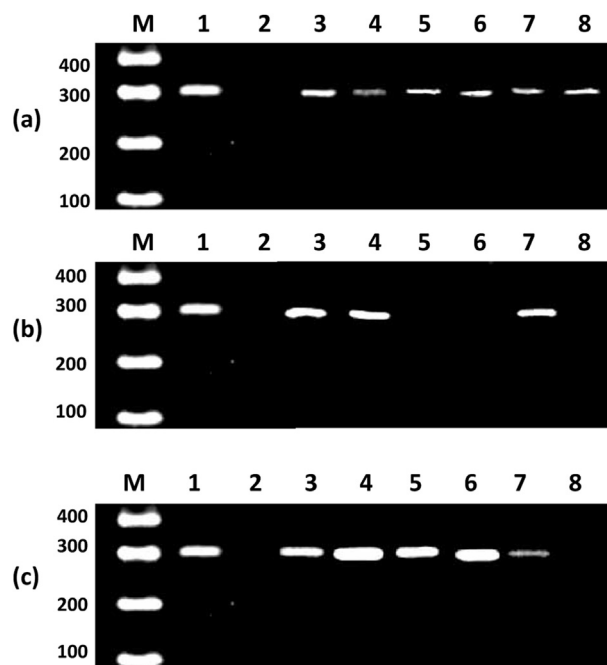


Fig. 5. Polymerase chain reaction (PCR) analysis of heart tissue at the day final day of experiment. (a) Shows untreated mice group, (b) Shows the group of mice treated with 4, (c) Shows the group of mice treated with 5. Lanes: M, base pair marker; 1, PCR positive control; 2, PCR negative control; 3–5, Non-immunosuppressed mice group; 6–8, Immunosuppressed mice group.

3. Results and discussion

3.1. In vitro trypanosomicidal evaluation

In order to get preliminary information, *in vitro* activities of 1–5 were evaluated against epimastigote, amastigote and trypomastigote forms of *T. cruzi*, as shown in Table 1. It was found that the more sensitive forms to all different compounds tested were the intracellular forms (amastigotes) reaching an effectiveness of 52 times higher than the reference drug in the case of 4. The activity of 5 was also remarkable once again against the amastigote forms, being 29-fold more active than Bz. The rest of the compounds also showed trypanosomicidal activity against the different forms of the parasite and the effect was always better than that of the reference drug; however, they all showed less than 15 times effectiveness compared with Bz. As a result, these two compounds were chosen to undergo an extra *in vitro* assay and deeper insight of the activity of these compounds was found in the infectivity assay, where the

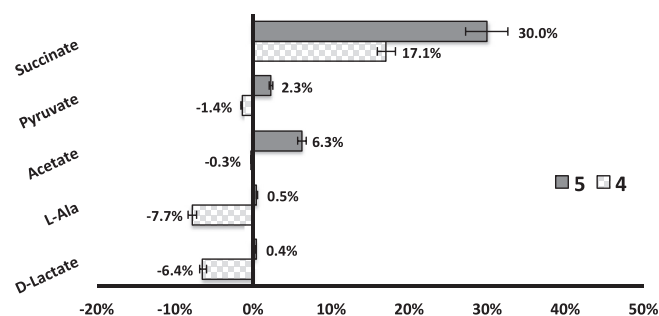


Fig. 6. Variation percentages in the height of the peaks corresponding to catabolites excreted by *T. cruzi* epimastigotes in the presence of 4 and 5 at their IC₂₅, compared to a control sample after 96 h of incubation.

process that takes place in the host of the lifecycle of *T. cruzi* in the presence of the drugs was reproduced *in vitro*. Once again, **4** was found to be the more active, decreasing the rate of infection in cells by 80% on the last day of the experiment, as shown in Fig. 2(a). It also decreased the average number of amastigote forms found per infected cell; these decreases reached the 38% for cells treated with **4** and 41% for those which received **5** as a treatment. Both cases were more efficient than Bz, which effectively only decreased the number by 15% compared to the control (Fig. 2(b)). The last data obtained from this assay were regarding the number of trypomastigote forms released by the infected cells; this effect was remarkable for both compounds, as can be seen in Fig. 2(c), where the effect showed a significant decrease of more than 75% for both compounds compared to the control assay.

3.2. *In vivo* trypanosomicidal evaluation

Since compounds **4** and **5** showed remarkable SI values with respect to Bz in the *in vitro* experiments, they were selected according to the criteria established by Ref. [25] for further *in vivo* studies in the chosen murine model. Their trypanozidal activity during the acute phase of Chagas disease [until 40 days post-infection (pi)] was first investigated. None of the animals treated with either the control or compounds **4** and **5** died during the treatment. As shown in Fig. 3, the reduction of parasitaemia in mice treated with compounds was evident from the very beginning of

the treatment and was maintained until the end, resulting in parasitaemia reduction values of 45% and 22% with respect to the control experiment for **4** and **5**, respectively. Although Bz data have not been included in Fig. 3 for easier visualisation, it must be noted that parasitaemia reductions originated by Bz at the dose of 5 mg/kg body mass were much smaller (16.7% on day 40 pi).

The next step was to evaluate the behaviour of the two compounds until the chronic phase. Therefore, the mice treated as described above were taken up to day 120 pi (advanced chronic phase), in order to evaluate the immune status and the disease extent of the mice at that stage; blood samples were extracted for determining parasitaemia and immunoglobulin G (Ig-G) levels in comparison with the corresponding non-immunosuppressed (control) subgroup of mice (Fig. 4). Concerning the parasitaemia reactivation, Fig. 4(a) shows a very illustrative three-dimensional graph indicating the percentage of parasitaemia reactivation for **4** and **5** in comparison with the control mice; very low percentages were obtained in the two cases, with values ranging from 9.8% to 48.1%, whereas a reactivation of 80.3% was found in the control mice. Bz data obtained from the 80% mice that survived after treatment gave a substantially higher parasitaemia reactivation of 36% at 5 mg/kg of body mass, indicating that one of the tested compounds was clearly more efficient than the reference drug.

The enzyme-linked immunosorbent assay (ELISA) was used for the detection of total Ig-G levels and the antigen source was the Fe-SOD enzyme isolated in our laboratory. The detection of total Ig G

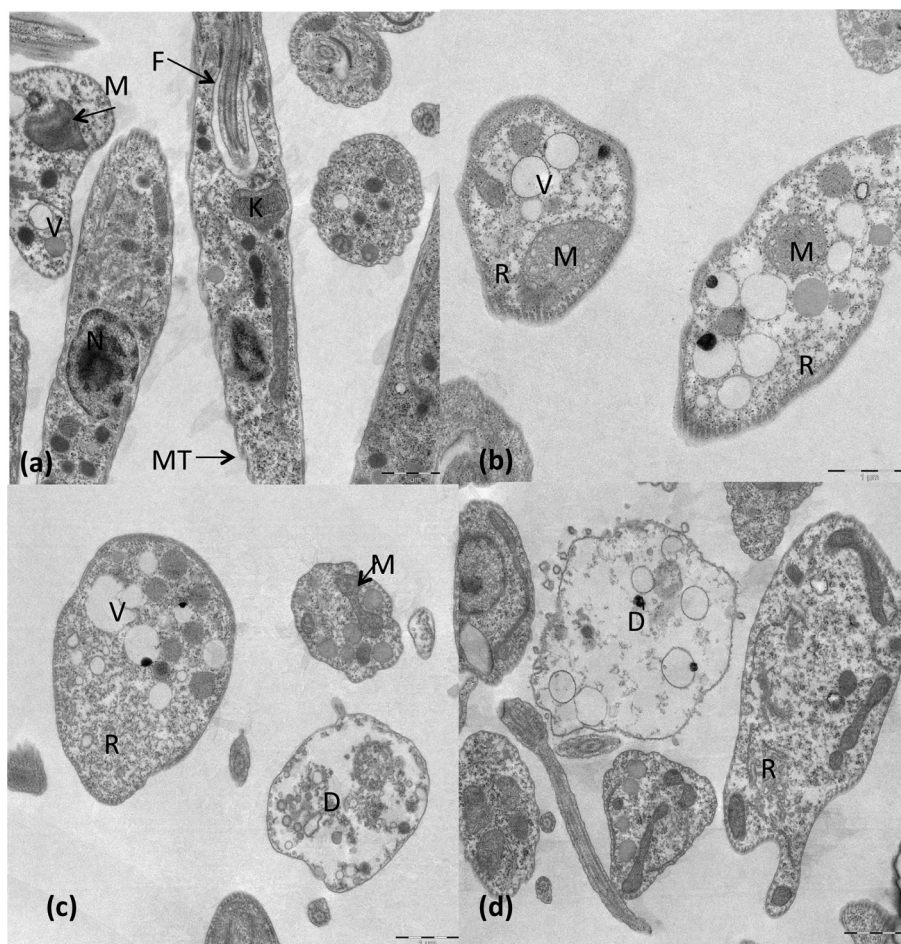


Fig. 7. Ultrastructural alterations shown by TEM in epimastigotes of *T. cruzi* treated with Phen **4** and **5** at IC_{25} concentration. (a) Control parasite showing typical organelles such as nucleus (N), mitochondrion (M), glycosomes (G), microtubules (MT), vacuole (V), reservosome (R), kinetoplast (K) and flagellum (F). (b) Treated with **4**. (c–d) Treated with **5**. Scale bar = 1 μ m.

allowed evaluation of the immune status of the mice [26], since that indicates the level of protection that should be attributed to the tested compounds, combined with the innate protection that mice have naturally [27]. Results obtained from the ELISA experiments were confirmed by the parasitaemia assay performed as indicated above. In accordance with the ELISA test, the group of mice treated with compounds **4** and **5** maintained levels of total Ig G (Fig. 4(b)), as did chronic infected mice, lower than that of the control group after being immunosuppressed, while the control group levels were increased as a consequence of the reactivation of parasitaemia. Finally, Fig. 5 shows the PCR results after necropsy. After removing the hearts, performing total DNA extraction and amplification of a fragment within the parasite SOD-gene, the hearts of control animals showed the ubiquitous presence of the parasite. In striking contrast, hearts in mice treated with **4** were relatively free from parasites (50%), thus confirming the partial curative effect of this compound at the studied dosage. Less significant was the effect of **5**, where only around the 17% of mice were free of parasites.

Clinical chemistry measurements are provided in Table 2. Changes in lactate dehydrogenase (LDH) and aspartate aminotransferase (AST) for the group of mice treated with **4** were the only differences found when compared to the control group, but these changes were insignificant since they were lower than 10%. This confirms the evidence that the compounds tested are not toxic in the murine model; in fact, this lack of toxicity added to the better efficacy of **4**, leading us to consider this compound as a promising candidate for the treatment of Chagas disease. Therefore, the compound should be followed-up in future clinical experiments.

3.3. Possible mechanism of action

Trypanosomatids are unable to completely degrade glucose to CO₂, so they excrete part of the hexose skeleton into the medium as partially oxidised fragments, the nature and percentage of which depend on the pathway used for glucose metabolism [28]. The catabolism products in *T. cruzi* are mainly succinate, acetate, D-lactate and L-alanine [29]. In order to obtain some information about the effects of **4** and **5** on the glucose metabolism of the parasite, we registered the ¹H NMR spectra of *T. cruzi* epimastigotes treated with the test compounds (spectra not shown); the final excretion products were identified qualitatively and quantitatively, and the results obtained were compared with those found for untreated control epimastigotes. Fig. 6 shows the differences found in every case with respect to the control.

Excretion of all metabolites was disturbed in the treatment with **5**, with succinate being the most affected, showing an increase of 30%, followed by acetate and pyruvate with increases of 6.3 and 2.3%, respectively. In general, all metabolites were increased in the medium when the parasites were treated with **5**. However, changes were notably less significant with **4** than **5**. In this case, all of the metabolites, with the exception of succinate, were slightly decreased. L-alanine and D-Lactate showed the most remarkable decreases of 7.7% and 6.4%, respectively. On the other hand, succinate was also disturbed and, as seen with **5**, it was overexpressed in the medium at 17.1%. All of these data could be interpreted on the basis of a change in the succinate, D-lactate, L-alanine pathways occurring in the presence of the compounds under investigation. It is well known that D-lactate and L-alanine originate from the transformation of PEP in pyruvate in the presence of pyruvate kinase or pyruvate phosphate dikinase [30]. On the other hand, it is interesting to note that the increase in succinate with **5** indicate catabolic changes that could be related to a malfunction of the mitochondria, due to the redox stress produced by inhibition of the mitochondrion-resident Fe-SOD enzyme [31], which should result

in decreased pyruvate metabolism and a consequent decrease of the succinate produced in mitochondria. Overall, these data should confirm that the modifications generated in organelles like glycosomes or mitochondria by the compounds assayed are the ultimate reason for the alterations observed in the excreted products of *T. cruzi*.

Modifications at the ultrastructural level caused after incubation of epimastigote forms of *T. cruzi* with the compounds under study in the current work, **4** and **5**, have been studied. Both compounds induced strong disturbances in the parasites' morphology and consequently death in some cases. At this level, **5** was found to be the more effective compound, causing more mortality in the parasite cultures compared to **4** when the IC₂₅ was administered. Although the survival rate was higher in parasites treated with **4**, the parasites were clearly morphologically disturbed when compared with the untreated assay, as shown in Fig. 7(a). Among the more common disturbances when **4** was added to the medium, as shown in Fig. 7(b), include the finding that mitochondria were swollen, without cristae and almost unrecognisable; the cytoplasm was also full of small vacuoles, there was a lack of ribosomes and low electron density was appreciated. Fig. 7(c) and (d) reveal the aspect of parasites that survived after treatment with **5**, where the most frequent change was vacuolisation with enormous empty

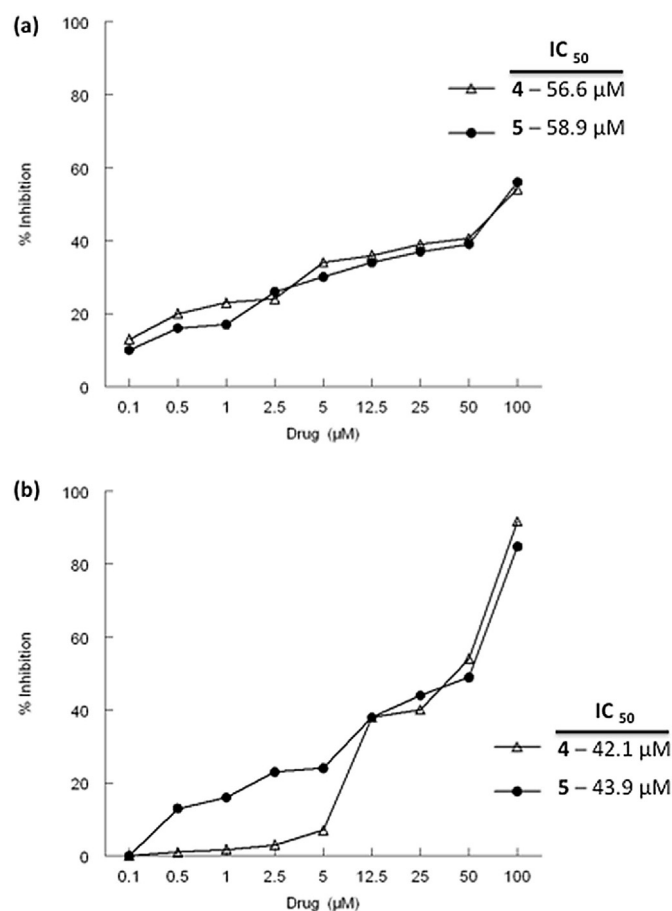


Fig. 8. (a) *In vitro* inhibition (%) of CuZn-SOD from human erythrocytes for compounds (activity 23.36 ± 4.21 U/mg). (b) *In vitro* inhibition (%) of Fe-SOD from *T. cruzi* epimastigotes for compounds (activity 20.77 ± 3.18 U/mg). Differences between the activities of the control homogenate and those ones incubated with compounds were obtained according to the Newman–Keuls test. Values are the average of three separate determinations.

vacuoles and swollen mitochondria combined with the low electron density and a lack of ribosomes, as seen with **4**.

These results prompted us to evaluate the inhibitory effect of compounds **4** and **5** on SOD activity to test their potential as enzyme inhibitors. The results obtained are shown in Fig. 8, with the corresponding IC₅₀ values that were calculated. Significant inhibitory values of Fe-SOD activity were found for the two tested compounds (Fig. 8(b)). Compounds **4** and **5** showed values close to 100% inhibition at 80 μM, with IC₅₀ values between 42.1 and 43.9 μM. The design of an effective drug that is able to inhibit parasite Fe-SOD without inhibiting human Cu/Zn-SOD is an interesting goal. Therefore, we also assayed the effect of compounds on Cu/Zn-SOD in human erythrocytes (Fig. 8(a)). The results obtained showed that the inhibition percentages for human Cu/Zn-SOD were lower than for Fe-SOD. Therefore, IC₅₀ values of 56.6 and 58.9 μM were reached in Cu/Zn-SOD for **4** and **5**, respectively.

Acknowledgements

F.O. is grateful for a FPU Grant (AP-2010-3562) from the Ministry of Education of Spain. I. C. thanks the Spanish Agency for the International Development and Cooperation (AECID) for a predoctoral grant.

References

- [1] R.L. Tarleton, J.W. Curran, Is Chagas disease really the “new HIV/AIDS of the Americas”? *PLoS Negl. Trop. Dis.* 6 (2012) e1861.
- [2] J.A. Urbina, Specific chemotherapy of Chagas disease: relevance, current limitations and new approaches, *Acta Trop.* 115 (2010) 55–68.
- [3] S.R. Wilkinson, M.C. Taylor, D. Horn, et al., A mechanism for cross-resistance to nifurtimox and Bz in trypanosomes, *Proc. Natl. Acad. Sci.* 105 (2008) 5022–5027.
- [4] E. Dumonteil, Vaccine development against *Trypanosoma cruzi* and *Leishmania* species in the post-genomic era, *Infect. Genet. Evol.* 9 (2009) 1075–1082.
- [5] Ramzi A. Mothana, Mansour S. Al-Said, Nawal M. Al-Musayeib, Ali A. El Gamal, Shaza M. Al-Massarani, Adnan J. Al-Rehaily, Majed Abdulkader, Louis Maes, *Int. J. Mol. Sci.* 15 (2014) 8360–8371.
- [6] Nur Tana, Macki Kalogaa, Oliver A. Radtkea, Albrecht F. Kiderlenc, Sevil Oksuz, Ayhan Ulubelenb, Herbert Kolodziejka, *Phytochemistry* 61 (2002) 881–884.
- [7] Tsholofelo A. Mokoka, Xolani K. Peter, Gerda Fouche, Nivan Moodley, Michael Adams, Matthias Hamburger, Marcel Kaiser, Reto Brun, Vinesh Maharaj, Neil Koorbanally, *South Afr. J. Bot.* 90 (2014) 93–95.
- [8] Nahoko Uchiyama, Fumiyuki Kiuchi, Michihiro Ito, Gisho Honda, Yoshio Takeda, Olimjon K. Khodzhimatov, Ozodbek A. Ashurmetov, *J. Nat. Prod.* 66 (2003) 128–131.
- [9] J.B.S. Bredenberg, J. Gripenberg, The chemistry of the natural order Cupressales. XIII. The presence of sugiol in the wood of *Juniperus communis*, *Acta Chem. Scand.* 8 (1954) 1728.
- [10] S. Yao, C.P. Tang, C.Q. Ke, et al., Abietane diterpenoids from the bark of *Cryptomeria fortunei*, *J. Nat. Prod.* 71 (2008) 1242–1246.
- [11] E.J. Alvarez-Manzaneda, R. Chahboun, E. Alvarez, et al., Synthesis of (+)-hanagokenol A, (+)-fortunins E, G, H, and (–)-sugikurojin A from abietic acid, *Synthesis* (2010) 3493–3503.
- [12] H.T.A. Cheung, T. Miyase, M.P. Lenguyen, et al., Further acidic constituents and neutral components of *Pinus massoniana* resin, *Tetrahedron* 49 (1993) 7903–7915.
- [13] E.J. Alvarez-Manzaneda, R. Chahboun, J.J. Guardia, et al., New route to 15-hydroxydehydroabietic acid derivatives: application to the first synthesis of some bioactive abietane and nor-abietane type terpenoids, *Tetrahedron Lett.* 47 (2006) 2577–2580.
- [14] J. Tellez-Meneses, A.M. Mejía-Jaramillo, O. Triana-Chavez, Biological characterization of *Trypanosoma cruzi* stocks from domestic and sylvatic vectors in Sierra Nevada of Santa Marta, Colombia, *Acta Trop.* 108 (2008) 26–34.
- [15] P. González, C. Marín, I. Rodríguez-González, A.B. Hitos, et al., In vitro activity of C20-diterpenoid alkaloid derivatives in promastigotes and intracellular amastigotes of *Leishmania infantum*, *Int. J. Antimicrob. Agents* 25 (2005) 136–141.
- [16] J. Cardoso, M.J. Soares, In vitro effects of citral on *Trypanosoma cruzi* metacyclogenesis, *Mem. Inst. Oswaldo Cruz* 5 (2010) 1026–1032.
- [17] R. Magán, C. Marín, M.J. Rosales, et al., Therapeutic potential of new Pt(II) and Ru(III) triazole-pyrimidine complexes against *Leishmania donovani*, *Pharmacology* 73 (2005) 41–48.
- [18] S. Cencig, N. Coltel, C. Truysens, et al., Parasitic loads in tissues of mice infected with *Trypanosoma cruzi* and treated with AmBisome, *PLoS Negl. Trop. Dis.* 5 (2011) e1216.
- [19] X. Ye, J. Ding, X. Zhou, et al., Divergent roles of endothelial NF-κB in multiple organ injury and bacterial clearance in mouse models of sepsis, *J. Exp. Med.* 205 (2008) 1303–1315.
- [20] A. Lopez-Céspedes, E. Villagran, K. Briceño-Alvarez, et al., *Trypanosoma cruzi*: seroprevalence detection in suburban population of Santiago de Queretaro (Mexico), *Sci. World J.* (2012), <http://dx.doi.org/10.1100/2012/914129>.
- [21] F. Olmo, C. Rotger, I. Ramírez-Macías, L. Martínez, C. Marín, L. Carreras, K. Urbanová, M. Vega, G. Chaves-Lemaur, A. Sampedro, M.J. Rosales, M. Sánchez-Moreno, A. Costa, Synthesis and biological evaluation of N,N'-squaramides with high in vivo efficacy and low toxicity: toward a low-cost drug against Chagas disease, *J. Med. Chem.* 57 (3) (2014 Feb 13) 987–999.
- [22] C. Fernandez-Becerra, M. Sanchez-Moreno, A. Osuna, et al., Comparative aspects of energy metabolism in plant trypanosomatids, *J. Eukaryot. Microbiol.* 44 (1997) 523–529.
- [23] M.M. Bradford, A refined and sensitive method for the quantification of microgram quantities of protein utilizing the principle of protein-dye binding, *Anal. Biochem.* 72 (1972) 248–254.
- [24] W.F. Beyer, I. Fridovich, Assaying for superoxide dismutase activity: some large consequences of minor changes in conditions, *Anal. Biochem.* 161 (1987) 559–566.
- [25] S. Nwaka, D. Besson, B. Ramirez, et al., Integrated dataset of screening hits against multiple neglected disease pathogens, *PLoS Negl. Trop. Dis.* 5 (2011) e1412.
- [26] A. El Bouhdidi, C. Truysens, M.T. Rivera, et al., *Trypanosoma cruzi* infection in mice induces a polyisotypic hypergammaglobulinaemia and parasite-specific response involving high IgG2a concentrations and highly avid IgG1 antibodies, *Parasite Immunol.* 16 (1994) 69–76.
- [27] H. Kayama, K. Takeda, The innate immuneresponse to *Trypanosoma cruzi* infection, *Microbes Infect.* 12 (2010) 511–517.
- [28] M. Ginger, *Trypanosomatid biology and euglenozoan evolution: new insights and shifting paradigms revealed through genome sequencing*, *Protist* 156 (2005) 377–392.
- [29] J.J. Cazzulo, Aerobic fermentation of glucose by trypanosomatids, *FASEB J.* 6 (1992) 3153–3161.
- [30] F. Bringaud, L. Riviere, V. Coustou, Energy metabolism of trypanosomatids: adaptation to available carbon sources, *Mol. Biochem. Parasitol.* 149 (2006) 1–9.
- [31] I.G. Kirkinezos, C.T. Moraes, Reactive oxygen species and mitochondrial diseases, *Cell Dev. Biol.* 12 (2001) 449–457.

Cite this: *RSC Adv.*, 2014, 4, 65108

Synthetic single and double aza-scorpianid macrocycles acting as inhibitors of the antioxidant enzymes iron superoxide dismutase and trypanothione reductase in *Trypanosoma cruzi* with promising results in a murine model†

F. Olmo,^{‡a} M. P. Clares,^{‡b} C. Marín,^{‡a} J. González,^{‡b} M. Inclán,^{‡b} C. Soriano,^{‡c} K. Urbanová,^{‡a} R. Tejero,^{‡d} M. J. Rosales,^{‡a} R. L. Krauth-Siegel,^{‡e} M. Sánchez-Moreno,^{‡*a} and E. García-España^{‡*b}

The anti-chagasic activity of a series of eleven derivatives of aza-scorpianid-like macrocycles, some of them newly synthesised, was assayed. The four compounds with the best selectivity indices *in vitro* were subjected to *in vivo* assays. Tests in a murine model of the acute phase of Chagas disease showed a two-fold reduction in parasitaemia compared to that with benznidazole. Furthermore, compounds **7** and **11**, with 4-pyridine and phenanthroline substituents in the lateral chain, caused a remarkable decrease in parasitaemia reactivation during the chronic phase after inducing immunosuppression in mice. These activity studies were complemented by measuring their inhibitory effect towards the antioxidant parasite-specific enzymes, iron superoxide dismutase (Fe-SOD) and trypanothione reductase, the metabolites excreted after treatment and ultrastructural alterations. The ability of the selected macrocycles to complex with Fe(II) and Fe(III) was studied using potentiometric methods. Detailed molecular dynamics studies provided interesting pointers about the way in which the compounds approach and modify the active centre of Fe-SOD. The activity, low toxicity, stability, low cost of the starting materials and straightforward synthesis make these compounds appropriate molecules for the development of affordable anti-chagasic agents.

Received 5th September 2014
Accepted 3rd November 2014

DOI: 10.1039/c4ra09866h

www.rsc.org/advances

Introduction

Chagas disease (CD) is a chronic, systemic, parasitic infection caused by the protozoan *Trypanosoma cruzi*¹ and is identified by the World Health Organisation (WHO) as one of the world's 17 most neglected tropical diseases.² This disease represents one of the main public health concerns in 21 countries in Latin America where about 7–8 million people are currently infected with *T. cruzi*.³ CD is also becoming an emerging health problem

in non-endemic areas, because the parasite has travelled outside South and Central America because of population migration (North America, Pacific region and Europe). Thus, CD is becoming a new worldwide epidemiological, economic, social and political challenge. However, as reported by the WHO, whereas research funding to combat HIV/AIDS, malaria and tuberculosis has been considerably increased in the last few years, that devoted to other infectious diseases associated with poverty, such as CD, has not been increased in the same manner.⁴

Currently, the main drugs used to treat CD are two nitro-aromatic heterocycles: the furane-based nifurtimox and the imidazole-based benznidazole (Bz).⁵ Both drugs are effective in the acute phase of the disease, although Bz shows a better safety and efficacy profile.⁶ However, their efficacies are very low during the chronic phase of the disease.⁷ Furthermore, these compounds have severe side effects, including anorexia, vomiting, peripheral polyneuropathy and allergic dermatopathy.⁸ The presence of nitro groups attached to the heterocyclic rings suggests that these drugs act on the parasite by nitro reduction, providing reduced intermediates that covalently modify biomolecules. However, their mode of action is currently under

^aDepartamento de Parasitología, Instituto de Investigación Biosanitaria IBS. Granada, Universidad de Granada, Granada, Spain. E-mail: msanchem@ugr.es

^bInstituto de Ciencia Molecular, Departamento de Química Inorgánica, Universidad de Valencia, E-46980 Paterna, Valencia, Spain. E-mail: enrique.garcia-es@uv.es

^cDepartamento de Química Orgánica, Universidad de Valencia, E-46100 Burjassot, Valencia, Spain

^dDepartamento de Química Física, Universidad de Valencia, E-46100 Burjassot, Valencia, Spain

^eBiochemie-Zentrum der Universität Heidelberg, Im Neuenheimer Feld 328, 69120 Heidelberg, Germany

† Electronic supplementary information (ESI) available. See DOI: 10.1039/c4ra09866h

‡ These authors have contributed equally to the work.

discussion.⁹ Their high toxicity in humans is probably the result of oxidative or reductive tissue damage and is inextricably linked to their antiparasitic activity.⁵ Recently, it has been proposed that the toxicity of these drugs could be linked to their microsomal nitroreduction to reactive metabolites inside the liver.¹⁰ Therefore, existing drug treatments for CD are far from satisfactory and the development of a vaccine is a goal yet to be achieved. The discovery of new low cost drugs circumventing the drawbacks of conventional drugs seems to be an urgent necessity.⁴

Research into anti-chagasic agents is mainly focused on key biochemical metabolic pathways or crucial parasite-specific enzymes. Sterol metabolism, kinetoplast DNA linked sites, trypanothione reductase, cysteine proteinase, hypoxanthine-guanine phosphoribosyltransferase, dihydrofolate reductase, and glyceraldehyde 3-phosphate dehydrogenase have been the main lines of investigation during the last few years.¹¹

Among the trypanosomatid specific enzymes, we have focused our attention on iron superoxide dismutase (Fe-SOD). This enzyme, not found in mammals which have only manganese and copper/zinc superoxide dismutases (Mn-SOD and Cu/Zn-SOD), plays an essential role in the defence of the parasite against oxidation generated by the host's immune system.¹² Indeed, it has been shown that parasitic protozoan survival is closely related to the ability of Fe-SOD to evade toxic free radical damage originated by their hosts.¹³ Because of the predominant role of the prosthetic groups, interaction with Fe-SOD active sites could be an efficient way of deactivating the antioxidant effect of the enzyme.

In regard to this point, in the last few years, our research group has designed a new family of polyamine compounds consisting of a macrocyclic pyridinophane core substituted with side chains containing additional donor atoms (Fig. 1).¹⁴ These macrocycles are termed *scorpiand ligands* because the side chain can fold towards the macrocyclic core following the binding of target guest species such as protons, anions or metal ions.^{14,15}

Recently, the *in vitro* action of several of these compounds against *T. cruzi* and two species of *Leishmania* (*Leishmania infantum* and *Leishmania braziliensis*) has been studied. The results showed that the synthetic aza-scorpiand-like macrocyclic derivatives are potentially promising agents for the treatment of trypanosomatid infections.¹⁶ In the present work, the *in vitro* antiparasitic activity of 11 new polyaminic compounds and their toxicity against Vero cells was tested. The new compounds were compared using Bz as a reference drug. Then, the compounds with the best selectivity indices were chosen for the *in vivo* assay of the trypanocidal activity tests in the acute and chronic phases using female BALB/c mice as an animal model. The effect of the compounds on the ultrastructure of *T. cruzi* was also studied using transmission electronic microscopy (TEM) experiments to confirm the type of damage caused to the parasite. Proton nuclear magnetic resonance (¹H-NMR) determination of the nature and percentage of excreted metabolites was performed to obtain information about the inhibitory effect of our compounds on the glycolytic pathway because this represents the prime energy source of the parasite. Furthermore, in order to check for metabolic

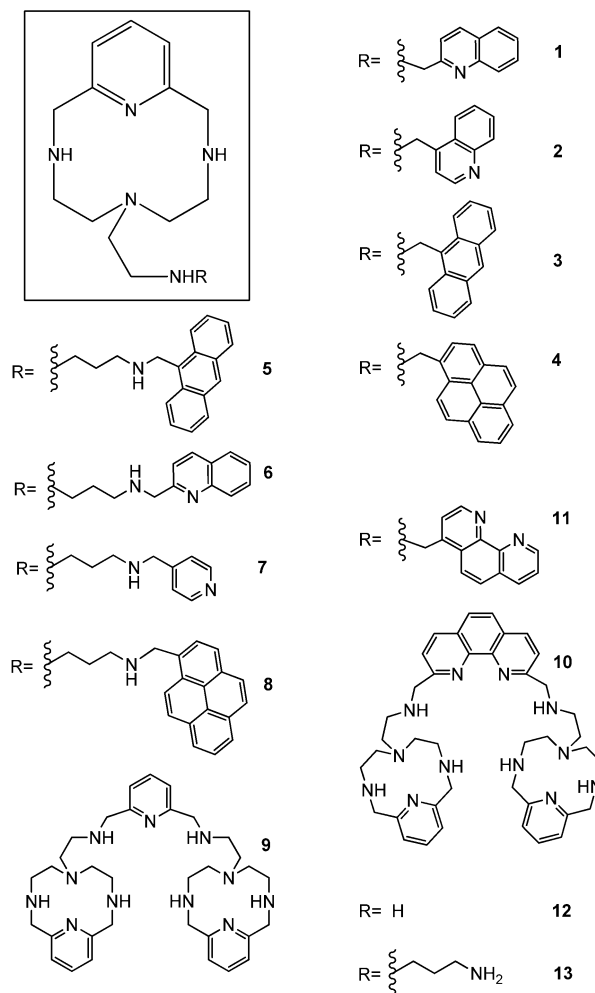


Fig. 1 Chemical formula of aza-scorpiand derivatives. The common core for compounds 1–8 is depicted in the inset.

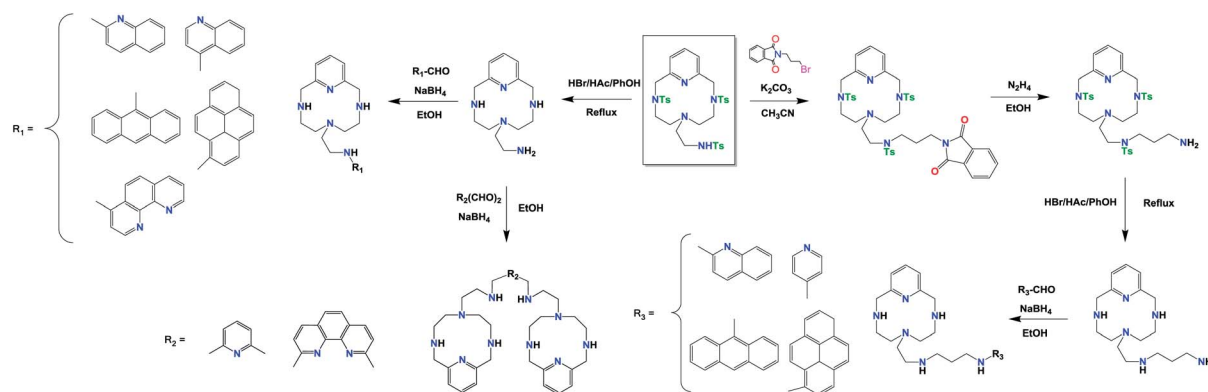
disturbances or abnormalities associated with treatment, representative biochemical parameters were measured for all groups of mice.

Previously, we have demonstrated that these derivatives are good inhibitors of Fe-SOD, not only in *T. cruzi*,^{16b} but also in *Leishmania* spp.^{16a} An evaluation of their effectiveness as putative inhibitors of Fe-SOD in relation to human CuZn-SOD and also of trypanothione reductase is presented. Finally, an exhaustive molecular dynamic study was carried out to determine the way in which these drugs approach and inhibit the active centre of Fe-SOD.

Results and discussion

Chemistry

Synthesis of the compounds. The synthesis of 1, 2, 3, 4, and 11 was accomplished as described previously^{14,17} following a modification of the Richman–Atkins procedure.¹⁸ First, pertosylated polyamine tris(2-aminoethyl)amine was reacted with 2,6-bis(bromomethyl)pyridine in a 1 : 1 molar ratio using potassium carbonate (K₂CO₃) as the base in refluxing



Scheme 1 Synthetic route for the preparation of compounds 1–13.

acetonitrile (CH_3CN) and this gave the tosylated compound **12**. Detosylation was carried out with hydrogen bromide (HBr)/acetic acid (HAc)/phenol (PhOH), and **12** was obtained as a hydrobromide salt. Compounds **1**, **2**, **3**, **4** and **11** were obtained by reacting **12**, in its free amine form, with the corresponding carboxaldehydes (Scheme 1) in dry ethanol followed by *in situ* reaction with sodium borohydride (NaBH_4). The compounds were finally precipitated as hydrochloride salts.

Compound **13** was obtained by the reaction of pertosylated polyamine **12** with *N*-(3-bromopropyl)phthalimide in a 1 : 1 molar ratio using K_2CO_3 as the base in refluxing CH_3CN . Deprotection and detosylation were carried out with hydrazine monohydrate and HBr/HAc/PhOH, respectively, obtaining **13** as a tetrahydrobromide salt.^{17a} Compounds **5**, **6**, **7** and **8** were obtained by reacting **13**, in its free amine form, with the corresponding carboxaldehydes (Scheme 1) in dry ethanol followed by *in situ* reaction with NaBH_4 . The compounds were finally precipitated as the hydrochloride salts.^{17a,19}

The synthesis of **9** and **10** was carried out by reacting two moles of **12** with one mole of pyridine-2,6-dicarboxaldehyde or 1,10-phenanthroline-2,9-dicarboxaldehyde, respectively, in dry ethanol, followed by *in situ* reduction with NaBH_4 . The compounds were finally precipitated as their hydrochloride salts.^{17b}

Degree of protonation of the compounds. An important parameter that must be considered when dealing with polyamines is their acid–base behaviour. The protonation state of the amine groups in the macrocycle affects their interaction with other substrates because it defines their donor capabilities and their behaviour as hydrogen bond donors or acceptors. Table S1 (see ESI[†]) presents the protonation constants determined by potentiometric titrations using a 0.15 M NaCl solution as ionic strength. As can be seen in Table S1,[†] the number of protonated species corresponds to the number of secondary or primary amino groups present either in the macrocyclic core or in the arms. Protonation of the tertiary amines or pyridine groups was not observed, at least in the 2.0–11.0 pH range of the potentiometric titrations. Only in the case of the two macrocycles containing a phenanthroline unit and of the macrocycle with a 4-pyridine unit in their arms (**10**, **11** and **7**, respectively) was a further protonation step inferred.

An interesting point for this discussion and for the posterior molecular dynamics study is to know the degree of protonation of the compounds at pH 7.4. Such data are shown in Fig. 2 and it can be seen that while all the simple, non-enlarged, azascorpiands **1–4** and **11** had degrees of protonation of approximately 2, the enlarged scorpiand molecules **5–9** reached a degree of protonation of 3. Tritopic macrocycles **9** and **10** were the most charged compounds, reaching a degree of protonation of almost 4 at this pH. Previous NMR studies have shown that the first two protons bind preferentially to the amino groups of the macrocyclic core of **1–4** and **11**.^{17b} The first three protons binding to **5–9** involve, apart from the two secondary amino groups of the core, one of the amine groups of the lateral chain.¹⁴

Interaction with iron. Because one of the potential targets of the studied compounds was the Fe-SOD of the parasites, it seemed interesting to evaluate the affinity of these chelating ligands for iron either in its II or III oxidation state. In Table S2,[†] estimates of the binding constants for **1**, **2** and **7** as representatives of this series are presented. As can be seen, all three compounds form stable complexes with either Fe(II) or Fe(III) and the stability of the latter ones was remarkable and comparable to that found for the Cu^{2+} complexes previously

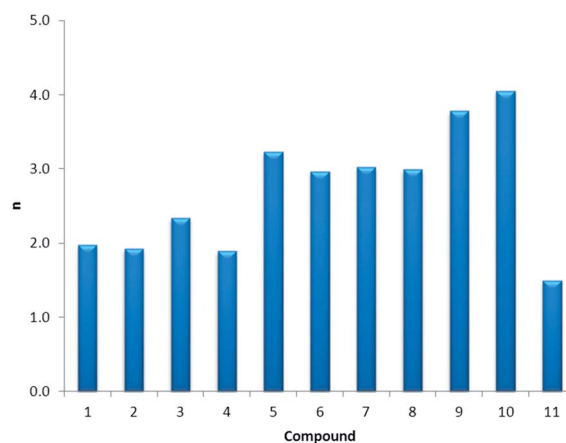


Fig. 2 Degree of protonation of the different compounds at pH 7.4.

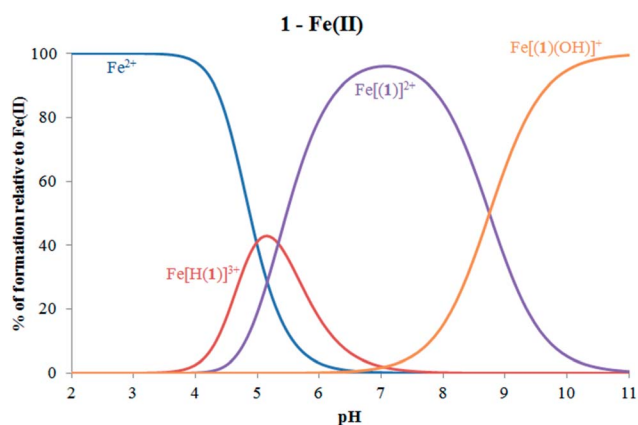


Fig. 3 Distribution diagrams of the Fe(II)–1 systems.

described.^{14,17,19} However, the stability of the Fe(III) complexes was not high enough to avoid the formation of hydroxo species and of Fe(III) hydroxide at basic pH values. Alternatively, Fe(III) systems might have been affected by the side oxidation of amine groups to imines and, therefore, the stability constants are presented as tentative values. However, in view of the distribution diagrams shown in Fig. 3 and S1,[†] it is clear that if the ligands approach the active site of Fe-SOD quite closely, some competition might be established with the primary ligands of the active centre for the capture of the metal ions.

Biological activity

In vitro trypanocidal evaluation. The *in vitro* activity of compounds 1–11 was evaluated against extracellular (epimastigote and trypomastigote) and intracellular (amastigote) forms of *T. cruzi*, as described in the Experimental section. More

indicative data were found with the assays performed on the intracellular amastigote forms, because epimastigotes are not the fully developed parasitic forms in vertebrate hosts. Finally, the compounds were tested against blood trypomastigotes, because these parasitic forms, together with the amastigotes, are responsible for the chronic phase of CD.

The IC₅₀ values (the concentration required to give 50% inhibition) obtained for the extracellular and intracellular forms are shown in the first three columns of Table 1, which also includes the data obtained for the reference drug Bz. Toxicity values were calculated against mammalian Vero cells after 72 h of culture and the selectivity indices (SI, calculated as IC₅₀ Vero cells toxicity/IC₅₀ activity of extracellular or intracellular forms of the parasite) are shown in the last three columns of Table 1. The numbers in brackets show the SI of the compound relative to that of Bz. This value indicates the *in vitro* potential of the test compounds compared to the reference drug.

All compounds showed activity against the three parasite stages, and some of them were more active than Bz. For the cytotoxicity against Vero cells, the compounds were substantially less toxic than the reference drug (see the IC₅₀ values in Table 1). Considering the more illustrative SI, compounds 1, 2, 7, and 11 were of potential interest with SI values 25 to 77-fold higher than those of Bz (Table 1). The SI values of the other compounds were lower, indicating that they are less suitable. However, when the Mn²⁺ complexes of compounds 1–7 and 11 were checked, a lower effect was observed (see ESI Table S3[†]). This can probably be attributed to the protective effect that the Mn²⁺ complexes of these ligands exert over free radicals generated in the oxidative metabolism.²⁰

Significant differences were found, however, in the unspecific cytotoxicity against Vero cells and, of course, in the SI resulting from these data. Despite this, there was not a clear

Table 1 *In vitro* activity, toxicity and selectivity index found for the aza-scorpian-like macrocyclic derivatives on the extracellular and intracellular forms of *T. cruzi*^c

Compound	IC ₅₀ ^a (μM)			Toxicity IC ₅₀ Vero cell (μM)	SI ^b		
	Epimastigote forms	Amastigote forms	Trypomastigote forms		Epimastigote forms	Amastigote forms	Trypomastigote forms
Bz	16.2 ± 0.8	23.6 ± 0.7	22.6 ± 0.8	13.6 ± 0.9	0.8	0.6	0.6
1	3.3 ± 0.5	6 ± 1	5 ± 2	187 ± 14	57 (71)	31 (52)	37 (62)
2	4.2 ± 0.7	3.2 ± 0.5	5 ± 1	146 ± 9	35 (44)	46 (77)	29 (48)
3	16 ± 2	13 ± 2	22 ± 3	214 ± 15	13 (16)	16 (27)	10 (17)
4	3.2 ± 0.3	4.2 ± 0.3	7.4 ± 0.7	83 ± 5	26 (33)	20 (33)	11 (18)
5	18.0 ± 0.5	14 ± 1	33 ± 2	131 ± 13	7 (9)	9 (15)	4 (7)
6	16 ± 1	8.4 ± 0.7	27 ± 2	88 ± 6	6 (8)	10 (17)	3 (5)
7	3.3 ± 0.2	2.8 ± 0.5	6.5 ± 0.4	98 ± 7	30 (38)	35 (58)	15 (25)
8	29 ± 2	2.5 ± 3	19.4 ± 0.8	84 ± 10	3 (4)	3 (5)	4 (7)
9	4.8 ± 0.5	5.1 ± 0.4	9 ± 1	76 ± 5	16 (20)	15 (25)	8 (13)
10	4.1 ± 0.6	3.6 ± 0.1	9.2 ± 0.8	94 ± 6	23 (29)	26 (43)	10 (17)
11	7.9 ± 0.6	5.2 ± 0.3	12 ± 1	202 ± 11	26 (33)	39 (65)	17 (28)

^a IC₅₀ = the concentration required to give 50% inhibition, calculated by linear regression analysis from the values at the concentrations employed (1, 10, 25, 50 and 100 μM). ^b Selectivity index = IC₅₀ Vero cells/IC₅₀ extracellular or intracellular form of the parasite. In brackets: the number of times that a compound exceeds the reference drug SI (for the extracellular and intracellular forms of *T. cruzi*). ^c The values are the average of three separate determinations.

relationship between toxicity and structure, and the more toxic compounds appeared to be the double scorpiands (9, 10) and the single scorpiands containing large aromatic pyrene units (4, 8). Taking into account all the data included in Table 1, compounds 1, 2, 7 and 11 were the best compounds, with SI values exceeding 50 times or more those of Bz, depending on the stage of the parasite used. According to some authors, only compounds with SI values exceeding 50 times the SI value of Bz are good enough to be considered as interesting as antiparasitic drugs.²¹

Before starting the *in vivo* analysis of compounds 1, 2, 7 and 11, an infectivity assay was performed. In such an assay, which is an *in vitro* reproduction of the life cycle of the parasite (see ESI, infectivity section and Fig. S2†), it can be observed that all four compounds selected, decreased the infection rate, *i.e.*, by 73%, 68%, 82% and 76%, respectively. In the same way, they decreased the number of amastigote forms per infected cell at rates higher than 50% and consequently, the release of trypomastigote forms into the media decreased to 60%, 44%, 80% and 69%.

***In vivo* activity of scorpiand-like azamacrocyclic derivatives.** The promising results obtained for the *in vitro* tests prompted us to study the *in vivo* activity of compounds 1, 2, 7 and 11 in a murine model (BALB/c mice).

The effectiveness of drugs currently in use against CD varies widely between the acute and chronic phases. Therefore, it was decided to evaluate the compounds in both phases. For acute phase experiments, the first 40 days after infection were considered, whereas the effect on the chronic phase was studied between days 40 and 120 after infection for those compounds with high efficiency during the acute phase.

Scheme S1 (see ESI†) provides a picture of all the *in vivo* experiments performed. The intraperitoneal administration route was preferred to the intravenous procedure because intraperitoneal treatment substantially reduces animal mortality.²²

In fact, none of the animals died in any of our experiments performed either with the control or with 1, 2, 7 and 11 at the concentrations used (5 mg kg⁻¹ of body mass). Female mice were inoculated with trypomastigotes, as described in the Experimental section. Treatment, *via* the intraperitoneal route (ip), with the compounds of interest began five days post infection and was maintained for an additional five days. Another group of mice was treated in the same manner, but with only the vehicle (control). During the study of acute phase activity, the levels of parasitaemia were determined every two days. Fig. 4 shows the number of trypomastigote forms found in the blood until 40 days post infection. On the days of maximum parasitic burden (peak days, 16–22 days post infection) all compounds greatly reduced the number of circulating parasites. Furthermore, this reduction lasted until day 40 and was more significant for the groups treated with the compounds under study than for those treated with Bz. The order of *in vivo* activity towards the trypomastigote forms in the acute phase was: 7 > 11 > 2 ≫ 1 > Bz.

Compounds 1 and 2 showed moderate activity, because between 30% and 63% of the parasites survived the treatment

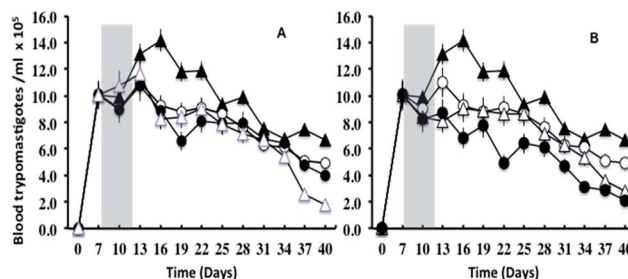


Fig. 4 Parasitaemia in the murine model of acute CD (A and B). In (A) (-▲-) control, (-●-) compound 1, (-△-) compound 2. In (B) (-▲-) control, (-●-) compound 7, (-△-) compound 11. All compounds were administered by the ip route with 5 mg kg⁻¹ of body mass of each compound. Grey shading represents the treatment period. Values are the means of the results for six mice ± standard deviation.

(Fig. 4A), while 7 and 11 displayed the highest activity during the acute phase (parasitaemia reduction greater than 80% by the end of the acute phase), as shown in Fig. 4B. So, in view of these results, the group of mice treated with compounds 7 and 11 were kept until 120 days post infection under the same conditions.

The experiment was accomplished by an immunosuppression test on the treated and control mice at day 120 post infection (late chronic phase, in which there are no parasites remaining in the bloodstream). Fig. 5A shows the reactivation of parasitaemia after immunosuppression. The control group recovered from its initial parasitaemia almost entirely, thus giving a reactivation of 100%. In contrast, mice treated with 11 showed a parasitaemia load of 60% relative to their previous burden, while mice treated with 7 displayed an even lower reactivation of only 50%.

Enzyme-linked immunosorbent assays (ELISA) were used as an alternative method for verifying the effectiveness of these two compounds in the chronic phase after being challenged with an immunosuppression cycle. According to the literature, IgG titres in Balb/c become stable during the chronic phase of the disease²³ and this was confirmed by the results shown in Fig. 5B, which shows the anti-*T. cruzi* IgG levels. The IgG levels of the control group increased by about 40% because of the presence of parasites in the bloodstream after immunosuppression. However, the differences between immunosuppressed and non-immunosuppressed groups were smaller in the case of 11 and not significant for those treated with 7. This means that the parasite-specific IgG level was not higher than the remaining amount of total unspecific level of IgG caused by the hypergammaglobulinaemia characteristic of infection with *T. cruzi*.^{23,24} Finally, Fig. 5C shows the PCR results of samples obtained after necropsy. The hearts were ground and used for total DNA extraction and amplification of a fragment within the parasite SOD-gene. The hearts of control animals confirmed the presence of parasites, while the hearts of mice treated with 7 were relatively clear of parasites (25% of the control value) thus confirming the degree of curative effect of 7.

It is concluded that the limited effectiveness of 7, the best compound found in this study, was because of the low dosage

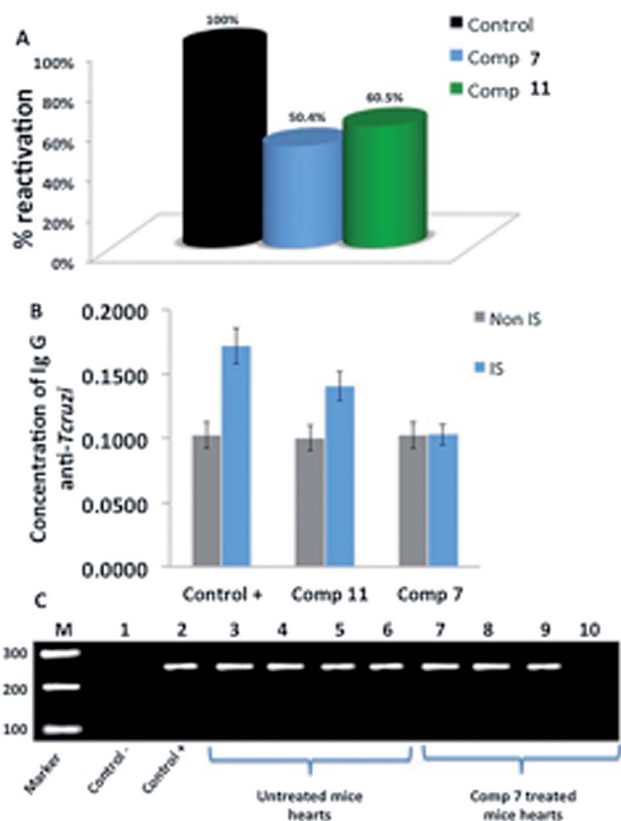


Fig. 5 Immunosuppression experiment in the mouse model. (A) Reactivation of parasitaemia after immunosuppression. (B) Total IgG levels of anti-*T. cruzi*. Values are the means of three separate experiments and the error bars represent the mean \pm standard deviation. (C) Polymerase chain reaction (PCR) analysis of heart tissue at 120 days after infection. All the mice from lanes 3–10 were infected.

used during the acute phase. Thus, these results will be taken into consideration in future experiments where the dosage will be increased and the schedule of treatment will also be modified to better expose the compound in the bloodstream. This increase in compound administration should not result in enhanced toxicity. Indeed, according to the data shown in Table S4,[†] all the biochemical parameters determined to obtain kidney, heart and liver profiles were maintained after compound administration and only the uric acid values showed an insignificant decrease of 10% (see the ESI[†]).

Molecular mechanisms of action

Metabolite excretion study. Because trypanosomatids are unable to completely degrade glucose to carbon dioxide, they excrete a considerable portion of their hexose skeleton as partially oxidised fragments in the form of fermented metabolites, whose nature and percentage depend on the pathway used for glucose metabolism.²⁵ The catabolism products in *T. cruzi* were acetate and succinate, with smaller percentages of L-alanine and D-lactate, results which were in agreement with data found in the literature.²⁶ The detection of large amounts of succinate as a major end product is a usual feature, because it relies on glycosomal redox balance, enabling re-oxidation of

NADH produced in the glycolytic pathway. Succinic fermentation requires only half of the phosphoenolpyruvate (PEP) produced to maintain the NAD⁺/NADH balance. The remaining pyruvate is converted inside the mitochondrion and the cytosol into acetate, D-lactate, L-alanine, or ethanol according to the degradation pathway followed by each species.²⁷

To obtain some information about the effect of the compounds tested on parasite glucose metabolism, we

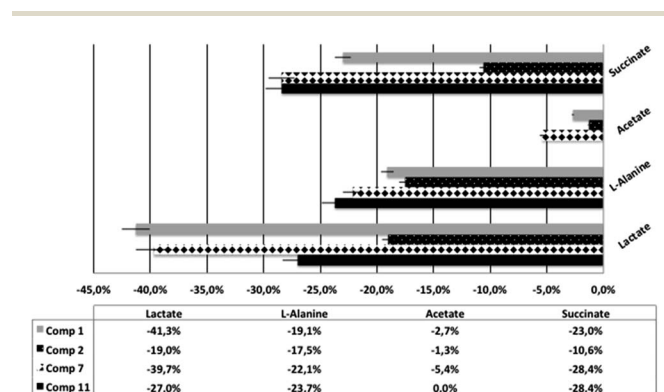


Fig. 6 Variation of percentages in the height of the peaks corresponding to metabolites excreted by *T. cruzi* epimastigotes in the presence of aza-scorpianid-like macrocycle derivatives at their IC₂₅ (the concentration required to give 25% inhibition) compared to a control sample. Values are the means of three separate experiments and error bars represent the standard deviation.

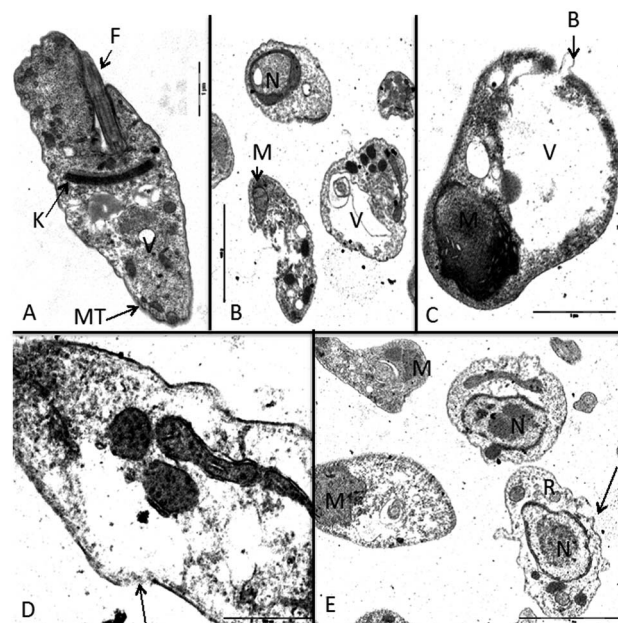


Fig. 7 Ultrastructural alterations shown by TEM in epimastigotes of *T. cruzi* treated with aza-scorpianid-like macrocycles 1, 2, 7 and 11. (A) Control parasite showing typical organelles; (B) treated with aza-scorpianid-like macrocycles 1; (C) treated with compound 2; (D) treated with compound 7 and (E), treated with compound 11, at the IC₂₅ concentration. Scale bar = 1 μ m. N = nucleus, M = mitochondria, G = glycosomes, MT = microtubules, V = vacuoles, R = reservosomes, K = kinetoplast and F = flagellum.

obtained the $^1\text{H-NMR}$ spectra of *T. cruzi* epimastigote forms after treatment with **1**, **2**, **7** and **11**. The final excretion products were identified qualitatively and quantitatively (spectra not shown). The results were compared with those obtained from parasites maintained in a cell-free medium (control) for 96 hours. The characteristic presence of acetate, succinate, D-lactate and L-alanine was confirmed in the control experiments. As expected, succinate and acetate were the most abundant end products identified. However, after treatment of the parasites with the selected compounds, the excretion of catabolites was substantially altered at the dosages employed. Fig. 6 shows the changes observed compared to the control. Remarkable differences in the catabolic pathway were observed, depending on the compound used, which seemed to be connected with the trypanocidal activity described previously. The main features found were substantial decreases in succinate and lactate and, to a lesser extent, alanine. The most active compounds **7** and **11** decreased succinate, D-lactate and L-alanine by -28.4% , -39.7% and -22.1% and -28.4% , -27.0% and -23.7% , respectively.

All these data can be interpreted on the basis of a change in the succinate, D-lactate, L-alanine pathways occurring in the presence of the most active compounds **7** and **11**. It is well-known that D-lactate and L-alanine originate from the transformation of PEP in pyruvate in the presence of pyruvate kinase or pyruvate-phosphate dikinase.²⁶ Therefore, it seems possible that **7** and **11** interact with the pyruvate kinase enzymes, thereby modifying the glucose metabolism of the parasite at the

pyruvate stage. On the other hand, it is interesting to note that the decrease in succinate observed with **7** and **11** could also be related to dysfunction of the mitochondria, because of the redox stress produced by inhibition of the Fe-SOD enzyme which is resident in the mitochondrion.²⁸ This should result in a decrease in pyruvate metabolism and a consequent decrease in succinate produced in the mitochondria. All these data prove that the severe modifications generated in organelles such as glycosomes or mitochondria by **7** and **11** is the ultimate reason for the alterations observed in the excretion products of *T. cruzi*.

Ultrastructural alterations. The trypanocidal activity shown by **1**, **2**, **7** and **11** should cause damage to parasite cells, therefore, we used TEM to study the epimastigote forms of *T. cruzi* treated with **1**, **2**, **7** and **11** to determine if this was true. As expected, significant morphological alterations were observed when compared with untreated control cells (Fig. 7). Without any doubt, the most effective compounds were **7** and **11**, which caused considerable disturbances in many parasites. Compound **1** (Fig. 7B) mainly caused disorganisation in the plasma membrane, enormous vacuoles inside the cell, and mitochondria were found to swollen and expanded. The nuclei were also swollen and vacuolated, and in some parasites, the cytoplasm was full of reservosomes. More drastic effects were caused by **2**, as can be seen in Fig. 7C, where some epimastigote forms were totally swollen with giant vacuoles which filled almost all the cytoplasm. Furthermore, the mitochondria were disorganised and swollen, with small crystals and a less electron dense zone than usual that could be related to a loss of function.

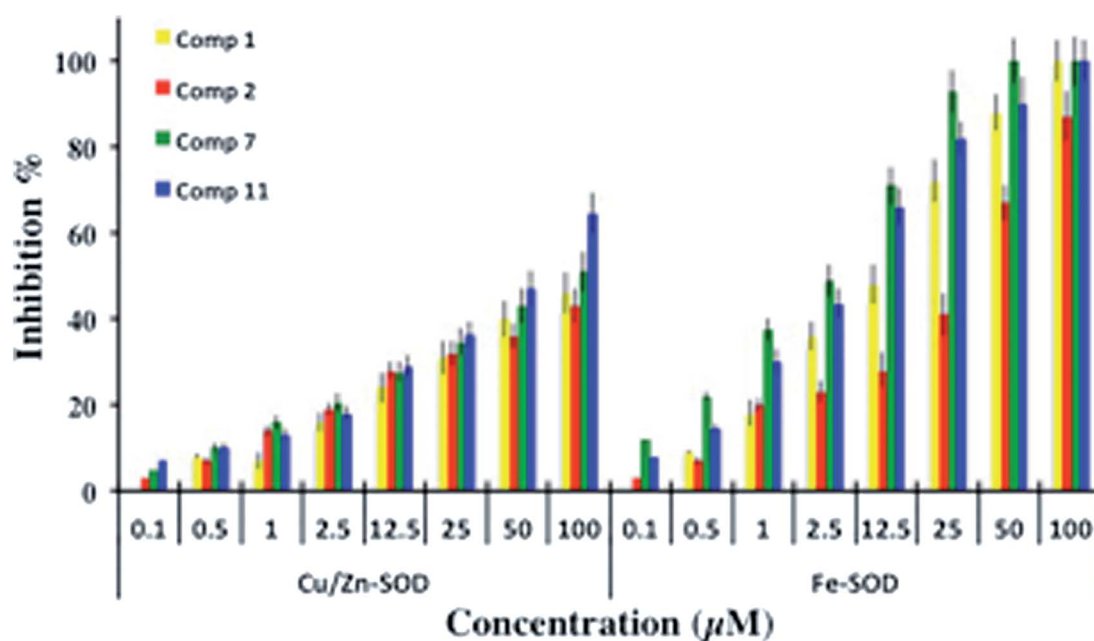


Fig. 8 *In vitro* inhibition (%) of CuZn-SOD from human erythrocytes for compounds (activity: $23.36/4.21 \text{ U mg}^{-1}$) and Fe-SOD from *T. cruzi* epimastigotes for compounds (activity $20.77/3.18 \text{ U mg}^{-1}$). The x-axis shows the compound concentrations given for each enzyme. Enzyme concentrations were kept constant in all the assays. Differences between the activities of the control homogenate and those incubated with test compounds were obtained using the Newman–Keuls method. Values in the legend represent the IC_{50} (the concentration required to give 50% inhibition) calculated using linear regression analysis from the K_c values at the concentrations employed (0.1–100 mM). IC_{50} values for Cu/Zn-SOD = $123 \mu\text{M}$, $172 \mu\text{M}$, $98 \mu\text{M}$ and $56 \mu\text{M}$, for compounds **1**, **2**, **7**, and **11**, respectively. IC_{50} values for Fe-SOD = $13 \mu\text{M}$; $42 \mu\text{M}$; $4 \mu\text{M}$ and $7 \mu\text{M}$, for compounds **1**, **2**, **7**, and **11**, respectively. Values are the average of three separate determinations and error bars represent the standard deviation.

The parasites treated with compound **11** (Fig. 7E) were totally disturbed, showing an empty cytoplasm, broken plasma membrane and some organelles were unrecognisable. Some similar alterations occurred when the epimastigote forms were treated with **7** (Fig. 7D), where ribosomes were very few and the electron density was decreased in the nucleus. Mitochondria were swollen and microtubules were discontinuous along the cytoplasm.

Inhibitory effect on the *T. cruzi* Fe-SOD enzyme. These results prompted us to evaluate the inhibitory effect of **1**, **2**, **7** and **11** on Fe-SOD activity. The results are shown in Fig. 8. Significant inhibitory values of Fe-SOD activity were found for the four compounds tested. Compounds **7** and **11** showed values close to 100% inhibition at 25–50 μM with IC_{50} values ranging from 4.2 to 6.6 μM . The design of an effective drug able to inhibit the parasite Fe-SOD without inhibiting human SOD is an interesting objective. Therefore, we also assayed the effect of these compounds on Cu/Zn-SOD from human erythrocytes. The results show that the inhibition percentages for human CuZn-SOD were lower than for Fe-SOD. The lead compounds **7** and **11** gave IC_{50} values of 98.0 and 55.8 μM , respectively, for Cu–Zn-SOD.

It should be noted that, as mentioned previously, these compounds not only showed greater alterations in glucose catabolism but they also led to greater levels of Fe-SOD inhibition. Because the Fe-SOD present in mitochondria is an essential part of the antioxidant protective response of the parasite, its inhibition would be related to a decrease in the rate of survival for the parasite. Because of this fact, it is hypothesised that compounds having a pyridine nitrogen on the side chain are able to get closer to the active centre of the enzyme, as is the case of compound **7**, so they might produce greater inhibition. Modelling studies were carried out to obtain further information about inhibition.

Modelling studies. In order to learn about possible ways in which the compounds yielding the best trypanocidal activity inhibit the active centre of Fe-SOD, out a molecular dynamics study was carried out in which the compounds were contacted to Fe-SOD *T. cruzi* protein PDB ID: 2GPC. As mentioned in more detail in the Experimental section, a distance restraint was applied between the heavy atoms of the active site residues and the heavy atoms of the compounds, using the $\langle r^{-6} \rangle^{-1/6}$ average of all the interaction distances to atoms of the groups. After the equilibration stage at 300 K, a total of 10 ns of molecular dynamics was performed. Finally, the five minimum energy conformers were selected from the trajectory and minimised by removing all the restrains.

T. cruzi Fe-SOD is a dimeric protein with polypeptide chains consisting of seven helical regions and three anti-parallel β -strands.²⁹ The substrates approach the active site through a funnel in which H31 and Y35 serve as the gateway and restrict the access of small molecules towards the active site (Fig. 9). The metal ion is coordinated in trigonal bipyramidal geometry to H27, H75, D160 and H164 and to a water molecule or a hydroxide anion. A hydrogen bond network involving the gateway residues Y35 and Q71 and the water molecule or hydroxide ion directly bound to the metal facilitate proton

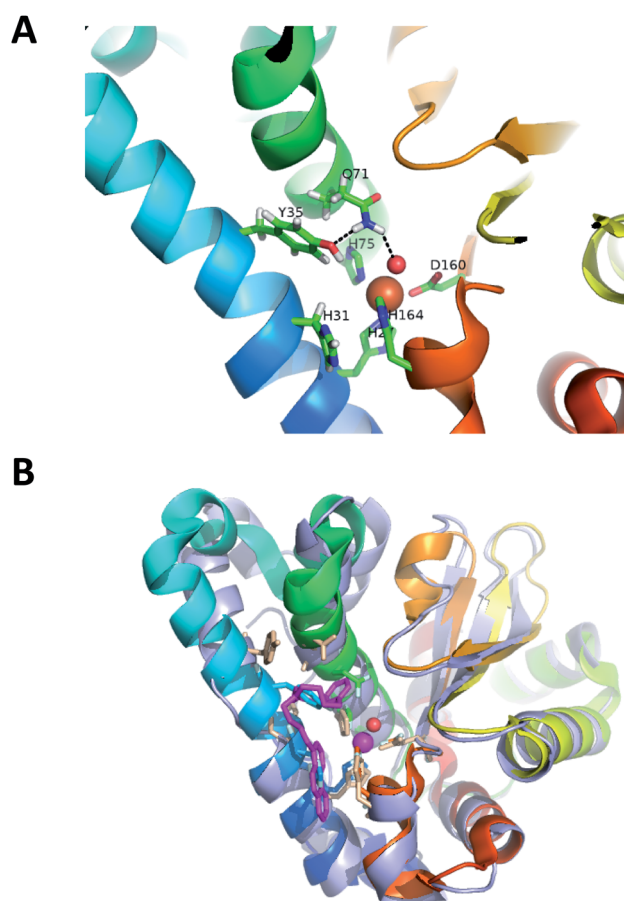


Fig. 9 (A) Representation of the active centre and residues forming the funnel gateway of Fe-SOD *T. cruzi* protein PDB ID 2GPC. Relevant hydrogen bond connections are presented as dotted lines. (B) Diagram representing the superimposition of the original 2GPC protein (rainbow colours) (only one chain) over the molecular dynamics minimum energy structure (pale blue) of the protein with compound **11** (magenta). Original residues have the corresponding rainbow colours whereas the final dynamic residues are pale brown. Helix I is represented on the left.

exchange between the active centre and the exterior of the protein.³⁰ Apart from this, residues E163 and Y167 extend towards the surface of the protein and help stabilise the dimer through hydrogen bonding with E163 and H31 of the other unit, respectively,^{30,31} (see Fig. S3, ESI†).

The molecular dynamics studies with compounds **1**, **2**, **7** and **11** revealed profound changes in the active site environment. Although all the compounds examined displaced the gateway amino acids H31 and Y35, two different contacting orientations were identified. For **1**, **2** and **11**, the quinoline and phenanthroline subunits at the arm lie towards the exterior of the funnel while the macrocyclic core approaches the active centre, whereas for **7**, the macrocycle is placed the other way around, extending its lateral chain containing the 4-pyridine units towards the metal site and leaving the macrocyclic core oriented outwards. Although in none of these examples do the donor atoms of the inhibitors bind directly to the metal ion, they produce drastic changes in the hydrogen bond network around the active site at

the time that they significantly alter helix 1 (see Fig. 9B and S4 (ESI[†])). Interestingly, the molecules approach the active site by taking advantage of a disrupted turn in the helix. The interaction of the compounds with the proteins pushes back the upper part of helix 1. As expected, all the compounds remove the hydrogen bond network formed by Y35 and Q71 and are involved in hydrogen bonding either with them and/or with H31. For example, while **1** forms hydrogen bonds with Y35 and Q71, **11** establishes hydrogen bonds with H31 and Q71 (Fig. S4 ESI[†]).

In its turn, **2** makes hydrogen bonds with Q71 and also with H164, which forms part of the first coordination sphere of the metal ion which places the 4-quinoline unit parallel to the shifted Y35 of the gateway. Finally, for **7**, hydrogen bonds between the inhibitor and Y35 and H31 are observed whereas Q72 does not participate in the hydrogen bonding network. Additionally, the hydrogen of **7** also bonds to a leucine residue (L26). There is one surprising and very interesting result regarding the way in which these molecules fit and close the funnel of the enzyme. As seen in the surface map of Fig. 10 and **11** (phenanthroline) completely occludes the funnel, preventing any other molecule from approaching the active site. The same event, although not to such a large extent, occurs for the other compounds (see Fig. S5 in the ESI[†]).

Trypanothione reductase (TR) inhibition assay. The best compounds were selected to evaluate their effects on *T. cruzi* trypanothione reductase (TR). All four compounds proved to be

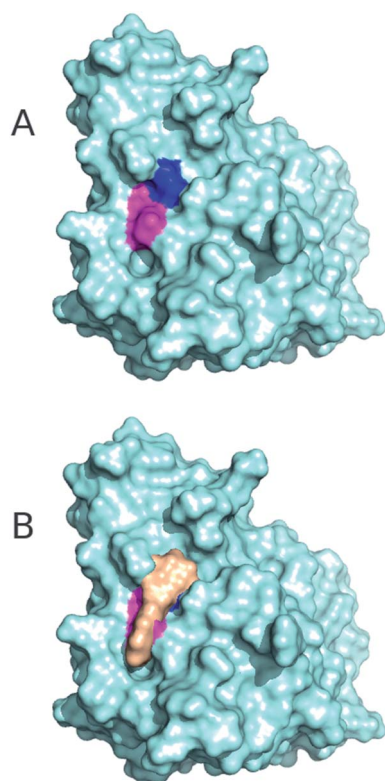


Fig. 10 Solvent accessible surface of (A) original 2GPC protein and (B) 2GPC and minimised compound **11** (light brown) showing the occlusion of the funnel. H31 and Y35 are presented in magenta and blue, respectively.

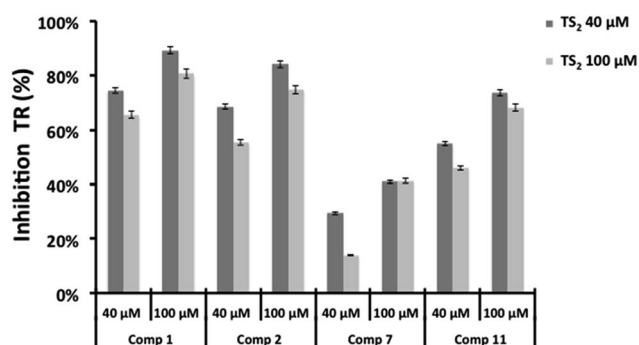


Fig. 11 Inhibition of TcTR by compounds **1**, **2**, **7** and **11**. The activity was measured following the NADPH consumption at 340 nm as described in the Experimental section. The control used to obtain 100% of activity was assayed without an inhibitor but the same amount of water was used to dissolve the compounds. The values are an average of two independent measurements and error bars show the standard deviation.

inhibitors of TR (Fig. 11). At fixed concentrations of 40 and 100 μM for both the inhibitor and the substrate trypanothione disulfide (TS₂), the degree of inhibition varied between 14% and

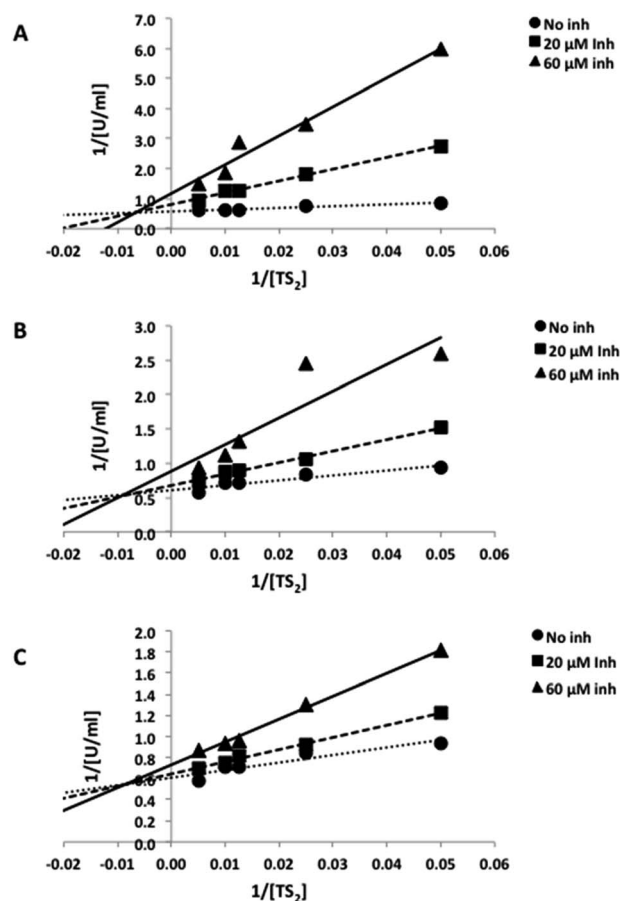


Fig. 12 Lineweaver–Burk plots for the inhibition of TcTR by compound **1** (A), **2** (B), and **11** (C). The assays contained 100 μM NADPH and no inhibitor (inh), 20 μM, or 60 μM fixed concentrations of the inh. The TS₂ concentration was varied between 20, 40, 80, 100 and 200 μM.

89%. The most active *in vivo* trypanocidal compound **7** had the lowest inhibitory activity (lower than 50%), which renders TR unlikely as a potential target. The other three compounds **1**, **2** and **11** caused 74% to 89% inhibition when 100 μM of the compound and 40 μM of TS_2 were applied, indicating that they are inhibitors of the enzyme. Notably, no significant difference (around 10%) in the degree of inhibition at the two TS_2 concentrations was observed. This strongly indicates that these compounds do not act as pure competitive inhibitors.

Trypanothione reductase kinetic study. To obtain insight into the molecular mode of action, the inhibitor constants and the type of inhibition were determined using Lineweaver–Burk plots, which revealed that all three compounds **1**, **2** and **11** behave as mixed type non-competitive inhibitors. Clearly, the lines cut in the double reciprocal plot above the x -axis.³² In the case of **1**, K_i and K_i' values of 4 and 53 μM , respectively, were obtained. Compound **2** was slightly less efficient giving K_i and K_i' values of 8 and 114 μM , respectively. Finally, for **11**, the K_i and K_i' values were 16 μM and >200 μM , respectively (Fig. 12). However, a higher affinity of the compound for the free enzyme compared to the enzyme–substrate complex was observed, as can be inferred from the calculated $K_i < K_i'$ values.

In silico pharmacokinetic evaluation. Compounds **1**, **2**, **7** and **11**, which showed the best trypanocidal activity, were also submitted to an *in silico* pharmacokinetic properties evaluation.

To evaluate the absorption rate, necessary for oral administration, the number of free rotatable bonds (n -ROTB) and Lipinski's "rule of five" was determined for the lead compounds. Lipinski's descriptors evaluate the molecular properties for drug pharmacokinetics in the human body, especially for oral absorption. The rule states that the most "druglike" molecules present $c \log P \leq 5$, molecular weight ≤ 500 , number of hydrogen bond acceptors (HBA) ≤ 10 , and hydrogen bond donors (HBD) ≤ 5 .³³ Lipinski's molecular descriptors and the predicted data of some absorption, distribution, metabolism, excretion and toxicity (ADMET) properties for **1**, **2** (which share the same predicted values), **7** and **11** are summarised in Table 2. The predominant species at pH 7.4 (H_2L^{2+} , for **1**, **2** and **11** and H_3L^{3+} for **7**) was chosen for the evaluation. **1**, **2**, **7** and **11** showed acceptable n -ROTB values (≤ 10) and fulfilled Lipinski's rule of five. In addition, ADMET properties were calculated using admetSAR (<http://www.admetexp.org/>), a freely accessible web-based application.³⁴ The predicted data for blood–brain barrier (BBB) penetration and human intestinal absorption (HIA) were positive for all the tested compounds. Caco-2 cell permeability was negative in all cases, but with a moderate probability value. For metabolism, various cytochromes P450 (CYP) were evaluated, showing similar patterns for all the compounds. In terms of toxicity, it was found that none of the

Table 2 Oral bioavailability, molecular properties and predicted ADMET properties of compounds **1**, **2**, **7** and **11**^a

	Compounds 1 and 2		Compound 7		Compound 11	
	Result	Probability (%)	Result	Probability (%)	Result	Probability (%)
Lipinski molecular descriptors						
HBA (≤ 10)	4		4		5	
HBD (≤ 5)	3		4		3	
$c \log P$ (≤ 5)	2.62		1.52		2.64	
MW (≤ 500)	393.56		400.59		444.61	
n -ROTB (≤ 10)	5		9		5	
Absorption						
BBB	+	87.9	+	67.7	+	87.9
HIA	+	72.2	+	74.1	+	72.2
Caco-2	–	61.6	–	65.9	–	61.6
Metabolism						
CYP450 2C9 substrate	NS	90.2	NS	89.8	NS	90.2
CYP450 2D6 substrate	S	63.0	S	55.9	S	63.1
CYP450 3A4 substrate	NS	77.0	NS	73.5	NS	77.0
CYP450 1A2 inhibitor	NI	89.5	NI	91.8	NI	89.5
CYP450 2C9 inhibitor	NI	96.0	NI	95.4	NI	96.0
CYP450 2D6 inhibitor	NI	69.5	NI	51.0	NI	69.5
CYP450 2C19 inhibitor	NI	95.1	NI	96.7	NI	95.1
CYP450 3A4 inhibitor	NI	90.0	NI	93.7	NI	90.0
Toxicity						
AMES toxicity	–	68.6	–	66.4	–	68.6
Carcinogens	–	93.2	–	93.9	–	93.2

^a n -ROTB, number of rotatable bonds; HBA, number of hydrogen bond acceptors; HBD, number of hydrogen bond donors; $c \log P$, logarithm of compound partition coefficient between n -octanol and water; MW, molecular weight; BBB, blood–brain barrier; HIA, human intestinal absorption; S, substrate; NS, non-substrate; NI, noninhibitor.

compounds showed mutagenic toxicity with the AMES test or other carcinogenic effects.

Conclusions

The trypanocidal properties of a family of simple and double aza-scorpian compounds, some of them newly synthesised, were examined both *in vivo* and *in vitro*. The experiments allowed us to select compounds displaying improved efficiency and lower toxicity than the reference drug. Parallel studies were carried out to establish the mechanism of action. Following this series of experiments, four compounds were selected as potential candidates to enter into clinical trials. Compounds **7** and **11** selectively inhibit the Fe-SOD enzyme of the parasites. Molecular dynamics studies indicated that these compounds block the access of substrates to the active site while they break the hydrogen bond pattern around the active site. Furthermore, compound **7** showed an *in vivo* cure rate of 25% at a safe standard dosage of 5 mg kg⁻¹ body mass. As shown by the NMR data, another mechanism of action of this series of compounds may be related to energetic mechanisms. Furthermore, **1** and **2** behaved as very effective TR inhibitors. The damage to the defence system of parasites produced by these compounds was reflected in the TEM ultrastructural analysis which showed high vacuolisation. Furthermore, the compounds of choice displayed low *in vivo* toxicity, as reflected by the fulfilment of the ADMET rules. Finally, it deserves to be mentioned that, because of their different mechanisms of action, combined therapies should be further considered to obtain improved efficiency. A patent (P201330699) has already been filed for this family of compounds.

Experimental

Chemistry

The ESI[†] contains the synthetic procedure for compounds **2** and **4** prepared for the first time and the characterisation data (NMR, mass spectrometry and elemental microanalysis) of all the compounds. Details of the potentiometric titrations, calculation of acid–base and stability constants and molecular modelling studies are also included in the ESI.[†]

Biological activity – *in vitro* assays

The parasites and mammalian cells used are described in the ESI.[†] The procedures to test the different compounds against all parasite forms and mammalian cells individually as well as the infectivity assay, which represents a reproduction of the life cycle *in vitro*, are also provided.

Biological activity – *in vivo* assays

Mouse infection and treatment. This experiment was performed using the rules and principles of the international guide for biomedical research in experimental animals and with the approval of the ethical committee of the University of Granada, Spain. Groups of six BALB/c albino female mice (6–8 weeks old, 25–30 g weight), maintained under a 12 h dark/light cycle (lights

on at 07 : 30 h) at a temperature of 22 ± 3 °C and provided with water and standard chow *ad libitum*, were inoculated *via* the ip route with 5 × 10⁵ blood trypomastigotes of *T. cruzi* obtained from previously infected mice blood. The animals were divided as follows: (I) positive control group (mice infected but not treated); (II) study group (mice infected and treated with the compounds under study). The administration of the tested compounds began on the seventh day of infestation once the infection was confirmed, and doses of 25 mg kg⁻¹ body weight per day were administered for five consecutive days (7–12 days post infection) by the ip route. Peripheral blood was obtained from the mandibular vein of each mouse (5 µL samples) and dissolved in 495 µL of a phosphate buffered saline (PBS) solution at a dilution of 1 : 100. The circulating parasite numbers were quantified using a Neubauer chamber for counting blood cells. The count was performed every three days for 40 days (acute phase). The number of bloodstream forms found was expressed as parasites per mL. From this point onwards, the disease was considered chronic. The assays that follow are detailed in the ESI,[†] where cyclophosphamide-induced immunosuppression and the assessment of cure are included.

Toxicity tests by clinical chemistry measurements. A fraction of the serum, obtained as shown above, was sent to the Biochemical Service at the University of Granada where a series of parameters was measured according to commercial kits acquired from Cromakit® using a BS-200 Chemistry Analyzer (Mindray, Shenzhen). With the levels obtained for different sets of sera ($n = 15$, $n = 6$), the mean value and standard deviation were calculated. Finally, the confidence intervals for the mean normal populations based on a confidence level of 95% ($100 \times (1 - \alpha) = 100 \times (1 - 0.05)\%$) were also calculated. The ranges obtained are shown in Table S4,[†] which allows for the comparison and analysis of the sera studied in this work.

Studies on the mechanism of action

Metabolite excretion study. Cultures of *T. cruzi* epimastigotes (initial concentration 5 × 10⁵ cells per mL) received IC₂₅ concentrations of the compounds under study (except for control cultures). After incubation for 96 h at 28 °C, the cells were centrifuged at 400 g for 10 min. The supernatant solution were collected to determine the excreted metabolites using ¹H-NMR. Chemical shifts were expressed in parts per million (ppm, δ scale), using sodium 2,2-dimethyl-2-silapentane-5-sulfonate as the reference signal. The chemical displacements used to identify the respective metabolites were consistent with those described previously.³⁵

Ultrastructural alterations. The epimastigotes of *T. cruzi* were cultured at a density of 5 × 10⁵ cells per mL in a suitable medium containing the compounds tested at their IC₂₅ concentrations. After 72 h, these cultures were centrifuged at 400 g for 10 min, and the pellets were washed with PBS and then mixed with 2% (v/v) paraformaldehyde–glutaraldehyde in 0.05 M cacodylate buffer (pH 7.4) for 4 h at 4 °C. Following this, the pellets were prepared for study using TEM with a previously described technique.³⁶

Superoxide dismutase (SOD) inhibition studies. The protocol to obtain the enzyme from the culture and the experimental measure of the inhibition assays are described in the ESI.†

Trypanothione reductase (TR) inhibition studies. Recombinant trypanothione reductase from *T. cruzi* (TcTR) was prepared following a published procedure.³⁷ TS₂ was generated enzymatically as described previously.³⁸ TR activity was measured in a total volume of 1 mL of 40 mM HEPES, 1 mM EDTA, pH 7.5, in the presence of 100 μM NADPH and varying concentrations of TS₂ (20, 40, 80, 100 and 200 μM) and/or inhibitor (0, 28 and 100 μM). The absorption decrease because of NADPH oxidation was followed at 340 nm and 25 °C. Stock solutions of the inhibitors were prepared in water according to their solubility.

The K_i and K_i' values were determined using the following equations:³²

$$K_i = \frac{[I]}{K_{m(\text{obs})} \left(1 + \frac{[I]}{K_i'} \right) - K_m}$$

$$K_i' = \frac{[I]}{\frac{V_{\text{max}}}{V_{\text{max}(\text{obs})}} - 1}$$

The ability of the compounds to induce the oxidase activity of TR was measured in the presence of 100 μM NADPH, with 40 and 100 μM of the compound in a total volume of 1 mL and about 2 U mL⁻¹ of TR. Under these conditions, spontaneous NADPH oxidation results in a minimal absorption decrease. This activity was not accelerated in the presence of the compounds tested, thus proving that they do not act as subversive substrates (data not shown).

Acknowledgements

Financial support for this study was received from the Spanish Ministry of Economy and Competitiveness (MINECO), CONSOLIDER-INGENIO 2010 CSD2010-00065 and Generalitat Valenciana PROMETEO 2011/008. F.O. is grateful for an FPU Grant from the Ministry of Education of Spain and he also thanks Natalie Dirdjaja and Dr Alejandro Leroux, Heidelberg, for their support with the kinetic analysis of TR.

Notes and references

- P. J. Hotez, D. H. Molyneuz, A. Fenwick, J. Kumaresan, S. E. Sachs, J. D. Sachs and L. Savioli, *N. Engl. J. Med.*, 2007, **357**, 1018–1027.
- WHO, *Global Report for Research on Infectious Diseases of Poverty*, 2013, ISBN: 9789241564489.
- WHO, Chagas disease (American trypanosomiasis), Fact sheet no. 340, update March 2013.
- A. M. Strosberg, K. Barrio, V. H. Stinger, J. Tashker, J. C. Wilbur, L. Wilson and K. Woo, Institute for One World Health (IOWH), San Francisco, CA, 2007, pp. 1–110, http://s3.amazonaws.com/zanran_storage/www.oneworldhealth.org/ContentPages/15710128.pdf.
- J. A. Urbina, *Curr. Pharm. Des.*, 2002, **8**, 287–295.
- R. Viotti, C. Vigliano, B. Lococo, M. G. Alvarez, M. Petti, G. Bertocchi and A. Armenti, *Expert Rev. Anti-Infect. Ther.*, 2009, **7**, 157–163.
- C. J. Schofield, J. Jannin and R. Salvatella, *Trends Parasitol.*, 2006, **22**, 583–588.
- (a) M. J. Pinazo, L. Guerrero, E. Posada, E. Rodríguez, D. Soy and J. Gascon, *Antimicrob. Agents Chemother.*, 2013, **57**, 390–395; (b) S. Cencig, N. Coltel, C. Truyens and Y. Carlier, *Int. J. Antimicrob. Agents*, 2012, **40**, 527–532.
- (a) J. D. Maya, D. K. Cassels, P. Iturriaga-Vasquez, J. Ferreira, M. Faúndez, N. Galanti, A. Ferreira and A. Morello, *Comp. Biochem. Physiol., Part A: Mol. Integr. Physiol.*, 2007, **146**, 601–620; (b) S. R. Wilkinson, C. Bot, J. M. Kelly and B. S. Hall, *Curr. Top. Med. Chem.*, 2011, **11**, 2072–2084.
- M. D. Mecca, L. Bartel and J. Castro, *Hum. Exp. Toxicol.*, 2013, **32**, 1305–1310.
- M. N. Soeiro and S. L. de Castro, *Expert Opin. Ther. Targets*, 2009, **13**(1), 105–121.
- (a) L. Piacenza, F. Irigoín, M. N. Alvarez, G. Peluffo, M. C. Taylor, J. M. Kelly, S. R. Wilkinson and R. Radi, *Biochem. J.*, 2007, **403**(2), 323–334; (b) I. A. Abreu and D. E. Cabelli, *Biochim. Biophys. Acta*, 2010, **1804**, 263–274; (c) A. F. Miller, *Curr. Opin. Chem. Biol.*, 2004, **8**, 162–168.
- (a) R. K. Mehlotra, *Crit. Rev. Microbiol.*, 1996, **22**(4), 295–314; (b) J. A. Atwood, D. B. Weatherly, T. A. Minning, B. Bundy, C. Cavola, F. R. Opperdoes, R. Orlando and R. L. Tarleton, *Science*, 2005, **309**, 473–476; (c) M. A. Muñoz-Fernández, M. A. Fernández and M. Fresno, *Immunol. Lett.*, 1992, **33**(1), 35–40; (d) V. M. Costa, K. C. Torres, R. Z. Mendonça, I. Gresser, K. J. Gollob and I. A. Abrahamssohn, *J. Immunol.*, 2006, **177**(5), 3193–3200.
- B. Verdejo, A. Ferrer, S. Blasco, C. E. Castillo, J. González, J. Latorre, M. A. Máñez, M. G. Basallote, C. Soriano and E. García-España, *Inorg. Chem.*, 2007, **46**, 5707–5719.
- V. Amendola, L. Fabbrizzi, C. Mangano and P. Pallavicini, *Acc. Chem. Res.*, 2001, **34**, 488–493.
- (a) C. Marín, M. P. Clares, I. Ramírez-Macías, S. Blasco, F. Olmo, C. Soriano, B. Verdejo, M. J. Rosales, D. Gómez-Herrera, E. García-España and M. Sánchez-Moreno, *Eur. J. Med. Chem.*, 2013, **62**, 466–477; (b) F. Olmo, C. Marín, M. P. Clares, S. Blasco, M. T. Albelda, C. Soriano, R. Gutiérrez-Sánchez, F. Arrebola-Vargas, E. García-España and M. Sánchez-Moreno, *Eur. J. Med. Chem.*, 2013, **70**, 189–198.
- (a) M. Inclán, M. T. Albelda, J. C. Frías, S. Blasco, B. Verdejo, C. Serena, C. Salat-Canela, M. L. Díaz, A. García-España and E. García-España, *J. Am. Chem. Soc.*, 2012, **134**, 9644–9656; (b) J. González, J. M. Llinares, R. Belda, J. Pitarch, C. Soriano, R. Tejero, B. Verdejo and E. García-España, *Org. Biomol. Chem.*, 2010, **8**(10), 2367–2376.

- 18 (a) J. E. Richman and T. J. Atkins, *J. Am. Chem. Soc.*, 1974, **96**, 2268–2270; (b) J. E. Richman, T. J. Atkins and W. F. Oetle, *Organic Synthesis*, J. Wiley & Sons, New York, 1988, vol. 6, p. 652; (c) B. L. Shaw, *J. Am. Chem. Soc.*, 1975, **97**, 3856–3857.
- 19 M. Inclán, M. T. Albelda, E. Carbonell, S. Blasco, A. Bauzá, A. Frontera and E. García-España, *Chem.-Eur. J.*, 2014, **20**, 1–13.
- 20 M. P. Clares, S. Blasco, M. Inclán, L. del Castillo Agudo, B. Verdejo, C. Soriano, A. Doménech, J. Latorre and E. García-España, *Chem. Commun.*, 2011, **47**, 5988–5990.
- 21 S. Nwaka and A. Hudson, *Nat. Rev. Drug Discovery*, 2006, **5**, 941–955.
- 22 C. F. Da Silva, M. M. Batista, D. G. J. Batista, E. M. de Souza, P. B. da Silva, G. M. de Oliveira, A. S. Meuser, A. R. Shareef, D. W. Boykin and M. N. C. Soeiro, *Antimicrob. Agents Chemother.*, 2008, **52**, 3307–3314.
- 23 A. el Bouhdidi, C. Truyens, M. T. Rivera, H. Bazin and Y. Carlier, *Parasite Immunol.*, 1994, **16**(2), 69–76.
- 24 M. A. Bryan, S. E. Guyach and K. A. Norris, *PLoS Neglected Trop. Dis.*, 2010, **4**(7), e733.
- 25 F. Bringaud, L. Riviere and V. Coustou, *Mol. Biochem. Parasitol.*, 2006, **149**, 1–9.
- 26 J. Turrens, *Parasitol. Today*, 1999, **15**, 346–348.
- 27 P. A. M. Michels, F. Bringaud, M. Herman and V. Hannaert, *Biochim. Biophys. Acta*, 2006, **1763**, 1463–1477.
- 28 I. G. Kirkinos and C. T. Moraes, *Semin. Cell Dev. Biol.*, 2001, **12**, 449–457.
- 29 J. F. R. Bacheга, M. V. A. S. Navarro, L. Bleicher, R. K. Bortoleto-Bugs, D. Dive, P. Hoffmann, E. Viscogliosi and R. C. Garratt, *Proteins*, 2009, **77**, 26–37.
- 30 T. Hunter, K. Ikebukuro, W. H. Bannister, J. V. Bannister and G. J. Hunter, *Biochemistry*, 1997, **36**, 4925–4933.
- 31 M. M. Whittaker and J. W. Whittaker, *J. Biol. Chem.*, 1998, **273**, 22188–22193.
- 32 M. Dixon and E. C. Webb, *Enzymes*, Longman Scientific & Technical, Harlow, Essex, England, 1986.
- 33 C. A. Lipinski, F. Lombardo, B. W. Dominy and P. J. Feeney, *Adv. Drug Delivery Rev.*, 2001, **46**, 3–26.
- 34 F. Cheng, W. Li, Y. Zhou, J. Shen, Z. Wu, G. Liu, P. W. Lee and Y. Tang, *J. Chem. Inf. Model.*, 2012, **52**, 3099–3105.
- 35 C. Fernández-Becerra, M. Sánchez-Moreno, A. Osuna and F. R. Opperdoes, *J. Eukaryotic Microbiol.*, 1997, **44**, 523–529.
- 36 I. Ramírez-Macias, C. Marín, R. Chahboun, I. Messouri, F. Olmo, M. J. Rosales, R. Gutierrez-Sánchez, E. Alvarez-Manzaneda and M. Sánchez-Moreno, *Am. J. Trop. Med. Hyg.*, 2012, **87**, 481–488.
- 37 F. X. Sullivan and C. T. Walsh, Cloning, sequencing, overproduction and purification of trypanothione reductase from *Trypanosoma cruzi*, *Mol. Biochem. Parasitol.*, 1991, **44**(1), 145–147.
- 38 M. A. Comini, N. Dirdjaja, M. Kaschel and R. L. Krauth-Siegel, Preparative enzymatic synthesis of trypanothione and trypanothione analogues, *Int. J. Parasitol.*, 2009, **39**, 1059–1062.

7.2. Publications submitted.

Publication	Journal (Impact Factor)	Category Name (Journal Rank in Category)	Quartile in Category
[7]. Olmo F, Urbanová K, Rosales MJ, Martín-Escolano R, Sánchez-Moreno M, Marín C. An in vitro iron superoxide dismutase inhibitor decreases the parasitemia levels of <i>Trypanosoma cruzi</i> in Balb/c mouse model during acute phase. <i>Int J Parasitol Drugs Drug Resist.</i>	International Journal for Parasitology: Drugs and Drug Resistance (2.514)	PARASITOLOGY (12)	Q2
		PHARMACOLOGY & PHARMACY (111)	Q2
[8]. Olmo F, Cussó O, Marín C, Rosales MJ, Urbanová K, Krauth-Siegel RL, Costas M, Ribas X, Sánchez-Moreno M. In vitro and in vivo identification of tetradentated polyamine complexes as highly efficient metallodrugs against <i>Trypanosoma cruzi</i> . <i>Acta Trop.</i> 2015	Acta Tropica (2.519)	PARASITOLOGY (11)	Q2
		TROPICAL MEDICINE (4)	Q1
[9]. Olmo F, Costas M, Marín C, Rosales MJ, Martín-Escolano R, Cussó O, Ribas X, Sánchez-Moreno M. Tetradentate polyamines as highly efficient metallodrugs for Chagas disease treatment in murine model. <i>Trans R Soc Trop Med Hyg.</i> 2015	Transactions of the Royal Society of Tropical Medicine & Hygiene (1.931)	PUBLIC ENVIRONMENTAL & OCCUPATIONAL HEALTH (64)	Q2
		TROPICAL MEDICINE (6)	Q2

Elsevier Editorial System(tm) for International Journal for Parasitology: Drugs and Drug
Resistance
Manuscript Draft

Manuscript Number:

Title: An in vitro iron superoxide dismutase inhibitor decreases the parasitemia levels of *Trypanosoma cruzi* in Balb/c mouse model during acute phase

Article Type: Full Length Article

Section/Category: unicell

Keywords: anti-chagasic, chemotherapy, Trypanosomiasis, hydroxyphthalazine derivatives.

Corresponding Author: Dr. Manuel Sanchez-Moreno,

Corresponding Author's Institution: FACULTAD DE CIENCIAS

First Author: Francisco Olmo

Order of Authors: Francisco Olmo; Kristína Urbanová; Maria J Rosales; Rubén Martín-Escolano;
Manuel Sanchez-Moreno; Clotilde Marín

Manuscript Region of Origin: SPAIN

Abstract: In order to identify new compounds to treat Chagas disease during the acute phase with higher activity and lower toxicity than the reference drug benznidazole (Bz), two hydroxyphthalazine derivatives compounds were prepared and their trypanocidal effects against *Trypanosoma cruzi* were evaluated by light microscopy through the determination of IC₅₀ values. Cytotoxicity was determined by flow cytometry assays against Vero cells. In vivo assays were performed in BALB/c mice, in which the parasitemia levels were quantified by fresh blood examination; the assignment of a cure was determined by reactivation of blood parasitemia levels after immunosuppression. The mechanism of action was elucidated at metabolic and ultra-structural levels, by ¹H NMR and TEM studies. Finally, as these compounds are potentially capable of causing oxidative damage in the parasites, the study was completed, by assessing their activity as potential iron superoxide dismutase (Fe-SOD) inhibitors. High-selectivity indexes observed in vitro were the basis of promoting one of the tested compounds to in vivo assays. The tests on the murine model for the acute phase of Chagas disease showed better parasitemia inhibition values than those found for Bz. Compound 2 induced a remarkable decrease in the reactivation of parasitemia after immunosuppression. Compound 2 turned out to be a great inhibitor of Fe-SOD. The high antiparasitic activity and low toxicity together with the modest costs for the starting materials render this compound an appropriate molecule for the development of an affordable anti-Chagas agent.

Suggested Reviewers: Fred Opperdoes
University of Louvain
opperdoes@bchm.ucl.ac.be

Carla Maia
Universidade Nova de Lisboa
carlamaia@ihmt.unl.pt



DEPARTAMENTO DE PARASITOLOGÍA
GRUPO CTS944 _ PARASITOLOGÍA MOLECULAR
FACULTAD DE CIENCIAS

Granada, 19/01/15

Dr. Manuel Sánchez Moreno
e-mail: msanchem@ugr.es

To: The Editor
International Journal for Parasitology: Drugs and Drug Resistance

Dear Editor,

Please find enclosed our manuscript entitled “**An in vitro iron superoxide dismutase inhibitor decreases the parasitemia levels of *Trypanosoma cruzi* in Balb/c mouse model during acute phase**” by Olmo et al. to be considered for publication in International Journal for Parasitology: Drugs and Drug Resistance.

In this work is evaluated the trypanocidal effect of two hydroxyphthalazine derivatives compounds against *Trypanosoma cruzi*. The high efficiency of these compounds against *T. cruzi* was shown through *in vitro* assays (improved efficiency and lower toxicity than the reference drug) and further confirmed by an additional *in vivo* study in a murine model that goes from the acute to the chronic phase of Chagas disease. The study includes a deep analysis to figure out the possible mechanism of action, attending to the inhibition of Superoxide dismutase, complemented with the study of the changes in the metabolites excreted by the parasite and disturbances caused by our compounds at ultrastructural level. Compound 2 induced a decrease in the reactivation of parasitemia after immunosuppression. Also, this compound turned out to be a great inhibitor of Fe-SOD. The high antiparasitic activity and low toxicity together with the modest costs for the starting materials render this compound an appropriate molecule for the development of an affordable anti-Chagas agent.

As it is mentioned in the article, the drugs currently used to treat Chagas disease are decades old and have many limitations including high toxicity, therefore the search for new drugs is urgently needed. We think that our contribution is interesting and

rather complete, including the deep approach *in vitro* and *in vivo* and also the mechanism of action of these pre-drugs, for hence this manuscript could be a quite interesting topic for the journal readers. For all the reasons explained before we believe that it merits publication in International Journal for Parasitology: Drugs and Drug Resistance.

Thank you very much for taking into account this manuscript.

Yours sincerely,

M. Sánchez-Moreno

CONFLICTS OF INTEREST

We wish to confirm that there are no known conflicts of interest associated with this publication and there has been no significant financial support for this work that could have influenced its outcome.

We confirm that the manuscript has been read and approved by all named authors and that there are no other persons who satisfied the criteria for authorship but are not listed. We further confirm that the order of authors listed in the manuscript has been approved by all of us.

We confirm that we have given due consideration to the protection of intellectual property associated with this work and that there are no impediments to publication, including the timing of publication, with respect to intellectual property. In so doing we confirm that we have followed the regulations of our institutions concerning intellectual property.

We further confirm that any aspect of the work covered in this manuscript that has involved either experimental animals has been conducted with the ethical approval of all relevant bodies and that such approvals are acknowledged within the manuscript.

We understand that the Corresponding Author is the sole contact for the Editorial process (including Editorial Manager and direct communications with the office). He is responsible for communicating with the other authors about progress, submissions of revisions and final approval of proofs. We confirm that we have provided a current, correct email address which is accessible by the Corresponding Author and which has been configured to accept email from (msanchem@ugr.es)

Signed by all authors as follows:

The image shows five distinct handwritten signatures in blue ink, arranged in two rows. The top row contains three signatures, and the bottom row contains two. The signatures are stylized and difficult to read, but they appear to be the names of the authors who signed the document.

1 An *in vitro* iron superoxide dismutase inhibitor decreases
2 the parasitemia levels of *Trypanosoma cruzi* in Balb/c
3 mouse model during acute phase

4

5

6 Francisco Olmo, Kristína Urbanová, Maria Jose Rosales, Ruben Martín-Escolano,
7 Manuel Sánchez-Moreno* and Clotilde Marín.

8

9

10

11 Departamento de Parasitología, Instituto de Investigación Biosanitaria
12 (ibs.GRANADA). Hospitales Universitarios De Granada/Universidad de Granada,
13 Granada, Spain.

14 *Corresponding author: phone, +34-958-242-369; fax, +34-958-243-862; e-mail,
15 msanchem@ugr.es

16

17

18

19 **Abstract**

20 In order to identify new compounds to treat Chagas disease during the acute phase with
21 higher activity and lower toxicity than the reference drug benznidazole (Bz), two
22 hydroxyphthalazine derivatives compounds were prepared and their trypanocidal effects
23 against *Trypanosoma cruzi* were evaluated by light microscopy through the
24 determination of IC₅₀ values. Cytotoxicity was determined by flow cytometry assays
25 against Vero cells. *In vivo* assays were performed in BALB/c mice, in which the
26 parasitemia levels were quantified by fresh blood examination; the assignment of a cure
27 was determined by reactivation of blood parasitemia levels after immunosuppression.
28 The mechanism of action was elucidated at metabolic and ultra-structural levels, by ¹H
29 NMR and TEM studies. Finally, as these compounds are potentially capable of causing
30 oxidative damage in the parasites, the study was completed, by assessing their activity
31 as potential iron superoxide dismutase (Fe-SOD) inhibitors. High-selectivity indexes
32 observed *in vitro* were the basis of promoting one of the tested compounds to *in vivo*
33 assays. The tests on the murine model for the acute phase of Chagas disease showed
34 better parasitemia inhibition values than those found for Bz. Compound **2** induced a
35 remarkable decrease in the reactivation of parasitemia after immunosuppression.
36 Compound **2** turned out to be a great inhibitor of Fe-SOD. The high antiparasitic
37 activity and low toxicity together with the modest costs for the starting materials render
38 this compound an appropriate molecule for the development of an affordable anti-
39 Chagas agent.

40 **Keywords:** anti-chagasic, chemotherapy, Trypanosomiasis, hydroxyphthalazine
41 derivatives.

42

43 1. Introduction

44 American trypanosomiasis is a potentially life-threatening parasitic disease caused by
45 *Trypanosoma cruzi*. There are more than 10-20 million people infected worldwide,
46 mostly in Latin America. Although not a uniform death sentence, *T. cruzi* infection is
47 far from innocuous, as an estimated 30-40% of infected individuals develop debilitating
48 and chronic disease, and this infection accounts for 20,000–50,000 deaths per year
49 (Tarleton et al., 2012). Currently, the available drugs used for the treatment of this
50 infection, Benznidazole (Bz) or nifurtimox, show limited therapeutic potential and are
51 associated with serious side effects, such as skin rashes, leucopenia, neurotoxicity,
52 fever, articular and muscular pain, peripheral neuropathy, lymphadenopathy,
53 agranulocytosis, and thrombocytopenic purpura (Wilkinson et al., 2008; Urbina, 2010).
54 Thus, there is an urgent need for the development of new anti-trypanosomal agents with
55 lower toxicity and greater activity, especially for the chronic phase of the disease. To
56 date, no vaccine has been developed against *T. cruzi* (Dumonteil, 2009). Therefore, the
57 search for new targets for chemotherapy and vaccines is a major challenge. Among the
58 targets, the parasite antioxidant system has attracted attention due to its uniqueness in
59 the trypanosomatids.

60 Taking into account this need for new drugs to combat *T. cruzi* parasites, we considered
61 studying the activity of two hydroxyphthalazine derivatives against the causing agent of
62 Chagas disease to be of great interest. These compounds are quite interesting, since their
63 synthesis starts from cheap substrates and the procedures are not very complicated in
64 most of the cases. In this work, their anti-proliferative activity and unspecific
65 mammalian cytotoxicity in the species considered were evaluated *in vitro*, and these
66 measures were complemented by infectivity assays on Vero cells. Furthermore, those in
67 whom *in vitro* activity showed remarkable effects were tested *in vivo*. Finally, the

68 parasites were submitted to a thorough study of the possible mechanisms of action of
69 the compounds assayed, as follows: (i) an ¹H-NMR study concerning the nature and
70 percentage of metabolite excretion was performed in order to obtain information on the
71 inhibitory effect of the compounds on the glycolytic pathway, since it represents the
72 primary source of energy for the parasite, (ii) alterations caused in the cell ultrastructure
73 of the parasites were recorded using transmission electronic microscopy (TEM), and
74 (iii) an enzymatic study of inhibition over the iron superoxide dismutase (Fe-SOD),
75 which represent one of the many mechanisms of antioxidant defence in trypanosomatids.

76 **2. Materials and methods**

77 ***2.1. Chemistry***

78 Samples of the tested hydroxyphthalazine derivatives **1** and **2** have been donated
79 by the Heterocyclic Synthetic Receptors research group of the Organic Chemistry
80 Department at the Universidad Complutense of Madrid ([Sánchez-Moreno et al., 2012](#),
81 [Figure 1](#)). They are part of a series of compounds that are being currently designed by
82 that group, and their synthesis, characterization and further antiparasitic properties will
83 be described elsewhere.

84 ***2.2. Parasite Strain Culture.***

85 Trypanosoma cruzi SN3 strain of IRHOD/CO/2008/SN3 was isolated from domestic
86 Rhodnius prolixus; biological origin is Guajira (Colombia) ([Téllez-Meneses et al.,](#)
87 [2008](#)). Epimastigote forms were grown in axenic Grace's insect medium (Gibco)
88 supplemented with 10% inactivated fetal bovine serum (FBS) at 28°C in tissue-culture
89 flasks, Roux flasks (Corning, USA) with a surface area of 75 cm², as described by
90 ([Gonzalez et al., 2005](#)).

91 ***2.3. Transformation of epimastigotes to metacyclic forms.***

92 Metacyclogenesis was induced by culturing a 5-day-old culture of epimastigote forms
93 of *T. cruzi* that was harvested by centrifugation at 7 000 g for 10 min at 10 °C according
94 to (Cardoso et al., 2010).

95 **2.4. Cell Culture and Cytotoxicity Tests.**

96 Vero cells (Flow) were grown in RPMI and MEM (Gibco), supplemented with 10%
97 iFBS and the procedure followed was as in (Magán et al., 2005).

98 **2.5. In Vitro Activity Assays, Extracellular Forms:**

99 **2.5.1. Epimastigotes assay.**

100 *T. cruzi* epimastigotes were collected in the exponential growth phase and distributed in
101 culture trays (with 24 wells) at a final concentration of 5×10^4 parasites/well. The
102 effects on the parasite growth were tested according to (Olmo et al., 2013).

103 **2.5.2. Blood Trypomastigote Forms Assay.**

104 Compounds 1 and 2 were also evaluated in blood trypomastigotes of *T. cruzi*. BALB/c
105 female mice infected with *T. cruzi* were used 7 days after infection. Blood was obtained
106 by cardiac puncture using 3.8% sodium citrate as an anticoagulant in a 7:3
107 blood:anticoagulant ratio. The parasitaemia in the infected mice was about 1×10^5
108 parasites/mL. The compounds were diluted in phosphate-buffered saline solution (PBS)
109 to give a final concentration 10, 25, and 50 μ M for each product. Aliquots (20 μ L) of
110 each solution were mixed in culture trays (96 wells) with 55 μ L of infected blood
111 containing the parasites at a concentration of approximately 1×10^6 parasites/mL.
112 Infected blood with PBS, at the same concentrations as the products, was used as
113 control. The plates were shaken for 10 min at room temperature and kept at 4°C for 24 h.
114 Each solution was examined microscopically (Olympus CX41) for parasite counting

115 using the Neubauer haemocytometric chamber (a dilution of 1:100 in PBS was
116 necessary to get into the range of counting). The activity (percent of parasites reduction)
117 was compared with that of the control.

118 ***2.6. In Vitro Activity Assays, Intracellular forms: Amastigotes Assay.***

119 Vero cells were cultured in RPMI medium supplemented with 10% iFBS, in a
120 humidified 95% air and 5% CO₂ atmosphere at 37 °C. Then the cells were infected and
121 treated as in ([Gonzalez et al., 2005](#)).

122 ***2.7. Infectivity Assay.***

123 Vero cells were cultured in RPMI medium supplemented with 10% iFBS as described
124 above. Afterward, the cells were infected in vitro with metacyclic trypomastigote forms
125 of *T. cruzi* at a ratio of 10:1. The assay was performed as in ([Gonzalez et al., 2005](#)).

126 ***2.8. In Vivo Trypanosomicidal Activity Assay:***

127 ***2.8.1. Mice infection and treatment***

128 This experiment was performed with the approval of the Ethical Committee of the
129 University of Granada, Spain. Two groups of six BALB/c albino female mice (6–8
130 weeks old, 25–30 g weight) were maintained with water and standard chow *ad libitum*,
131 under a 12-h dark/light cycle and 22 ± 3°C temperature. Each mouse was inoculated by
132 intraperitoneal route with 5 x 10⁵ blood trypomastigotes of *T. cruzi* obtained from
133 previously infected mice blood. Group I was positive control group (mice infected but
134 not treated) and group II was study group (mice infected and treated with the
135 compounds under study). On seventh day of infestation was begun the administration of
136 the selected compounds at doses of 25 mg/kg body mass per day for 5 consecutive days
137 (7–12 days post-infection). Parasitemia levels were evaluated from peripheral blood

138 obtained from the mandibular vein of each mouse (5 μ L samples) and dissolved in 495
139 μ L of a PBS solution at a dilution of 1:100. The circulating parasite numbers were
140 quantified with a Neubauer's chamber for counting blood cells and the number of
141 bloodstream forms was expressed as parasites/mL. This counting was performed every
142 3 days during a 40 day period (acute phase) (Olmo et al., 2014).

143 2.8.2. *Cyclophosphamide-induced immune suppression and assessment of* 144 *cure*

145 After day 60, parasitaemia showed progressively decreasing levels and it is established
146 that the animals entered the chronic phase of the experiment. Therefore, on day 120,
147 parasitaemia was shown to be undetectable by fresh blood microscopic examination,
148 and the mice received 4 intraperitoneal injections of 200 mg/kg of body mass of
149 cyclophosphamide monohydrate (CP) (ISOPAC®) on alternate days, as previously
150 described (Cencig et al., 2011). Seven days after of the last CP injection, parasitaemia
151 was evaluated according to the procedure described for acute phase to quantify the
152 presence of blood trypomastigote forms as reactivation rate. Finally, mice were bled out,
153 under gaseous anaesthesia (CO₂), via heart puncture and blood was collected. To obtain
154 the serum, blood was incubated for 2 hours/37°C and then overnight/4°C, followed by
155 centrifuging the supernatant twice at 1000 and 2700 g, consecutively. The serum was
156 aliquoted and used for ELISA and biochemical analysis, as explained below. Hearts
157 were harvested and immediately flushed free of blood by gentle infusion of 10 ml of
158 pre-warmed PBS through the left ventricle (Ye et al., 2008) in order to avoid
159 contamination of the collected tissue with blood parasites. After this, samples were
160 frozen at -80°C and stored until used for DNA extraction (Olmo et al., 2014).

161 2.8.3. *ELISA tests*

162 Fe-SOD excreted from the parasite, cultured and processed as described in (Lopez-
163 Cespedes et al., 2012), was used as the antigen fraction. The ELISA test to measure the
164 antibodies against *T. cruzi* used was performed as in (Olmo et al., 2014).

165 2.8.4. *Toxicity tests by clinical chemistry measurements.*

166 A fraction of the serum obtained as it was shown above was send to the Biochemical
167 service in the University of Granada where a series of parameters were measured
168 according to their commercial kits acquired from Cromakit® by BS-200 Chemistry
169 Analyzer Shenzhen Mindray (Bio-medical Electronics Co., LTD). With the levels
170 obtained for different populations of sera (n = 15, n = 6) we calculated the mean value
171 and standard deviation. Finally, we also calculated the confidence interval for the mean
172 normal populations based on a confidence level of 95% ($100 \times (1-\alpha) = 100 \times (1-.05)\%$).
173 The ranges obtained are shown in Table 2, which allows comparison and analysis of the
174 sera studied in this work.

175 2.9. Assays to figure out the mechanism of action:

176 2.9.1. *Metabolite Excretion*

177 Cultures of *T. cruzi* epimastigote forms (initial concentration of 5×10^5 cells/mL)
178 received IC₂₅ of the compounds (except for the control cultures). After incubation for 96
179 h at 28°C, the cells were centrifuged at 400 g for 10 min. The supernatants were
180 collected in order to determine the excreted metabolites through ¹H NMR, and the
181 chemical shifts were expressed in parts per million (ppm), using dimethyl sulphoxide
182 (DMSO) as the reference signal. One-dimensional ¹H NMR spectra were acquired on
183 VARIAN DIRECT DRIVE 400 MHz Bruker spectrometer with AutoX probe using
184 D₂O. The assignments of metabolites were based on 1D NMR spectrum. The chemical
185 shifts used to identify the respective metabolites were consistent with those described

186 previously by our group ([Fernandez-Becerra et al., 1997](#)). In addition, the human
187 metabolome database (<http://www.hmdb.ca/>) was also used for this purpose. The
188 spectral region of 1.0 to 5.5 ppm was bucketed into a frequency window of 0.1 ppm.
189 The region corresponding to water (4.5 to 5.5 ppm) was excluded during binning to
190 avoid artefacts due to pre-saturation of water, and the region corresponding to glucose
191 (3.4 to 3.8 ppm) was also excluded. The aromatic region was excluded because the
192 signal to noise ratio in this region was poorer compared to that of the aliphatic region.
193 The peak (2.6 ppm) corresponding to DMSO was removed before binning. The
194 resulting integrals were normalised to the working region (1.0 to 3.4) ppm of the
195 spectrum to correct for inter-sample differences in dilution. The binning and
196 normalisations were achieved using Mestrenova 9.0 software. The matrix obtained in
197 Mestrenova was imported to Microsoft Excel for further data analyses.

198 2.9.2. *Ultrastructural alterations*

199 The parasites were cultured at a density of 5×10^5 cells/mL in each corresponding
200 medium containing the compounds tested at the concentration of IC_{25} . After 96 h, these
201 cultures were centrifuged at 400 g for 10 min and the pellets produced were washed in
202 PBS before being mixed with 2% (v/v) paraformaldehyde/glutaraldehyde in 0.05 M
203 cacodylate buffer (pH 7.4) for 24 h at 4°C. Following this, the pellets were prepared for
204 transmission electron microscopy study using a technique described by our group
205 ([Gonzalez et al., 2005](#)).

206 2.9.3. *Superoxide dismutase inhibition assay*

207 The parasites cultured as described above were centrifuged. The pellet was suspended in
208 3 mL of STE buffer (0.25 M sucrose, 25 mM Tris-HCl, 1 M EDTA, pH 7.8) and
209 disrupted by three cycles of sonic disintegration, 30 s each at 60 W. The sonicated

210 homogenate was centrifuged at 1500 g for 5 min at 4°C, and the pellet was washed three
211 times in ice-cold STE buffer. This fraction was centrifuged (2500 g for 10 min at 4°C)
212 and the supernatant was collected. The protein concentrations were determined using the
213 Bradford method (Bradford, 1972). Iron and copper–zinc superoxide dismutases (Fe-
214 SOD and CuZn-SOD) activities were determined using the method described by Beyer
215 and Fridovich (Beyer et al., 1987).

216 3. Results and Discussion

217 3.1. *In Vitro Trypanosomicidal Evaluation*

218 In order to get preliminary information, *in vitro* activities of **1** and **2** were evaluated
219 against epimastigote, amastigote and trypomastigote forms of *T. cruzi*, as shown in
220 Table 1. It was found that the more sensitive forms to all different compounds tested
221 were the intracellular forms (amastigotas) reaching an effectiveness of 48 times higher
222 than the reference drug in the case of **2**. The compound **1** also showed trypanosomicidal
223 activity against the different forms of the parasite and the effect was always better than
224 that of the reference drug; however, against all forms it showed less than 15 times
225 effectiveness compared with Bz. As a result, compound **2** was chosen to undergo an
226 extra *in vitro* assay and deeper insight of the activity of this compound was found in the
227 infectivity assay, where the process that takes place in the host of the lifecycle of *T.*
228 *cruzi* in the presence of the drugs was reproduced *in vitro*. Once again, **2** was found to
229 be the more active than the reference drug, decreasing the rate of infection in cells by
230 80% on the last day of the experiment, as shown in Figure 2A. It also decreased the
231 average number of amastigote forms found per infected cell; these decreases reached
232 the 57% for cells treated with **2** being more efficient than Bz, which effectively only
233 decreased the number by 15% compared to the control (Figure 2B). The last data
234 obtained from this assay were regarding the number of trypomastigote forms released

235 by the infected cells, as can be seen in [Figure 2C](#), where the effect showed a significant
236 decrease of 43% compared to the control assay.

237 3.2. *In Vivo Trypanosomicidal Evaluation*

238 Since compound **2** showed remarkable SI values with respect to Bz in the *in vitro*
239 experiments, it was selected for being close to the criteria established by [Nwaka et al.,](#)
240 [2011](#) for further *in vivo* studies in the chosen murine model. Its trypanozidal activity
241 during the acute phase of Chagas disease [until 40 days post-infection (pi)] was first
242 investigated. None of the animals treated with either the control or compound **2** died
243 during the treatment. As shown in [Figure 3](#), the reduction of parasitaemia in mice
244 treated with the compound was evident from the very beginning of the treatment and
245 was maintained until the end, resulting in parasitaemia reduction with respect to the
246 control experiment for **Bz** and **2**.

247 The next step was to evaluate the behaviour of the compound until the chronic phase.
248 Therefore, the mice treated as described above were taken up to day 120 pi (advanced
249 chronic phase), in order to evaluate the immune status and the disease extent of the mice
250 at that stage; blood samples were extracted for determining parasitaemia and
251 immunoglobulin G (Ig-G) levels in comparison with the corresponding non-
252 immunosuppressed (control) subgroup of mice ([Figure 4](#)). Concerning the parasitaemia
253 reactivation, [Figure 4A](#) shows a very illustrative three-dimensional graph indicating the
254 percentage of parasitaemia reactivation for **2** in comparison with the control mice; lower
255 percentages were obtained in the treated case with 54.1% of reactivation, whereas a
256 reactivation of 80.3% was found in the control mice.

257 The enzyme-linked immunosorbent assay (ELISA) was used for the detection of total
258 Ig-G levels and the antigen source was the Fe-SOD enzyme isolated in our laboratory.

259 The detection of total Ig G allowed evaluation of the immune status of the mice (el
260 Bouhdidi et al., 1994), since that indicates the level of protection that should be
261 attributed to the tested compounds, combined with the innate protection that mice have
262 naturally (Kayama et al., 2010). Results obtained from the ELISA experiments were
263 confirmed by the parasitaemia assay performed as indicated above. In accordance with
264 the ELISA test, the group of mice treated with compound **2** almost maintained levels of
265 total Ig G (Figure 4B), as did chronic infected mice, lower than that of the control group
266 after being immunosuppressed, while the control group levels were increased as a
267 consequence of the reactivation of parasitaemia.

268 Clinical chemistry measurements are provided in Table 2. Changes in the transaminases
269 and the total bilirubin were observed for the group of mice treated with **2** were the only
270 differences found when compared to the control group, but these changes were
271 insignificant since they only reached the 10%. This confirms the evidence that the
272 compounds tested are not toxic in the murine model; in fact, this lack of toxicity added
273 to the better efficacy of **2**, leading us consider this compound as a promising candidate
274 for the treatment of Chagas disease. Therefore, the compound should be followed-up in
275 future clinical experiments.

276 3.3. *Possible Mechanism of Action*

277 Trypanosomatids are unable to completely degrade glucose to CO₂, so they excrete part
278 of the hexose skeleton into the medium as partially oxidised fragments, the nature and
279 percentage of which depend on the pathway used for glucose metabolism (Ginger,
280 2005). The catabolism products in *T. cruzi* are mainly succinate, acetate, D-lactate and
281 L-alanine (Cazzulo, 1992). In order to obtain some information about the effects of **2** on
282 the glucose metabolism of the parasite, we registered the ¹H NMR spectra of *T. cruzi*
283 epimastigotes treated with the test compounds (spectra not shown); the final excretion

284 products were identified qualitatively and quantitatively, and the results obtained were
285 compared with those found for untreated control epimastigotes. [Figure 5](#) shows the
286 differences found in every case with respect to the control.

287 Excretion of almost all metabolites was disturbed in the treatment with **2**, with
288 succinate being the most affected, showing an increase of 90%, followed by acetate and
289 D-lactate with decreases of 31% and increases of 12%, respectively. All of these data
290 could be interpreted on the basis of a change in the succinate, D-lactate, pathways
291 occurring in the presence of the compound under investigation. It is well known that D-
292 lactate and L-alanine originate from the transformation of PEP in pyruvate in the
293 presence of pyruvate kinase or pyruvate phosphate dikinase ([Bringaud et al., 2006](#)). On
294 the other hand, it is interesting to note that the increase in succinate indicate catabolic
295 changes that could be related to a malfunction of the mitochondria, due to the redox
296 stress produced by inhibition of the mitochondrion-resident Fe-SOD enzyme
297 ([Kirkinetzos et al., 2001](#)), which should result in decreased pyruvate metabolism and a
298 consequent decrease of the succinate produced in mitochondria. Overall, these data
299 should confirm that the modifications generated in organelles like glycosomes or
300 mitochondria by the compounds assayed are the ultimate reason for the alterations
301 observed in the excreted products of *T. cruzi*.

302 Modifications at the ultrastructural level caused after incubation of epimastigote forms
303 of *Trypanosoma cruzi* with the compound under study in the current work, **2**, have been
304 studied. This compound induced strong disturbances in the parasites' morphology and
305 consequently death in some cases. At this level, **2** was found to be the more effective
306 compound, causing more mortality in the parasite cultures compared to the control when
307 the IC₂₅ was administered. The parasites were clearly morphologically disturbed when
308 compared with the untreated assay, as shown in [Figure 6.A](#). Among the more common

309 disturbances when **2** was added to the medium, as shown in [Figure 6.B](#), include the
310 finding that mitochondria were swollen, without cristae and almost unrecognisable; the
311 cytoplasm was also full of small vacuoles, there was a lack of ribosomes and low
312 electron density was appreciated.

313 These results prompted us to evaluate the inhibitory effect of compound **2** on SOD
314 activity to test their potential as enzyme inhibitors. The results obtained are shown in
315 [Figure 7](#), with the corresponding IC₅₀ values that were calculated. Significant inhibitory
316 values of Fe-SOD activity were found for the tested compound. Compound **2** showed
317 values close to 100% inhibition at 100 µM, with IC₅₀ values around 27 µM. The design
318 of an effective drug that is able to inhibit parasite Fe-SOD without inhibiting human
319 Cu/Zn-SOD is an interesting goal. Therefore, we also assayed the effect of the
320 compound **2** on Cu/Zn-SOD in human erythrocytes. The results obtained showed that the
321 inhibition percentages for human Cu/Zn-SOD were lower than for Fe-SOD. Therefore,
322 162 µM of the studied compound was needed to give a 50% of inhibition.

323 In conclusion, the trypanocidal properties of compounds **1** and **2** have been examined
324 both *in vivo* and *in vitro*. The two compounds of the present study were chemical
325 modifications of the most efficient compounds previously tested by our group ([Sanchez-
326 Moreno et al., 2012](#)). As in the field of medicinal chemistry, any modifications within
327 the structure of the compounds makes that it had to restart the assays from the very first
328 phase. The purpose of this change was the inclusion of a hydroxy group in one of the
329 rings of the phthalazine, this group besides being a new structure with higher polar
330 properties allows for future chemical conjugation to add new groups and radicals.
331 Although the compounds did not improved the tripanozidal activity *in vitro*, it was found
332 that *in vivo* the toxicity was greatly reduced and therefore permit the administration of
333 higher doses. Also, once again revealed that these chemical structures highly inhibit the

334 parasite enzyme Fe-SOD, as it was anticipated in molecular modeling studies previously
335 performed, (Sanchez-Moreno et al., 2012) confirming once again to be the target for
336 these compounds.

337 The experiments allowed us to select compound 2, that displayed improved efficiency
338 and lower toxicity than the reference drug. Parallel studies have been carried to establish
339 the mechanisms of action. Compound 2 selectively inhibits the Fe-SOD enzyme of the
340 parasite. Moreover, compound 2 showed an *in vivo* failure of reactivation in parasitaemia
341 after immunosuppression at a dosage of 125 mg/kg body mass. Finally, owing to their
342 promising activity, a further high-level study should be considered to obtain an improved
343 efficiency.

344 4. Acknowledgments

345 We acknowledge financial support from the Spanish Ministry of Economy and
346 Competitiveness (MINECO), CONSOLIDER-INGENIO 2010 CSD2010-00065. F.O. is
347 grateful for a FPU Grant (AP2010-3562) from the Ministry of Education of Spain.

348 REFERENCES:

349 Beyer, W.F., Fridovich, I., 1987. Assaying for superoxide dismutase activity: some
350 large consequences of minor changes in conditions. *Anal. Biochem.* 161: 559–566.

351 Bradford, M.M., 1972. A refined and sensitive method for the quantification of
352 microgram quantities of protein utilizing the principle of protein-dye binding. *Anal.*
353 *Biochem.* 72: 248–254.

354 Bringaud, F., Riviere, L., Coustou, V., 2006. Energy metabolism of Trypanosomatids:
355 adaptation to available carbon sources. *Mol. Biochem. Parasitol.* 149: 1-9.

356 Cardoso, J., Soares, M.J., 2010. In vitro effects of citral on *Trypanosoma cruzi*
357 metacyclogenesis. Mem. Inst. Oswaldo Cruz. 5: 1026-1032.

358 Cazzulo, J.J., 1992. Aerobic fermentation of glucose by trypanosomatids. FASEB J. 6:
359 3153-3161.

360 Cencig, S., Coltel, N., Truyens, C., Carlier, Y., 2011. Parasitic loads in tissues of mice
361 infected with *Trypanosoma cruzi* and treated with AmBisome. PLoS Negl. Trop. Dis. 5:
362 e1216.

363 Dumonteil, E., 2009. Vaccine development against *Trypanosoma cruzi* and *Leishmania*
364 *species* in the post-genomic era. Infect. Genet. Evol. 9: 1075-1082.

365 el Bouhdidi, A., Truyens, C., Rivera, M.T., Bazin, H., Carlier, Y., 1994. *Trypanosoma*
366 *cruzi* infection in mice induces a polyisotypic hypergammaglobulinaemia and parasite-
367 specific response involving high IgG2a concentrations and highly avid IgG1 antibodies.
368 Parasite Immunol. 16: 69-76.

369 Fernandez-Becerra, C., Sánchez-Moreno, M., Osuna, A., Opperdoes F.R. 1997.
370 Comparative aspects of energy metabolism in plant trypanosomatids. J. Eukaryot.
371 Microbiol. 44: 523-529.

372 Ginger, M.L., 2005. Trypanosomatid biology and euglenozoan evolution: new insights
373 and shifting paradigms revealed through genome sequencing. Protist. 156: 377-392.

374 González, P., Marín, C., Rodríguez-González, I., Hitos, A.B., Rosales, M.J., Reina, M.,
375 Díaz, J.G., González-Coloma, A., Sánchez-Moreno, M., 2005. In vitro activity of C20-
376 diterpenoid alkaloid derivatives in promastigotes and intracellular amastigotes of
377 *Leishmania infantum*. Int. J. Antimicrob. Agents. 25: 136-141.

378 Kayama, H., Takeda, K., 2010. The innate immuneresponse to *Trypanosoma cruzi*
379 infection. *Microbes Infect.* 12: 511- 517.

380 Kirkinezos, I.G., Moraes, C.T., 2001. Reactive oxygen species and mitochondrial
381 diseases. *Cell Dev. Biol.* 12: 449-457.

382 Lopez-Cespedes, A., Villagran, E., Briceño-Alvarez, K., de Diego, J.A., Hernández-
383 Montiel, H.L., Saldaña, C., Sánchez-Moreno, M., Marín, C., 2012. *Trypanosoma cruzi*:
384 seroprevalence detection in suburban population of Santiago de Queretaro (Mexico). *Sci.*
385 *World J.* doi: 10.1100/2012/914129.

386 Magán, R., Marín, C., Rosales, M.J., Salas, J.M., Sánchez-Moreno, M., 2005.
387 Therapeutic potential of new Pt(II) and Ru(III) triazole-pyrimidine complexes against
388 *Leishmania donovani*. *Pharmacology.* 73: 41-8.

389 Nwaka, S., Besson, D., Ramirez, B., Maes, L., Matheeussen, A., Bickle, Q., Mansour,
390 N.R., Yousif, F., Townson, S., Gokool, S., Cho-Ngwa, F., Samje, M., Misra-
391 Bhattacharya, S., Murthy, P.K., Fakorede, F., Paris, J.M., Yeates, C., Ridley, R., Van
392 Voorhis, W.C., Geary, T., 2011. Integrated dataset of screening hits against multiple
393 neglected disease pathogens. *PLoS Negl. Trop. Dis.* 5: e1412.

394 Olmo, F., Marín, C., Clares, M.P., Blasco, S., Albelda, M.T., Soriano, C., Gutiérrez-
395 Sánchez, R., Arrebola-Vargas, F., García-España, E., Sánchez-Moreno, M., 2013.
396 Scorpiand-like azamacrocycles prevent the chronic establishment of *Trypanosoma cruzi*
397 in a murine model. *Eur. J. Med. Chem.* 70: 189-198.

398 Olmo, F., Rotger, C., Ramírez-Macías, I., Martínez, L., Marín, C., Carreras, L.,
399 Urbanová, K., Vega, M., Chaves-Lemaur, G., Sampedro, A., Rosales, M.J., Sánchez-
400 Moreno, M., Costa, A., 2014. Synthesis and Biological Evaluation of N,N'-Squaramides

401 with High in Vivo Efficacy and Low Toxicity: Toward a Low-Cost Drug against
402 Chagas Disease. *J. Med. Chem.* 57: 987-999.

403 Sánchez-Moreno, M., Gómez-Contreras, F., Navarro, P., Marín, C., Olmo, F., Yunta,
404 M.J., Sanz, A.M., Rosales, M.J., Cano, C., Campayo L., 2012. Phthalazine derivatives
405 containing imidazole rings behave as Fe-SOD inhibitors and show remarkable anti-*T.*
406 *cruzi* activity in immunodeficient-mouse mode of infection. *J. Med. Chem.* 26: 9900-
407 9913.

408 Tarleton, R.L., Curran, J.W., 2012. Is Chagas disease really the "new HIV/AIDS of the
409 Americas"? *PLoS Negl. Trop. Dis.* 6: e1861.

410 Téllez-Meneses, J., Mejía-Jaramillo, A.M., Triana-Chávez, O., 2008. Biological
411 characterization of *Trypanosoma cruzi* stocks from domestic and sylvatic vectors in
412 Sierra Nevada of Santa Marta, Colombia. *Acta Trop.* 108: 26–34.

413 Urbina, J.A., 2010. Specific chemotherapy of Chagas disease: relevance, current
414 limitations and new approaches. *Acta Trop.* 115: 55–68.

415 Wilkinson, S.R., Taylor, M.C., Horn, D., Kelly, J.M., Cheeseman, I., 2008. A
416 mechanism for cross-resistance to nifurtimox and Bz in trypanosomes. *Proc. Natl.*
417 *Acad. Sci.* 105: 5022-5027.

418 Ye, X., Ding, J., Zhou, X., Chen, G., Liu, S.F., 2008. Divergent roles of endothelial NF-
419 kappaB in multiple organ injury and bacterial clearance in mouse models of sepsis. *J.*
420 *Exp. Med.* 205: 1303–1315.

421 FIGURE LEGENDS:

422

423 Figure 1. Chemical structure of the compounds assayed.

424 Figure 2. Reduction of the infectivity of *T. cruzi* in Vero cells treated with 2 and Bz. (a)
425 Rate of infection, (b) mean number of amastigotes per infected Vero cell and (c)
426 number of trypomastigotes in the culture medium. Control group is represented with
427 filled circles; filled squares represent Bz; filled triangles represent 2. Measured at IC25.
428 Values are the means of three separate experiments.

429 Figure 3. Parasitemia in the murine model of acute Chagas disease: filled circles
430 represent control, filled squares and filled triangles represent group treated with Bz and
431 2, respectively, with a final dose received of 125 mg/kg of body mass administered by
432 the intraperitoneal route. Grey shade represents the treatment days.

433 Figure 4. Immunosuppression *in vivo* assay for mice untreated and treated with 125
434 mg/kg of body mass of 2. (a) Shows the reactivation of blood parasitemia after the
435 immunosuppression cycles by fresh blood counting comparing to the peak day of
436 parasitemia during acute phase. (b) Shows differences in the Ig G levels measured by
437 ELISA at different day post infection for immunosuppressed and non-
438 immunosuppressed group of mice.

439 Figure 5. Variation percentages in the height of the peaks corresponding to catabolites
440 excreted by *T. cruzi* epimastigotes in the presence of 2 at IC25, compared to a control
441 sample after 96 hours of incubation.

442 Figure 6. Ultrastructural alterations shown by TEM in epimastigotes of *T. cruzi* treated
443 with 2 at IC25 concentration. (A) Control parasite showing typical organelles such as
444 nucleus (N), mitochondrions (M), glycosomes (G), microtubules (MT), vacuoles (V),
445 reservosomes (R), kinetoplast (K) and flagellum (F). (B) Treated with 2. Scale bar =
446 1 μ m.

447 Figure 7. *In vitro* inhibition (%) of CuZn-SOD from human erythrocytes and Fe-SOD
448 from *T. cruzi* epimastigotes for compound 2 (Cu/Zn-SOD activity 23.36 ± 4.21 U/mg)
449 (Fe-SOD activity 20.77 ± 3.18 U/mg). Differences between the activities of the control
450 homogenate and those ones incubated with compounds were obtained according to the
451 Newman–Keuls test. IC₅₀ values are shown in brackets. Values are the average of three
452 separate determinations.

453

FIGURES & LEGENDS:

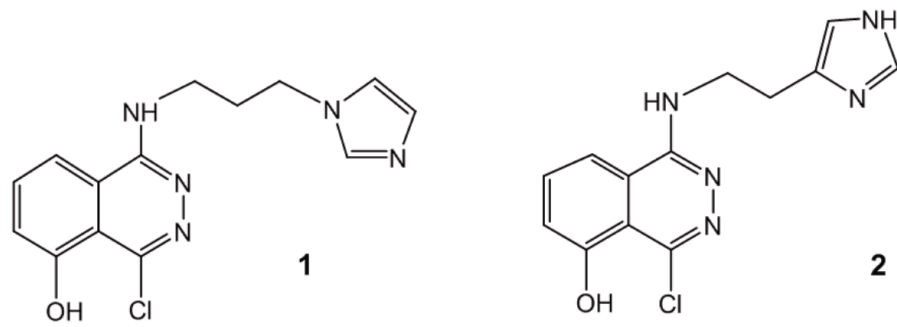


Figure 1. Chemical structure of the compounds assayed.

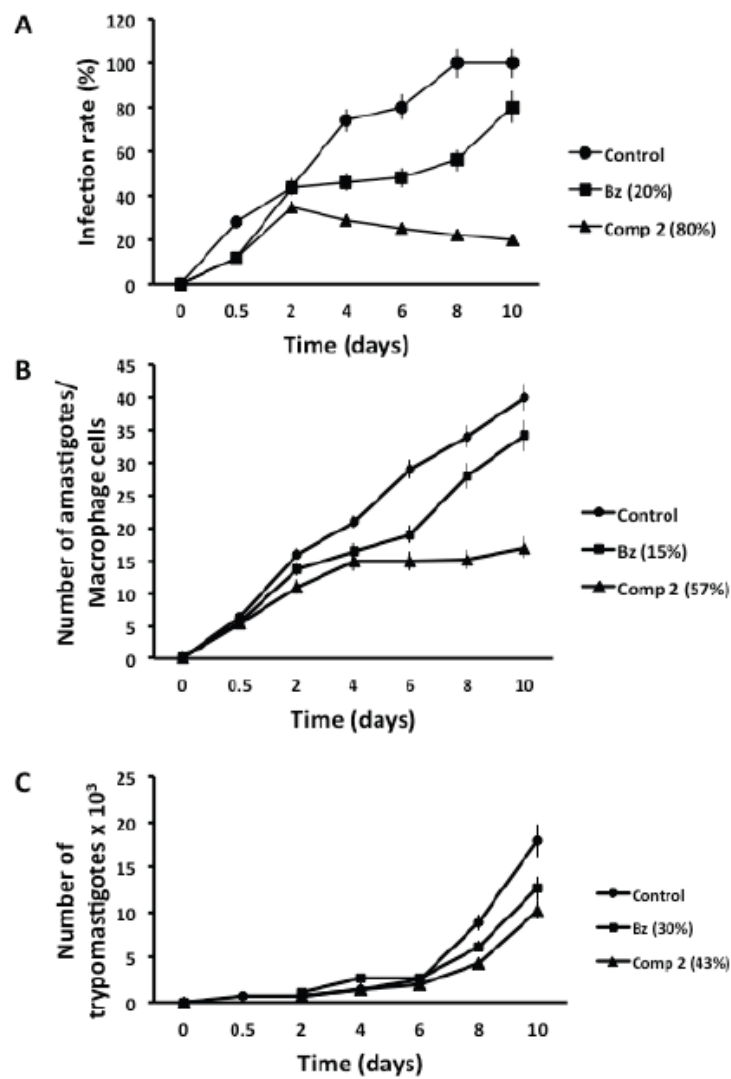


Figure 2. Reduction of the infectivity of *T. cruzi* in Vero cells treated with **2** and Bz. (a) Rate of infection, (b) mean number of amastigotes per infected Vero cell and (c) number of trypomastigotes in the culture medium. Control group is represented with filled circles; filled squares represent Bz; filled triangles represent **2**. Measured at IC₂₅. Values are the means of three separate experiments.

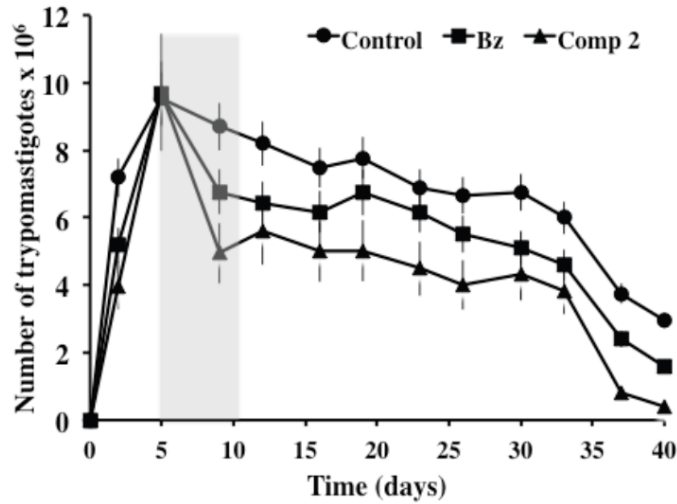


Figure 3. Parasitemia in the murine model of acute Chagas disease: filled circles represent control, filled squares and filled triangles represent group treated with **Bz** and **2**, respectively, with a final dose received of 125 mg/kg of body mass administered by the intraperitoneal route. Grey shade represents the treatment days.

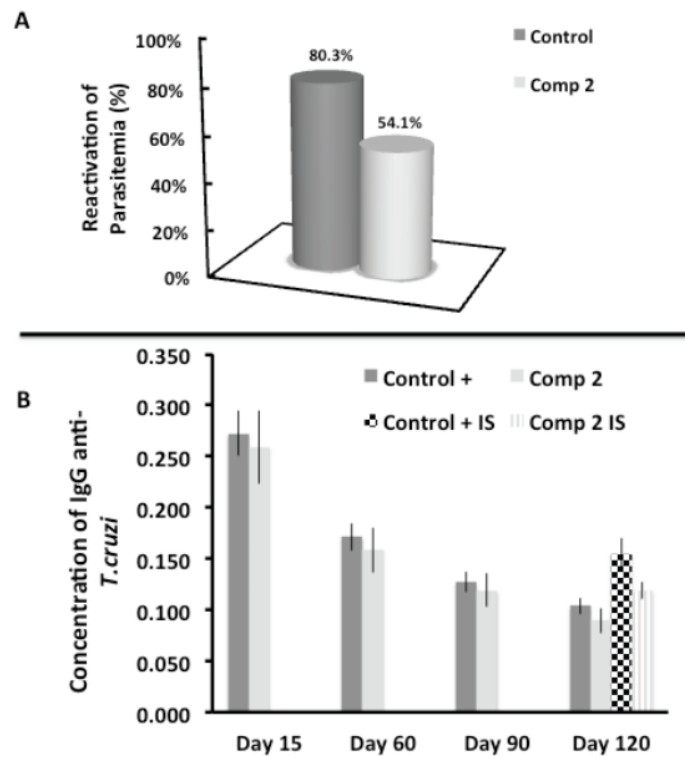


Figure 4. Immunosuppression in vivo assay for mice untreated and treated with 125 mg/kg of body mass of **2**. (a) Shows the reactivation of blood parasitemia after the immunosuppression cycles by fresh blood counting comparing to the peak day of parasitemia during acute phase. (b) Shows differences in the Ig G levels measured by ELISA at different day post infection for immunosuppressed and non-immunosuppressed group of mice.

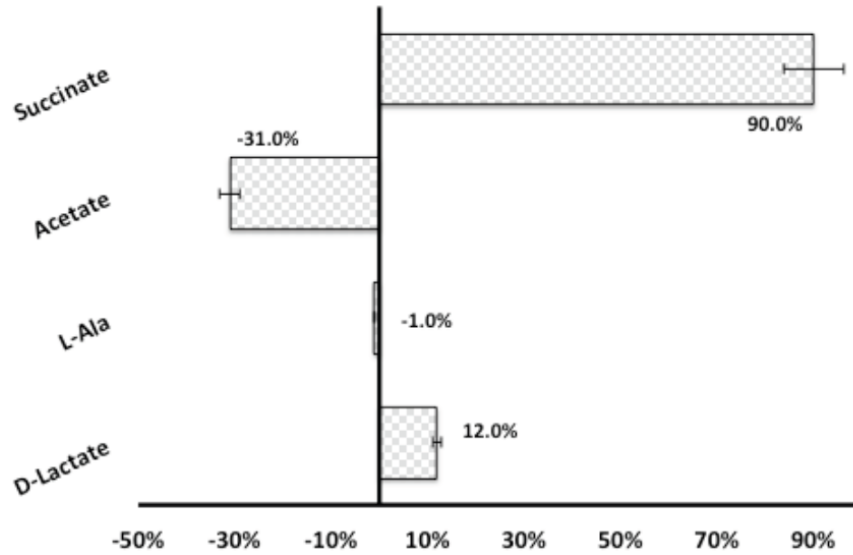


Figure 5. Variation percentages in the height of the peaks corresponding to catabolites excreted by *T. cruzi* epimastigotes in the presence of **2** at IC_{25} , compared to a control sample after 96 hours of incubation.

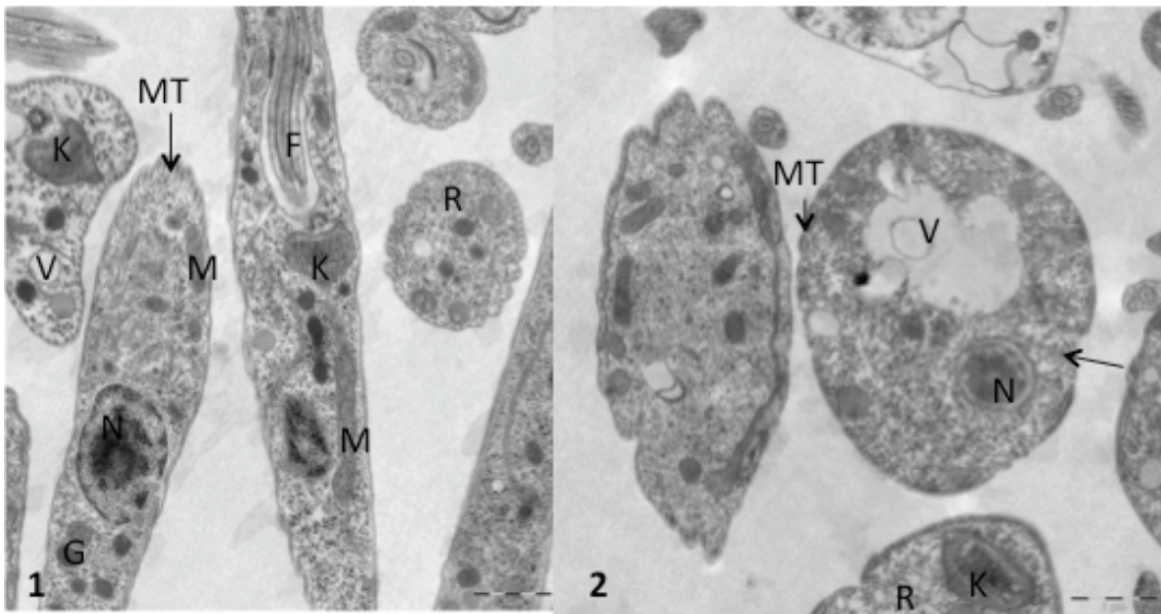


Figure 6. Ultrastructural alterations shown by TEM in epimastigotes of *T. cruzi* treated with **2** at IC_{25} concentration. (a) Control parasite showing typical organelles such as nucleus (N), mitochondrion (M), glycosomes (G), microtubules (MT), vacuoles (V), reservosomes (R), kinetoplast (K) and flagellum (F). (1) Untreated. (2) Treated with **2**. Scale bar = $1\mu\text{m}$.

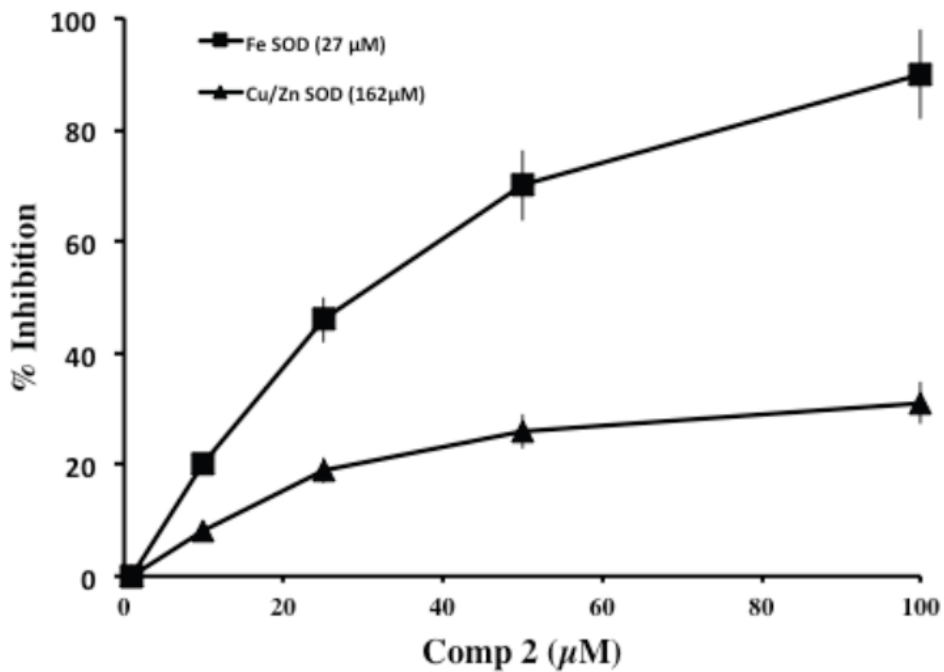


Figure 7. *In vitro* inhibition (%) of CuZn-SOD from human erythrocytes and Fe-SOD from *T. cruzi* epimastigotes for compound **2** (Cu/Zn-SOD activity 23.36 ± 4.21 U/mg) (Fe-SOD activity 20.77 ± 3.18 U/mg). Differences between the activities of the control homogenate and those ones incubated with compounds were obtained according to the Newman-Keuls test. IC_{50} values are shown in brackets. Values are the average of three separate determinations.

Table 1. In Vitro Activity, Toxicity and Selectivity Index found for the compounds and the reference drug on extracellular and intracellular forms of *Trypanosoma cruzi*.

Compounds	IC ₅₀ (μM) ^a			Toxicity IC ₅₀ Vero Cell (μM) ^b	SI ^c		
	Epimastigote forms	Amastigote forms	Trypomastigotes forms		Epimastigote forms	Amastigote forms	Trypomastigotes forms
Bz	15.8±1.1	23.3±4.6	22.4±1.9	13.6±0.9	0.8	0.6	0.6
Comp 1	39.2±2.1	20.8±1.7	29.5±0.8	148.8±3.1	4 (5)	7 (12)	5 (8)
Comp 2	8.5±5.7	7.4±2.2	10.8±0.8	214.7±4.6	25 (31)	29 (48)	20 (33)

^aIC₅₀ = the concentration required to give 50% inhibition, calculated by linear regression analysis from the Kc values at concentrations employed (1, 10, 25, 50 and 100 μM). ^bTowards Cell Vero after 72 h of culture. ^cSelectivity index = IC₅₀ Cell Vero/IC₅₀ extracellular and intracellular form of parasite. In brackets: number of times that compound SI exceeds the reference drug SI. Results are averages of three separate determinations.

Table 2. Summarizes the Biochemical clinical parameters tested in different groups of Balb/c Mice infected with *Trypanosoma cruzi* at different experimental situations.

	Kidney markers profile			Liver markers profile		
	UREA (mg/dL)	URIC ACID (mg/dL)	AST/GOT (U/L)	ALT/GPT (U/L)	TOTAL BILIRUBIN(mg/dL)	PHOSPHATASE ALKALYNE (U/L)
UNINFECTED MICE (n=15)	39 [36-43]	5 [4.3-5.5]	126 [103-148]	46 [37-54]	0.23 [0.17-0.28]	133 [104-161]
INFECTED MICE-ACUTE PHASE (n=15)	49 [39-60]	4.5 [3.7-5.5]	129 [100-157]	48 [38-58]	0.15 [0.12-0.18]	231 [161-300]
INFECTED MICE-CHRONIC PHASE (n=15)	49	4.3	148	53	0.12	186
120 days POST INFECTION MICE and Comp 2 125 mg/kg.w TREATED (n=6)	=	=	+	+	+	=

Key: =, variation no larger than 10%; +, up to 10% of increasing over the range; ++, up to 30% of increasing over the range; +++, up to 40% of increasing over the range; +++++, more than 50% of increasing over the range; -, up to 10% of decreasing over the range; --, up to 30% of decreasing over the range; ---, up to 40% of decreasing over the range; ----, more than 50% of decreasing over the range.

Manuscript Number:

Title: In vitro and in vivo identification of tetradentated polyamine complexes as highly efficient metallodrugs against *Trypanosoma cruzi*

Article Type: Research Paper

Keywords: trypanosomiasis, chemotherapy, polyamines, murine model, Chagas

Corresponding Author: Dr. Manuel Sánchez-Moreno,

Corresponding Author's Institution:

First Author: Francisco Olmo

Order of Authors: Francisco Olmo; Olaf Cussó; Clotilde Marín; Maria J Rosales; Kristína Urbanová; R. Luise Krauth-Siegel; Miquel Costas; Xavi Ribas; Manuel Sánchez-Moreno

Abstract: In order to identify new compounds to treat Chagas disease during the acute phase with higher activity and lower toxicity than the reference drug benznidazole (Bz), a series of tetraamine-based compounds was prepared and their trypanocidal effects against *Trypanosoma cruzi* were evaluated by light microscopy through the determination of IC₅₀ values. Cytotoxicity was determined by flow cytometry assays against Vero cells. In vivo assays were performed in BALB/c mice, in which the parasitemia levels were quantified by fresh blood examination; the assignment of a cure was determined by PCR and reactivation of blood parasitemia levels after immunosuppression. The mechanism of action was elucidated at metabolic and ultra-structural levels by ¹H NMR and TEM studies. Finally, as tetraamines are potentially capable of causing oxidative damage in the parasites, the study was completed by assessing their activity as potential iron superoxide dismutase (Fe-SOD) and trypanothione reductase (TR) inhibitors. High-selectivity indexes observed in vitro were the basis of promoting three of the tested compounds to in vivo assays. The tests on the murine model for the acute phase of Chagas disease showed better parasitemia inhibition values than those found for Bz. Tetraamines 2 and 3 induced a remarkable decrease in the reactivation of parasitemia after immunosuppression and curative rates of 33 and 50%, respectively. Tetraamine 3 turned out to be a great inhibitor of Fe-SOD and TR. The high anti-parasitic activity and low toxicity render these tetraamines appropriate molecules for the development of an affordable anti-Chagas agent.

Dear Editor,

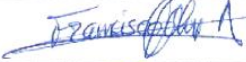
Please find enclosed our manuscript entitled “***In vitro and in vivo identification of tetradentate polyamines and their manganese-based complexes as highly efficient metallodrugs against Trypanosoma cruzi***” by Olmo et al. to be considered for publication in *Acta Tropica*.

In this multidisciplinary work, where it has been teamed up Chemistry group with Biochemistry and Parasitology groups, we describe the synthesis and antiprotozoal activity of tetradentate polyamines against *Trypanosoma cruzi*. The high efficiency of these polyamines against *T. cruzi* was shown through *in vitro* assays and further confirmed by an additional *in vivo* study in a murine model that goes from the acute to the chronic phase of Chagas disease. The study includes a deep analysis to figure out the possible mechanism of action, attending to the inhibition of Superoxide dismutase and Trypanothione reductase enzymes, complemented with the study of the changes in the metabolites excreted by the parasite and disturbances caused by our compounds at ultrastructural level.

Regarding to the format, we try to simplify the article standing out *Result and Discussion* section in the manuscript and providing the *Experimental* with a quite complete pack of references for an easier and direct understanding of the content, without losing the scientific rigour required, in order to give the proper information to reproduce any assay.

As it is mentioned in the article, the drugs currently used to treat Chagas disease are decades old and have many limitations including high toxicity, therefore the search for new drugs is urgently needed. We think that our contribution is interesting and rather complete, including the deep approach *in vitro* and *in vivo* and also the mechanism of action of these pre-drugs, for hence this manuscript could be a quite interesting topic for the journal readers. For all the reasons explained before we believe that it merits publication in *Acta Tropica*.

All authors of this research paper directly participated in the planning, execution, or analysis of the study and they have seen and approved this version of the manuscript. Hence, all authors approve the submission of the manuscript, accept full responsibility for the study, had access to the data, and controlled the decision to publish.

Name	Signature
Olmo, Francisco	
Cussó, Olaf	
Marín, Clotilde	
Rosales, María J.	
Urbanová, Kristína	
Krauth-Siegel, Luise	Krauth-Siegel
Costas, Miquel	
Ribas, Xavi	
Sánchez-Moreno, Manuel	

Thank you very much for taking into account this manuscript.

Best regards,

Yours sincerely,

Graphical Abstract



1
2
3
4
5
6
7
8
9
10
11
12
13
14
15
16
17
18
19
20
21
22
23
24
25
26
27
28
29
30
31
32
33
34
35
36
37
38
39
40
41
42
43
44
45
46
47
48
49
50
51
52
53
54
55
56
57
58
59
60
61
62
63
64
65

***In vitro* and *in vivo* identification of tetradentated
polyamine complexes as highly efficient metallodrugs
against *Trypanosoma cruzi***

Francisco Olmo,¹ Olaf Cussó,² Clotilde Marín,¹ Maria José Rosales,¹ Kristína Urbanová,¹ R. Luise Krauth-Siegel,³ Miquel Costas,² Xavi Ribas,² Manuel Sánchez-Moreno^{1,*}

¹Departamento de Parasitología, Facultad de Ciencias, Universidad de Granada, E-18071 Granada, Spain.

²QBIS Research Group, Institut de Química Computacional i Catàlisi (IQCC), and Departament de Química, Universitat de Girona. Campus de Montilivi, E-17071, Girona, Spain.

³Biochemie-Zentrum der Universität Heidelberg, Im Neuenheimer Feld 328, 69120 Heidelberg, Germany

*Corresponding author. Tel: +34-958-242369; Fax: +34-958-243174; E-mail: msanchem@ugr.es

Abstract

1
2
3 In order to identify new compounds to treat Chagas disease during the acute phase with
4 higher activity and lower toxicity than the reference drug benznidazole (Bz), a series of
5 tetraamine-based compounds was prepared and their trypanocidal effects against
6 *Trypanosoma cruzi* were evaluated by light microscopy through the determination of
7 IC_{50} values. Cytotoxicity was determined by flow cytometry assays against Vero cells.
8 *In vivo* assays were performed in BALB/c mice, in which the parasitemia levels were
9 quantified by fresh blood examination; the assignment of a cure was determined by
10 PCR and reactivation of blood parasitemia levels after immunosuppression. The
11 mechanism of action was elucidated at metabolic and ultra-structural levels by 1H NMR
12 and TEM studies. Finally, as tetraamines are potentially capable of causing oxidative
13 damage in the parasites, the study was completed by assessing their activity as potential
14 iron superoxide dismutase (Fe-SOD) and trypanothione reductase (TR) inhibitors. High-
15 selectivity indexes observed *in vitro* were the basis of promoting three of the tested
16 compounds to *in vivo* assays. The tests on the murine model for the acute phase of
17 Chagas disease showed better parasitemia inhibition values than those found for Bz.
18 Tetraamines **2** and **3** induced a remarkable decrease in the reactivation of parasitemia
19 after immunosuppression and curative rates of 33 and 50%, respectively. Tetraamine **3**
20 turned out to be a great inhibitor of Fe-SOD and TR. The high anti-parasitic activity and
21 low toxicity render these tetraamines appropriate molecules for the development of an
22 affordable anti-Chagas agent.
23
24
25
26
27
28
29
30
31
32
33
34
35
36
37
38
39
40
41
42
43
44
45
46
47
48
49
50

51
52
53 **Keywords:** trypanosomiasis, chemotherapy, polyamines, murine model, Chagas
54
55
56
57
58
59
60
61
62
63
64
65

1. Introduction

The World Health Organisation (WHO) lists Chagas disease as one of the most neglected tropical diseases. Chagas disease is endemic in Latin America; it is estimated that 10 million people are infected worldwide and more than 25 million are living at risk of infection ([World Health Organization, 2012](#)). The main drugs used for the treatment of Chagas disease are benznidazole (Bz, LAFEPE) and nifurtimox (Lampit[®], Bayer), which present significant side effects and cure <20% of patients with chronic Chagas disease ([Mckerrow et al., 2009](#)). Thus, many researchers have combined efforts to discover drugs against new targets, looking for lower toxicity and a greater tolerance in patients, aiming not only for efficiency in the acute phase, but also in the chronic phase.

One of the self-defence strategies of *Trypanosoma cruzi* (the etiological agent of Chagas disease) is its highly active and exclusive iron superoxide dismutase (Fe-SOD), which differs from Cu–Zn-SOD or Mn-SOD operating in mammals. Fe-SOD is an extremely efficient enzyme for preventing any oxidative damage from the host in combination with peroxidases. The other self-defence strategy is trypanothione, a parasitic molecule involved in protozoan protection against oxidative stress, which is now considered a virulence factor of Chagas disease ([Piacenza et al., 2013](#)). Thus, the use of molecules that interfere with the enzyme trypanothione reductase (TR), which keep the trypanothione molecule in its reduced status, may lead to parasite death. In this sense, we focused on complexes capable affecting or interfering with these exclusive enzymes of *T. cruzi*.

In previous work, we designed iron and manganese coordination complexes containing polyamine ligands, which are capable of generating highly oxidising species ([Cussó et al., 2013](#); [García-Bosch et al., 2012](#); [Company et al., 2011](#)) Highly reactive Mn(IV)=O and

1 Fe(IV)=O species embedded in these ligand scaffolds have been prepared and their
2 oxidative reactivity studied. Furthermore, these polyamine ligands bind very strongly to
3 iron and manganese ions, forming coordination complexes that are stable under highly
4 acidic and oxidative conditions.
5
6
7
8
9

10 Herein, we report on the *in vitro* and *in vivo* anti-trypanosomal properties of Mn-based
11 polyamines and polyamine complexes (**Figure 1**), which represent a class of
12 compounds that have, so far, only rarely been explored for Chagas disease
13 chemotherapy. Finally, we analyse the possible mechanism of action over the parasite
14 structure and function as well as the protective enzymes mentioned above.
15
16
17
18
19
20
21
22

23 **2. Materials and methods**

24 **2.1. Chemistry**

25
26
27
28
29 Most of our compounds (**1**, **2**, **4** and **5**) have been previously synthesized for organic
30 synthesis purposes (Cussó et al., 2013; Costas and Que, 2002) On the other hand, the
31 compound **3** has been designed as a structural variant of compound **2** and synthesized for
32 the first time in this work. The structures are shown in **Figure 1**.
33
34
35
36
37
38
39

40 **2.2. Compound 3 synthesis**

41
42
43 A suspension of Mn(OTf)₂ (69.7 mg, 0.16mmol) in anhydrous dichloromethane (1 mL)
44 was added dropwise to a vigorously stirred solution of (R,R)-^{dMM}BPMC_N (Cussó et al.,
45 2013) (55.8 mg, 0.16 mmol) in dichloromethane (1 mL). After a few seconds the solution
46 became cloudy and a white precipitate appeared. After stirring for 1 hour the solution was
47 filtered off and the resultant white solid dried under vacuum. This solid was solved in
48 CH₂Cl₂ (3 mL) and the solution filtered off through celite©. Slow diethyl ether diffusion
49 over the resultant solution afforded, in a few days, 81 mg of white crystals (0.10 mmol,
50 yield 65 %). Anal. Calcd for C₂₈H₄₀F₆MnN₄O₈S₂: C, 42.37; H, 5.08; N, 7.06 %. Found: C,
51
52
53
54
55
56
57
58
59
60
61
62
63
64
65

1
2
3
4
5
6
7
8
9
10
11
12
13
14
15
16
17
18
19
20
21
22
23
24
25
26
27
28
29
30
31
32
33
34
35
36
37
38
39
40
41
42
43
44
45
46
47
48
49
50
51
52
53
54
55
56
57
58
59
60
61
62
63
64
65

42.13; H, 4.89; N, 7.13 %. FT-IR (ATR) ν , cm^{-1} : 2934 – 2872 (C-H) sp^3 , 1599, 1479, 1306, 1233, 1211, 1158, 1081, 1026, 879, 633, 511. ESI-HRMS calcd. for $\text{C}_{27}\text{H}_{40}\text{F}_3\text{MnN}_4\text{O}_5\text{S}$ [M-OTf] $^+$: 644.2047, found: 644.2061

2.3. Parasite Strain Culture

Trypanosoma cruzi SN3 strain of IRHOD/CO/2008/SN3 was isolated from domestic Rhodnius prolixus; biological origin is Guajira (Colombia) (Téllez-Meneses et al., 2008). Epimastigote forms were grown in axenic Grace's insect medium (Gibco) supplemented with 10% inactivated fetal bovine serum (FBS) at 28°C in tissue-culture flasks, Roux flasks (Corning, USA) with a surface area of 75 cm^2 , as described by us (González et al., 2005).

2.4. Transformation of epimastigotes to metacyclic forms

Metacyclogenesis was induced by culturing a 5-day-old culture of epimastigote forms of *T. cruzi* that was harvested by centrifugation at 7 000 g for 10 min at 10 °C according to Cardoso and Soares, 2010.

2.5. Cell Culture and Cytotoxicity Tests

Vero cells (Flow) were grown in RPMI and MEM (Gibco), supplemented with 10% iFBS and the procedure followed was as in González et al., 2005.

2.6. In Vitro Activity Assays, Extracellular Forms:

2.6.1. Epimastigotes assay

T. cruzi epimastigotes were collected in the exponential growth phase and distributed in culture trays (with 24 wells) at a final concentration of 5×10^4 parasites/well. The effects on the parasite growth were tested according to Olmo et al., 2013.

2.6.2. Blood Trypomastigote Forms Assay

1
2
3 Compounds 4-5 were also evaluated in blood trypomastigote forms of *T. cruzi*. BALB/c
4
5 female mice infected with *T. cruzi* were used 7 days after infection. Blood was obtained
6
7 by cardiac puncture using 3.8% sodium citrate as an anticoagulant in a 7:3
8
9 blood:anticoagulant ratio. The parasitaemia in the infected mice was about 1×10^5
10
11 parasites/mL. The compounds were diluted in phosphate-buffered saline solution (PBS)
12
13 to give a final concentration 10, 25, and 50 μM for each product. Aliquots (20 μL) of
14
15 each solution were mixed in culture trays (96 wells) with 55 μL of infected blood
16
17 containing the parasites at a concentration of approximately 1×10^6 parasites/mL.
18
19 Infected blood with PBS, at the same concentrations as the products, was used as
20
21 control. The plates were shaken for 10 min at room temperature and kept at 4°C for 24 h.
22
23 Each solution was examined microscopically (Olympus CX41) for parasite counting
24
25 using the Neubauer haemocytometric chamber (a dilution of 1:100 in PBS was
26
27 necessary to get into the range of counting). The activity (percent of parasites reduction)
28
29 was compared with that of the control.
30
31
32
33
34
35
36
37

2.7. *In Vitro* Activity Assays, Intracellular forms: Amastigotes Assay

38
39 Vero cells were cultured in RPMI medium supplemented with 10% iFBS, in a
40
41 humidified 95% air and 5% CO₂ atmosphere at 37 °C. Then the cells were infected and
42
43 treated as in [Olmo et al., 2013](#).
44
45
46
47
48

2.8. Infectivity Assay

49
50 Vero cells were cultured in RPMI medium supplemented with 10% iFBS as described
51
52 above. Afterward, the cells were infected in vitro with metacyclic trypomastigote forms
53
54 of *T. cruzi* at a ratio of 10:1. The assay was performed as in [Olmo et al., 2013](#).
55
56
57
58
59
60
61
62
63
64
65

2.9. In Vivo Trypanosomicidal Activity Assay:

2.9.1. Mice infection and treatment

This experiment was performed using the rules and principles of the International Guide for Biomedical Research in Experimental Animals and with the approval of the ethical committee of the University of Granada, Spain. Groups of six BALB/c albino female mice (6–8 weeks old, 25–30 g weight), maintained under a 12-h dark/light cycle (lights on at 07:30 h) at a temperature of $22 \pm 3^\circ\text{C}$ and provided with water and standard chow *ad libitum*, were inoculated via the intraperitoneal route with 5×10^5 blood trypomastigotes of *T. cruzi* obtained from previously infected mice blood. The animals were divided as follows: I, positive control group (mice infected but not treated); II, study group (mice infected and treated with the compounds under study). The administration of the testing compounds was begun on the seventh day of infestation once the infection was confirmed, and doses of 5 mg/kg body mass per day were used for 5 consecutive days (7–12 days post-infection). Peripheral blood was obtained from the mandibular vein of each mouse (5 μL samples) and dissolved in 495 μL of a PBS solution at a dilution of 1:100. The circulating parasite numbers were quantified with a Neubauer's chamber for counting blood cells. This counting was performed every 3 days during a 40 day period (acute phase). The number of bloodstream forms was expressed as parasites/mL.

2.9.2. Cyclophosphamide-induced immune suppression and assessment of cure

After day 60, the animals entered the chronic phase of the experiment where parasitaemia showed progressively decreasing levels independent of the treatment. Therefore, on day 120, parasitaemia was shown to be undetectable by fresh blood

1 microscopic examination, and the mice received 4 intraperitoneal injections of 200
2 mg/kg of body mass of cyclophosphamide monohydrate (CP) (ISOPAC®) on alternate
3 days, as previously described ([Cecing et al., 2011](#)). Within 1 week of the last CP
4 injection, parasitaemia was evaluated according to the procedure described for acute
5 phase to quantify the presence of blood trypomastigote forms as reactivation rate.
6
7 Finally, mice were bled out, under gaseous anaesthesia (CO₂), via heart puncture and
8 blood was collected. Blood was incubated for 2 hours at 37°C and then over night at 4°C
9 in order to allow clotting and then the serum was obtained from samples after
10 centrifuging the supernatant twice at 1000 and 2700 g, consecutively. The serum was
11 aliquoted and used for ELISA and biochemical analysis, as explained below. Hearts
12 were harvested and immediately flushed free of blood by gentle infusion of 10 ml of
13 pre-warmed PBS through the left ventricle ([Ye et al., 2008](#)) in order to avoid
14 contamination of the collected tissue with blood parasites. After this, samples were
15 frozen at -80°C and stored until used for DNA extraction.
16
17
18
19
20
21
22
23
24
25
26
27
28
29
30
31
32

33 **2.9.3. ELISA tests**

34
35 Fe-SOD excreted from the parasite, cultured and processed as described in [Lopez-
36 Cespedes et al., 2012](#), was used as the antigen fraction. The ELISA test to measure the
37 antibodies against *T. cruzi* used was performed as in [Olmo et al., 2014](#).
38
39
40
41
42
43
44
45

46 **2.9.4. DNA extraction and PCR**

47
48
49 Hearts were defrosted and then ground using a Potter-Elvehjem to follow the
50 purification procedure of the Wizard® Genomic DNA Purification Kit (Promega). PCR
51 was performed using two primers designed in our laboratory ([Olmo et al., 2014](#)), based
52 on the published sequence of the enzyme superoxide dismutase *T. cruzi* CL Brenner
53 (GenBank accession No. XM_808937), which amplifies a fragment of approximately
54
55
56
57
58
59
60
61
62
63
64
65

1
2
3
4
5
6
7
8
9
300bp belonging to the superoxide dismutase gene b of *T. cruzi*. The PCR was run in a total volume of 20µl. Next, the amplification products were subjected to electrophoresis on 1.6% agarose gel containing 1:10000 GelRed™ Nucleic Acid Gel Stain, for 90 minutes at 90 V.

10 11 12 13 14 15 16 17 18 19 20 21 22 23 24 25 26 27 28 29 30 31 32 33 34 35 36 37 38 39 40 41 42 43 44 45 46 47 48 49 50 51 52 53 54 55 56 57 58 59 60 61 62 63 64 65

2.9.5. Toxicity tests by clinical chemistry measurements.

A fraction of the serum obtained as it was shown above was send to the Biochemical service in the University of Granada where a series of parameters were measured according to their commercial kits acquired from Cromakit® by BS-200 Chemistry Analyzer Shenzhen Mindray (Bio-medical Electronics Co., LTD). With the levels obtained for different populations of sera (n = 15, n = 6) we calculated the mean value and standard deviation. Finally, we also calculated the confidence interval for the mean normal populations based on a confidence level of 95% ($100 \times (1-\alpha) = 100x (1-.05)\%$). The ranges obtained are shown in **3**, which allows comparison and analysis of the sera studied in this work.

2.10. Assays to figure out the mechanism of action:

2.10.1. Ultrastructural alterations

The parasites were cultured at a density of 5×10^5 cells/mL in each corresponding medium containing the compounds tested at the concentration of IC₂₅. After 96 h, these cultures were centrifuged at 400 g for 10 min and the pellets produced were washed in PBS before being mixed with 2% (v/v) paraformaldehyde/glutaraldehyde in 0.05 M cacodylate buffer (pH 7.4) for 24 h at 4°C. Following this, the pellets were prepared for transmission electron microscopy study using a technique described by our group ([Fernández-Becerra et al., 1997](#)).

2.10.2. Metabolite Excretion

1 Cultures of *T. cruzi* epimastigote forms (initial concentration of 5×10^5 cells/mL)
2 received IC₂₅ of the compounds (except for the control cultures). After incubation for 96
3 h at 28°C, the cells were centrifuged at 400 g for 10 min. The supernatants were
4 collected in order to determine the excreted metabolites through ¹H NMR, and the
5 chemical shifts were expressed in parts per million (ppm), using dimethyl sulphoxide
6 (DMSO) as the reference signal. One-dimensional ¹H NMR spectra were acquired on
7 VARIAN DIRECT DRIVE 400 MHz Bruker spectrometer with AutoX probe using
8 D₂O. The assignments of metabolites were based on 1D NMR spectrum. The chemical
9 shifts used to identify the respective metabolites were consistent with those described
10 previously by our group (Fernández-Becerra et al., 1997). In addition, the human
11 metabolome database (<http://www.hmdb.ca/>) was also used for this purpose. The
12 spectral region of 1.0 to 5.5 ppm was bucketed into a frequency window of 0.1 ppm.
13 The region corresponding to water (4.5 to 5.5 ppm) was excluded during binning to
14 avoid artefacts due to pre-saturation of water, and the region corresponding to glucose
15 (3.4 to 3.8 ppm) was also excluded. The aromatic region was excluded because the
16 signal to noise ratio in this region was poorer compared to that of the aliphatic region.
17 The peak (2.6 ppm) corresponding to DMSO was removed before binning. The
18 resulting integrals were normalised to the working region (1.0 to 3.4) ppm of the
19 spectrum to correct for inter-sample differences in dilution. The binning and
20 normalisations were achieved using Mestrenova 9.0 software. The matrix obtained in
21 Mestrenova was imported to Microsoft Excel for further data analyses.

2.10.3. Superoxide dismutase inhibition assay

22 The parasites cultured as described above were centrifuged. The pellet was suspended in
23 3 mL of STE buffer (0.25 M sucrose, 25 mM Tris-HCl, 1 M EDTA, pH 7.8) and
24 disrupted by three cycles of sonic disintegration, 30 s each at 60 W. The sonicated
25
26
27
28
29
30
31
32
33
34
35
36
37
38
39
40
41
42
43
44
45
46
47
48
49
50
51
52
53
54
55
56
57
58
59
60
61
62
63
64
65

1 homogenate was centrifuged at 1500 g for 5 min at 4°C, and the pellet was washed three
2 times in ice-cold STE buffer. This fraction was centrifuged (2500 g for 10 min at 4°C)
3 and the supernatant was collected. The protein concentrations were determined using the
4 Bradford method (Bradford, 1972). Iron and copper–zinc superoxide dismutases (Fe-
5 SOD and CuZn-SOD) activities were determined using the method described by Beyer
6 and Fridovich (Beyer and Fridovich, 1987).
7
8
9
10
11
12
13
14

15 **2.10.4. TR inhibition studies.**

16 Recombinant TR from *Trypanosoma cruzi* (TcTR) was prepared following a published
17 procedure (Sullivan and Walsh, 1991). TS₂ was generated enzymatically as described
18 previously (Comini et al., 2009). The TR activity was measured in a total volume of 1 mL
19 of 40 mM Hepes and 1 mM EDTA at pH 7.5 in the presence of 100 μM NADPH by
20 varying the concentrations of TS₂ (20, 40, 80, 100 and 200 μM) and/or the inhibitor (0, 28
21 and 100 μM). The absorption decrease, owing to NADPH oxidation, was followed at 340
22 nm and 25°C. Stock solutions of the inhibitors were prepared in water according to their
23 solubility.
24
25
26
27
28
29
30
31
32
33
34
35
36
37
38

39 The K_i and K_i' values were determined using the following equations (Dixon and Webb,
40 1986):
41
42
43
44

$$45 K_i = \frac{[I]}{\frac{K_{m(\text{obs})} \left(1 + \frac{[I]}{K_i'}\right)}{K_m} - 1}$$

$$46 K_i' = \frac{[I]}{\frac{V_{\text{max}}}{V_{\text{max}(\text{obs})}} - 1}$$

47
48
49
50
51
52
53
54
55
56 The ability of the compounds to induce the oxidase activity of TR was measured in the
57 presence of 100 μM NADPH and about 2 U/mL of TR, with 40 or 100 μM of the specified
58
59
60
61
62
63
64
65

1 compound in a total volume of 1 mL. Under these conditions, spontaneous NADPH
2 oxidation results in a minimal absorption decrease. This activity was not accelerated in the
3 presence of the compounds, ruling out the possibility that they act as subversive substrates
4 (data not shown).
5
6
7
8
9

10 **3. Results and Discussion**

11 **3.1. Chemistry**

12
13 Manganese-based coordination complexes (**1–3**) were selected for their ability to generate
14 high-oxidation-state compounds, which are potentially capable of causing oxidative
15 damage in the parasite. Additionally, water-soluble compounds (**4, 5**) were studied to
16 evaluate potential Fe-chelation in causing Fe-SOD dysfunction and inducing parasite death.
17
18
19
20
21
22
23
24
25

26 **3.2. *In vitro* trypanosomicidal evaluation**

27
28 All five polyamines showed better selectivity indexes ($SI = IC_{50} \text{ Vero cells}/IC_{50}$
29 extracellular and intracellular forms of *T. cruzi*) compared to the reference drug Bz. As
30 summarised in **Table 1**, compound **2**, with SI values 108 and 93 times higher than those of
31 Bz, was the best compound, independent of the parasite stage. This activity meets the
32 criteria given by Nwaka and co-workers ([Nwaka et al., 2011](#)) and Romanha and co-
33 workers ([Romanha et al., 2010](#)) and is, therefore, considered as a strong candidate to
34 undergo *in vivo* studies. On the other hand, compounds **3** and **5** also showed quite good
35 trypanocidal activity, thus resulting SI values that were even better than those of Bz.
36
37
38
39
40
41
42
43
44
45
46
47
48
49

50 To obtain more accurate information about the most active polyamines (**2, 3, and 5**), the
51 development of the parasites in Vero cells was studied by measuring the rates of infection
52 and the average number of amastigote and trypomastigote forms present during a ten-day
53 treatment period. Vero cells were infected with metacyclic forms of *T. cruzi* and the
54 gradual differentiation into amastigote forms was followed. During the observation time, in
55
56
57
58
59
60
61
62
63
64
65

1 the control group, the rate of infection of the host cells gradually increased, reaching 99%
2 invasion at the end of the experiment (**Figure 2a**). The test was repeated in the presence of
3 the reference drug and in the presence of compounds **2**, **3** or **5** at their IC₂₅ concentrations.
4
5 It was found that the rate of infection decreased in all cases, with respect to the control, and
6
7 compounds **2**, **3** and **5** showed reductions in the infection rate of 84, 66 and 55%,
8
9 respectively, thus with much a higher efficiency than Bz (19% reduction).
10
11
12
13
14

15 In terms of the average number of amastigote forms per Vero cell (**Figure 2a**), the results
16 were consistent with those mentioned above for infection rates. After treatment,
17
18 compounds **2**, **3** and **5** significantly reduced the number of amastigote forms per cell by 81,
19
20 59 and 56%, respectively, whereas Bz showed reduction of only a 39%. The average
21
22 number of amastigote forms increased to a maximum on the sixth day of culture, but
23
24 decreased thereafter (**Figure 2b**); the rupture of Vero cells released trypomastigote forms.
25
26 In terms of the number of trypomastigote forms found per millilitre of culture medium
27
28 (**Figure 2c**), a maximum was reached on day 10 (9.5×10^3 trypomastigote forms/mL) for
29
30 the control, whereas this value was substantially reduced by the reference drug (41%), but
31
32 even more so by compounds **2**, **3** and **5** (84, 76 and 72%, respectively). In summary, the
33
34 results of the parasite spreading in Vero cells are in agreement with those of the
35
36 trypanocidal activity reported in **Table 1** for intracellular and extracellular forms of *T.*
37
38 *cruzi*, with compound **2** being much better than any of the other drug candidates tested.
39
40
41
42
43
44
45
46
47

48 **3.3. *In vivo* activity of tetradentate polyamines**

49

50
51 The promising *in vitro* results prompted us to study the *in vivo* activity of these polyamines
52
53 in female BALB/c mice. As the effectiveness of the drugs currently in use against Chagas
54
55 disease varies widely between the acute and chronic phase, we decided to evaluate the
56
57 impact of our compounds on both phases. For the acute phase experiments, we considered
58
59
60
61
62
63
64
65

1 the first 40 days after infection (dpi), whereas the effect on the chronic phase was studied
2 between days 40 and 120 after infection. The intraperitoneal (i.p.) doping route was
3 preferred over the intravenous procedure, because it is well known that i.p. treatment
4 substantially reduces animal mortality (Da Silva et al., 2008). In fact, no mouse died in any
5 of our experiments with either the control or with the compounds assayed at the
6 concentrations used (15 mg/kg of body mass). However, the survival percentage for the
7 mice treated with Bz was only about 80%. The female mice were inoculated with
8 trypomastigote forms, as described in the Experimental section, and i.p. treatment with the
9 compounds was started five days post-infection and maintained for five consecutive days.
10 A group of mice (control group) was treated in the same manner, but using only the vehicle.
11 During the study of acute-phase activity, the level of parasitemia was determined every
12 two days. **Figure 3** shows the number of trypomastigote forms found during the acute
13 phase (1–40 dpi). On the day of maximum parasite burden (20–22 days after infection), all
14 of the tested compounds greatly reduced the number of blood trypomastigote forms
15 compared with the control group. Furthermore, compounds **2**, **3** and **5** lowered the level of
16 parasitemia on day 40 by 59, 35 and 27%, respectively. This effect was significantly
17 greater than that found for the reference drug (11%). The decreasing order of *in vivo*
18 activity on trypomastigote forms in the acute phase was found to be **2** >> **3** > **5** > Bz.
19
20
21
22
23
24
25
26
27
28
29
30
31
32
33
34
35
36
37
38
39
40
41
42
43

44 The chemical structure of these coordination complexes (**2**, **3** and **5**) is fundamentally
45 different from that of Bz. Therefore, the mechanisms underlying their anti-trypanosomal
46 activity most likely differ, and simple structure–activity correlations should be regarded
47 with caution.
48
49
50
51
52
53
54

55 Therefore, these group of mice, treated with polyamines **2** and **3**, where kept until 120 dpi
56 was achieved under the same conditions. The experiment was concluded with an
57 immunosuppression test on the treated mice 120 days after p.i. (late chronic phase, in
58
59
60
61
62
63
64
65

1 which there are no parasites remaining in the bloodstream that are quantifiable by fresh
2 blood analysis). **Figure 4a** shows the reactivation of parasitemia after immunosuppression.
3
4 It can be appreciated that the control group recovers half of its initial peak of parasitemia,
5 with a reactivation of 55.5 %. In contrast, the treated groups show a parasitemia load of
6
7 only 10.1% with respect to their burden peak when the mice have been administered with
8
9 compound **2**, as well as a low reactivation (12.7 %) for those treated with compound **3**; less
10
11 significant was the decrease in reactivation for the group treated with compound **5**, which
12
13 was closer to that of the untreated group (40.2 %). ELISA assays offer an alternative
14
15 method for verifying the effectiveness of these three compounds in the chronic phase after
16
17 being challenged with an immunosuppression cycle. **Figure 4b** shows the total Ig-G levels
18
19 of anti-*T. cruzi* and, according to previous reports, the titer of Ig-G in Balb/c becomes
20
21 stable during chronic phase of the disease ([el Bouhdidi et al., 1994](#)); this is confirmed in
22
23 **Figure 4b**. The control group showed an almost triplication in the Ig-G levels in response
24
25 to the presence of the parasite in the bloodstream after immunosuppression. However, in
26
27 the treated group, the differences between immunosuppressed (IS) and non-
28
29 immunosuppressed (non-IS) groups were smaller and not significant in the case of
30
31 compounds **2** and **3**; however, treatment with compound **5** showed a doubled Ig-G value
32
33 compared to the non-IS group. This means that the parasite-specific Ig-G levels were not
34
35 higher than the remaining amount of total unspecific Ig-G caused by the
36
37 hypergammaglobulinaemia characteristic of the infection by *Trypanosoma cruzi* ([Bryan et](#)
38
39 [al., 2010](#)).

40
41
42
43
44
45
46
47
48
49
50
51
52 Finally, **Figure 4c** shows the polymerase chain reaction (PCR) results after necropsy. The
53
54 hearts were grinded and underwent a total DNA extraction and amplification of a fragment
55
56 within the parasite SOD gene; the hearts of the control animals showed the ubiquitous
57
58 presence of the parasite. In contrast, the hearts from mice treated with compound **2** were
59
60
61
62
63
64
65

1 relatively clean from parasites (33%) and 50% were clean when treated with compound **3**,
2 thus confirming the partial curative effect of these compounds at this dosage. No mice
3 were clean of parasites when they were treated with compound **5**.
4
5

6
7
8 The *in vivo* study clearly showed that compounds **2** and **3** were the two most effective
9 compounds; therefore, they were selected for a deeper study to gain insight into their
10 mechanism of action. In order to improve the effectiveness of compounds **2** and **3**, we must
11 take into consideration an increase in the dosage for future experiments and modify the
12 schedule of treatment for a better exposure of the compound in the bloodstream.
13
14
15

16
17
18 Biochemical clinical parameters were tested in different groups of BALB/c mice infected
19 with *Trypanosoma cruzi* in different experimental situations (**Table 2**), showing that an
20 increase in the dosage does not cause a toxicity risk. All biochemical parameters tested,
21 regarding the kidney, heart and liver profiles, were not altered after compound
22 administration, with the exception of compound **3**, for which the uric acid, urea and CK-
23 MB values increased significantly. The latter could be related to its excretion, which could
24 cause some abnormalities in kidney function. Regarding compound **2**, this analysis could
25 allow us to increase the dosage for a better efficacy, considering that no toxicity was
26 observed. It also remarkable how the LDH parameter, which is a marker of heart damage
27 associated with the presence of parasites, decreased between a 30 and 40% in both
28 treatments compared to the untreated group.
29
30
31
32
33
34
35
36
37
38
39
40
41
42
43
44
45
46

47 **3.4. Metabolite excretion study**

48
49
50
51
52 As trypanosomatids are unable to completely degrade glucose to CO₂, they excrete a
53 considerable portion of their hexose skeleton as partially oxidised fragments in the form of
54 fermented metabolites, whose nature and percentage depend on the pathway used for
55 glucose metabolism ([Bringaud et al., 2006](#); [Ginger, 2005](#)). The catabolism products in
56
57
58
59
60
61
62
63
64
65

1
2
3
4
5
6
7
8
9
10
11
12
13
14
15
16
17
18
19
20
21
22
23
24
25
26
27
28
29
30
31
32
33
34
35
36
37
38
39
40
41
42
43
44
45
46
47
48
49
50
51
52
53
54
55
56
57
58
59
60
61
62
63
64
65

Trypanosoma cruzi were acetate and succinate, with smaller percentages of L-alanine and D-lactate, in agreement with the data in previously published reports (Turrens, 1999). Detection of large amounts of succinate as a major end product is an usual feature, because it relies on glycosomal redox balance, enabling re-oxidation of the NADH produced in the glycolytic pathway. Succinic fermentation requires only half of the phosphoenolpyruvate produced to maintain the NAD⁺/NADH balance, and the remaining pyruvate is converted inside the mitochondria and the cytosol is converted into acetate, D-lactate, L-alanine or ethanol, according to the degradation pathway followed by each species (Michels et al., 2006). In order to obtain some information concerning the effect of the tested compounds on glucose metabolism in the parasites, we obtained ¹H NMR spectra of *T. cruzi* epimastigote forms after treatment with compounds **2** and **3**, from which the final excretion products were identified qualitatively and quantitatively (spectra not shown). The results were compared with those obtained from parasites maintained in a cell-free medium (control) for four days after inoculation with the parasite. The characteristic presence of acetate, succinate, D-lactate and L-alanine was confirmed in the control experiments. As expected, succinate and acetate were the most abundant end products identified. However, after treatment of the parasites with compounds **2** and **3**, the excretion of metabolites was slightly altered at the dosages employed. **Figure 5** displays these modifications with respect to the control at the height of the spectral peaks, corresponding to the most representative final excretion products. Marked differences in the catabolic pathways appeared, which seemed to be connected with the trypanocidal activity mentioned above. The most actives compounds **2** and **3** decreased the amount of succinate by 11 and 10%, respectively; in addition, an increase in the amount of acetate, D-lactate and L-alanine by 22, 21 and 12%, respectively, was found upon treatment with compound **2**, whereas the same metabolites increased by 25, 14 and 15% upon treatment with compound **3**. So, in

1 conclusion, even though the disturbances were quantifiable, we could not attribute the
2 metabolism of the involved enzymes to the direct targets of the compounds.
3

4 5 **3.5. Ultra-structural alterations** 6

7
8 The ultra-structural alterations produced by compounds **2** and **3** were studied against the
9 epimastigote forms of *Trypanosoma cruzi*. As shown in **Figure 6**, comparing to the control
10 (**Figure 6a**), all parasites showed some common disturbances, but we also found some
11 specific alterations. Compound **2** is more active, causing excessive expansion and swelling
12 at the flagellar pocket (FP) and the Golgi apparatus (GA), as shown in **Figure 6b**. The
13 mitochondria appeared extremely swollen and, in some cases, they were empty with a few
14 crypts (**Figure 6c,d**). The number of lipid vacuoles was higher than usual and, in some
15 parasites, there were vesicles in the plasma membrane. This disturbance in the plasma
16 membrane was exclusive at this level and the microtubules were properly engaged. A
17 higher number in ribosomes with a strong density were also noticed. The kinetoplast (K)
18 lost its helical structure and appeared as a dark stain within the mitochondria.
19
20
21
22
23
24
25
26
27
28
29
30
31
32
33
34
35

36 Similar, but less intense, effects were produced by compound **3** (**Figure 6e,f**), in which the
37 mitochondria were much more swollen and disorganised, as in the previous item, and were
38 also present in a lighter shade than usual. The most degenerated structure was that of K,
39 which was almost unrecognisable, showing an enormous size and being completely
40 disorganised. To a lesser extent, the mitochondria were swollen and altered, and a
41 dilatation of the FP could be appreciated. Cytoplasm of the epimastigote forms was filled
42 with vacuoles of different types, some were empty and some contained debris, electron-
43 granules or concentric myelin bands and many lipid vacuoles. The plasma membrane was
44 also altered, with small blisters
45
46
47
48
49
50
51
52
53
54
55
56
57
58

59 **3.6. Inhibitory effect on *T. cruzi* Fe-SOD** 60 61 62 63 64 65

1 The effect of compounds **2** and **3** on *T. cruzi* Fe-SOD was assayed at concentrations
2 ranging from 0.5 to 100 μM . We used epimastigote forms of *T. cruzi*, which excrete Fe-
3 SOD when cultured in a medium lacking inactivated foetal calf serum (FCS) (Villagran et
4 al., 2005). The results are summarised in **Figure 7** together with the corresponding IC_{50}
5 values. **Figure 7b** shows the respective data for Cu–Zn-SOD from human erythrocytes. A
6 comparison of **Figure 7a** and **7b** reveals that, in the case of compound **3**, Fe-SOD was
7 clearly inhibited, whereas the effect on the human Cu–Zn-SOD was substantially lower.
8 Compound **3** caused 100% inhibition of Fe-SOD, even at a concentration of 25 μM , and
9 thus showed a lower IC_{50} value compared to human SOD. Compound **2** did not
10 significantly interfere with any of the SOD species.
11
12
13
14
15
16
17
18
19
20
21
22
23
24

25 Thus, in addition to their effect in glucose catabolism, the compounds interfere with the
26 parasite Fe-SOD. As the mitochondria are an essential part of the antioxidant protective
27 response (Piacenza et al., 2007) the inhibition of Fe-SOD suggests that compound **3** could
28 be a good candidate for the target mentioned. Future modelling studies will be carried out
29 to further investigate this point.
30
31
32
33
34
35
36
37

38 **3.7. Inhibition of TR**

39
40

41 The two polyamines **2** and **3** with the highest anti-parasitic activity were also studied as
42 inhibitors of *T. cruzi* TR. Neither of the compounds showed spontaneous oxidation of
43 NADPH by themselves. At fixed concentrations of 40 and 100 μM of both inhibitor and
44 the substrate trypanothione disulfide (TS_2), the degree of inhibition varied between 23 and
45 72% (**Figure 8**). Compound **3** showed a higher inhibitory activity, reaching 72% at 100
46 μM of the compound and 40 or 100 μM TS_2 , suggesting an inhibition mechanism that is
47 independent of the substrate concentration. Compound **2** was less effective, yielding 23%
48 inhibition when 100 μM of the compound and 40 μM TS_2 were applied. To obtain a deeper
49
50
51
52
53
54
55
56
57
58
59
60
61
62
63
64
65

1 insight into the mode of inhibition, compound **3** was subjected to a detailed kinetic analysis.

2
3 Indeed, Lineweaver–Burk analysis revealed that compound **3** behaves as a mixed-type
4 inhibitor of TR (**Figure 9**). The calculation of the inhibition constants, as described in
5 the Materials and Methods section ([Dixon and Webb, 1986](#)), yielded average K_i and K_i'
6 values of 7 and 49 μM , respectively ($K_i = 40$; $K_i' = 6$ for 28 μM inhibitor and $K_i = 58$; K_i'
7 = 8 for 100 μM inhibitor), so the values for the different concentrations of inhibitor do
8 not differ from the average by more than 12 or 16% for K_i or K_i' , respectively. The lines
9 in the double-reciprocal plot cut above the x -axis, and thus $K_i < K_i'$, which indicates that
10 compound **3** has a higher affinity for the free enzyme compared to the TR–substrate
11 complex.
12
13
14
15
16
17
18
19
20
21
22
23

24 25 **Conclusion**

26
27 The trypanocidal properties of a series of compound derivatives have been examined both
28 *in vivo* and *in vitro*. The experiments allowed us to select compounds that displayed
29 improved efficiency and lower toxicity than the reference drug. Parallel studies have been
30 carried to establish the mechanisms of action. Compound **3** selectively inhibits the Fe-SOD
31 and TR enzymes of the parasite. Moreover, polyamine **3** showed an *in vivo* cure rate of
32 50% at a security standard dosage of 15 mg/Kg body mass. Finally, owing to their
33 promising activity, a further high-level study should be considered to obtain an improved
34 efficiency.
35
36
37
38
39
40
41
42
43
44
45
46
47
48

49 **4. Acknowledgments**

50
51 We acknowledge Generalitat de Catalunya for an ICREA Academia Award (X.R. and
52 M.C.). F.O. is grateful for a FPU Grant from the Ministry of Education of Spain and he
53 also thanks Natalie Dirdjaja and Dr. Alejandro Leroux for their support with the kinetic
54 analysis of TR.
55
56
57
58
59
60
61
62
63
64
65

5. Financial & competing interests disclosure

This work was supported by: Spanish Ministry of Economy and Competitiveness (MINECO), CONSOLIDER-INGENIO 2010 CSD2010-00065. European Research Foundation for Project ERC-2009-StG-239910, MICINN for project CTQ2009-08464. INNPLANTA project INP-2011-0059-PCT-420000-ACT1. Authors declare no conflicts of interest. No written assistance has been required for the content but the English has been corrected by the company *Proof Reading Service* (Devonshire Business Centre. Works Road. Letchworth Garden City. SG6 1GJ. United Kingdom).

REFERENCES:

1
2
3 Beyer, W.F., Fridovich, I. 1987. Assaying for superoxide dismutase activity: some large
4 consequences of minor changes in conditions. *Anal. Biochem.* 161, 559–566.
5
6

7
8
9 Bradford, M.M. 1972. A refined and sensitive method for the quantification of microgram
10 quantities of protein utilizing the principle of protein-dye binding. *Anal. Biochem.* 72,
11 248–254.
12
13
14

15
16
17 Bringaud, F., Rivière, L., Coustou, V. 2006. Energy metabolism of trypanosomatids:
18 adaptation to available carbon sources. *Mol. Biochem. Parasitol.* 149, 1-9.
19
20

21
22
23 Bryan, M.A., Guyach, S.E., Norris, K.A. 2010. Specific humoral immunity versus
24 polyclonal B cell activation in *Trypanosoma cruzi* infection of susceptible and resistant
25 mice. *PLoS Negl. Trop. Dis.* 4, e733.
26
27
28

29
30
31 Cardoso, J., Soares, M.J. 2010. In vitro effects of citral on *Trypanosoma cruzi*
32 metacyclogenesis. *Mem Inst Oswaldo Cruz.* 5, 1026-32.
33
34

35
36
37 Cencig, S., Coltel, N., Truyens, C., et al. 2011. Parasitic loads in tissues of mice infected
38 with *Trypanosoma cruzi* and treated with AmBisome. *PLoS Negl Trop Dis.* 5, e1216.
39
40

41
42
43 Comini, M.A., Dirdjaja, N., Kaschel, M., et al. 2009. Preparative enzymatic synthesis of
44 trypanothione and trypanothione analogues. *Int. J. Parasitol.* 39, 1059–1062.
45
46

47
48
49 Company, A., Prat, I., Frisch, J.R., et al. 2011. Modeling the cis-oxo-labile binding site
50 motif of non-heme iron oxygenases: water exchange and oxidation reactivity of a non-
51 heme iron(IV)-oxo compound bearing a tripodal tetradentate ligand. *Chem. Eur. J.* 17,
52 1622 – 1634.
53
54
55
56
57
58
59
60
61
62
63
64
65

1
2
3
4
5
6
7
8
9
10
11
12
13
14
15
16
17
18
19
20
21
22
23
24
25
26
27
28
29
30
31
32
33
34
35
36
37
38
39
40
41
42
43
44
45
46
47
48
49
50
51
52
53
54
55
56
57
58
59
60
61
62
63
64
65

Costas, M., Que, L.Jr. 2002. Ligand topology tuning of iron-catalyzed hydrocarbon oxidations. *Angew. Chem. Int. Ed.* 41, 2179-218.

Cussó, O., Garcia-Bosch, I., Font, D., *et al.* 2013. Highly stereoselective epoxidation with H₂O₂ catalyzed by electron-rich aminopyridine manganese catalysts. *Org Lett.* 15, 6158-61.

Cussó, O., Garcia-Bosch, I., Ribas, X., *et al.* 2013. Asymmetric epoxidation with H₂O₂ by manipulating the electronic properties of non-heme iron catalysts. *J. Am. Chem. Soc.* 135, 14871–14878.

Cussó, O., Garcia-Bosch, I., Ribas, X., *et al.* 2013. Asymmetric epoxidation with H₂O₂ by manipulating the electronic properties of non-heme iron catalysts. *J. Am. Chem. Soc.* 135, 14871–14878.

Da Silva, C.F., Batista, M.M., Batista, D.G.J., *et al.* 2008. In vitro and in vivo studies of the Trypanocidal activity of a diarylthiophene diamidine against *Trypanosoma cruzi*. *Antimicrob. Agents Chemother.* 9, 3307–3314.

Dixon, M., Webb, E.C. 1986. *Enzymes*; Logman Scientific & Technical: Harlow, Essex, England.

el Bouhdidi, A., Truyens, C., Rivera, M.T., *et al.* 1994. *Trypanosoma cruzi* infection in mice induces a polyisotypic hypergammaglobulinaemia and parasite-specific response involving high IgG2a concentrations and highly avid IgG1 antibodies. *Parasite Immunol.* 16, 69-76.

Fernandez-Becerra, C., Sánchez-Moreno, M., Osuna, A. *et al.* 1997. Comparative aspects of energy metabolism in plant trypanosomatids. *J Eukaryotic Microbiol.* 44, 523–529.

1 Garcia-Bosch, I., Gómez, L., Polo, A., *et al.* 2012. Stereoselective Epoxidation of Alkenes
2 with Hydrogen Peroxide using a Bipyrrolidine-Based Family of Manganese Complexes.
3
4 Adv. Synth. Catal. 354, 65 – 70.
5
6

7
8 Ginger, M.L. 2005. Trypanosomatid biology and euglenozoan evolution: new insights and
9 shifting paradigms revealed through genome sequencing. Protist. 156, 377-92.
10

11
12
13 González, P., Marín, C., Rodríguez-González, I., Hitos, A.B., *et al.* 2005. In vitro activity
14 of C20-diterpenoid alkaloid derivatives in promastigotes and intracellular amastigotes of
15
16
17
18
19 Leishmania infantum. Int J Antimicrob Agents. 25, 136-141.
20

21
22 Lopez-Cespedes, A., Villagran, E., Briceño-Alvarez, K., *et al.* 2012. Trypanosoma cruzi:
23 seroprevalence detection in suburban population of Santiago de Queretaro(Mexico). Sci
24
25
26
27 World J,DOI: 10.1100/2012/914129.
28

29
30 Mckerrow, J.H., Doyle, P.S., Engel, J.C., *et al.* 2009. Two approaches to discovering and
31
32
33
34 developing new drugs for Chagas disease. Mem Inst Oswaldo Cruz. 104, 263–269.
35

36
37 Michels, P.M.A., Bringaud, F., Herman, M., *et al.* 2006. Metabolic functions of
38
39
40
41
42 glycosomes in trypanosomatids. Biochimica et Biophysica Acta 1763, 1463-1477.
43

44
45 Nwaka, S., Besson, D., Ramirez, B., *et al.* 2011. Integrated dataset of screening hits against
46
47
48
49
50 multiple neglected disease pathogens. PLoS Negl. Trop. Dis. 5, e1412.
51

52
53 Olmo, F., Escobedo-Ortegón, J., Palma, P., *et al.* 2014. Specific primers design based on
54
55
56
57
58
59
60
61
62
63
64
65 the superoxide dismutase b gene for Trypanosoma cruzi as a screening tool: Validation
method using strains from Colombia classified according to their discrete typing unit.
Asian Pac J Trop Med. 854-859.

1
2
3
4
5
6
7
8
9
10
11
12
13
14
15
16
17
18
19
20
21
22
23
24
25
26
27
28
29
30
31
32
33
34
35
36
37
38
39
40
41
42
43
44
45
46
47
48
49
50
51
52
53
54
55
56
57
58
59
60
61
62
63
64
65

Olmo, F., Marín, C., Clares, M.P., *et al.* 2013. Scorpiand-like azamacrocycles prevent the chronic establishment of *Trypanosoma cruzi* in a murine model. *Eur J Med Chem.* 70, 189-198.

Olmo, F., Rotger, C., Ramírez-Macías, I., Martínez, L., Marín, C., Carreras, L., Urbanová, K., Vega, M., Chaves-Lemaur, G., Sampedro, A., Rosales, M.J., Sánchez-Moreno, M., Costa, A. 2014. Synthesis and Biological Evaluation of N,N'-Squaramides with High in Vivo Efficacy and Low Toxicity: Toward a Low-Cost Drug against Chagas Disease. *J Med Chem.* 13;57(3), 987-99.

Piacenza, L., Irigoín, F., Alvarez, M.N., *et al.* 2007. Mitochondrial superoxide radicals mediate programmed cell death in *Trypanosoma cruzi*: cytoprotective action of mitochondrial iron superoxide dismutase overexpression, *Biochem. J.* 403, 323-334.

Piacenza, L., Peluffo, G., Alvarez, M.N., *et al.* 2013. *Trypanosoma cruzi* antioxidant enzymes as virulence factors in Chagas disease. *Antioxid Redox Signal.* 19, 723-34.

Romanha, A.J., Lisboa de Castro, S., Correia Soeiro, M.N., *et al.* 2010. In vitro and in vivo experimental models for drug screening and development for Chagas disease. *Mem Inst Oswaldo Cruz* 105, 233-238.

Sullivan, F.X., Walsh, C.T. 1991. Cloning, sequencing, overproduction and purification of trypanothione reductase from *Trypanosoma cruzi*. *Mol. Biochem. Parasitol.* 44, 145-147.

Téllez-Meneses, J., Mejía-Jaramillo, A.M., Triana-Chávez, O. 2008. Biological characterization of *Trypanosoma cruzi* stocks from domestic and sylvatic vectors in Sierra Nevada of Santa Marta, Colombia. *Acta Trop.* 108, 26–34.

Turrens, J. 1999. More differences in energy metabolism between trypanosomatidae. *Parasitol. Today* 15, 346-348.

1 Villagran, M.E., Marin, C., Rodriguez-González, I., *et al.* 2005. Use of an iron superoxide
2 dismutase excreted by *T. cruzi* in the diagnosis of Chagas disease: Seroprevalence in rural
3 zones of the state of Queretaro, Mexico. *Am. J. Trop. Med. Hyg.* 73, 510–516.
4
5

6
7
8 World Health Organization. Chagas disease (American trypanosomiasis). WHO, Geneva,
9 Switzerland (2012). Fact sheet No. 340.
10

11
12
13 Ye, X., Ding, J., Zhou, X., *et al.* 2008. Divergent roles of endothelial NF-kappaB in multiple
14 organ injury and bacterial clearance in mouse models of sepsis. *J Exp Med.* 205, 1303–
15 1315.
16
17
18
19
20
21
22
23
24
25
26
27
28
29
30
31
32
33
34
35
36
37
38
39
40
41
42
43
44
45
46
47
48
49
50
51
52
53
54
55
56
57
58
59
60
61
62
63
64
65

FIGURES & LEGENDS

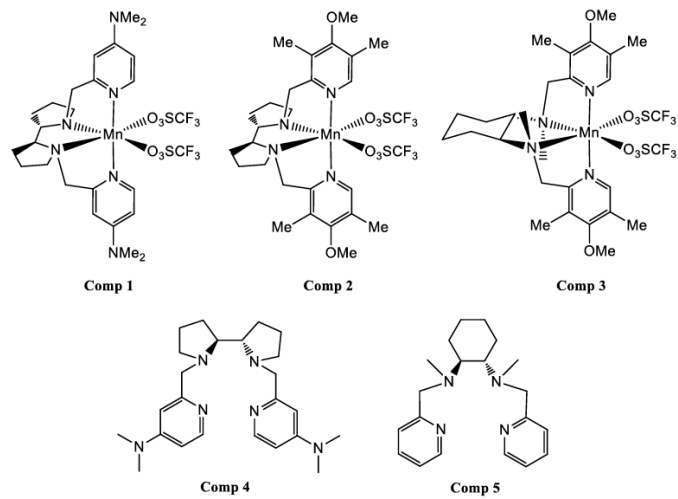


Figure 1. Structure of the tetraamine-based compounds screened in this study.

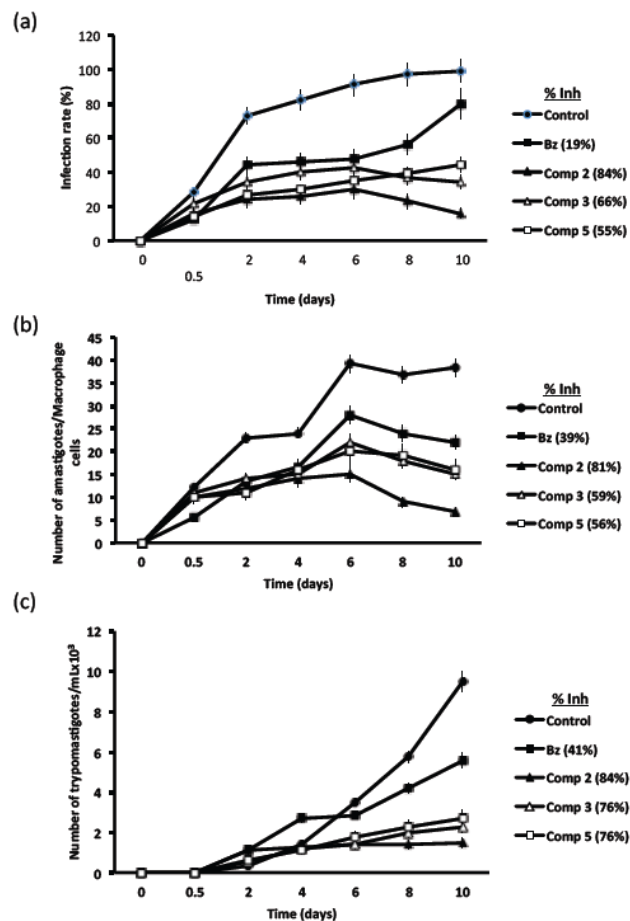


Figure 2. Effect of compounds 2, 3, 5 and Bz on the infectivity of *T. cruzi* in Vero cells. (a) Rate of infection, (b) mean number of amastigote forms per infected Vero cell and (c) number of trypomastigote forms in the culture medium after treatment with the IC₂₅ of the control (filled circles), Bz (filled squares), compound 2 (filled triangles), compound 3 (open triangles) and compound 5 (open squares). The results are the mean values of three separate experiments and the error bars represent the mean \pm standard deviation.

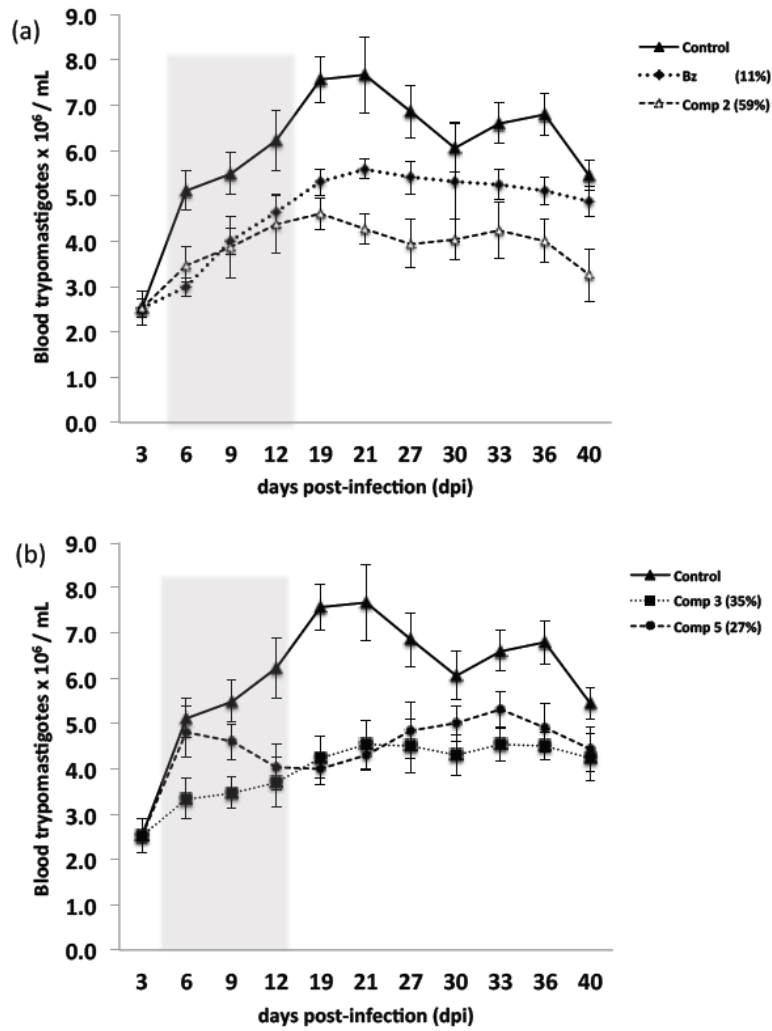


Figure 3. Parasitemia in the murine model of acute Chagas disease (a and b). Control (filled triangles) and doses of 15 mg/kg body mass of Bz (filled rhombus), compound 2 (open triangles), compound 3 (filled squares) and compound 5 (filled circles). The grey shading represents the days of treatment. Values are the means of six separate mice and error bars represent the mean +/- standard deviation.

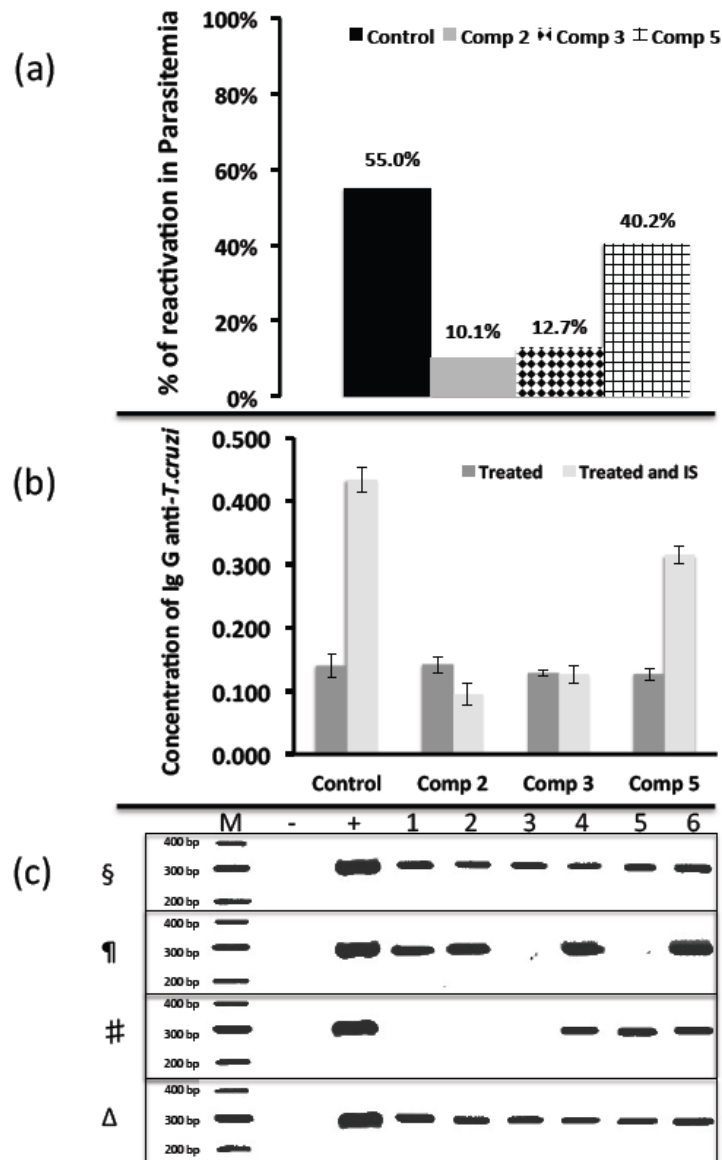


Figure 4. Post-mortem analyses on the final day after necropsy. (a) Percentage of reactivation of blood parasitemia after immunosuppression, (b) total Ig-G levels of anti-*T. cruzi*, where the error bars represent the mean \pm standard deviation and (c) PCR of mouse heart tissue. M, marker; -, PCR negative control; +, PCR positive control; lanes 1–3 represent the non-IS mice in the final days of the experiment; lanes 4–6 represent the IS mice; §, infection control group; ¶, infected and treated with compound 2; #, infected and treated with compound 3; Δ, infected and treated with compound 5.

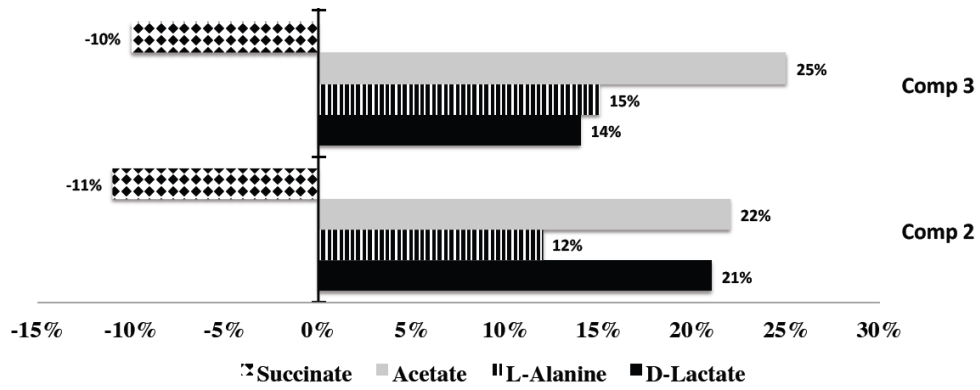


Figure 5. Variation percentages in the height of the peaks corresponding to metabolites excreted by *T. cruzi* epimastigote forms in the presence of tetradentate polyamines at their IC₂₅ compared to a control sample. Values are the means of three separate experiments and error bars represent the mean +/- standard deviation.

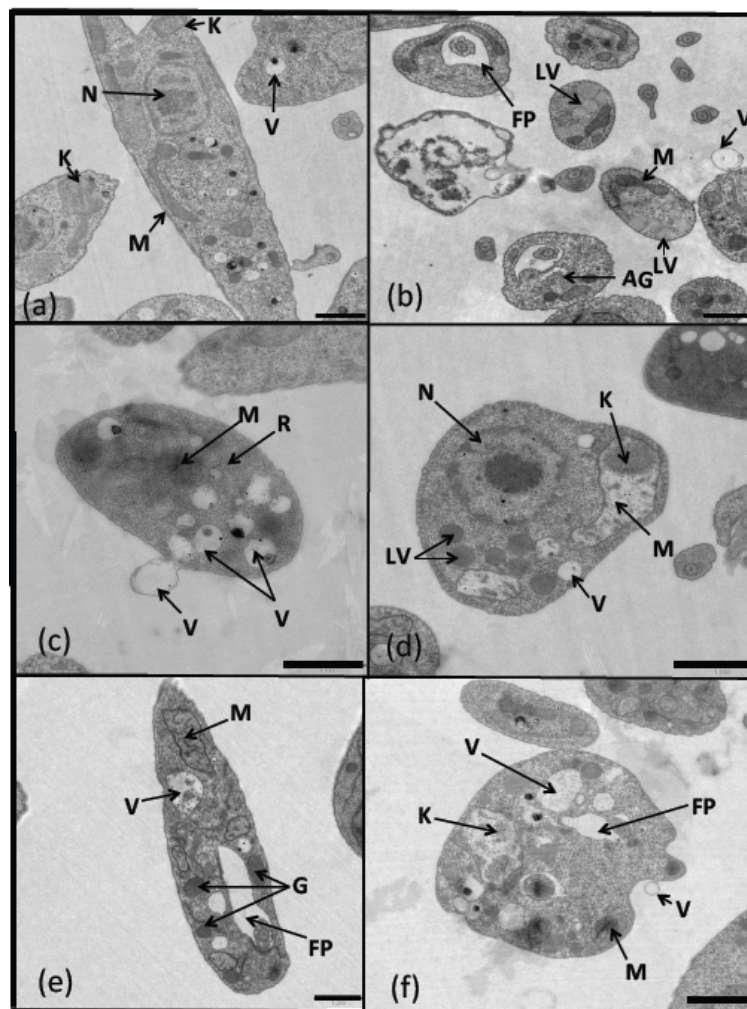


Figure 6. Ultra-structural alterations of epimastigote forms of *Trypanosoma cruzi* treated with tetradentate polyamines. (a) Control of *T. cruzi* with typical aspect, (b–d) epimastigote forms treated with compound 2, (e–f) epimastigote forms treated with compound 3. Structures codes: nucleus (N), mitochondrion (M), kinetoplast (K), ribosomes (R), glycosomes (G), Flagellar pocket (FP), lipid vacuoles (LV) and vacuoles (V). Scale bar = 1 μ m.

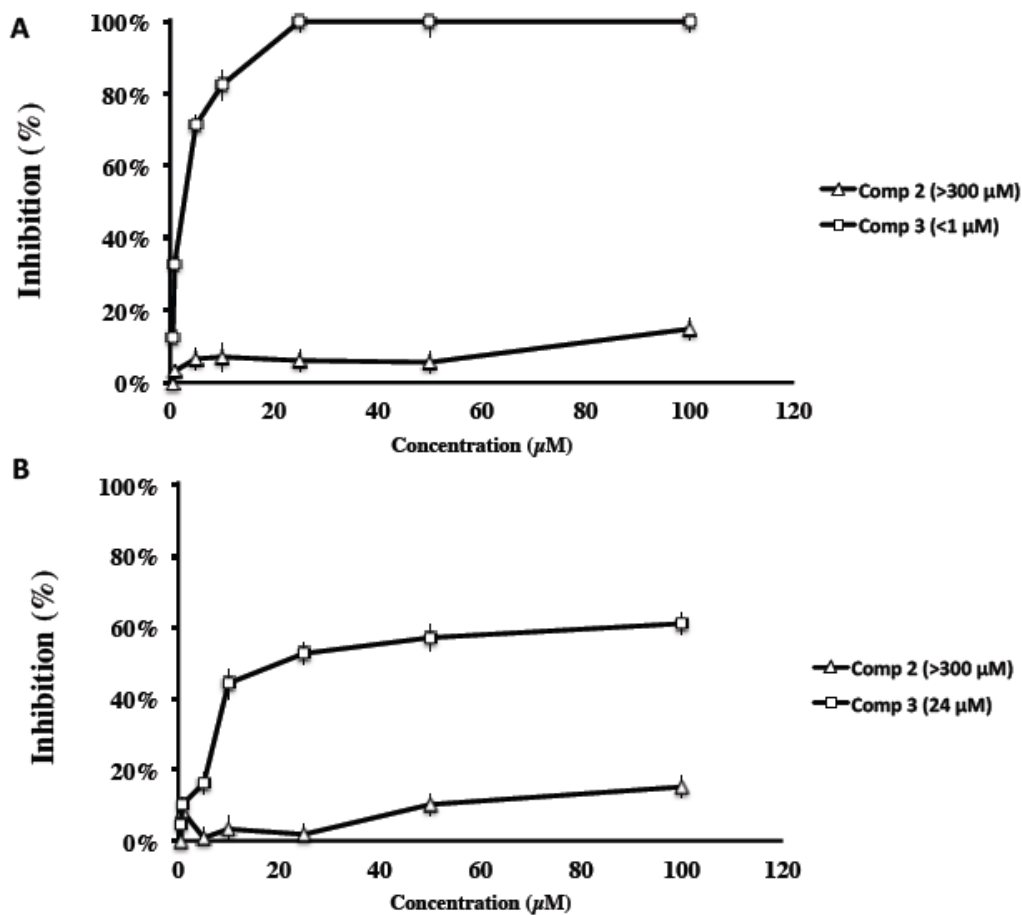


Figure 7. (a) *In vitro* inhibition (%) of Fe-SOD from *T. cruzi* epimastigote forms by the compounds (activity 20.77/3.18 U/mg). (b) *In vitro* inhibition (%) of Cu-Zn-SOD from human erythrocytes for the compounds (activity 23.36/4.21 U/mg). The differences between the activities of the control homogenate and those incubated with compounds were obtained according to the Newman-Keuls test. Values in the legend represented in brackets are the IC_{50} , which is the concentration required to give 50% inhibition and was calculated by linear-regression analysis from the K_c values at the concentrations employed (0.5–100 μM). The values are the average of three separate determinations and the error bars represent the mean \pm standard deviation.

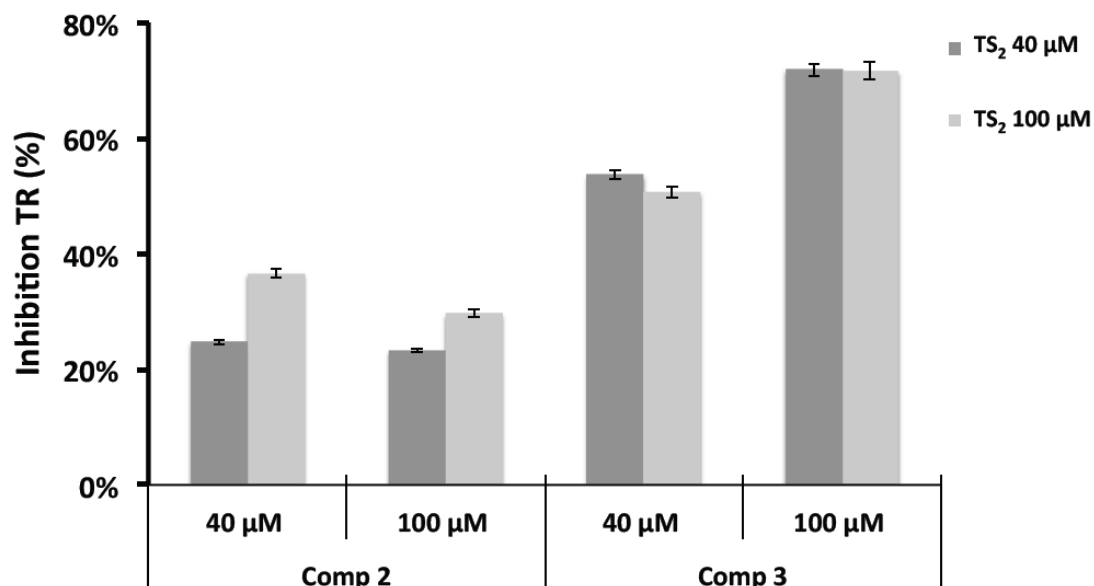


Figure 8. Inhibition of TcTR by polyamines **2** and **3**. The activity was measured following the NADPH consumption at 340 nm, as described in the Experimental Section. The control used to obtain 100% activity was assayed without an inhibitor, but the same amount of water used to dissolve the compound. The values are the average of two independent measurements and the error bars show the mean \pm standard deviation.

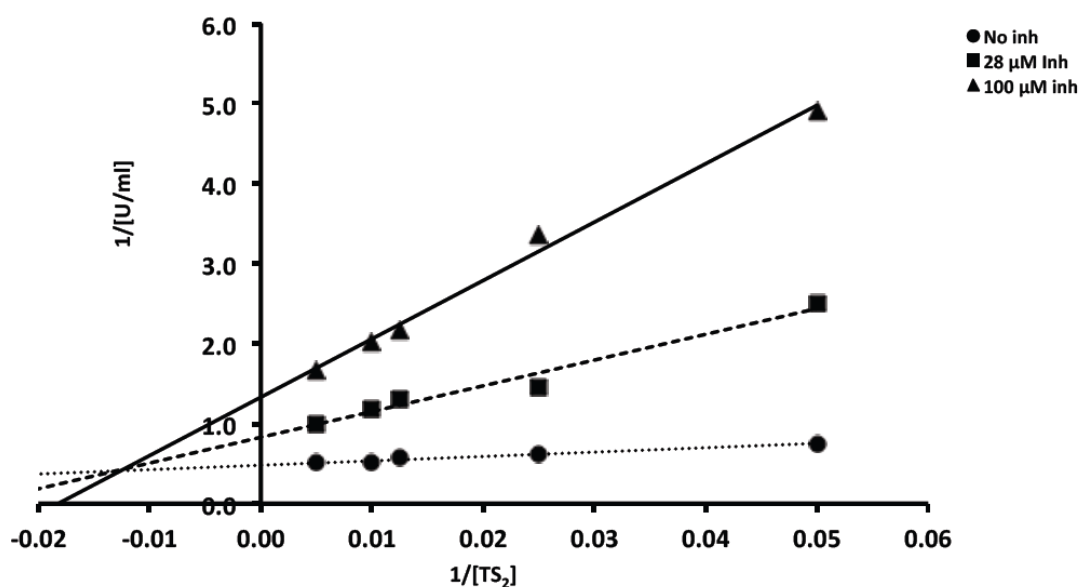


Figure 9. Lineweaver–Burk plot for the inhibition of TcTR by compound **3**. The assays contained 100 μM NADPH and either zero or a fixed concentration of inhibitor, as indicated in the graph. The TS₂ concentration was varied between 20, 40, 80, 100 and 200 μM.

Table 1. In vitro activity, toxicity and selectivity index for the polyamine compounds and complexes on different forms of *Trypanosoma cruzi*.

Compound	IC ₅₀ (μM) ^a			Toxicity IC ₅₀ Vero Cell (μM)			SI ^b		
	Epimastigote forms	Amastigote forms	Trypomastigote forms	Epimastigote forms	Amastigote forms	Trypomastigote forms	Epimastigote forms	Amastigote forms	Trypomastigote forms
Bz	15.8±1.1	23.3±4.6	22.4±1.9	13.6±0.9	0.8	0.6	0.6		
Comp 1	41.5±3.0	22.7±1.4	23.5±1.8	31.0±2.3	0.7 (1)	1.4 (2)	1.3 (2)		
Comp 2	8.2±0.6	1.2±0.2	1.4±0.2	78.0±11.0	9.5 (12)	65 (108)	55.7 (93)		
Comp 3	13.6±0.9	9.1±0.3	4.4±0.2	88.1±12.0	6.5 (8)	9.7 (16)	20 (33)		
Comp 4	33.6±0.7	14.5±0.8	9.5±0.5	108.0±10.0	3.2 (4)	7.5 (12)	11.4 (19)		
Comp 5	10.4±0.3	14.4±0.5	13.6±0.7	248.3±8.6	23.9 (30)	17.2 (29)	18.3 (30)		

The values are the mean plus standard deviation derived from four separate determinations. ^aIC₅₀ = the concentration that inhibits cell proliferation by 50%. In each case, the IC₅₀ was estimated using the regression function with higher goodness of fit (R²), at six different concentrations (0.1 to 100 μM). ^b Selectivity Index = IC₅₀ Vero cells/IC₅₀ *T. cruzi*. The numbers in parenthesis give the ratio of SI values for the compound compared to the reference drug benznidazole (Bz).

Table 2. Summarizes the Biochemical clinical parameters tested in different groups of Balb/c Mice infected with *Trypanosoma cruzi* at different experimental situations.

	Kidney markers profile		Heart markers profile			Liver markers profile		
	UREA (mg/dL)	URIC ACID (mg/dL)	CK-MB (U/L)	LDH (U/L)	AST/GOT (U/L)	ALT/GPT (U/L)	TOTAL BILIRUBIN(mg/dL)	ALKALYNE PHOSPHATASE (U/L)
UNINFECTED MICE (n=15)	39 [36-43]	5 [4.3-5.5]	453 [215-690]	3086 [2108-4064]	126 [103-148]	46 [37-54]	0.23 [0.17-0.28]	133 [104-161]
INFECTED MICE- ACUTE PHASE (n=15)	49 [39-60]	4.5 [3.7-5.5]	681 [400-950]	2910 [1589-4232]	129 [100-157]	48 [38-58]	0.15 [0.12-0.18]	231 [161-300]
120 days POST INFECTION MICE (n=6)	40	4.56	742	3104	133	52.34	0.209	164.5
120 days POST INFECTION and TREATED MICE (n=6)	=	-	=	--	--	=	=	=
120 days POST INFECTION and TREATED MICE (n=6)	+++	+	+++	--	--	=	=	=

Key: = variation no larger than 10 %; +, up to 10% of increasing over the range; ++, up to 30% of increasing over the range; +++, up to 40% of increasing over the range; +++++, more than 50% of increasing over de range; -, up to 10% of decreasing over the range; --, up to 30% of decreasing over the range; ---, up to 40% of decreasing over the range; ----, more than 50% of decreasing over de range.

TRSTMH

Tetradentate polyamines as highly efficient metallodrugs for Chagas disease treatment in murine model --Manuscript Draft--

Article Type:	Full Length Article
Full Title:	Tetradentate polyamines as highly efficient metallodrugs for Chagas disease treatment in murine model
Abstract:	<p>Background: to identify new compounds to treat Chagas disease during acute phase with higher activity and less toxicity than the reference drug benznidazole is a current challenge for Tropical Medicine.</p> <p>Methods: a series of compound-based compounds was prepared and their trypanocidal effects against <i>Trypanosoma cruzi</i> and cytotoxicity were determined through the determination of IC50 values. In vivo assays were performed in mice, where parasitaemia levels were quantified by fresh blood examination and the assignment of a cure was determined by PCR and reactivation of blood parasitaemia levels after immunosuppression. The mechanisms of action were elucidated at metabolic and ultra-structural levels, by 1H NMR, Fe-SOD inhibition, and TEM studies</p> <p>Results: high-selectivity indexes observed in vitro were the basis of promoting one of the tested compounds to in vivo assays. Compound 6 induced a remarkable decrease in the reactivation of parasitaemia after immunosuppression and curative rates of 33%. Compound 6 turned out to be a great inhibitor of Fe-SOD.</p> <p>Conclusions: The experiments allowed us to select a compound that displayed improved efficiency and lower toxicity than the reference drug. Compound 6 is a promising candidate for treating Chagas disease, but a further high-level study should be considered to obtain an improved efficiency.</p>
Manuscript Number:	TRSTMH-D-14-00357
Order of Authors:	Francisco Olmo Miquel Costas Clotilde Marín Maria José Rosales Rubén Martín-Escolano Olaf Cussó Xavi Ribas Manuel Sánchez-Moreno, PhD
Suggested Reviewers:	Enrique Gracia-España enriquegarcia-es@uv.es Fred Opperdoes opperdoes@bchm.ucl.ac.be Juan Manuel Salas Peregrín jsalas@ugr.es
Opposed Reviewers:	



DEPARTAMENTO DE PARASITOLOGÍA
GRUPO CTS944 _ PARASITOLOGÍA MOLECULAR
FACULTAD DE CIENCIAS

Granada, 09/12/14

Dr. Manuel Sánchez Moreno
e-mail: msanchem@ugr.es

To: The Editor
Transactions of the Royal Society of Tropical Medicine & Hygiene

Dear editor,

Please find enclosed the manuscript entitled "Tetradentate polyamines as highly efficient metallodrugs for Chagas disease treatment in murine model." by Olmo et al. to be considered for publication in Transactions of the Royal Society of Tropical Medicine & Hygiene (TRSTMH).

In this article we describe the synthesis and antiprotozoal activity of tetradentate polyamines against different *in vitro* morphological forms of *Trypanosoma cruzi* and *in vivo* activity in murine model. Most derivatives showed *in vitro* activities similar or higher than those of the reference drug benznidazole; this fact, along with low unspecific cytotoxicities against Vero cells shown by some of them, led to very good selectivity indexes (SI). The high efficiency of these derivatives against *T. cruzi* was confirmed by further *in vitro* studies on infection rates and by an additional *in vivo* study in a murine model from the acute to the chronic phase of Chagas disease. Complementary analyses of the changes in the metabolites excreted by the parasite and on the ultrastructural disturbances induced after treatment with the most efficient derivatives were also conducted. As mentioned in the article, the drugs currently used to treat Chagas disease are decades old and have many limitations including high toxicity; therefore the search for new drugs is urgently needed; we think that our contribution is interesting and rather complete, including *in vitro* and *in vivo* preclinical studies in a model of acute and chronic Chagas disease and also search for its mechanism of action. For all the reasons explained before we believe that it merits publication in Transactions of the Royal Society of Tropical Medicine & Hygiene.

Thank you very much for taking in count this manuscript.

Yours sincerely,

Dr. Manuel Sánchez Moreno
Professor in Parasitology
Departamento de Parasitología.
Facultad de Ciencias (Edificio Mecenaz) Severo Ochoa s/n
18001-Granada. España
Phone: +34-958-242369
Fax: +34-958-243174
e-mail: msanchem@ugr.es

Tetradentate polyamines as highly efficient metalloodrugs for Chagas disease treatment in murine model

**Francisco Olmo,¹ Miquel Costas,² Clotilde Marín,¹ Maria José Rosales,¹ Rubén
Martín-Escolano,¹ Olaf Cussó,² Xavi Ribas,² Manuel Sánchez-Moreno^{1,*}**

¹Departamento de Parasitología, Facultad de Ciencias, Universidad de Granada, E-18071
Granada, Spain.

²QBIS Research Group, Institut de Química Computacional i Catàlisi (IQCC), and
Departament de Química, Universitat de Girona. Campus de Montilivi, E-17071, Girona,
Spain.

*Corresponding author. Tel: +34-958-242369; Fax: +34-958-243174; E-mail:
msanchem@ugr.es

ABSTRACT

Background: to identify new compounds to treat Chagas disease during acute phase with higher activity and less toxicity than the reference drug benznidazole is a current challenge for Tropical Medicine.

Methods: a series of compound-based compounds was prepared and their trypanocidal effects against *Trypanosoma cruzi* and cytotoxicity were determined through the determination of IC₅₀ values. *In vivo* assays were performed in mice, where parasitaemia levels were quantified by fresh blood examination and the assignment of a cure was determined by PCR and reactivation of blood parasitaemia levels after immunosuppression. The mechanisms of action were elucidated at metabolic and ultra-structural levels, by ¹H NMR, Fe-SOD inhibition, and TEM studies

Results: high-selectivity indexes observed *in vitro* were the basis of promoting one of the tested compounds to *in vivo* assays. Compound **6** induced a remarkable decrease in the reactivation of parasitaemia after immunosuppression and curative rates of 33%. Compound **6** turned out to be a great inhibitor of Fe-SOD.

Conclusions: The experiments allowed us to select a compound that displayed improved efficiency and lower toxicity than the reference drug. Compound **6** is a promising candidate for treating Chagas disease, but a further high-level study should be considered to obtain an improved efficiency.

Keywords: trypanosomiasis, chemotherapy, polyamines, murine model

Introduction

The World Health Organisation (WHO) lists Chagas disease as one of the most neglected tropical diseases. Chagas disease is endemic in Latin America; it is estimated that 10 million people are infected worldwide and more than 25 million are living at risk of infection.¹ The main drugs used for the treatment of Chagas disease are benznidazole (Bz, LAFEPE) and nifurtimox (Lampit[®], Bayer), which present significant side effects and cure <20% of patients with chronic Chagas disease.² Thus, many researchers have combined efforts to discover drugs against new targets, looking for lower toxicity and a greater tolerance in patients, aiming not only for efficiency in the acute phase, but also in the chronic phase.

One of the self-defence strategies of *Trypanosoma cruzi* (the etiological agent of Chagas disease) is its highly active and exclusive iron superoxide dismutase (Fe-SOD), which differs from Cu–Zn-SOD or Mn-SOD operating in mammals. Fe-SOD is an extremely efficient enzyme for preventing any oxidative damage from the host in combination with peroxidases. The other self-defence strategy is trypanothione, a parasitic molecule involved in protozoan protection against oxidative stress, which is now considered a virulence factor of Chagas disease.³ Thus, the use of molecules that interfere with the enzyme trypanothione reductase (TR), which keep the trypanothione molecule in its reduced status, may lead to parasite death. In this sense, we focused on complexes capable affecting or interfering with these exclusive enzymes of *T. cruzi*.

In previous work, we designed iron and manganese coordination complexes containing polyamine ligands, which are capable of generating highly oxidising species.^{4–6} Highly reactive Mn(IV)=O and Fe(IV)=O species embedded in these ligand scaffolds have been prepared and their oxidative reactivity studied. Furthermore, these polyamine ligands bind

very strongly to iron and manganese ions, forming coordination complexes that are stable under highly acidic and oxidative conditions.

Herein, we report on the *in vitro* and *in vivo* anti-trypanosomal properties of Mn-based polyamines and polyamine complexes (**Figure 1**), which represent a class of compounds that have, so far, only rarely been explored for Chagas disease chemotherapy. Finally, we analyse the possible mechanism of action over the parasite structure and function as well as the protective enzymes mentioned above.

Materials and methods

Chemistry

Comp 4 was purchased from Catexcel. Compounds 1,⁷ 3,⁸ 5,⁷ 6,⁹ were prepared as described in the literature.

Synthesis of comp 2: Comp **4** (47.1 mg, 0.14 mmols) was dissolved in acetonitrile (1 mL). A solution of FeCl₂ (36.2 mg, 0.28 mmols) in acetonitrile (2 mL) was prepared under inert atmosphere. The solution of FeCl₂ was added dropwise at room temperature to the solution of **4**, the mixture turned pale yellow and was stirred at room temperature for 1 hour. Then, AgClO₄ (114.7 mg, 0.55 mmols) was added and the formation of a white precipitate was observed. The mixture was stirred over 30 minutes. Afterwards a white powder and a purple solution were clearly distinguished. The purple solution was filtered through syringe filters (25 mm Ø) and the white precipitate was washed with CH₃CN until the filtrates become colorless. 121 mg of purple crystals (0.11 mmols, 80 %) were obtained after diffusion with ethyl ether. Molecular structure was confirmed by single crystal X-ray diffraction. Crystals loose acetonitrile upon drying under vacuum, but color is instantaneously recovered upon solution in acetonitrile. **ESI/MS (CH₃CN):** 749.1 [M - 6CH₃CN - ClO₄]⁺, 685.0 [Fe^{II}₂(ClO₄)₂(OH)(H₂O)(TACN₂)]⁺. **¹H-NMR (CD₃CN):** 110.7,

103.3, 65.8, 38.4, 36.0, 33.1 ppm. **Elemental analysis:** Anal Calcd. for $[(C_{18}H_{40}N_6)Fe(CH_3CN)_3](ClO_4)_4$: C, 29.62 %; N, 12.95 %; H, 5.07%. Found: C, 28.9 %; N, 12.95 %; H, 5.08 %.

Biological activity: *In vitro* assays

Antimicrobial properties of the compounds were firstly evaluated *in vitro* against epimastigote, amastigote and trypomastigote forms of *T. cruzi*, and Vero cells were used for the determination of unspecific cytotoxicity, according to the methodology described by us.¹⁰ These studies were complemented by infectivity assays on Vero cells with the most active compounds, representing a reproduction of the lifecycle *in vitro*.

Biological activity: *In vivo* assays

The *in vivo* trypanocidal activities of the compounds were studied using a murine model from acute to chronic phases of Chagas disease, according to our previously published procedures.¹¹ Toxicity testing was also included to determinate the potential damage that the compounds could cause for the host, which was measured by analysing different biochemical parameters as markers of the kidney, heart and liver profiles.

Mechanism of action

In order to get an insight into the molecular mode of action of the compounds, a ¹H NMR study was conducted, according to a previously published procedure,¹⁰ and the changes in the nature and quantity of the excreted metabolites were examined to gain information about the effect of the compounds on the energetic metabolism of parasites. In addition, ultra-structural alterations of the parasites treated with the compounds were investigated using transmission electron microscopy (TEM). The ability of the compounds to interfere with the antioxidant defence of the parasites was evaluated by studying them as putative inhibitors of Fe-SOD (in contrast to human Cu–Zn-SOD).¹¹

Results and discussion

In vitro trypanosomicidal evaluation

Five out of seven of the polyamines showed better selectivity indexes ($SI = IC_{50}$ Vero cells/ IC_{50} extracellular and intracellular forms of *T. cruzi*) compared to the reference drug Bz. As summarised in **Table 1**, compound **6**, with SI values 13, 17 and 21 times higher than those of Bz, was the best compound, independent of the parasite stage (epimastigote, amastigote and trypomastigote forms, respectively). This activity meets good criteria to consider it as a strong candidate to undergo *in vivo* studies.

To obtain more accurate information about the most active polyamine, **6**, the development of the parasites in Vero cells was studied by measuring the rates of infection and the average number of amastigote and trypomastigote forms present during a ten-day treatment period. Vero cells were infected with metacyclic forms of *T. cruzi* and the gradual differentiation into amastigote forms was followed. During the observation time, in the control group, the rate of infection of the host cells gradually increased, reaching 99% invasion at the end of the experiment (**Figure 2A**). The test was repeated in the presence of the reference drug and in the presence of compound **6**, at their IC_{25} concentrations. It was found that the rate of infection decreased in all cases, with respect to the control, and compound **6** showed reductions in the infection rate of 81% thus with much a higher efficiency than Bz (19% reduction).

In terms of the average number of amastigote forms per Vero cell (**Figure 2B**), the results were consistent with those mentioned above for infection rates. After treatment, compound **6** significantly reduced the number of amastigote forms per cell by 56%, whereas Bz showed reduction of only a 39%. The average number of amastigote forms increased to a

maximum on the sixth day of culture, but decreased thereafter; the rupture of Vero cells released trypomastigote forms. In terms of the number of trypomastigote forms found per millilitre of culture medium (**Figure 2C**), a maximum was reached on day 10 (9.5×10^3 trypomastigote forms/mL) for the control, whereas this value was substantially reduced by the reference drug (41%), but even more so by compounds **6** (88%). In summary, the results of the parasite spreading in Vero cells are in agreement with those of the trypanocidal activity reported in **Table 1** for intracellular and extracellular forms of *T. cruzi*, with compound **6** being much better than any of the other drug candidates tested.

***In vivo* activity of tetradentate polyamines**

The promising *in vitro* results prompted us to study the *in vivo* activity of this polyamine in female BALB/c mice. As the effectiveness of the drugs currently in use against Chagas disease varies widely between the acute and chronic phase, we decided to evaluate the impact of our compound on both phases. For the acute phase experiments, we considered the first 40 days after infection (dpi), whereas the effect on the chronic phase was studied between days 40 and 120 after infection. The intraperitoneal (i.p.) doping route was preferred over the intravenous procedure, because it is well known that i.p. treatment substantially reduces animal mortality.¹² In fact, no mouse died in any of our experiments with either the control or with the compounds assayed at the concentrations used (15 mg/kg of body mass). However, the survival percentage for the mice treated with Bz was only about 80%. The female mice were inoculated with trypomastigote forms, as described in the material and methods section, and i.p. treatment with the compounds was started five days post-infection and maintained for five alternated days. A group of mice (control group) was treated in the same manner, but using only the vehicle. During the study of acute-phase activity, the level of parasitaemia was determined every two days. **Figure 3** shows the number of trypomastigote forms found during the acute phase (1–40 dpi). On

the day of maximum parasite burden (20–22 days after infection), the tested compound greatly reduced the number of blood trypomastigote forms compared with the control group. Furthermore, compounds **6**, lowered the level of parasitaemia on day 40 by 61%, being this effect significantly greater than that found for the reference drug (11%).

The chemical structure of these coordination complexes is fundamentally different from that of Bz. Therefore, the mechanisms underlying their anti-trypanosomal activity most likely differ, and simple structure–activity correlations should be regarded with caution.

Therefore, these group of mice, treated with polyamine **6** where kept until 120 dpi was achieved under the same conditions. The experiment was concluded with an immunosuppression test on the treated mice 120 days after p.i. (late chronic phase, in which there are no parasites remaining in the bloodstream that are quantifiable by fresh blood analysis). **Figure 4A** shows the reactivation of parasitaemia after immunosuppression. It can be appreciated that the control group recovers half of its initial peak of parasitaemia, with a reactivation of 55 %. In contrast, the treated group show a parasitaemia load of 37.2% with respect to their burden peak when the mice have been administered with compound **6**. ELISA assays offer an alternative method for verifying the effectiveness of these three compounds in the chronic phase after being challenged with an immunosuppression cycle. **Figure 4B** shows the total Ig-G levels of anti-*T. cruzi* and, according to previous reports, the titer of Ig-G in Balb/c becomes stable during chronic phase of the disease;¹³ this is confirmed in **figure 4B**. The control group showed an almost doubling in the Ig-G levels in response to the presence of the parasite in the bloodstream after immunosuppression. However, in the treated group, the differences between immunosuppressed (IS) and non-immunosuppressed (non-IS) groups were smaller and not significant in the case of compound **6**. This means that the parasite-specific Ig-G levels were not higher, just proportional, than the remaining amount of total unspecific Ig-G

caused by the hypergammaglobulinaemia characteristic of the infection by *Trypanosoma cruzi*.¹⁴

Finally, **figure 4C** shows the polymerase chain reaction (PCR) results after necropsy. The hearts were grinded and underwent a total DNA extraction and amplification of a fragment within the parasite SOD gene; the hearts of the control animals showed the ubiquitous presence of the parasite. In contrast, the hearts from mice treated with compound **6** were relatively clean from parasites 33%, thus confirming the partial curative effect of these compounds at this dosage. Biochemical clinical parameters were tested in different groups of BALB/c mice infected with *Trypanosoma cruzi* in different experimental situations (**Table 2**), showing that an increase in the dosage does not cause a toxicity risk. All biochemical parameters tested, regarding the kidney, heart and liver profiles, were not altered after compound administration.

In order to improve the effectiveness of compound **6**, we must take into consideration an increase in the dosage for future experiments and modify the schedule of treatment for a better exposure of the compound in the bloodstream.

Metabolite excretion study

As trypanosomatids are unable to completely degrade glucose to CO₂, they excrete a considerable portion of their hexose skeleton as partially oxidised fragments in the form of fermented metabolites, whose nature and percentage depend on the pathway used for glucose metabolism.^{15,16} The catabolism products in *Trypanosoma cruzi* were acetate and succinate, with smaller percentages of L-alanine and D-lactate, in agreement with the data in previously published reports.¹⁷ Detection of large amounts of succinate as a major end product is an usual feature, because it relies on glycosomal redox balance, enabling re-oxidation of the NADH produced in the glycolytic pathway. Succinic fermentation

requires only half of the phosphoenolpyruvate produced to maintain the NAD^+/NADH balance, and the remaining pyruvate is converted inside the mitochondria and the cytosol is converted into acetate, D-lactate, L-alanine or ethanol, according to the degradation pathway followed by each species.¹⁸ In order to obtain some information concerning the effect of the tested compounds on glucose metabolism in the parasites, we obtained ^1H NMR spectra of *T. cruzi* epimastigote forms after treatment with compound **6**, from which the final excretion products were identified qualitatively and quantitatively (spectra not shown). The results were compared with those obtained from parasites maintained in a cell-free medium (control) for four days after inoculation with the parasite. The characteristic presence of acetate, succinate, D-lactate and L-alanine was confirmed in the control experiments. As expected, succinate and acetate were the most abundant end products identified. However, after treatment of the parasites with compound **6**, the excretion of metabolites was slightly altered at the dosages employed. **Figure 5** displays these modifications with respect to the control at the height of the spectral peaks, corresponding to the most representative final excretion products. Marked differences in the catabolic pathways appeared, which seemed to be connected with the trypanocidal activity mentioned above. The most remarkable differences were the decreased amount of succinate by 17%; in addition, an increase in the amount of acetate, D-lactate and L-alanine by 17, 18 and 21%, respectively, was found upon treatment with compound **6**. So, in conclusion, even though the disturbances were quantifiable, we could not attribute the metabolism of the involved enzymes to the direct targets of the compounds.

Ultra-structural alterations

The ultra-structural alterations produced by compound **6** were studied against the epimastigote forms of *Trypanosoma cruzi*. As shown in **Figure 6**, comparing to the control (**Figure 6A**), where all parasites showed typical structures as nucleus (N), mitochondrion

(M), kinetoplast (K), ribosomes (R) and vacuoles (V), the treated parasites (**Figure 6B**) showed some common disturbances, specially the cytoplasm of the epimastigote forms was filled with vacuoles of different types, some were empty and some contained debris. The mitochondria appeared extremely swollen.

Inhibitory effect on *T. cruzi* Fe-SOD

The effect of compound **6** on *T. cruzi* Fe-SOD was assayed at concentrations ranging from 0.5 to 100 μM . We used epimastigote forms of *T. cruzi*, which excrete Fe-SOD when cultured in a medium lacking inactivated foetal calf serum (FCS).¹⁹ The results are summarised in **Figure 7** together with the corresponding IC_{50} values. It shows the respective data for Cu–Zn-SOD from human erythrocytes and Fe-SOD from the parasite. A comparison reveals that, in the case of the Cu/Zn- SOD the IC_{50} values are over 100 μM , while the same inhibition it is obtained for the Fe-SOD with only 18 μM of compound **6**.

Thus, in addition to their effect in glucose catabolism, the compounds interfere with the parasite Fe-SOD. As the mitochondria are an essential part of the antioxidant protective response,²⁰ the inhibition of Fe-SOD suggests that compound **6** could be a good candidate for the target mentioned. Future modelling studies will be carried out to further investigate this point.

Conclusion

The trypanocidal properties of a series of compound derivatives have been examined both *in vivo* and *in vitro*. The experiments allowed us to select compounds that displayed improved efficiency and lower toxicity than the reference drug. Parallel studies have been carried to establish the mechanisms of action. Compound **6** selectively inhibits the Fe-SOD of the parasite. Moreover, compound **6** showed an *in vivo* cure rate of 33% at a security

standard dosage of 15 mg/Kg body mass. Finally, owing to their promising activity, a further high-level study should be considered to obtain an improved efficiency.

Acknowledgment

We acknowledge Generalitat de Catalunya for an ICREA Academia Award (X.R. and M.C.). F.O. is grateful for a FPU Grant (AP2010-3562) from the Ministry of Education of Spain.

REFERENCES:

- [1] World Health Organization. Chagas disease (American trypanosomiasis). WHO, Geneva, Switzerland (2012) Fact sheet No. 340.
- [2] Mckerrow JH, Doyle PS, Engel JC, et al. Two approaches to discovering and developing new drugs for Chagas disease. *Mem Inst Oswaldo Cruz* 2009;104(1):263–269.
- [3] Piacenza L, Peluffo G, Alvarez MN, Martínez A, Radi A. *Trypanosoma cruzi* antioxidant enzymes as virulence factors in Chagas disease. *Antioxid Redox Signal* 2013;19(7):723-34.
- [4] Cussó O, Garcia-Bosch I, Ribas X, et al. Asymmetric epoxidation with H₂O₂ by manipulating the electronic properties of non-heme iron catalysts. *J Am Chem Soc* 2013;135:14871–14878.
- [5] Garcia-Bosch I, Gómez L, Polo A, et al. Stereoselective Epoxidation of Alkenes with Hydrogen Peroxide using a Bipyrrolidine-Based Family of Manganese Complexes. *Adv Synth Catal* 2012;354:65 – 70.
- [6] Company A, Prat I, Frisch JR, et al. Modeling the cis-oxo-labile binding site motif of non-heme iron oxygenases: water exchange and oxidation reactivity of a non-heme iron(IV)-oxo compound bearing a tripodal tetradentate ligand. *Chem Eur J* 2011;17:1622 – 1634.
- [7] Company A, Gómez L, Fontrodona X, et al. A Novel Platform for Modeling Oxidative Catalysis in Non-Heme Iron Oxygenases with Unprecedented Efficiency. *Chem Eur J* 2008;14:5727-5731.

- [8] Garcia-Bosch I, Company A, Fontrodona X, et al. Efficient and Selective Peracetic Acid Epoxidation Catalyzed by a Robust Manganese Catalyst. *Org Lett* 2008;10:2095-2098.
- [9] Wieghardt K, Schoeffmann E, Nuber B, et al. Syntheses, properties and electrochemistry of transition-metal complexes of the macrocycle 1,4,7-tris(2-pyridylmethyl)-1,4,7-triazacyclononane (L). Crystal structures of [NiL](ClO₄)₂, [MnL](ClO₄)₂, and [PdL](PF₆)₂ containing a distorted-square-base-pyramidal PdIIN5 core. *Inorg Chem* 1986;25:4877-4883.
- [10] Olmo F, Marín C, Clares MP, et al. Scorpiand-like azamacrocycles prevent the chronic establishment of *Trypanosoma cruzi* in a murine model. *Eur J Med Chem* 2013;70:189-198.
- [11] Olmo F, Rotger C, Ramírez-Macías I, et al. Synthesis and biological evaluation of N,N'-squaramides with high in vivo efficacy and low toxicity: toward a low-cost drug against Chagas disease. *J Med Chem* 2014;57(3):987-99.
- [12] Da Silva CF, Batista MM, Batista DGJ, et al. In vitro and in vivo studies of the Trypanocidal activity of a diarylthiophene diamidine against *Trypanosoma cruzi*. *Antimicrob Agents Chemother* 2008;9:3307–3314.
- [13] el Bouhdidi A, Truyens C, Rivera MT, et al. *Trypanosoma cruzi* infection in mice induces a polyisotypic hypergammaglobulinaemia and parasite-specific response involving high IgG2a concentrations and highly avid IgG1 antibodies. *Parasite Immunol* 1994;16(2):69-76.

- [14] Bryan MA, Guyach SE, Norris KA. Specific humoral immunity versus polyclonal B cell activation in *Trypanosoma cruzi* infection of susceptible and resistant mice. PLoS Negl Trop Dis 2010;4(7):e733.
- [15] Bringaud F, Rivière L, Coustou V. Energy metabolism of trypanosomatids: adaptation to available carbon sources. Mol Biochem Parasitol 2006;149(1):1-9.
- [16] Ginger ML. Trypanosomatid biology and euglenozoan evolution: new insights and shifting paradigms revealed through genome sequencing. Protist 2005;156(4):377-92.
- [17] Turrens J. More differences in energy metabolism between trypanosomatidae, Parasitol Today 1999;15:346-348.
- [18] Michels PAM, Bringaud F, Herman M, et al. Metabolic functions of glycosomes in trypanosomatids. Biochimica et Biophysica Acta 2006;1763: 1463-1477.
- [19] Villagran ME, Marin C, Rodriguez-González I, et al. Use of an iron superoxide dismutase excreted by *T. cruzi* in the diagnosis of Chagas disease: Seroprevalence in rural zones of the state of Queretaro, Mexico. Am J Trop Med Hyg 2005;73:510–516.
- [20] Piacenza L, Irigoien F, Alvarez MN, et al. Mitochondrial superoxide radicals mediate programmed cell death in *Trypanosoma cruzi*: cytoprotective action of mitochondrial iron superoxide dismutase overexpression. Biochem J 2007;403:323-334.

FIGURES & LEGENDS:

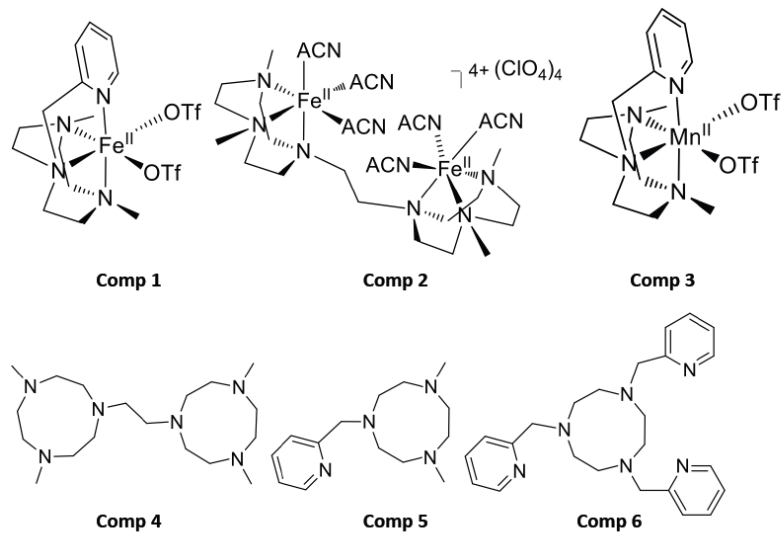


Figure 1. Structure of the tetraamine-based compounds screened in this study.

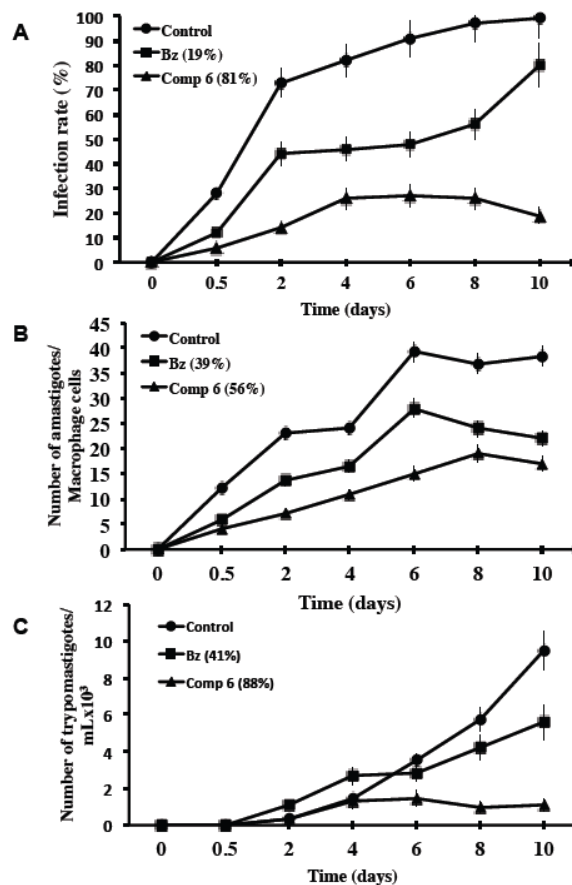


Figure 2. Effect of compound 6, and Bz on the infectivity of *T. cruzi* in Vero cells. (A) Rate of infection, (B) mean number of amastigote forms per infected Vero cell and (C) number of trypomastigote forms in the culture medium after treatment with the IC₂₅ of the control (filled circles), Bz (filled squares), compound 6 (filled triangles). The results are the mean values of three separate experiments and the error bars represent the mean \pm standard deviation.

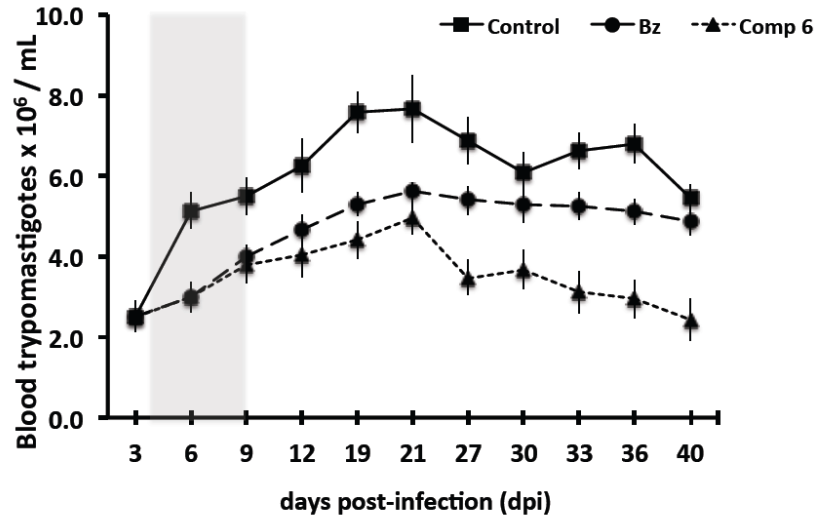


Figure 3. Parasitemia in the murine model of acute Chagas disease. Control (filled squares) and doses of 15 mg/kg body mass of Bz (filled circles), compound **6** (filled triangles). The grey shading represents the days of treatment. Values are the means of six separate mice and error bars represent the mean +/- standard deviation.

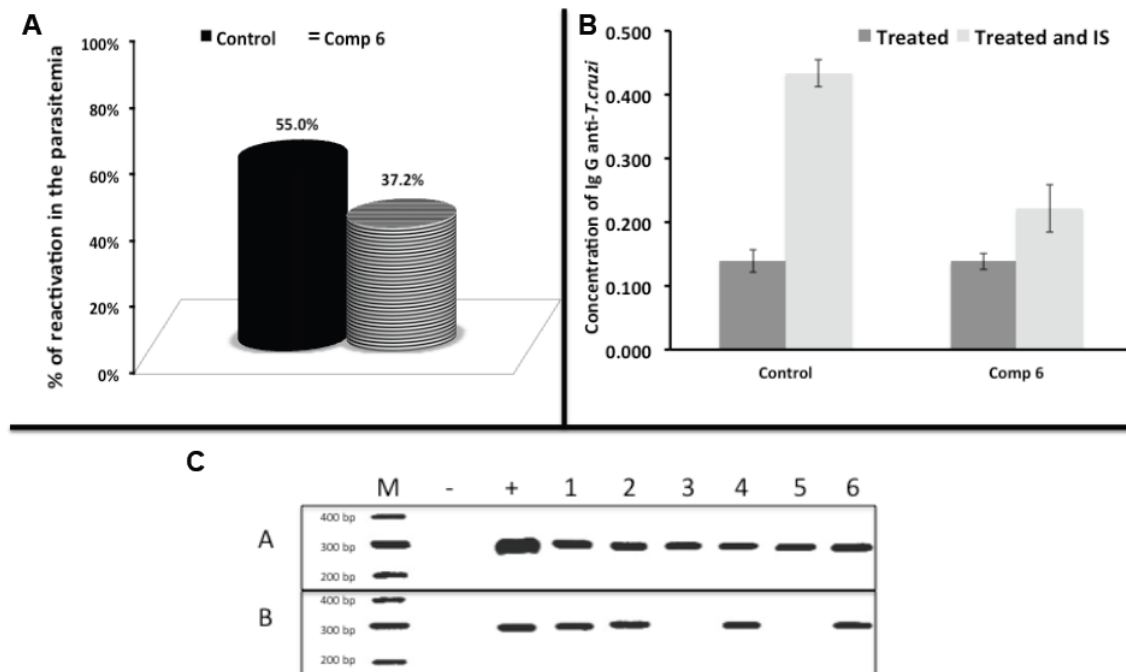


Figure 4. Post-mortem analyses on the final day after necropsy. (A) Percentage of reactivation of blood parasitemia after immunosuppression, (B) total Ig-G levels of anti-*T. cruzi*, where the error bars represent the mean +/- standard deviation of three mice and (C) PCR of mouse heart tissue. M, marker; -, PCR negative control; +, PCR positive control; lanes 1–3 represent the non-IS mice in the final days of the experiment; lanes 4–6 represent the IS mice; A, infection control group; B, infected and treated with compound **6**.

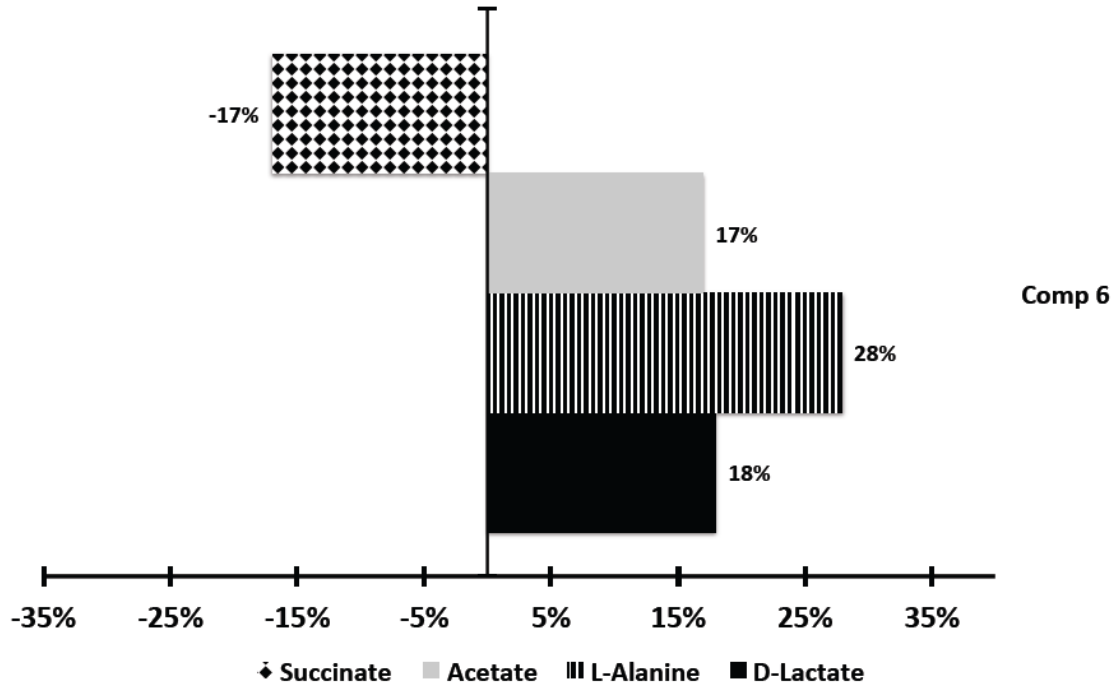


Figure 5. Variation percentages in the height of the peaks corresponding to metabolites excreted by *T. cruzi* epimastigote forms in the presence of comp 6 at its IC₂₅ compared to a control sample.

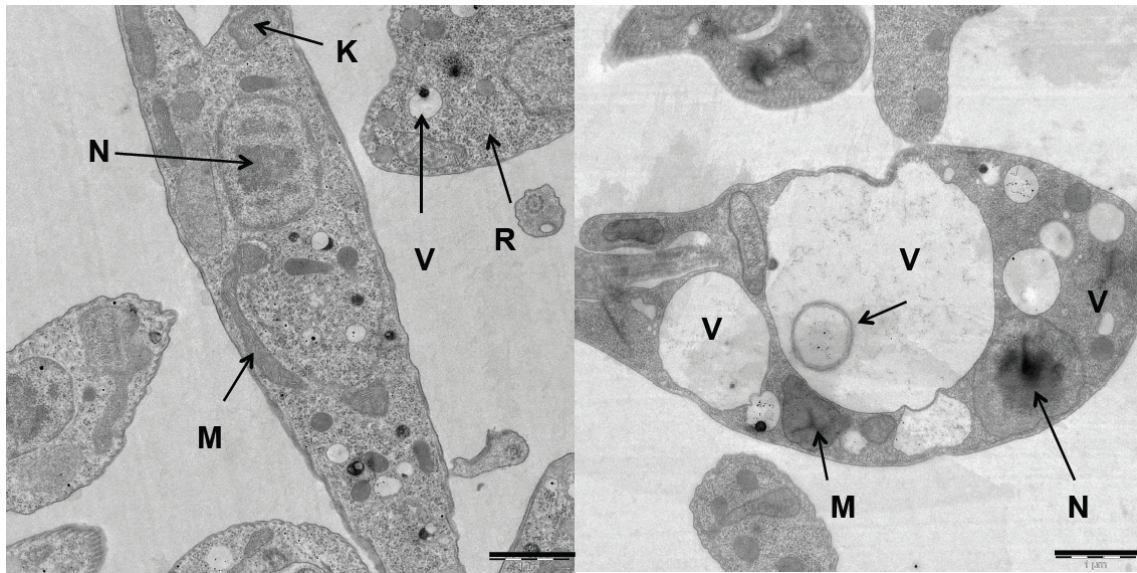


Figure 6. Ultra-structural alterations of epimastigote forms of *Trypanosoma cruzi* treated with comp 6. Left panel represents the control group of *T. cruzi* with typical aspect; Right panel represents epimastigote forms treated with compound 6. Structures codes: nucleus (N), mitochondrion (M), kinetoplast (K), ribosomes (R), glycosomes (G), Flagellar pocket (FP), lipid vacuoles (LV) and vacuoles (V). Scale bar = 1 μ m.

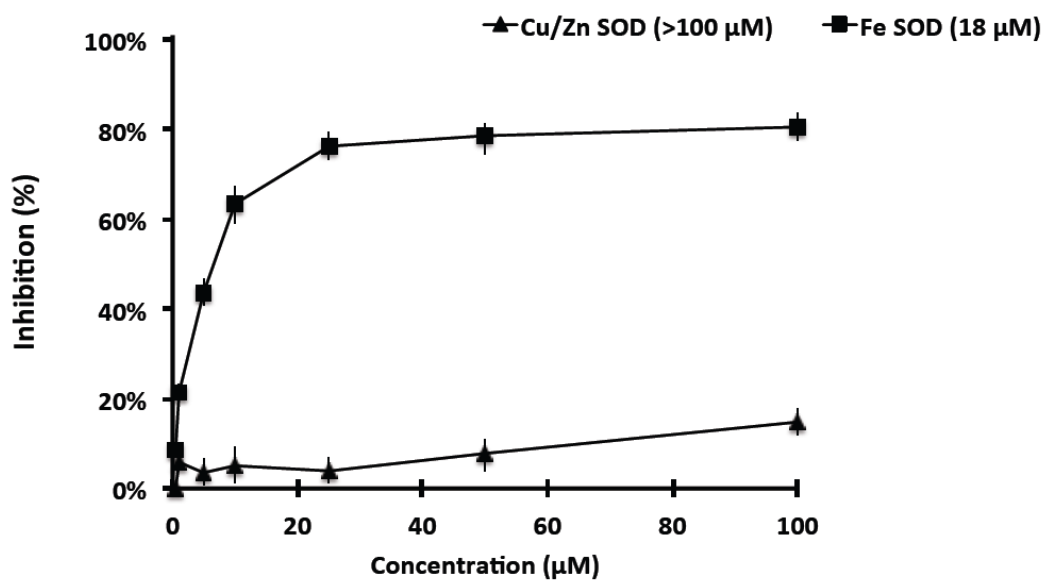


Figure 7. *In vitro* inhibition (%) by the comp 6 of Fe-SOD from *T. cruzi* epimastigote forms (activity 20.77/3.18 U/mg Cu–Zn-SOD from human erythrocytes for the compounds (activity 23.36/4.21 U/mg). The differences between the activities of the control homogenate and those incubated with compounds were obtained according to the Newman–Keuls test. Values in the legend represented in brackets are the IC₅₀, which is the concentration required to give 50% inhibition and was calculated by linear-regression analysis from the *Kc* values at the concentrations employed (0.5–100 µM). The values are the average of three separate determinations and the error bars represent the mean +/- standard deviation.

Table 1. In Vitro Activity, Toxicity and Selectivity Index found for polyaminic compounds complex on extracellular and intracellular forms of *Trypanosoma cruzi*.

Compounds	IC ₅₀ (μM) ^a			Toxicity IC ₅₀ Vero Cell (μM) ^b	SI ^c		
	Epimastigote forms	Amastigote forms	Trypomastigotes forms		Epimastigote forms	Amastigote forms	Trypomastigotes forms
Bz	15.8±1.1	23.3±4.6	22.4±1.9	13.6±0.9	0.8	0.6	0.6
Comp 1	40.7±2.1	20.8±1.7	19.0±0.8	17.9±3.1	0.4 (1)	0.9 (1)	0.9 (2)
Comp 2	69.9±5.7	19.5±2.2	16.3±0.8	95.6±4.6	1.4 (2)	4.9 (8)	5.9 (10)
Comp 3	52.5±8.5	21.5±2.6	30.0±1.4	80.0±7.7	1.44 (2)	3.7 (6)	2.66 (4)
Comp 4	180.0±8.7	49.5±3.4	44.8±3.7	55.1±2.4	0.3 (1)	1.1 (2)	1.2 (2)
Comp 5	93.8±9.1	34.9±2.3	23.8±0.5	80.2±9.0	0.8 (1)	2.3 (4)	3.4 (6)
Comp 6	7.3±0.8	7.0±0.9	5.7±0.8	71.6±6.3	9.8 (13)	10.2 (17)	12.6 (21)

Results are averages of four separate determinations. ^aIC₅₀ = the concentration required to give 50% inhibition, calculated by linear regression analysis from the Kc values at concentrations employed (1, 10, 25, 50 and 100 μM). ^bTowards Cell Vero after 72 h of culture. ^cSelectivity index =IC₅₀ Cell Vero/IC₅₀ extracellular and intracellular form of parasite. In brackets: number of times that compound exceeds the reference drug SI (on extracellular and intracellular forms of *T. cruzi*).

Table 2. Summarizes the Biochemical clinical parameters tested in different groups of Balb/c Mice infected with *Trypanosoma cruzi* at different experimental situations.

	Kidney markers profile			Heart markers profile			Liver markers profile		
	UREA (mg/dL)	URIC ACID (mg/dL)	CK-MB (U/L)	LDH (U/L)	AST/GOT (U/L)	ALT/GPT (U/L)	TOTAL BILIRUBIN(mg/dL)	PHOSPHATASE ALKALYNE (U/L)	
UNINFECTED MICE (n=15)	39 [36-43]	5 [4.3-5.5]	453 [215-690]	3086 [2108-4064]	126 [103-148]	46 [37-54]	0.23 [0.17-0.28]	133 [104-161]	
INFECTED MICE-ACUTE PHASE (n=15)	49 [39-60]	4.5 [3.7-5.5]	681 [400-950]	2910 [1589-4232]	129 [100-157]	48 [38-58]	0.15 [0.12-0.18]	231 [161-300]	
INFECTED MICE- CHRONIC PHASE (n=15)	49	4.3	800	2536	148	53	0.12	186	
120 days POST INFECTION MICE and Comp 6 15 mg/kg.w TREATED (n=6)	=	=	+	+	+	+	+	=	

Key: =, variation no larger than 10 %; +, up to 10% of increasing over the range; ++, up to 30% of increasing over the range; ++++, up to 40% of increasing over the range; +++++, more than 50% of increasing over de range; -, up to 10% of decreasing over the range; --, up to 30% of decreasing over the range; ---, up to 40% of decreasing over the range; ----, more than 50% of decreasing over de range.

7.3. Unpublished results

7.3.1. *In vitro* drug-combination

According to the data obtained from the *in vivo* tests, we selected a series of compounds to improve/enhance the action of the drugs with the aim of performing drug-combination assays by building isoboles and calculating their corresponding combination coefficients (Ci). The criteria followed for making such combinations are considered in the discussion and conclusions section, but basically, we combined the compounds that showed the best *in vitro* IC₅₀ against each form of the parasite, as well as those that *in vivo* showed the best cure rates or lower parasitemia reactivation after immunosuppression. In all combinations, the basic compound has been the best IC₅₀ against amastigotes (Comp 61), as these forms of the parasite are primarily responsible for the chronic form of the infection. This has been combined with:

- Combination 1: Comp 17 third-best compound against amastigotes (as the second-best compound can not be combined because of its solubility properties).
- Combination 2: Comp 32 best compound against trypomastigotes.
- Combination 3: Comp 44 best compound against epimastigotes.

The results are shown in the following table:

Ci= da/Da+db/Db						
Concentration in μM required for an inhibition of 50% in growth						
	Combination 1		Combination 2		Combination 3	
Da	Comp 61	7.9	Comp 61	7.9	Comp 61	7.9
Db	Comp 17	9.4	Comp 32	13.3	Comp 44	8
da	Comp 61 combined	3.9	Comp 61 combined	2.2	Comp 61 combined	7.5
db	Comp 17 combined	4.6	Comp 32 combined	2.9	Comp 44 combined	3
Ci	0.98		0.50		1.32	

[RESULTS]

As is shown, according to their C_i , Combination 3 was excluded in further assays because a C_i higher than 1 means antagonism between the two compounds, while combinations 1 and 2 were selected for the last *in vivo* assay, as both combinations displayed a C_i of lower than 1, thus indicating synergism between the compounds. For a graphical view of this result, the following figure shows the isoboles constructed for the three combinations.

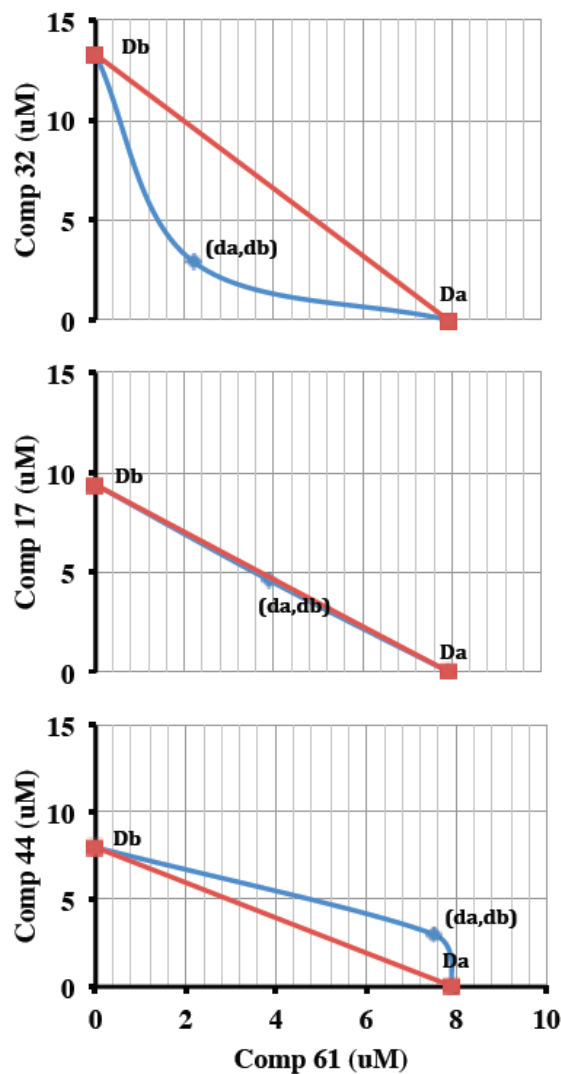


Chart 3 Isobologram of the three drug-combination assayed *in vitro*.

7.3.2. *In vivo* drug-combination

Acute phase treatment trials for the compounds tested were performed as explained in the materials and methods section. The drug was administered orally and the parasite strain used was different (*T. cruzi* CLBr) from that used previously for the *in vivo* assays in our lab. Treated mice showed no significant infection differences compared to the control group, as is shown in the following figure:

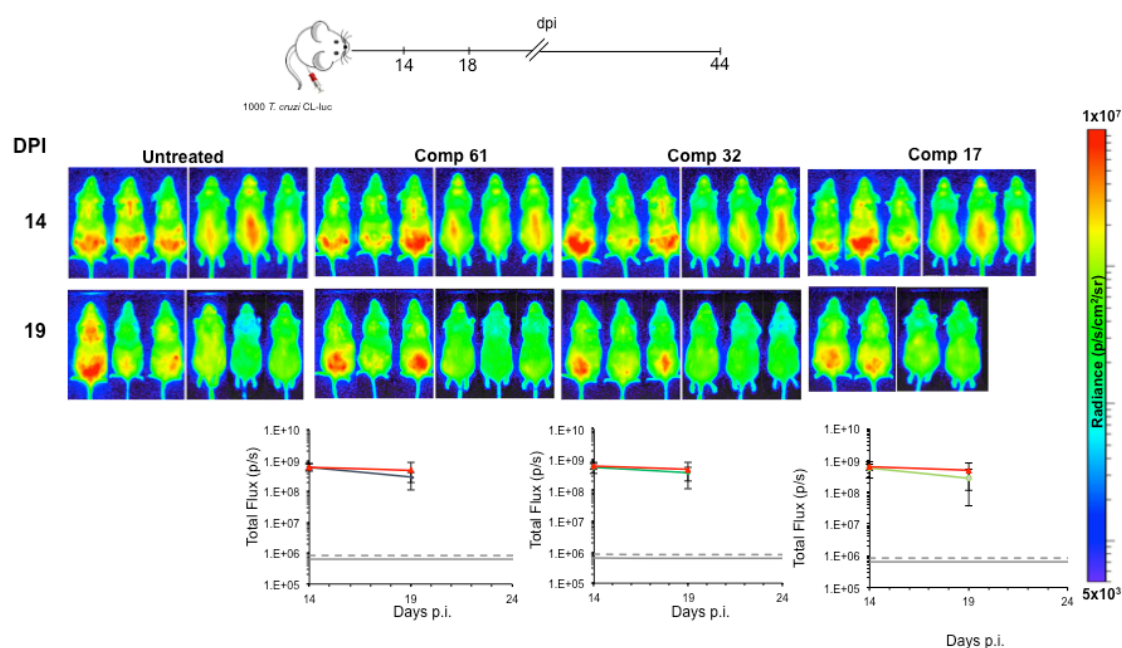


Figure 13. Evaluation by *in vivo* bioluminescence imaging of the compounds in mice infected with *T. cruzi* during the acute phase.

On the other hand, the trials in the chronic phase with both synergistic combinations, determined by their $C_i < 1$, showed different effectiveness as can be seen in the following figure. Combination 1 was not much more effective than the control, since parasitemia levels were very close to those in the control group, while in the case of combination 2, the parasitemia levels showed a decrease for several days following treatment. Due to the fact that parasitaemia did not disappear completely, the experiment was not continued to the immunosuppression phase, as this is only required

[RESULTS]

if the disappearance of parasitemia suggests that there has been a cure; in this case there were still parasites in the blood 10 days after treatment as shown in the figure.

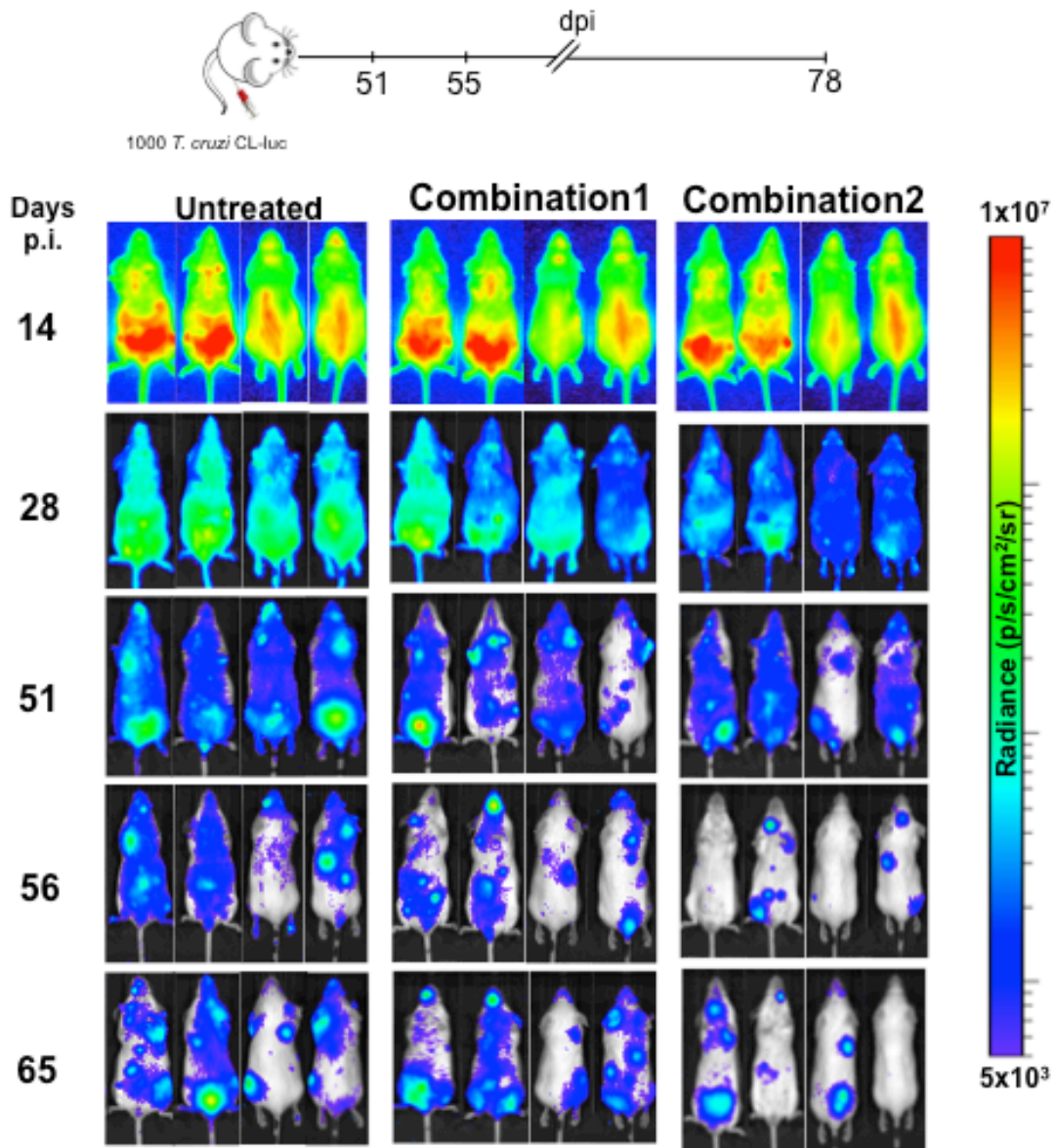


Figure 14. Evaluation by *in vivo* bioluminescence imaging of the drug-combination in mice infected with *T. cruzi* during the chronic phase

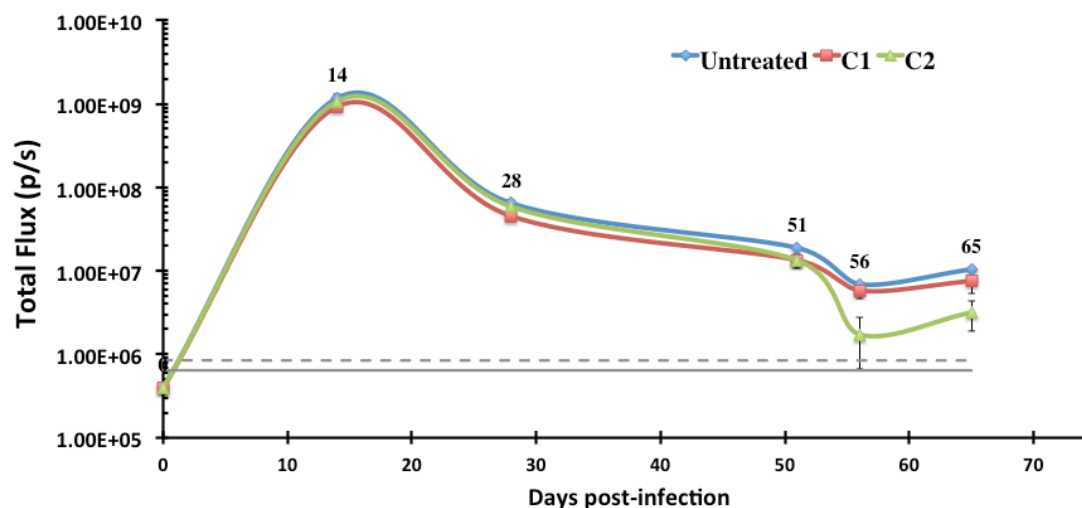


Chart 4. Results of the evaluation by *in vivo* bioluminescence imaging of the drug-combination in mice during the chronic phase of infection with *T. cruzi*.

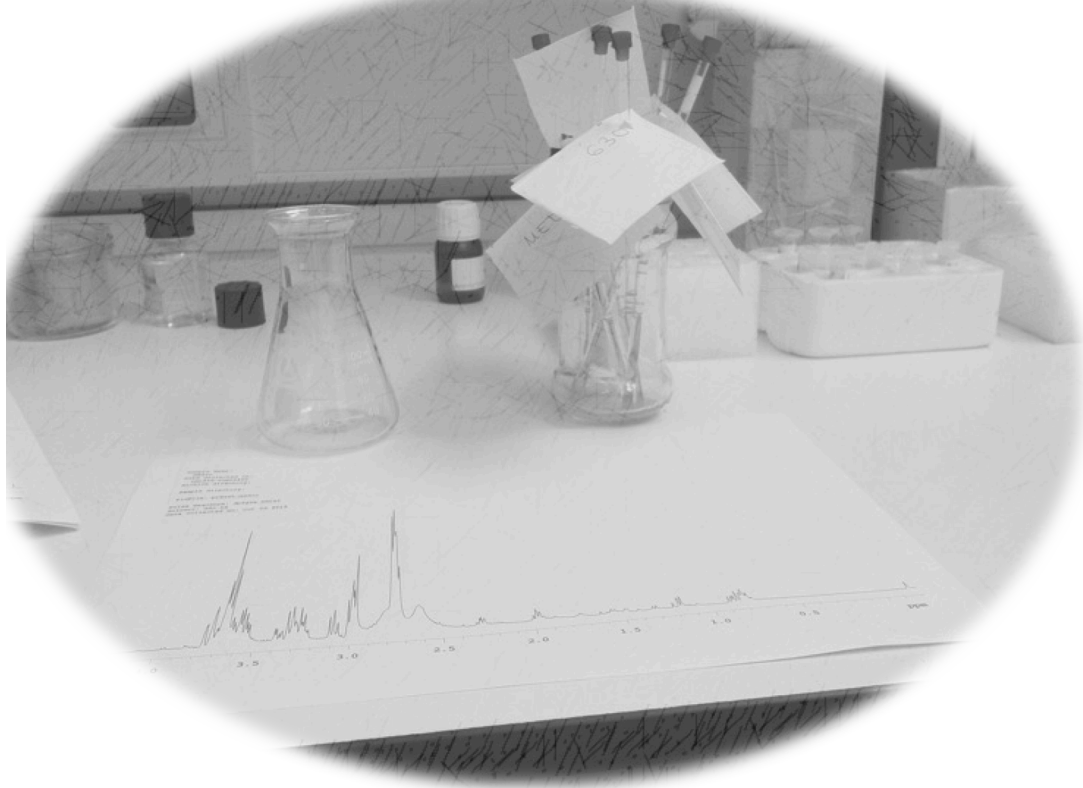
7.4. Invention Patents

The following intention patents have been registered:

- Title: Scorpiand-like macrocycles derivatives and their use as antiparasitic.
 - Record: Spanish Patent and Trademark Office (SPTO)
 - Application Number: P201132035
 - Entity holding: Department of Inorganic Chemistry, Institute of Molecular Science, University of Valencia and Institute of Biotechnology, Faculty of Science, University Granada
 - Countries: Spain Date 16/12/2011
 - Industrial Property type: Invention Patent
 - Inventors / Authors / breeders: Garcia-Spain-Monsonís, Enrique; Clares-Garcia, Maria Paz; Marin Sánchez, Clotilde; Blasco-Llopis, Salvador Soriano-Soto, Conxa; Gonzalez-Garcia, Jorge; Olmo Arévalo, Francisco; Verdejo, Begoña; Inclan, Mariano.
- Title: Complejos metálicos que comprenden compuestos poliamínicos y dichos compuestos para su uso como agentes antiparasitarios.
 - Record: Spanish Patent and Trademark Office (SPTO)
 - Application Number: P201331559
 - Entity holding: Faculty of Science, University Granada;
 - Countries: Spain Date 23/10/2013

[RESULTS]

- Industrial Property type: Invention Patent
 - Inventors / Authors / breeders: Xavi Ribas Salamaña; Miquel Costas Salgueiro; Olaf Cussó Forest; Anna Company Casadevall; Julio Lloret Fillol; Manuel Sánchez Moreno; Clotilde Marín Sánchez; María José Rosales Lombardo; Francisco Olmo Arévalo
3. Title: Compuestos poliamínicos y complejos metálicos que los comprendenara su uso como agentes antiparasitarios.
- Record: Spanish Patent and Trademark Office (SPTO)
 - Application Number: P201331558
 - Entity holding: Faculty of Science, University Granada;
 - Countries: Spain Date 23/10/2013
 - Industrial Property type: Invention Patent
 - Inventors / Authors / breeders: Xavi Ribas Salamaña; Miquel Costas Salgueiro; Olaf Cussó Forest; Anna Company Casadevall; Julio Lloret Fillol; Manuel Sánchez Moreno; Clotilde Marín Sánchez; María José Rosales Lombardo; Francisco Olmo Arévalo.
4. Title: Actividad antiparasitaria de escuaramidas.
- Record: Spanish Patent and Trademark Office (SPTO)
 - Application Number: P201330699
 - Entity holding: Faculty of Science, University Granada;
 - Countries: Spain Date 23/10/2013
 - Industrial Property type: Invention Patent
 - Inventors / Authors / breeders: Antoni Costas; Manuel Sánchez Moreno; Clotilde Marín Sánchez; Carme Rotger; Francisco Olmo Arévalo.



8. DISCUSSION & CONCLUSIONS

"Quality is never an accident; it is always the result of intelligent effort"

John Ruskin

A study of over sixty compounds belonging to 5 different chemical families (Scorpiands, Squaramides, Phthalazines, Tetradentated polyamines and Abietane Acid Derivatives) has been performed. This study is the most extensive and rigorous possible, according to the methods and instrumentation available, to determine the trypanocidal activity of the compounds as potential agents against the protozoan *Trypanosoma cruzi*, both *in vitro* and *in vivo* (in a murine model). The process involved screening, followed by selection for the next stage of those compounds which met the criteria of efficacy established in the literature. Therefore, the process was completely comprehensive, with those compounds for which efficiency was not expected in the next step being discarded.

Although we tried to standardize the method used, because this study is the result of over four years of dynamic work, small changes and modifications have been made with the aim of improving and updating the work. These modifications are attempts to adapt to new methods, techniques, equipment and more effective measurement systems to improve the screening process; increasing the number of replicates, gathering data more accurately through mechanized techniques, applying new software, reducing the degree of severity in animal experimentation, and other similar changes.

Table 8 summarizes the most effective among the tested compounds, as well as the most significant *in vitro* and *in vivo* results that justify why these compounds were selected. Among them, are the best IC₅₀ against each form of the parasite, as well as their corresponding selectivity indices (SI), the doses used in the mouse model for treatments that were administered during the acute phase of the infection as well as in a pattern of five intraperitoneal administrations. Also shown are percentages of parasitaemia reactivation after immunosuppression, and cure rates following negative PCR (considering the heart as the target organ). It is precisely this last aspect that is

[DISCUSSION & CONCLUSIONS]

currently on the agenda of the international scientific community. The discussion focuses on those mice where the target organ (the heart in this case) was free of parasites and produced a negative PCR, but showed some percentage (even if minimal) of parasites in the blood. This would mean that the curative effect is being overestimated, and it would be reasonable to assume that there are other microhabitats in the mouse's body where the parasite may be maintained during the chronic phase. The characteristics of this niche must be that there is limited exposure to the compounds (as could be the case of fat) or it is a tissue the immune system can only access at low intensities or which shows high tolerance (such as the digestive tract). This would allow the parasite to survive in low levels (minimised by the immune system), and it is only when the mouse is subjected to immunosuppressive treatment that the parasite is released from this unexpected habitat allowing it to return to the blood stream.

Another parameter that was followed closely throughout the experiments was the total IgG measured by the ELISA tests, in order to know the immune status of the mice through the process, also allowing confirmation of infection, progression, and finally determination of whether or not the induced immunosuppression was too severe.

Having been subjected to this series of assays, including screening in our laboratory, the compounds that eventually became potential candidates have been studied in depth, to gain an understanding of their mechanisms of action and therapeutic targets. Therefore, **Table 8** also reflects the potential therapeutic targets for each compound based on the tests performed. It is necessary to note that the attribution of the target is not exclusive, meaning that according to our method we can deduce that this target is being inhibited by the compound, but is not necessarily the only target on which the compound is acting. Indeed, in some situations the same compound was

active against two independently tested *in vitro* targets, such as Fe-SOD and TR antioxidant enzymes (Comp 32).

Table 8. Summary of the most effective activity found in the assayed compounds.

Compound	*IC ₅₀ (μM) “in vitro”	Selectivity Index	**Dosage used “in vivo”	Effectivity “in vivo”	Potential target
Scorpion-like azamacrocyclic 4 (Comp 44)	8 (e)	53	5 mpk	6 % react 85 % cure	SOD
Phthalazine 2 (Comp 20)	8.7 (e)	49	15 mpk	4 % react nd % cure	SOD/ mitochondria
Aza-scorpian derivative 11 (Comp 61)	5.2 (a)	39	5 mpk	60 % react 33 % cure	TR
Abietic acid derivative 4 (Comp 28)	7.1 (a)	31	25 mpk	9.8% react 50% cure	Unknown
Squaramide 17 (Comp 17)	8.5 (a)	53	40 mpk	3% react 83 % cure	Unknown
Tetradentated polyamine 3 (Comp 32)	4.4 (t)	65	15 mpk	13 % react 50 % react	SOD / TR

*(e):epimastigotes,(a):amastigotes;(t):trypomastigotes. **mpk: mg per kg of body mass

In other cases, which have been reported in several of our publications, such as studies of ¹H-NMR and TEM, the mechanism of action is an overview of how a certain compound affects the metabolism and ultrastructure. For a more focused view, in order to elucidate the degree of involvement of each of the subcomponents individually acting over this whole system, more specific assays are required. In other words, this approach, involving the implications of the compounds on the energetic metabolism of the parasite, confirming that it has been producing a general alteration of a process with respect to a normal or control situation, changes in light of the fact that the results are speculative. New hypotheses could be developed by applying new trials aimed at achieving a higher degree of specificity, and determining whether or not the compound acts on a specific

[DISCUSSION & CONCLUSIONS]

enzyme, receptor, organelle, biomolecule, and so on. However, the results of certain assays allow us to strongly support that hypothesis that the presence of the compound induces a disturbance in the normal functioning of the parasite, causing loss of viability. We must not lose sight of assays for metabolism and ultrastructure parasites were performed in low concentrations of compound (IC_{25}), since the assay tried not to cause massive death, and consequently see a variety of intermediate stages of damage.

In an attempt to go one step further in the preclinical studies of our compounds, once the efficacy data of all the compounds individually was known, we tried combination therapy in order to see if whether or not drug-combinations of these compounds improves their effectiveness. To do this, we performed the combination assays. To this end, the compound that showed the greatest activity *in vitro* against amastigotes was selected, since amastigotes are responsible for the maintenance of chronic infection, and Compound 61 was considered the fixing compound for the different combinations. The first combination was prepared with the most active compound against amastigotes (third in the list since the solubility properties of the second do permit it to be combined), Comp 17. The second and third combinations used the most active against epimastigotes (Compound 44) and trypomastigotes (Compound 32), respectively. During the *in vitro* stage, the second combination (Comp 61/44) was discarded as it displayed antagonistic behaviour. The remaining two combinations were tested *in vivo* with a novel system in the London School of Hygiene and Tropical Medicine; only one showed a slight improvement in the treated mice during the chronic phase. Note that this last experiment was a challenge for the compounds, as it was performed using a detection system that is more sensitive for the parasitemia, the compounds were administered orally, which is a less efficient absorption route, and finally, for the first time the compounds were administered during the chronic phase of

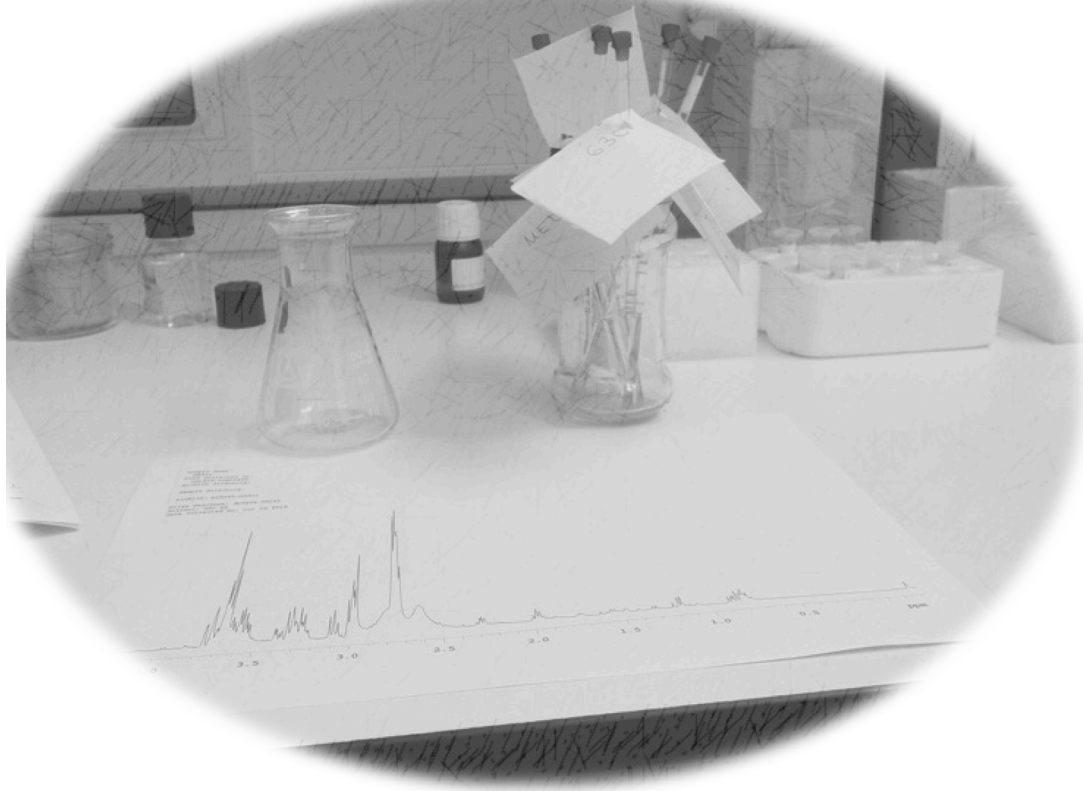
infection, where, as mentioned above, the parasite is less accessible. In addition, it is worth noting that the strain the trial was conducted with was different than that used in all previous tests.

Finally, after all the experimental work undertaken for the purposes of this study, we can draw the following **CONCLUSIONS**:

1. All the most effective compounds had IC₅₀ values lower than 9 μM and selectivity indices higher than 30 against at least one of the forms of the parasite.
2. The most efficient compounds against extracellular forms (epimastigotes and trypomastigotes) presented as the action target of Fe-SOD enzyme, together with TR in the case of Comp 32, and had serious effects on the mitochondria in the case of Comp 20.
3. For the most efficient compounds against intracellular forms (amastigotes), the therapeutic targets remain unknown (Compounds 17 and 28), with the exception of Comp 61, which proved to target enzyme TR.
4. Of the 62 starting compounds less than a third (20) reached the *in vivo* phase, and of these 20 compounds only 4 were used in the combination phase. Finally just 2 compounds have proved to be an efficient combination for the *in vivo* model in the chronic phase.
5. The most efficient drug-combination contains a compound highly effective against amastigotes and another against trypomastigotes, both acting on TR and Fe-SOD enzymes. They showed a combined potential efficacy *in vitro* (Ci synergistic of 0.5), confirmed in the chronic phase of infection *in vivo*.

[DISCUSSION & CONCLUSIONS]

6. The limitation of the *in vivo* efficacy of the drug-combination in the treatments is due to the oral administration (less efficient than the intraperitoneal route) and the short duration of treatment (5 days) for the chronic phase, which is a long one in the case of Chagas disease.
7. In cases where Fe-SOD or TR are considered the therapeutic target, their IC₅₀ were below 30 μ M.
8. The tested *in vivo* doses are generally very low in all experiments, both the concentrations of the compounds and the number of doses. Therefore, an improvement in this treatment regimen may improve efficiency, and for this a better understanding of the pharmaco-kinetics of the compounds used in the experimental model is required.
9. Since *in vitro* synergistic combinations are faithful representations of *in vivo* extrapolation a multiple combination of more than two compounds could result in a combination therapy against different forms of the parasite and against various targets that could approximate a complete cure of the infection.



8. DISCUSIÓN & CONCLUSIONES

"La calidad nunca es un accidente; siempre es el resultado de un esfuerzo de la inteligencia"

John Ruskin

Se ha realizado un estudio de más de sesenta compuestos, pertenecientes a 5 familias químicas diferentes (Scorpiands, Squaramides, Phthalazines, Tetradentated polyamines and Abietane Acid derivatives), del modo más amplio y riguroso posible de acuerdo a la metodología e instrumentación disponible, para determinar su actividad como potenciales agentes trypanocidas frente al protozoo *Trypanosoma cruzi*, tanto *in vitro* como *in vivo* en modelo murino. Ha sido un proceso de cribado por fases, en las cuales solo han sido seleccionados los compuestos que cumplían unos criterios de eficacia establecidos en la literatura. Por ello, el proceso ha sido cada vez más exhaustivo, descartando aquellos compuestos de los cuales no se esperaba una acción potencialmente eficiente en la siguiente fase.

Pese a que intentamos homogeneizar la metodología utilizada, dado que la presente memoria de tesis doctoral es el resultado de más de 4 años de trabajo dinámico dentro de la línea de estudio, pueden observarse pequeños cambios o modificaciones que se han realizado como mejora y actualización de los estudios. Estas modificaciones han tenido la finalidad de adaptar las técnicas a nuevas metodologías, aparataje y nuevos sistemas de medición más eficaces con objeto de mejorar el proceso de cribado; aumentando el número de réplicas, hacer más precisa la obtención de datos mediante su mecanización, aplicación de nuevos softwares, disminuir el grado de severidad en la experimentación animal conforme a la legislación vigente, entre otros cambios.

La siguiente **Tabla 8** resume los mejores compuestos de entre los ensayados, así como los resultados *in vitro* e *in vivo* más significativos que justifican porque han sido seleccionados dichos compuestos. Entre ellos, podemos encontrar las mejores IC₅₀ frente a cada forma del parásito, así como, sus correspondientes índices de selectividad (IS o SI), las dosis empleadas en el modelo murino en los tratamientos que siempre han sido administrados durante la fase aguda de la infección y en una pauta de cinco

[DISCUSIÓN & CONCLUSIONES]

administraciones intraperitoneales. Igualmente sus porcentajes de reactivación de la parasitemia tras la inmunosupresión, porcentajes de curación considerados tras la PCR negativa del órgano diana. Y es precisamente en este aspecto en el que se abre un debate de discusión, que se encuentra actualmente sobre la mesa de la comunidad científica internacional. El debate se centra en aquellos ratones en los que el órgano diana (corazón en este caso) resultó libre de parásitos al obtener una PCR negativa, pero mostró algún porcentaje (por mínimo que fuere) de parásitos en sangre. Lo que significa que se estaría sobreestimando su curación, haciéndonos pensar con buen criterio que debe existir otro microhábitat en el organismo donde se mantiene el parásito durante la fase crónica. Las características de este nicho deben ser que tiene limitado acceso para los compuestos (como pudiese ser el tejido adiposo) o bien ser un tejido al cual el sistema inmune accede de forma poco intensa o con alta tolerancia (como puede ser el aparato digestivo). Ello permite la supervivencia del parásito en bajos niveles, reduciendo su dispersión con ayuda del sistema inmune; y es precisamente cuando el ratón se somete al tratamiento inmunosupresor cuando se permite la liberación desde este inesperado hábitat permitiendo el retorno del parásito al sistema circulatorio.

Otro parámetro que hemos seguido con detenimiento durante todos los experimentos ha sido el título de IgG totales. Para ello, mediante la técnica de ELISA hemos tenido una referencia del estado inmunológico en que se encontraban los ratones durante todo el proceso, permitiendo además confirmar la infección, su progresión y finalmente que la inmunosupresión inducida no haya sido excesivamente severa.

Tras haber sido sometidos a esta sucesión de ensayos, como estrategia de cribado puesta a punto en nuestro laboratorio, aquellos compuestos que finalmente apuntaban como candidatos potenciales han sido estudiados en mayor profundidad con objeto de conocer su mecanismo de acción o diana terapéutica. Por ello, en la **Tabla 8**

se puede ver también reflejada la diana terapéutica potencial para cada compuesto en base a los ensayos realizados. Cabe a este respecto reflexionar detenidamente, pues la atribución que se hace a la diana no es exclusiva. Esto quiere decir que por nuestra metodología descrita, podemos deducir que esa diana está siendo inhibida por el compuesto, pero no es la única diana sobre la que pudiese estar actuando; de hecho en algunas situaciones el mismo compuesto tiene actividad sobre dos dianas diferentes ensayadas in vitro de forma independiente, como son las enzimas antioxidantes Fe-SOD y TR (Comp 32). En otros casos, que pueden encontrarse en las diversas publicaciones, como los estudios de $^1\text{H-NMR}$ y TEM la visión de actuación del compuesto determinado con respecto al metabolismo y la ultraestructura es de carácter global, para una visión más concreta se precisarían unos ensayos específicos que permitan dilucidar el grado de implicación de cada uno de los subcomponentes de este todo de forma individualizada. Significaría que, las aproximaciones a la actuación de los compuestos sobre el metabolismo energético del parásito confirma que se está produciendo una alteración general sobre algún proceso con respecto a una situación normal o de control, las alteraciones a la luz de los resultados son de carácter especulativo y nuevas hipótesis podrían ser elaboradas, aplicando para ello nuevos ensayos que permitan llegar a un grado de concreción superior y determinar si la actuación del compuesto es sobre una enzima específica, un receptor, un orgánulo, una biomolécula específica, etc. No obstante, los resultados obtenidos en determinados ensayos permiten establecer fuertemente que la presencia del compuesto induce un fuerte cambio en el funcionamiento normal del parásito causando pérdida de viabilidad, tampoco hay que perder de vista que para los ensayos de metabolismo y ultraestructura los parásitos son sometidos a unas concentraciones bajas de compuesto (IC_{25}) con objeto de no causar la muerte masiva y poder ver los estadios intermedios o variedad de daños causados.

Tabla 8. Resumen de la mejor actividad encontrada en los compuestos ensayados.

Compound	*IC ₅₀ (μM) “in vitro”	Selectivity Index	**Dosage used “in vivo”	Effectivity “in vivo”	Potential target
Scorpion-like azamacrocyclic 4 (Comp 44)	8 (e)	53	5 mpk	6 % react 85 % cure	SOD
Phthalazine 2 (Comp 20)	8.7 (e)	49	15 mpk	4 % react nd % cure	SOD/ mitochondria
Aza-scorpian derivative 11 (Comp 61)	5.2 (a)	39	5 mpk	60 % react 33 % cure	TR
Abietic acid derivative 4 (Comp 28)	7.1 (a)	31	25 mpk	9.8% react 50% cure	Unknown
Squaramide 17 (Comp 17)	8.5 (a)	53	40 mpk	3% react 83 % cure	Unknown
Tetradentated polyamine 3 (Comp 32)	4.4 (t)	65	15 mpk	13 % react 50 % react	SOD / TR

*(e):epimastigotes,(a):amastigotes;(t):trypomastigotes. **mpk: mg per kg of body mass

En un intento de dar un paso más allá en la fase preclínica de estudio de estos compuestos, una vez conocidos los datos de eficacia de todos los compuestos de un modo individual, surgió la idea de una terapia combinada con objeto de ver si la aplicación conjunta de estos compuestos supondría una mejora en su eficacia; para ello, se procedió a realizar los ensayos de combinación. Con esta finalidad, fue seleccionado el compuesto que mayor actividad presentaba *in vitro* frente a formas amastigotas, que son las responsables del mantenimiento crónico de la infección, siendo el compuesto (Comp 61) considerado el compuesto base de las diferentes combinaciones. La primera combinación se hizo con el siguiente compuesto mas activo frente a formas amastigotas (tercero en la lista pues el segundo no permite una combinación por sus propiedades químicas de solubilización) que fue el Comp 17. También se combinó con el más activo frente a epimastigotes (Comp 44) y trypomastigotes (Comp 32). Ya en esta fase de combinación *in vitro* se excluyó la una de las combinaciones (Comp 61/44) por ser

antagónica y de las dos combinaciones restantes que se ensayaron in vivo y con un sistema novedoso llevado a cabo en el London School of Hygiene and Tropical Medicine, solo una consiguió una ligera mejora en los ratones tratados durante la fase crónica. Cabe mencionar que este último experimento ha supuesto un desafío para los compuestos, pues se ha realizado con un sistema de detección de parasitemia más sensible, se ha utilizado una administración por una vía menos eficiente de absorción (oral) y por primera vez se ha administrado el compuesto durante la fase crónica de la infección, donde la distribución del parásito como hemos mencionado anteriormente es mas inaccesible. Además, también cabe destacar que la cepa sobre la que se ha realizado el ensayo ha sido diferente a la que se ha utilizado en todos los ensayos previos.

Finalmente, después de todo el trabajo realizado con objeto de esta tesis doctoral expuesta, podemos extraer las siguientes **CONCLUSIONES:**

1. Todos los compuestos más efectivos presentan IC_{50} menores de $9 \mu M$ e índices de selectividad mayores a 30, frente al menos alguna de las formas del parásito.
2. Los compuestos más eficientes frente a formas extracelulares (epimastigotes y trypomastigotes presentaron como diana de acción la enzima Fe-SOD, junto con la Trypanothione reductase en el caso del Comp 32 y graves efectos sobre la mitocondria en el caso del Comp 20.
3. Para los compuestos más eficientes frente a formas intracelulares (amastigotes), sus dianas terapéuticas permanecen desconocidas (Comp 17 y 28), con la salvedad del Comp 61 cuya diana resulto ser la enzima Trypanothione reductase.
4. De los 62 compuestos de partida menos de un tercio (20) pasaron a la fase in vivo, y de estos solo 4 han sido llevados a la fase de combinación, para

- finalmente solo 2 han resultado una combinación eficiente para el modelo in vivo de fase crónica.
5. La combinación más eficiente contiene un compuesto altamente eficaz frente a amastigotes y otro trypomastigotes, ambos actuando sobre las enzimas Tripanothione reductase y Fe-SOD. Mostrando una eficacia combinada potencial *in vitro* (Ci sinérgico de 0.5) y confirmada sobre la fase crónica de la infección *in vivo*.
 6. La limitación de la eficacia de los tratamientos *in vivo* se debe a la vía de administración oral que (menos eficiente que la vía intraperitoneal) así como a la corta duración del tratamiento (5 días) para una fase crónica tan prolongada como es la enfermedad de Chagas.
 7. En los casos en que la Fe-SOD o la TR han sido consideradas la diana terapéutica, sus IC₅₀ han sido inferiores a 30 µM.
 8. Las dosis ensayadas *in vivo* han sido muy bajas en general en todos los experimentos, tanto en la concentración de compuesto, como en el número de dosis administradas. Por tanto, una mejora en esta pauta de tratamiento podría mejorar su eficacia, para ello se precisa un mayor conocimiento farmacocinético de los compuestos en el modelo experimental utilizado.
 9. Dado que las combinaciones sinérgicas *in vitro* son fieles representaciones de su extrapolación *in vivo* una combinación múltiple de más de dos compuestos podría crear una terapia combinada frente a las diferentes formas del parásito y frente a diversas dianas que pueden aproximar la pauta de tratamiento para una curación completa de la infección.

Granada patentará un fármaco contra el chagas

Es la tercera enfermedad tropical más propagada en el mundo y existen 30.000 españoles diagnosticados, pero su tratamiento hasta ahora es tóxico y poco eficaz

de ANGELES PEÑALVER

La Organización Mundial de la Salud dice que es una enfermedad desatendida, pero dos grupos científicos de Granada han investigado añosamente sobre el mal de chagas y las soluciones médicas son cada día más abundantes y mejores. La OMS ha calificado esta enfermedad tropical como la tercera más propagada en todo el mundo. afecta a más de 30.000 personas en España, es endémica en el continente americano y en el mundo la su-
en más de 10 millones de personas y elevados índices de mortalidad. La migración de personas infectadas plantea un serio problema, ya se han registrado casos de transmisión por productos sanguíneos en España, Canadá y Estados Unidos. Entre el 20% y el 30% sufrirá alteraciones cardíacas, alteraciones digestivas y en el porcentaje neurológicas. Los medicamentos utilizados hasta ahora en esta patología eran muy tóxicos y tenían hipersensibilizantes. Y una vez puestos en marcha poco existían posibilidades de la medicina para mejorarlos, ayer se han registrado en España más de 200 millones de euros en gastos de investigación, expli-



El catedrático Manuel Sánchez Moreno al frente del equipo universitario que ha participado en el hallazgo. RAMÓN L. PÉREZ

consistieron en probar la toxicidad de los compuestos en células de mamíferos, además de su actividad antiparasitaria. Entre todas las moléculas se seleccionaron los productos más efectivos para estudiar tanto la fase aguda como crónica del mal, la inhibición de los parásitos y las posibles alteraciones en órganos vitales de ratones. «Ahora queda hacer los ensayos en animales más grandes, tipo perros, y completar la fase de ensayos en humanos, lo que puede costar unos dos millones de euros», asegura Sánchez Moreno, expli-

(más de 40 días de tratamiento) y presenta una toxicidad muy elevada. El nuestro es diez veces más eficaz». El grupo multidisciplinar en el que él participa como responsable ha sido financiado con 4 millones de

euros por un proyecto Consolider del Ministerio de Economía y Competitividad. En él hay además investigadores de Valencia, Girona, Illes Balears, Cádiz y la Complutense de Madrid, así como del Hospital Joan

23 de Tarragona. Estos científicos acaban de cumplir la primera mitad de su calendario y su siguiente objetivo es el desarrollo de nuevos agentes terapéuticos antiparasitarios, antiinflamatorios o antitumorales.

Otro grupo halla cómo detectar la gravedad de los pacientes

de A. P.

GRANADA. El chagas se transmi-

La enfermedad tiene una fase aguda

de Salud Carlos III por los doctores Pérez y Car-

tura

9. REFERENCES

" Be yourself the remaining seats are already occupied "

(" Sé tu mismo los demás puestos ya están ocupados. ")

Oscar Wilde

References used during the thesis.

References published as part of this thesis

References submitted as part of this thesis

- Aguilar VHM**, Abad-Franch F, Racines VJ, et al. Epidemiology of Chagas disease in Ecuador. A brief review. *Mem Inst Oswaldo Cruz* 1999; 94 (suppl 1): 387–93.
- Bern C**, Montgomery SP, Herwaldt BL, et al. Evaluation and treatment of Chagas disease in the United States: a systematic review. *JAMA* 2007; 298: 2171–81.
- Bern C**, Montgomery SP. An estimate of the burden of Chagas disease in the United States. *Clin Infect Dis* 2009; 49: e52–54.
- Bringaud F**, Riviere L, Coustou V. Energy metabolism of trypanosomatids: Adaptation to available carbon sources. *Molecular & Biochemical Parasitology* 2006;149: 1–9.
- Britto CC**. Usefulness of PCR-based assays to assess drug efficacy in Chagas disease chemotherapy: value and limitations. *Memorias do Instituto Oswaldo Cruz* 2009; 1: 122–135.
- Buckner FS**, Navabi N. Advances in Chagas Disease Drug Development: 2009-2010. *Curr. Opin. Infect. Dis.* 2010; 23: 609–616.
- Bursell E**. The role of proline in energy metabolism. In: Downer RGH, editor. Energy metabolism in insects. New York: Plenum Press; 1981. p.135–54.
- Caldas S**, Santos FM, de Lana M, et al. Trypanosoma cruzi: acute and long-term infection in the vertebrate host can modify the response to benznidazole. *Exp Parasitol.* 2008; 118(3): 315-23.

[REFERENCES]

- Camargo EP.** Perspectives of vaccination in Chagas disease revisited. *Mem Inst Oswaldo Cruz* 2009; 104 (Suppl 1): 275–280.
- Campbell DA,** Westenberger SJ, Sturm NR. The determinants of Chagas disease: connecting parasite and host genetics. *Current Molecular Medicine* 2004; 4: 549–562.
- Cannata JJ,** Cazzulo JJ. The aerobic fermentation of glucose by *Trypanosoma cruzi*. *Comp Biochem Physiol B* 1984; 79: 297–308.
- Castro JA,** de Mecca MM, Bartel LC. Toxic side effects of drugs used to treat Chagas' disease (American trypanosomiasis). *Hum Exp Toxicol.* 2006; 25(8): 471-9.
- Cevallos AM,** Segura-Kato YX, Merchant-Larios H et al. *Trypanosoma cruzi*: multiple actin isoforms are observed along different developmental stages. *Exp Parasitol.* 2011; 127: 249–259.
- Chamond N,** Gregoire C, Coatnoan N, et al. Biochemical characterization of proline racemases from the human protozoan parasite *Trypanosoma cruzi* and definition of putative protein signatures. *J Biol Chem* 2003; 278: 15484–94.
- Chatelain E.** Chagas Disease Drug Discovery: Toward a New Era. *J Biomol Screen.* 2015; 20(1): 22-35.
- Clayton J.** Chagas Disease: Pushing through the Pipeline. *Nature* 2010; 465: S12–S15.
- Co EM,** Denucci RA, Reinbold DD, et al. Assessment of malaria in vitro drug combination screening and mixed-strain infections using the malaria Sybr green I-based fluorescence assay. *Antimicrob Agents Chemother.* 2009; 53(6): 2557-63.
- de Souza W.** Structural organization of *Trypanosoma cruzi*. *Mem Inst Oswaldo Cruz,* Rio de Janeiro, Vol. 104 (Suppl. I): 89-100, 2009.

- Demoro B**, Rossi M, Caruso F, et al. Potential Mechanism of the Anti-Trypanosomal Activity of Organoruthenium Complexes with Bioactive Thiosemicarbazones. *Biol. Trace Elem. Res.* 2013; 153: 371–381.
- Duffy T** et al. Accurate real-time PCR strategy for monitoring bloodstream parasitic loads in Chagas disease patients. *PLoS Neglected Tropical Diseases* 2009; 3: 419.
- El-Sayed NM**, Myler PJ, Bartholomeu DC, et al. The genome sequence of *Trypanosoma cruzi*, etiologic agent of Chagas disease. *Science* 2005; 309: 409–15.
- Fabbro DL**, Streiger ML, Arias ED, et al. Trypanocide treatment among adults with chronic Chagas disease living in Santa Fe city (Argentina), over a mean follow-up of 21 years: parasitological, serological and clinical evolution. *Rev Soc Bras Med Trop* 2007; 40: 1–10.
- Fairlamb AH**, Opperdoes FR. Carbohydrate metabolism in African trypanosomes, with special reference to the glycosome. In: Morgan MJ, editor. Carbohydrate metabolism in cultured cells. *Plenum Publishing Corporation* 1986; p.183–224.
- Ferreira AV**, Segatto M, Menezes Z, et al. Evidence for *Trypanosoma cruzi* in adipose tissue in human chronic Chagas disease. *Microbes Infect.* 2011; 13(12-13): 1002-5.
- Filardi LS**, Brener Z. Susceptibility and natural resistance of *Trypanosoma cruzi* strains to drugs used clinically in Chagas disease. *Trans R Soc Trop Med Hyg* 1987; 81: 755–759.
- Freilij H**, Altcheh J. Congenital Chagas' disease: diagnostic and clinical aspects. *Clin Infect Dis* 1995; 21: 551–55.
- Gascon J**, Bern C, Pinazo MJ. Chagas disease in Spain, the United States and other non-endemic countries. *Acta Trop* 2009; DOI:10.1016/j.actatropica.2009.07.019.

[REFERENCES]

- Gomes YM**, Lorena VM, Luquetti AO. Diagnosis of Chagas disease: what has been achieved? What remains to be done with regard to diagnosis and follow up studies? *Mem Inst Oswaldo Cruz* 2009; 104 (suppl 1): 115–21.
- Guerra-Guttenberg RA**, Grana DR, Ambrosio G, et al. Chagas cardiomyopathy: Europe is not spared! *Eur Heart J* 2008; 29: 2587–91.
- Henriques C**, Henriques-Pons A, Meuser-Batista M, et al. In vivo imaging of mice infected with bioluminescent *Trypanosoma cruzi* unveils novel sites of infection. *Parasit Vectors*. 2014; 3,7:89.
- Jamison DT**. Disease control priorities in developing countries. 2nd ed, *New York, Oxford University Press*, 2006.
- Keenan M**, Abbott MJ, Alexander PW, et al. Analogues of fenarimol are potent inhibitors of *Trypanosoma cruzi* and are efficacious in a murine model of Chagas disease. *J Med Chem* 2012; 10,55(9): 4189-204.
- Kropf SP**, Sá MR. The discovery of *Trypanosoma cruzi* and Chagas disease (1908-1909): tropical medicine in Brazil. *Hist Cienc Saude Manguinhos*. 2009; 16 Suppl 1: 13-34.
- Lewis MD**, Ma J, Yeo M, et al. Genotyping of *Trypanosoma cruzi*: systematic selection of assays allowing rapid and accurate discrimination of all known lineages. *Am J Trop Med Hyg*. 2009; 81: 1041–1049.
- Lewis MD**, Fortes Francisco A, Taylor MC, et al. Bioluminescence imaging of chronic *Trypanosoma cruzi* infections reveals tissue-specific parasite dynamics and heart disease in the absence of locally persistent infection. *Cell Microbiol* 2014; 16(9): 1285-300.

- Luquetti AO**, Ponce C, Ponce E et al. Chagas' disease diagnosis: a multicentric evaluation of Chagas Stat-Pak, a rapid immunochromatographic assay with recombinant proteins of *Trypanosoma cruzi*. *Diagnostic Microbiology and Infectious Disease* 2003; 46: 265–271.
- Macedo AM**, Machado CR, Oliveira RP, et al. *Trypanosoma cruzi*: genetic structure of populations and relevance of genetic variability to the pathogenesis of Chagas disease. *Mem Inst Oswaldo Cruz* 2004; 99: 1–12.
- Manoel-Caetano FS**, Silva AE. Implications of genetic variability of *Trypanosoma cruzi* for the pathogenesis of Chagas disease. *Cad Saude Publica* 2007; 23: 2263–74.
- Marín C**, Ramírez-Macías I, López-Céspedes A, et al. In vitro and in vivo trypanocidal activity of flavonoids from *Delphinium staphisagria* against Chagas disease. *J Nat Prod* 2011 25; 74(4): 744-50.
- Mateo H**, Sánchez-Moreno M, Marín C. Enzyme-linked immunosorbent assay with purified *Trypanosoma cruzi* excreted superoxide dismutase. *Clin Biochem* 2010; 43(15): 1257-64.
- Mathers CD**, Lopez A, Murray C. The burden of disease and mortality by condition: data, methods, and results for the year 2001. In: Lopez AD et al, eds. *Global burden of disease and risk factors*. New York, Oxford University Press, 2006.
- Melo LDB**, Sant'anna C, Reis SA et al. Evolutionary conservation of actin-binding proteins in *Trypanosoma cruzi* and unusual subcellular localization of the actin homologue. *Parasitol* 2008; 135: 955–965.

[REFERENCES]

- Miles MA**, Llewellyn MS, Lewis MD, et al. The molecular epidemiology and phylogeography of *Trypanosoma cruzi* and parallel research on *Leishmania*: looking back and to the future. *Parasitology* 2009, 136: 1509–1528.
- Ministério da Saúde**. Secretaria de Vigilância em Saúde. Brazilian Consensus on Chagas disease. *Rev Soc Bras Med Trop* 2005; 38 (suppl 3): 7–29 (in Portuguese).
- Moncayo A**, Silveira AC. Current epidemiological trends for Chagas disease in Latin America and future challenges in epidemiology, surveillance and health policy. *Mem Inst Oswaldo Cruz* 2009, 1: 17–30.
- Moncayo A**. Chagas disease: current epidemiological trends after the interruption of vectorial and transfusional transmission in the Southern Cone countries. *Mem Inst Oswaldo Cruz* 2003; 98: 577–91.
- Mora MC**, Sanchez Negrette O, Marco D, et al. Early diagnosis of congenital *Trypanosoma cruzi* infection using PCR, hemoculture, and capillary concentration, as compared with delayed serology. *J Parasitol* 2005; 91: 1468–73.
- Moser DR**, Kirchhoff LV, Donelson JE. Detection of *Trypanosoma cruzi* by DNA amplification using the polymerase chain reaction. *J. Clin. Microbiol.* 1989; 27: 1477–1482.
- Mott KE**, Desjeux P, Moncayo A, et al. Parasitic diseases and urban development. *Bulletin of the World Health Organization*, 1990; 68: 691–698.
- Murta SM**, Romanha AJ. In vivo selection of a population of *Trypanosoma cruzi* and clones resistant to benznidazole. *Parasitology* 1998; 116: 165-171.

- Nogueira FB**, Krieger MA, Nirdé P, et al. Increased expression of iron-containing superoxide dismutase-A (TcFeSOD-A) enzyme in *Trypanosoma cruzi* population with in vitro-induced resistance to benznidazole. *Acta Trop.* 2006; 100: 119-132.
- Nozaki T**, Engel JC, Dvorak, JA. Cellular and molecular biological analyses of nifurtimox resistance in *Trypanosoma cruzi*. *Am J Trop Med Hyg.* 1996; 55: 111-117.
- Olmo F**, Clares MP, Marín C, et al. Synthetic single and double aza-scorpianid macrocycles acting as inhibitors of the antioxidant enzymes iron superoxide dismutase and trypanothione reductase in *Trypanosoma cruzi* with promising results in a murine model. *RSC Adv.* 2014; 4: 65108–65120.
- Olmo F**, Costas M, Marín C, et al. Tetradentate polyamines as highly efficient metallodrugs for Chagas disease treatment in murine model. *Trans R Soc Trop Med Hyg.* 2015 (Submitted).
- Olmo F**, Cussó O, Marín C, et al. In vitro and in vivo identification of tetradentated polyamine complexes as highly efficient metallodrugs against *Trypanosoma cruzi*. *Acta Trop.* 2015 (Submitted)
- Olmo F**, Escobedo-Ortegón J, Palma P, et al. Specific primers design based on the superoxide dismutase b gene for *Trypanosoma cruzi* as a screening tool: Validation method using strains from Colombia classified according to their discrete typing unit. *Asian Pac J Trop Med.* 2014; 7(11):854-859.
- Olmo F**, Guardia JJ, Marin C, et al. Prospects of an alternative treatment against *Trypanosoma cruzi* based on abietic acid derivatives show promising results in Balb/c mouse model. *Eur J Med Chem.* 2014; 89C: 683-690.

[REFERENCES]

- Olmo F**, Marin C, Clares MP, et al. Scorpiand-like azamacrocycles prevent the chronic establishment of *Trypanosoma cruzi* in a murine model. *Eur J Med Chem.* 2013; 70C: 189 - 198.
- Olmo F**, Rotger C, Ramírez-Macías I, Martínez L, Marín C, Carreras L, Urbanová K, Vega M, Chaves-Lemaur G, Sampedro A, Rosales MJ, Sánchez-Moreno M, Costa A. Synthesis and biological evaluation of N,N'-squaramides with high in vivo efficacy and low toxicity: toward a low-cost drug against Chagas disease. *J Med Chem.* 2014; 57(3): 987-99.
- Olmo F**, Urbanová K, Rosales MJ, et al. An in vitro iron superoxide dismutase inhibitor decreases the parasitemia levels of *Trypanosoma cruzi* in Balb/c mouse model during acute phase. *Int J Parasitol Drugs Drug Resist.* 2015 (Submitted)
- Organizacion Panamericana de la Salud.** Estimacion cuantitativa de la enfermedad de Chagas en las Americas. Montevideo, Uruguay: Organizacion Panamericana de la Salud, 2006 (in Spanish).
- Pellegrini A**, Carrera-Silva EA, Arocena A, et al. *Trypanosoma cruzi* antigen immunization induces a higher B cell survival in BALB/c mice, a susceptible strain, compared to C57BL/6 B lymphocytes, a resistant strain to cardiac autoimmunity. *Med Microbiol Immunol.* 2011; 200(4): 209-18.
- Petropoulos CJ**, Parkin NT, Limoli KL, et al. A novel phenotypic drug susceptibility assay for human immunodeficiency virus type 1. *Antimicrob Agents Chemother.* 2000; 44(4): 920-8.
- Quijano-Hernandez I**, Dumonteil E. Advances and challenges towards a vaccine against Chagas disease. *Hum Vaccin.* 2011; 7(11): 1184-91.

- Ramón-García S**, Ng C, Anderson H, et al. Synergistic drug combinations for tuberculosis therapy identified by a novel high-throughput screen. *Antimicrob Agents Chemother.* 2011; 55(8): 3861-9.
- Rassi A Jr.**, Rassi A, Marin-Neto JA. Chagas disease. *The Lancet* 2010; 375: 1388–1402.
- Rodrigues JC**, Godinho JL, de Souza W. Biology of human pathogenic trypanosomatids: epidemiology, lifecycle and ultrastructure. *Subcell Biochem.* 2014; 74: 1-42.
- Salvatella AR**, Vignolo W. Una aproximación a los costos de internación por cardiopatía Chagásica en Uruguay. *Revista da Sociedade Brasileira de Medicina Tropical* 1996; 29: 114–118.
- Sánchez-Moreno M**, Gómez-Contreras F, Navarro P, et al. Phthalazine Derivatives Containing Imidazole Rings Behave as Fe-SOD Inhibitors and Show Remarkable Anti-*T. cruzi* Activity in Immunodeficient-Mouse Mode of Infection. *J Med Chem.* 2012; 55(22): 9900-13.
- Santos DM**, Martins TA, Caldas IS, et al. Benznidazole alters the pattern of Cyclophosphamide-induced reactivation in experimental *Trypanosoma cruzi*-dependent lineage infection. *Acta Trop.* 2010; 113(2): 134-8.
- Schenone H**. Human infection by *Trypanosoma cruzi* in Chile: epidemiology estimates and costs of care and treatment of the chagasic patient. *Boletín chileno de parasitología* 1998; 53: 23–26.
- Schijman AG**, Bisio M, Orellana L, et al. International study to evaluate PCR methods for detection of *Trypanosoma cruzi* DNA in blood samples from Chagas disease patients. *PLoS Negl Trop Dis.* 2011; 5: 931.

[REFERENCES]

- Schmunis GA.** Epidemiology of Chagas disease in non-endemic countries: the role of international migration. *Mem Inst Oswaldo Cruz* 2007; 102 (suppl 1): 75–85.
- Schmunis GA.** *Trypanosoma cruzi*, the etiologic agent of Chagas' disease: status in the blood supply in endemic and nonendemic countries. *Transfusion* 1991; 31: 547–557.
- Schofield CJ, Dias JC.** A cost-benefit analysis of Chagas disease control. *Mem Inst Oswaldo Cruz* 1991; 86: 285–295.
- Silva JJ, Guedes PM, Zottis A, et al.** Novel Ruthenium Complexes as Potential Drugs for Chagas' Disease: Enzyme Inhibition and In Vitro/In Vivo Trypanocidal Activity. *Br. J. Pharmacol.* 2010; 160: 260–269.
- Soeiro MNC, Dantas AP, Daliry A, et al.** Experimental Chemotherapy for Chagas Disease: 15 Years of Research Contributions from In Vivo and In Vitro Studies. *Mem. Inst. Oswaldo Cruz* 2009; 104: 301–310.
- Soeiro MNC, de Castro SL.** Screening of Potential Anti- *Trypanosoma cruzi* Candidates: In vitro and In Vivo Studies. *Open Med. Chem. J.* 2011; 5: 21–30.
- Sosa Estani S, Segura EL, Ruiz AM, et al.** Efficacy of chemotherapy with benznidazole in children in the indeterminate phase of Chagas' disease. *Am J Trop Med Hyg* 1998; 59: 526–29.
- Tarleton RL.** Chagas disease: a role for autoimmunity? *Trends Parasitol.* 2003; 19: 447–451.
- Tarleton RL.** Immune system recognition of *Trypanosoma cruzi*. *Curr Opin Immunol.* 2007; 19: 430–434.

- Taylor MC**, Kelly JM. Optimizing bioluminescence imaging to study protozoan parasite infections. *Trends Parasitol.* 2014; 30(4): 161-2.
- Teixeira DE**, Benchimol M, Crepaldi PH, et al. Interactive Multimedia to Teach the Life Cycle of *Trypanosoma cruzi*, the Causative Agent of Chagas Disease. *PLoS Negl Trop Dis* 2012; 6(8): e1749.
- Tielens AG**, van Hellemond JJ. Surprising variety in energy metabolism within Trypanosomatidae. *Trends Parasitol.* 2009; 25(10): 482-90.
- Toledo MJ**, Bahia MT, Veloso VM, et al. Effects of specific treatment on parasitological and histopathological parameters in mice infected with different *Trypanosoma cruzi* clonal genotypes. *J Antimicrob Chemother.* 2004; 53(6): 1045-53.
- Tyler KM**, Olson CL, Engman DM. The Life Cycle Of *Trypanosoma cruzi*. American Trypanosomiasis. *World Class Parasites* 2003;Vol 7: 1-11.
- Umezawa ES**, Bastos SF, Camargo ME et al. Evaluation of recombinant antigens for serodiagnosis of Chagas' disease in South and Central America. *J Clin Microbiol.* 1999; 37: 1554–1560.
- Vallejo GA**, Guhl F, Chiari E, et al. Species specific detection of *Trypanosoma cruzi* and *Trypanosoma rangeli* in vector and mammalian hosts by polymerase chain reaction amplification of kinetoplast minicircle DNA. *Acta Trop.* 1999; 72: 203–212.
- Viotti R**, Vigliano C, Lococo B, et al. Side effects of benznidazole as treatment in chronic Chagas disease: fears and realities. *Expert Rev Anti Infect Ther* 2009; 7: 157–63.
- WHO**. Control of Chagas disease: report of a WHO expert committee. Geneva, World Health Organization, 2002.

[REFERENCES]

- WHO.** Control of Chagas disease. Second report of the WHO Expert Committee. Technical report series no 905. Geneva: World Health Organization, 2002.
- WHO.** Control of Chagas' disease: report of a WHO Expert Committee. Geneva, World Health Organization, 1991.
- WHO.** Technical Report of the TDR Disease Reference Group on Chagas Disease, Human African Trypanosomiasis and Leishmaniasis. WHO, 2012.
- Wilkinson SR,** Taylor MC, Horn D, et al. A mechanism for crossresistance to nifurtimox and benznidazole in trypanosomes. *Proc Natl Acad Sci U S A.* 2008; 105: 5022-5027.
- Yun O,** Lima MA, Ellman T, et al. Feasibility, drug safety, and effectiveness of etiological treatment programs for Chagas disease in Honduras, Guatemala, and Bolivia: 10-year experience of Medecins Sans Frontieres. *PLoS Negl Trop Dis.* 2009; 3: 488.
- Zingales B,** Andrade SG, Briones MR, et al. A new consensus for *Trypanosoma cruzi* intraspecific nomenclature: second revision meeting recommends TcI to TcVI. *Mem Inst Oswaldo Cruz.* 2009; 104: 1051–1054.
- Zingales B,** Miles MA, Campbell DA, et al. The revised *Trypanosoma cruzi* subspecific nomenclature: Rationale, epidemiological relevance and research applications. *Infect Genet Evol.* 2012; 12: 240–253.

